The acoustics of the steel string guitar

Author:
Inta, Ra Ata

Publication Date:
2007

DOI:

License:

THE ACOUSTICS OF THE STEEL STRING GUITAR

By
Ra Inta

To the memory of Tamzin Sherwood
(1977-2000)
Sic Transit Gloria Astra

Table of Contents

Abstract

To improve the replication of acoustic guitars, measurements of three Martin OOO style steel-string guitars were made at various stages of their construction. The guitars were constructed in parallel, as similar to each other as possible, with the exception of the soundboard material—which were made of Sitka spruce, Engelmann spruce and Western Red cedar.

To improve the similarity of the instruments, methods were developed to measure and control the material properties of key components before their incorporation into the instruments, including a device to measure the thickness of a guitar soundboard attached to the back and sides of the instrument.

Some of these measurements were compared to numerical models of the instrument and, after the establishment of a lexicon to describe guitar sounds, some physical factors contributing towards the timbre of guitar sounds were determined.

The results of these investigations may be developed to improve the consistency in the manufacture of stringed musical instruments.

Acknowledgements

Thankfully, this is not an Academy Awards™ speech, so I am able to properly thank the following, without whom this project would have been *impossible*. These truly are debts I will not ever be able to repay.

First, I would like to thank my supervisor, Prof. Joe Wolfe, who was supportive and generous well above and beyond the usual obligatory demands placed on supervisors. Joe has not only been a mentor in my scientific life, but also contributed much to my broader existence, both in the day-to-day, and the philosophical sense. A true captain of men as well as sailing ships.

Gerard Gilet, my industrial supervisor: I am indebted to his extraordinary foresight in recognising the importance of research on improving the construction of the guitar—especially in an industry with such 'slim overheads'. This is evident not only in his support of this project, but in his history of supporting research in a collegial and intelligent manner. I hope I have helped in some small way.

Dr John Smith, my co-supervisor: I am grateful for his continuous suggestions and expertise offered, as well as his broad knowledge, which helped me solve innumerable problems with his many great ideas. One day I hope I will visit Mileto, too.

(The) John Tann: No amount of muffins would equal the accumulated help I have received from this man. From my very first day on this project (helping him make an anechoic chamber) until the *very(!)* last minute, help support and inspiration was ungrudgingly, nay, willingly, offered.

An acknowledgement of foresight and support rightly belongs to the Australian

x

Why study the acoustics of the guitar? (An overview)

0.1 Introduction

"[A] clear overall understanding of the structural dynamics of the instrument is a critical element in understanding how to produce a quality instrument. All good luthiers intuitively understand this, but...much of musical instrument development proceeds in an empirical, Edison-like way, guided by individuals with keen ears experienced in their construction" —M. French & G. Bissinger French and Bissinger [2001]

After the voice, the guitar is probably the most popular musical instrument in the Western world. Basic physical and engineering properties of the guitar have been well studied over the last four decades, driven by the needs and curiosity of players and instrument builders, as well as the interest of scientific researchers. Much of the fundamental behaviour of the instrument is well understood but less well known are the various effects on the overall sound due to interactions among elements of the instrument. Most scientific investigation has been on the acoustic, as opposed to the electric, guitar. The electric guitar is outside the scope of the present work and hence the term *guitar* will hereafter refer to the *acoustic guitar* and will usually

mean the *steel-string* (folk) guitar specifically.

Guitar-makers (or *luthiers*) have traditionally developed techniques that were passed onto them by their predecessors. Adjustments are generally made to construction processes according to the needs of musicians; methods are improved through newly available technologies and the innovation of their colleagues. Experimentation usually involves modification of a preexisting technique, often with the desire to adhere to some particular guidance principle. The experiments that are deemed successful are retained, whilst the unsuccessful endeavours are either modified further or discarded. Developments have been influenced by the 'environment' determined by the technology and æsthetic tastes of the time. For example, one of the principal aims in acoustic guitar design has been to produce a louder instrument Morrish [1997]. This led to an increase in the surface area of the soundboard and, as a consequence, the plates of the guitar had to be reinforced with braces (*struts*) in order to maintain structural integrity Romanillos [1987]. The mechanical attributes of the bracing system influence the guitar's sound. Much of the innovation in the last few decades has involved some alteration of the bracing system; for example the Australian luthier, Greg Smallman, produces instruments with carbon fibre/balsawood composite braces in a lattice shape Fletcher and Rossing [1998], and Michael Kasha, among others, experimented with asymmetric bracing designs Kasha [1995], Eban [1985], Margolis [1986]. Many of these experiments are successful. However, in general, there have been few strong, specific, guiding principles obtained through scientific research and development for a luthier to follow in making design and construction innovations. Further, most luthiers have a strong personal intuition about

the overall effect of design and production changes, but it is usually very hard to communicate intuition objectively.

The lack of clear measurable objective goals may be attributed to a number of reasons, including:

- a lack of isolation of important measurable parameters leading to an optimisation of these parameters (assuming these parameters exist: §1.3) and;

- the complexity of engineering the instrument and characterising the construction materials, and;

- many guitar manufacturers do not (or do not feel able to) hold this as a high priority

Probably the factor most retarding progress in understanding the vibrational behaviour of the guitar is because of the last reason: although many guitar manufacturers see research and development of the guitar as an important issue, it is often perceived as a frivolous activity. Perhaps if more specific goals were isolated, more manufacturers would be more willing to invest more in innovation. Although there are many areas that would benefit from a more scientific understanding, this thesis is a series of investigations of some specific questions raised by the guitar manufacturer, Gerard Gilet.

0.2 Outstanding problems of interest

Many phenomena associated with sound production of the guitar may be understood through the application of physical principles. For example, the loudness of the instrument depends on the fraction of the string's vibrational energy radiated as sound and, consequently, one might assume that this would be simple to optimise. However, this is not as straight-forward as would seem at first; musicians tend to desire qualities of guitar sounds such that there is usually a compromise between the 'loudness' and the 'tone quality' (including the sustain and 'intonation') of the instrument, which has been noted in industry Gerken [2001].

Gerard Gilet is interested in the mechanisms behind a range of issues related to the construction of the guitar: How would it be best to control the material properties of important components, such as the braces and soundboards? How to characterise the finished instrument in a meaningful way? How do different species of wood affect the behaviour of the soundboard? How would he better quantify the subjective demands on the timbre of the instrument?

0.3 The approach in this thesis

This thesis addresses some of the problems described in §0.2. The approach is mostly experimental and relates to work done specifically on the steel-stringed acoustic guitar and some related simple systems. The main questions addressed are:

1. How important is the soundboard material and what are the important properties?

2. How important are the brace dimensions and techniques associated with the bracing?

3. How do vibratory properties of components influence the final instrument?

Three high quality steel-string acoustic guitars, all OOO models with solid wooden soundboards, were constructed, in parallel, by the author. They were built as similarly as possible—with the exception of the soundboard material: one was made of Engelmann spruce (*Picea engelmannii*), one of Sitka spruce (*Picea sitchensis*) and the last of Western Red cedar (*Thuya plicata*).

A primary goal was a scientific study of some of the vibratory and acoustic properties at various stages of construction. Care had been taken to control or to select some important material properties of components, *before they were incorporated into the instruments*, to minimise cross-instrumental variation. To control the components (except the soundboard) it was necessary to match these properties. Construction was performed at the *Gilet Guitars*[1] guitar manufacturing workshop under the supervision of the master luthier, Gerard Gilet. The OOO design was chosen because it is a model made with a relatively high level of consistency at this workshop. The Gilet workshop was also a stockist of guitar woods, making a selection of materials possible from a number of specimens.

---

[1] *Gilet Guitars*, Unit 8-10 Booralee St, Botany, Sydney, Australia

0.4   Overview

Chapter 1 reviews the understanding of the operation and behaviour of the guitar, its acoustic and vibratory behaviour. It also surveys some useful methods relating to the timbre of the instrument and the history of the instrument.

Chapter 2 introduces the guitar and some relevant technical developments. The essential concepts and nomenclature are discussed, because there are important differences in the language used for similar concepts between scientists and luthiers. Some basic mechanical models of systems related to the guitar, such as the Helmholtz resonator, the two and three mass coupled oscillator model, normal vibratory modes of plates and beams, and the radiativity of simple systems are included.

Chapter 3 covers technical details involved in the construction of the guitar, including the materials and design heuristics employed by luthiers. There is a detailed discussion on the properties of wood. These are important in ascertaining the use of scientific studies in improving the instrument. A physical interpretation behind some common techniques traditionally used in making the guitar is given.

Chapter 4 summarises numerical modelling work performed by David Vernet, Davy Laille and Matthieu Maziere, in collaboration with myself, on the guitars studied in this thesis, as well as some simpler vibratory systems. Models using the software packages CASTEM and CATIA, are compared to experiments to examine

the validity of the assumption of material anisotropy and to examine the relationships that adhesive bonds and free plate modes have on the finished instrument.

Chapter 5 describes experimental work on the selection of materials for use in constructing a guitar. The importance of testing material properties of components is emphasised.

Chapter 6 describes experimental work done on the soundboards and bodies of the guitars before completion. Differences among the three guitars are tracked during construction. A description of an invention developed by John Smith and myself to measure the thickness distribution of a guitar soundboard is given.

Chapter 7 presents experimental work done on the completed instruments. Results of tests done on pressure and dynamic mass responses as a function of frequency are reported, and compared to Chladni figures made at the same time. Analyses of the Helmholtz, coupling and free-plate frequencies are presented. The use of these are examined with regards to characterising particular instruments.

Chapter 8 consists of two studies on the subjective impressions of guitar timbre. The first establishes a lexicon for describing acoustic guitar sounds. This lexicon is used as a tool in the second study, which examines the effect of some physical variables on recorded guitar sounds, through the use of psychoacoustic techniques.

Chapter 9 concludes the study with a discussion on the usefulness and relevance

of the work presented here to those in the guitar making industry, as well as to those interested in the physical behaviour of the acoustic guitar. Problems encountered in this work are highlighted and some suggestions are made as to the direction of possible further work to be done.

Chapter 1

Previous work

"My secret is one you have witnessed many times, and one that I can't leave to posterity, because it must with my body go to the grave, for it consists of the tactile senses in my finger pads, in my thumb and index finger that tell the intelligent builder if the top is or is not well made, and how it should be treated to obtain the best tone from the instrument"—Antonio de Torres Jurado (1817-1892) [Romanillos, 1987]

This chapter discusses previous work, firstly on stringed instruments in general, and then to the guitar in particular. A small history of the instrument and a brief overview of the psychoacoustics of music are included. Detailed treatment of some of the methods described in this section are given in Chapter 2. The terminology of components of the guitar are given in §2.1.

1.1   A brief history of the guitar

There is much written on the history of the guitar. The traditional ancestors of the modern guitar are a four course 'guitarra' family (guitarra morisca and guitarra

Date	Event
1265	Reference to guitarra in 'Ars Musica' (Juan Gil of Zamora)
1283-1350	References to guitarra in poetry (Archpriest of Hita)
1306	Guitarra played at the Feast of Westminster
1400's	Vihuela developed
1600-1650	Much music for the guitar. Popularity rivalling the lute. 5th course added
1770-1800	Sixth string added, courses[1] replaced by single strings
1800-1850	Guitar popular, in performing and publishing
1850	Scalloped cross bracing developed (C. F. Martin)
1850-1892	Guitar design modernised (Torres)
1900	Steel strings used on some acoustic guitars
1902	OOO model guitar developed (C. F. Martin company)
1916	First guitar performance in a concert hall (Segovia)
1928	First electric guitar advertised
1929	14th body fret on steel-string guitars
1948	Gut strings wholly replaced by nylon (partly due to Segovia)
1980	Carbon fibre used in lattice brace system (Greg Smallman)

Table 1.1: A brief history of the guitar (From [Morrish, 1997, Longworth, 1975, Richardson, 1995b, Atherton, 1990])

latina, then popularly used for strummed accompaniment), and the Spanish vihuela, a six course instrument with a small body, similar to the lute. Both were in use throughout the 15th century. The guitarra had a fairly rotund body, not unlike that of gourd-based instruments, with a relatively small soundboard and a carved 'rose', similar to those of the traditional lute. The vihuela was even smaller and was fairly unrefined [Morrish, 1997]. The popularity of the lute has left an etymological remnant: a maker of guitars, violins or lutes is known as a *luthier*.

A five string guitar, incorporating features of the vihuela and the guitarra, appeared in the 16th century when the popularity of the vihuela had diminished. The lute was still widely used at this time, but was surpassed in popularity by the guitar in the late 17th century. The number of strings was not standardised to 6 until the

late 18th century, although not all modern guitars have 6 strings. The 4, 12 and, to a lesser degree, the 7 and 8 string guitars, also find some modern usage.

There were many prolific performers, composers and publishers of guitar music in the classical and romantic periods, including Fernando Sor, Mauro Guilliani, Matteo Carcassi, and Fernando Carulli. The violinist Niccolò Paganinni played, and Antonio Stradivari made, some guitars. Guitar concerts were common and Sor played the first solo guitar concert at the London Philharmonic Concert (1817). The fingerboard was made longer and the body was joined at the 12th fret (halfway along the string's active length) to enable playing the higher range more easily in the chitarra battente, an antecedent of the guitar [Bethancourt, 1999]. The bridge was moved to a more central position in the soundboard and a saddle was added to improve sound clarity, around the middle of 1600's at the earliest.

The guitar declined in popularity until Francisco Tárrega (1852-1909) who did much to improve the image of the instrument. He transcribed many pieces for the guitar and introduced the technique of playing with the fingernail, thereby increasing the timbral range; prior to this the instrument had mostly been an accompaniment and was usually strummed.

The Spanish luthier Antonio de Torres Jurado (1817-1892) is often dubbed the 'father of the modern guitar' and had much to do with refining the design to obtain an instrument that is essentially the same as the majority of classical and flamenco guitars made today. Torres was concerned with increasing the loudness of the instrument and made many major design changes, notably by increasing the surface area and by introducing bracing to the soundboard and back plate to structurally

reinforce against the increased string tension and mass [Romanillos, 1987]. The development of the traditional 'fan' bracing arrangement is commonly attributed to him, although his predecessors Josef Pagés and Louis Panormo used similar systems [Richardson, 1997]. Torres was also interested in improving the guitar through better understanding of the underlying mechanics. There is a popular anecdote that he constructed an instrument with a conventional spruce guitar soundboard—but the back and sides were made of papier-mâché—to demonstrate the acoustic importance of the soundboard. He once stated that he could not teach his secret to others because it was impossible to communicate the subjective tactile feedback system between thumb and index finger that was deemed indispensable in the quality control process [Romanillos, 1987]. Other influential luthiers from the early 20th century include Santos Hernández and Manuel Ramirez.

The guitarist Andres Segovia (1893-1987), influenced by Tarrega, helped make the guitar a respected concert instrument. He travelled widely and inspired many people to contribute to the playing and composition of music for guitars and their manufacture. Segovia is credited with the replacement of strings made of catgut (dehydrated sheep intestines) with those of nylon [Huber, 1991].

To further improve the loudness and the sustain of the instrument, strings made of steel wire (already used in the mandolin) were used to make the *steel string guitar* at the beginning of the 20th century by the luthiers Orville Gibson and Christian Frederick Martin [Gilbert, 1999]. However, the increased static tension of the strings requires substantial alteration of the soundboard and bridge structure. The soundboard reinforcement system known as *cross bracing* (§2.2) was developed in the

1800's and first used on parlour guitars. It only gained widespread use upon its application to the steel string guitar, because of its superior structural strength, and is now commonly used in steel-string guitars. The process of scalloping braces (§3.4) was originally developed by Christian Frederick Martin (1796-1873) in the the 1840's [Longworth, 1975]. The OOO model guitar was also developed by the C. F. Martin company, in 1902 by Frank Henry Martin (1866-1948), as a further attempt to compete with the comparatively loud stringed instruments such as banjos and mandolins. The OOO designation arose from the use of the symbol 'OM' by the C. F. Martin company to represent their 'Orchestra Model' and was shortened to 'O' [Longworth, 1975]. A larger size (in terms of body volume and soundboard area) was the 'OO'. The OOO model is larger yet again. This company was also responsible for another innovation widely used in steel-string guitars: joining the body to the finger board at the 14th fret [Longworth, 1975], to enable playing at higher registers (for comparison, this fret is the 12th for classical guitars and the electric guitar is generally made to be accessible to the 22nd or even the 24th fret).

Many popular musical movements feature the guitar as a central instrument, including the blues, some strains of jazz, many strains of pop, modern folk, skiffle, rock 'n' roll, country and western, bluegrass, hippy/psychedelic/folk/hard rock, Latin American salsa, industrial/death/thrash/glam/heavy/nu metal and grunge. This spans a large fraction of the major popular musical movements from the 1950's until the present day, representing a huge global market[2].

---

[2]For example, in 2002 guitar sales produced over $US900 million in revenue and almost one million new electric, and almost one million new acoustic, guitars were sold in the United States alone [Cruz, 2003].

The increase in popularity from the 1950's until the present has seen a corresponding increase in acoustic guitar production. However, despite this, the majority of design modifications over this period have been æsthetic or improvements to the pick-up and amplification system, with the exception of the increasing use of alternative construction materials. Perhaps the most striking of these attempts has been the introduction of carbon fibre lattice bracing on the classical guitar soundboard in 1980 by the Australian luthier, Greg Smallman [Atherton, 1990]. There are guitars that are partially or wholly made of carbon fibre (such as the Rainsong™guitars) and there is research into the application of other synthetic materials to the guitar [Besnainou, 1995].

1.2 Early work in acoustics

The study of the acoustics of musical instruments is one of the earliest mathematical sciences. It is widely believed that the Pythagoreans were inspired to search for mathematical order in nature because of their work on the harmonic relationships of the vibrations of strings; this is the first known example of experimental physics [Sedgwick and Tyler, 1917]. Many prominent physicists have contributed to the field of acoustics, including Galileo Galilei, Isaac Newton, Chandrasekhara Raman and Julian Schwinger. However, two great works from the late 19th century serve to summarise most of the field of acoustics and vibration up to then, and are still widely referred to in the literature: Hermann L. F. Helmholtz's 1885 text *On the Sensations of Tone as a Physiological Basis for the Theory of Music* [Helmholtz, 1885], and the two volume *The Theory of Sound* [Strutt, 1869] written by John William Strutt (3rd Baron Rayleigh) in 1869.

An excellent summary of music acoustics is *The Physics of Musical Instruments* [Fletcher and Rossing, 1998] by N. H. Fletcher and T. D. Rossing, although there are many other good examples [Benade, 1990, 1960, Hall, 1980, Pollard and Harris, 1979, Rossing, 1990].

1.3 Previous work on stringed musical instruments and related systems

Much of the work done on other stringed instruments can be easily applied to the behaviour of the acoustic guitar—in fact a large number of studies have been on the violin, which are usually applicable to the guitar. For example, a work that has provided inspiration for research in the field of stringed musical instruments in general is Carleen Hutchins' article *The science of the violin* [Hutchins, 1962]. Relevant material presented here is treated in more technical detail in Chapter 2.

Aside from the study of vibrating strings mentioned at the beginning of §1.2, the first detailed investigations into the acoustics of stringed instruments were most probably made by instrument makers. There is anecdotal evidence that luthiers from northern Italy in the 16th to mid 18th century (culminating most notably in the Amati, Stradivari and Guarneri families) used a 'tap-tone' method to characterise instrument wood and to 'tune' the free-plates of violins before assembly [Hutchins, 1993]. The earliest known quantitative measurements of the vibratory properties of

stringed instrument bodies were made by Felix Savart and the violin maker J. B. Vuillaume in the early 19th Century [Hutchins, 1999, Bissinger, 2001].

The majority of stringed musical instruments rely on a soundboard or stretched membrane coupled to an air cavity. The soundboard, and usually the back and sides, is a system of thin plates and therefore the vibratory properties of plates are important in characterising the behaviour of these instruments (§2.9). One of the first investigations into the vibrations of plates was made by Sophie Germaine [Germaine, 1821] and there is also a very good treatment by Rayleigh [Strutt, 1869]. Because the plates used on stringed instruments are generally very anisotropic, and the geometry often complex, the mathematical analysis of the vibratory properties can be fairly involved [Szilard, 1974, Lekhitskii, 1968, 1963]. Therefore theoretical treatments of complicated plates are largely restricted to numerical models (*e.g.* [Chaigne, 2002]) (§4).

Much of the research in guitar acoustics has concentrated on the resonance or normal modes of plates, because this determines many of the important features of the output intensity spectrum of the instrument, and some of the transient behaviour. This combination is often referred to as the *character* of the instrument, although it is unclear what this musical term exactly refers to in terms of spectral and transient features [McIntyre and Woodhouse, 1978].

The motion of the air is important in sound production. At low frequencies the air in the internal cavity of the guitar is similar to that of a Helmholtz resonator, where a 'plug' of air vibrates in the throat of a rigid vessel enclosing a volume of air (§2.4), first studied by Hermann Helmholtz in the 1860's [Helmholtz, 1885].

At higher frequencies, standing waves somewhat similar to the simple air modes

found in a long pipe (with both ends closed) are produced in the internal air cavity, first characterised in the guitar and the violin by Erik Jansson [Jansson, 1977].

Beams and elastic properties. The soundboard of the guitar is usually reinforced with wooden beams, or *braces* (§2.2). To understand the contribution the braces have on the vibratory behaviour, it is necessary to study the dynamics of vibrating beams or bars [Timoshenko, 1934, Rossing, 2000]. This type of analysis requires some knowledge of the material properties, *viz.* the elastic moduli, damping and mass density. The study of vibrating beams provides an important means of characterising these properties (§2.7) [Dunlop and Shaw, 1991, Harjono, 1998]. It has long been recognised that the material properties of woods used to make stringed instruments are worth investigation to the luthier [Richardson, 1994], and this is reflected in the volume of material published on the subject [Bucur, 1995, Schleske, 1990, Forest Products Laboratory, 1999, Bodig and Jayne, 1982]. A more difficult quantity to measure in wood is the damping factor [Haines, 2000] (§3.2).

Electromechanical analogies. Stringed musical instruments are a complicated engineering system. It is useful to draw on the substantial work done on analogous systems. The modern study of mechanical vibration and acoustics exploits analogies made to electronic circuit theory, enabling vibratory structures to be studied in the same way as circuit networks [Skudrzyk, 1968]. There are also acoustic applications of some techniques developed in the field of quantum mechanics [Levine and Schwinger, 1948, Forbes and Pike, 2004, Cummings, 1977]. The modelling of

instruments using electrical analogues and transmission line theory is helpful in quantitative calculation as well as giving insights into the behaviour of the instrument. Notably, John Schelleng gave a remarkable and influential model of the violin as an electrical circuit [Schelleng, 1963]. The model treats all the important vibratory components (the bowed string, bridge, soundboard and back-plate and the f-holes and internal air cavity) as effective circuits, able to interact. Colin Gough examined the transmission of string energy to the body of stringed instruments as an electrical transmission line system [Gough, 1981]. Analogously to electrical transformers, the body of a stringed musical instrument functions acts as an apparatus to match (imperfectly) the mechanical impedance of the string vibration to that of the air, such that power transfer from the strings to the air is reasonably efficient. However, it is not desirable to have an extremely high transmission efficiency; both of these works have given insights into coupling between the strings and the body, elucidating the problem of the 'wolf-note,' which is a result of too strong coupling between a particular string and body mode, which gives rise to a very loud, irritating, inharmonic sound which is harsh but has very little sustain. String-body coupling is dependent on the interaction between the player's finger and the string [Pavlidou, 1997], and the motion of the string in polarisations perpendicular and parallel to the plane of the soundboard [Richardson, 1997]. To give a more realistic sensation of timbre, synthesised tones from a plucked guitar string require modelling of how the string couples with the body in both polarisations [Lewney, 2000, Chaigne, 2002]. The strength of string-body coupling contributes to the compromise between sustain (or 'tone') and loudness noted by guitar makers and players [Gerken, 2001].

Simple models of the guitar. Models presented for the guitar (or violin) system have various levels of detail. Because the body of the guitar has a finite stiffness and a relatively large area, there is some coupling between the body and the motion of the air—in fact this is, at least implicitly, an important design factor. A simple model for the low frequency coupling between the air and the soundboard, assuming each is a simple oscillator able to interact, was first investigated by Jürgen Meyer [Meyer, 1974] and developed by Ian Firth [Firth, 1977], Graham Caldersmith [Caldersmith, 1978], Ove Christensen and Bo Vistisen [Christensen and Vistisen, 1980] (§2.5). These models predict the observation of additional soundboard modes due to coupling with the guitar body effectively behaving as a Helmholtz resonator. The soundboard and air motion are in opposite phase at frequencies below the Helmholtz resonance and are in phase above it [Christensen and Vistisen, 1980]. These predictions agree well with the experiments reported in these studies.

Investigations of the low frequency behaviour of the guitar can give information on many effective quantities (equivalent piston area, effective masses) and it is possible to calculate the strength of coupling between the soundboard and the air in the cavity [Christensen and Vistisen, 1980]. Knowledge of these parameters enable fairly descriptive models to be made of the pressure response of the instrument [Wright, 1996, Bécache et al., 2005].

The back-plate may be modelled as an additional oscillator [Christensen, 1984] (§2.6). As with the case of string-body coupling, there is an optimisation problem concerning body-air coupling: too little coupling leads to poor overall sound production, whereas coupling that is too high will lead to undesirably sharp peaks in the output sound spectrum. Extensions of these models for higher frequencies have been

developed by Ove Christensen [Christensen, 1983], Howard Wright [Wright, 1996] and Antoine Chaigne *et al.* [Bécache et al., 2005].

Results from [Christensen and Vistisen, 1980] show the coupling strengths for classical guitars to be about 0.8 for the guitars studied, compared to 0.63 for a violin measured by Ian Firth [Firth, 1976/77]. A related parameter, the *radiation efficiency* (the fraction of energy put into the bridge that is converted into sound) is also an important quantity. Joseph Lai and Marion Burgess measured mean efficiencies of 13% and 14% for two guitars over the range $50 \rightarrow 550$ Hz [Lai and Burgess, 1990].

Effects of plate bracing. Investigations into the bracing effects of the guitar have been conducted by Jürgen Meyer [Meyer, 1983a], Bernard Richardson [Richardson, 1982], Thomas Rossing [Rossing and Eban, 1999] and by M. J. Elejabarrieta *et al.* [Elejabarrieta et al., 2000,?]. Nearly all of these studies are on the bracing of the classical guitar. However, there is at least one study on the effect of the cross-bracing used on a steel-string guitar [Ross and Rossing, 1979] which shows a difference in the phase of the sound pressure radiated by a fan-braced guitar (with respect to the motion of the bridge) compared to a cross-braced instrument. Thomas Rossing then compared the vibratory behaviour of guitar soundboards before and after the bracing was added, finding that, without bracing, the soundboard behaved much like a simple rectangular plate, which was complicated greatly by the addition of the braces [Rossing, 1982]. The modes of the guitar are very sensitive to changes made in the soundboard bracing and greatly affect how the strings drive the body [Lewney, 2000].

Much of the experimental work done by luthiers is unpublished and/or hard

to obtain. However, there are a few specialised repositories and forums for the discussion of scientifically technical applications in luthiery, including the (now defunct) *Journal of the Catgut Acoustical Society*, the (also defunct) *Guild of American Luthierie Quarterly* and the *leftbrain luthier* internet discussion board. Many journals on acoustics also feature papers on stringed instruments, including the *Journal of the Acoustical Society of America*, *Acta Acustica* and the *Journal of Sound and Vibration*.

Many of the scientific projects involving luthiers could be classed in two categories: luthiers who welcome the application of principles from physics to the manufacture of their instrument, and trained physicists or engineers applying their science to luthiery. It would be fair to say the former group are in the majority, but the distinction is not exact; the manufacture of high quality instruments is an exacting process and therefore attracts those with a highly technical inclination. Well-known examples of the former include Antonio de Torres Jurado, Greg Smallman and Manuel Velázquez. The scientist/luthiers include Carleen Hutchins [Hutchins, 1998], Bernard Richardson [Richardson, 1995b], Graham Caldersmith [Caldersmith, 1985], Michael Kasha [Kasha, 1995] and Simon Marty [Marty, 1987a]. Members of both of these groups have done much to promote the advancement of scientific application to luthiery and most of these people have had many students or apprentices who have made important contributions to the field. There are also many examples of long-term collaborative projects between groups of luthiers and scientists, such as those involving Erik Jansson [Jansson, 2002], Thomas Rossing [Ross and Rossing, 1979, Rossing and Eban, 1999] and Antoine Chaigne [Chaigne and Rosen, 1999].

Timbre and the guitar

Although loudness is regarded as important, it is not the only characteristic of the sound produced by the acoustic guitar. The *timbre* of the guitar sound is more complicated to define (for example "The quantity determining discrimination between two complex tones having the same pitch and loudness") [Acoustical Society of America, 1960] and to measure. Without a working definition of timbre it is difficult to determine the perceived effects of physical modification to a guitar sound. The importance of understanding aspects of timbre is recognised and investigations on timbre range from telephony [Szlichcinski, 1979] to the interpretation of sonar sounds [Salomon, 1958].

Much of the work has focussed on determining the number of dimensions of the semantic space of timbre, derived from factor analysis of responses to acoustic stimuli. Previous investigations into the dimensionality of timbre [Grey, 1977, 1978, Kerrick et al., 1969, Lichte, 1941, McGee, 1964, Salomon, 1958, Terhardt, 1978, von Bismarck, 1974b,a, Wedin and Goude, 1972, Wessel, 1978] have given a dimensionality of 3-8, although some of these studies relate to sounds not in a musical context, or to tones that have a constant temporal character. For example, John Grey [Grey, 1977] defines a three-dimensional timbral space (transient behaviour, synchronicity of transients and the spectral energy distribution) as a result of multidimensional scaling of responses to sound stimuli.

A three dimensional model for timbre was also identified in [Jensen and Arnspang, 1999], which claimed a relationship among the spectral envelope, the temporal envelope and the level of noise of the stimulus. Other three factor models for timbre,

resulting from the reduction of a number of descriptors, give dimensions of 'activity', 'pleasantness' and 'high' [Kerrick et al., 1969] (accounting for 90% of the variance of the stimuli given) 'balanced', 'power' and 'thin' [Enomoto and Yoshida, 1968] (90% of the variance), and 'brightness,' 'roughness,' and 'fullness' [Lichte, 1941]. A four-factor model ('sharpness', 'compactness', 'fullness' and 'colour') for timbre, accounting for 91% of the total variance of steady tones, is presented in [von Bismarck, 1974b]. An eight factor model specifying the dimensions 'magnitude', 'æsthetic', 'clarity', 'security', 'relaxed', 'familiarity' and 'colour' (the eighth factor was not specified but has the attributes 'scraping,' 'soft' and 'smooth') accounted for 42% of the variance of complex sonar sounds [Salomon, 1958]. The variation in the number of dimensions of these studies suggest that care is required in the universal application of the results.

An obvious extension of this type of study is to relate measurable features to the timbre of a sound. For example, [Wold et al., 1996] give the principal components 'loudness', 'pitch', 'brightness', 'bandwidth' and 'harmonicity'.) A study by John Grey suggests that purely (long time averaged) spectral features may account for much of the timbre for some tones (*e.g.* those made by the bassoon) while others may be determined by temporal cues (such as those made by the clarinet or trumpet) [Grey, 1978].

The guitar is potentially able to express a considerable range in timbre, both through variations in playing technique and instrument design [Schneider, 1977, 1985]. The effect on the perceived timbre of the instrument due to alterations is

obviously important to luthiers, and many have an intuitive idea of the results of changes made gained from experience. For example, a list of construction factors that have an important effect on the timbre of the guitar is given in [McLeod and Welford, 1971]:

Shape and size of the body   Acoustic properties of the woods
Thickness of body members   Details of bracing
Glue bonds/joints   Fingerboard geometry
Bridge/saddle/nut   String properties
Size and placement of the soundhole

However, it is difficult to develop and to control parameters based on purely intuitive concepts. Tests have been constructed to examine the nature of timbre in the guitar. Erik Jansson showed that trained listeners broadly agree upon the 'quality' of guitars in a listening test [Jansson, 2002]. Responses to changes made to the structure of the guitar show that the level should be high in the range $80 - 1000$ Hz to give a 'full' sound, high in the range $1 - 3$ kHz to give 'brilliance' and 'clarity' (although too high a level here gives 'harsh' sound), a high level above 3 kHz is good for chords, affecting the tone just after plucking (too high a component also gives harshness) [Meyer, 1983b]. High pass filtering of the sound of the guitar at 4 kHz gives only sounds associated with plucking transients. Sounds low-pass filtered at 2 kHz sound 'dull' and 'hollow', and below 500 Hz gives a 'dull' sound, with indistinct attack. Finally, high-pass filtering of guitar sounds above 500 Hz gives the perception of a 'clear' but 'thin' tone [Jansson, 2002]. Studying four guitars with a range in quality, Ricardo Boullosa *et al.*, found that the perceived quality of a guitar was determined largely by the least *mean tuning error*[3] and the greatest *radiation*

---

[3]Defined, in cents, as: $1200 \log_2(\frac{\text{measured frequency}}{\text{nominal frequency}})$

efficiency [Boullosa et al., 1999]. Antoine Chaigne, Anders Askenfelt and Erik Jansson used synthesised guitar tones to show that dominant resonances can strongly influence perceived quality by synthesising guitar tones after asking participants to choose the guitar sound among other recordings of real plucked stringed instruments [Chaigne et al., 1992]. Howard Wright, in analysing responses due to changes in modal parameters of a synthesised model of the guitar, concluded that the modal parameters most influential on perceived tone quality are the effective area, followed by the effective mass, the mode frequency and then the Q-value of the particular mode [Wright, 1996].

If it is determined exactly what players and listeners want from the timbre of a guitar, a luthier may then experiment with design modifications until the desired sound is achieved. Unfortunately there is not even a lexicon agreed upon to describe guitar timbre sensations, let alone established physical measures relating to aspects of the timbre. One way to better quantify musical timbre is to develop an agreed set of descriptors to describe the sound of the guitar, and then to test a number of people to determine which of these are highly valued, in response to stimuli in the form of guitar sounds. The determination of physical measures (*e.g.* spectral or temporal features) relating to these timbral dimensions is then possible, enabling the instrument maker to develop instruments that are optimised in particular timbral dimensions by applying the appropriate physical principles to their craft.

The effect of components on timbre. The material properties of the components of the guitar contribute to the sensation of the timbre of the instrument. By

synthesising the sound of xylophone bars of varying material properties, and testing the psychoacoustic response of participants to the synthesis, Vincent Roussarie, Stephen McAdams and Antoine Chaigne found that slight changes in material properties have a significant effect on the perceived timbre of the struck bars [Roussarie et al., 1998]. The way in which the individual components of the instrument interact are also important. Carleen Hutchins found that the difference in frequency between a particular air cavity mode (A1) and a body mode (B1) largely determined whether a violin would be suitable for a solo, orchestral or chamber instrument [Hutchins, 1989].

The techniques developed in Chapter 5 might be used to enhance the techniques that luthiers use to select appropriate material for components of the guitar and could be further developed for a routine testing programme in the workshop. Although an improved testing programme would not necessarily guarantee any particular instrument would be made 'better' *per se*, it would reduce the failure rate—which is high, even for the most experienced luthiers [Gilet, 2000, Richardson, 1995b]. By making this selection process more quantitative, the ability to replicate a particular instrument would be improved. It would then also be possible to communicate the results to other luthiers.

There appear to be no simple and clear means of determining universal 'quality predictors,' and it is not even certain these predictors exist, even on a subjective level. However, isolation of such predictors would be highly beneficial. For example one of the more obvious and easily measured parameters is the loudness of the

instrument; it was largely with this well defined objective that the Greg Smallman guitar design was developed, having a very light soundboard and stiff back and sides [Atherton, 1990]. An obvious selection criterion for the bracing material is to have a high Young's modulus in the longitudinal direction (§5.5). The density is also important for many components. An optimal measure for the soundboard material is not known. In the absence of definite optimisation strategies, emulation of successful instruments is inevitable, in which case it would be useful to build a database of appropriate measures such as the Young's moduli or radiation ratio [Schelleng, 1963, Harjono and Dunlop, 1998] (§5.4) of the components of desired instruments. Knowing the properties of the components, it is then possible to control, or select components from a supply, for the desired properties.

A quantitative relationship between the behaviour of the free soundboard and that of the soundboard attached to the back and sides would be very useful. However, considering the difficulties in finding this relationship reported by others (*e.g.* [Schleske, 2000]) such a relationship is not expected to be found without great difficulty. For example, the nodal topology of the free soundboards tends to be 'open' while that of the soundboards attached to the sides tends to be 'closed' (§6.7).

An accurate simulation of the behaviour of the guitar would enable luthiers to anticipate the result of changes to a design of the instrument without going through the expensive process of construction. Given sufficiently accurate measurements of the material properties of components, an accurate model may be made of the components and, consequently, modifications to the design of the guitar.

The use of psychoacoustics, as part of a programme to further the field of music acoustics, would be beneficial to the guitar maker because the instruments are designed (apart from physical and technical limitations) according to human preference. A proper treatment would require an *ad hoc* study on guitar sounds, which might allow the maker to determine the psychoacoustic effects of components of the guitar [Meyer, 1983a].

Chapter 2

How the guitar produces sound

"The profound study of nature is the most fertile source of mathematical discoveries"
— Joseph Fourier

In this chapter, sound production by the guitar is examined, with regard to the application of physical principles to the manufacture of guitars. Some mathematical derivations of useful quantities are given, as well as some means of interpreting these quantities with regard to experiments on the instrument. Some examples are illustrated with my own measurements.

2.1   The basic anatomy of the guitar

There is a rich terminology associated with the guitar, in both making and playing the instrument. The modern guitar consists of a long thin *neck* and an *air cavity* enclosed by the *body*, a box formed by five or six plates glued together. The *sides* (or *ribs*) separate the *top-plate* (or *soundboard*) from the back-plate. The overall shape of the body is shown in Figure 2.1.

The part of the body between the neck and the soundhole is called the *upper*
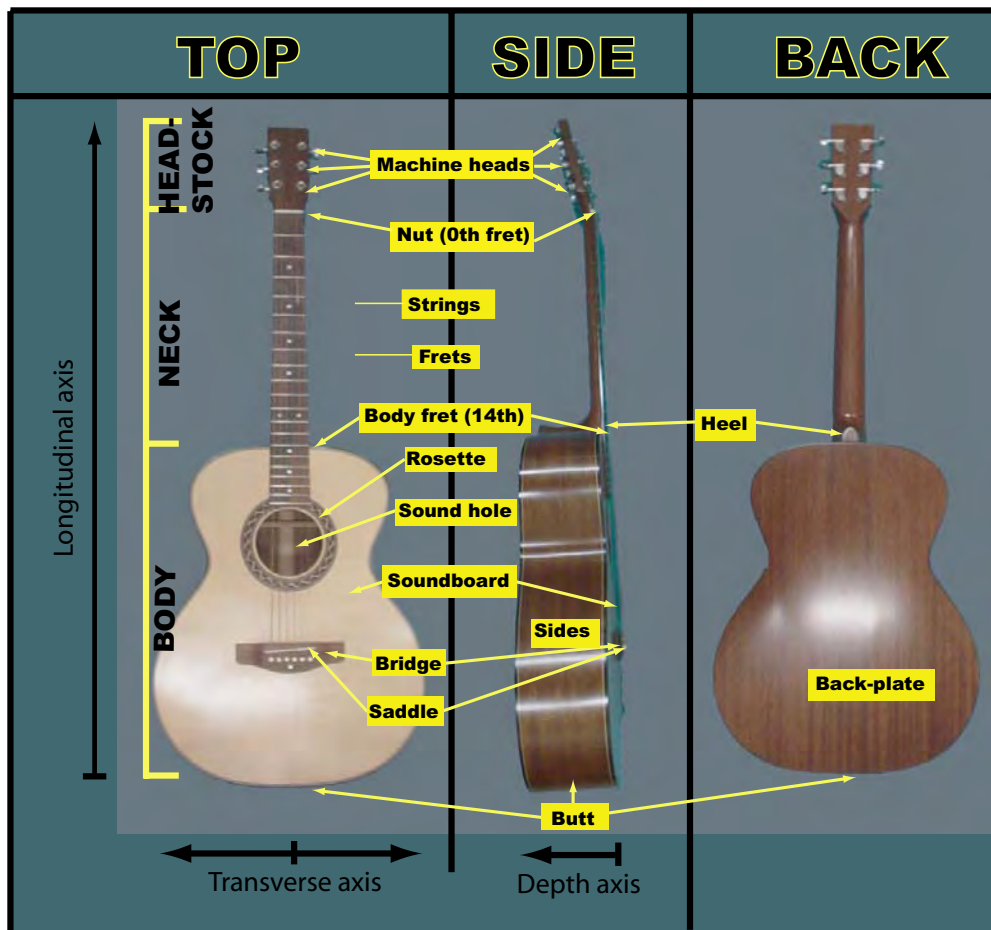
Figure 2.1: The important elements of a modern steel-string acoustic guitar. The guitar shown is the Gilet OOO-style with an Engelmann spruce soundboard.

bout. The larger area, the *lower bout*, on the soundboard is separated from the up-per bought by the *soundhole*, which allows air to flow in and out of the air cavity. The soundhole is usually bounded by a ring of wood (the *rosette* or *rose* §3.4). The neck extends from the edge of the upper bout and follows the main symmetry axis of the guitar (the *centre-line* or *longitudinal axis*.) The concave area between the upper and lower bouts is called the *waist*.

The modern acoustic steel-string (sometimes called a *folk* guitar) guitar usually has 6 parallel metal wires (*strings*) running from the *bridge* (a piece of dense wood located in the centre of the lower bout of the sound board) and terminating on the *head-stock*, at the end of the neck. There are variants with 4, 7, 8 or 12 strings but we shall hereby be concentrating solely on the 6 string variety.

The tension of each string is controlled, for tuning, by a separate *machine head* (or *tuning head*), a simple geared screw located on the head-stock. The linear mass density of each string is chosen so that standard tuning requires a tension of about $100 \rightarrow 140$ Newton each (Table 2.1). Because of the finite bending stiffness, lower pitched strings usually have additional wire wrapped around a core, to increase the linear mass density.

The *fingerboard* or *fret board* is the playing surface of the neck. It is directly be-low the strings and is made of durable wood and inlaid with small metal bars (*frets*) running perpendicular to the strings. A piece of bone or ivory (the *nut*) holds the strings in place at the point where the fingerboard joins the head-stock. The strings are firmly stopped at the other end by the *saddle*, a thin sliver of bone/ivory/hard

String	Open note	Frequency (Hz)	Diameter (mm)	Static tension (nominal) (N)	$\frac{\text{Tension}}{\text{Length}}$ (Nm^{-1})
1	E4	329.6	0.30	103.6	159.9
2	B3	246.9	0.41	103.6	159.9
3	G3	196.0	0.61	134.3	207.2
4	D3	146.8	0.81	135.5	209.2
5	A2	110.0	1.07	132.9	205.1
6	E2	82.4	1.35	115.5	178.3

Table 2.1: Typical mechanical properties of steel guitar strings (D'Addario EJ16 Phosphor Bronze/Light 0.012″ → 0.053″). The fundamental frequencies and tensions assume a 648mm ($25\frac{1}{2}$″) scale length and standard tuning (concert pitch A2=110 Hz). Strings 3-6 have wire coiled around the core to increase the linear mass density.

polymer[1] on the upper surface of the bridge. The saddle strongly restricts the motion of the strings at this point. The distance between the nut and the saddle (the active vibratory region of the string) is known as the *scale length* (typically 648 mm for steel stringed guitars).

The player shortens the effective length of a string by pressing a finger behind a fret. The frets are spaced such that the pitch increases by a semi-tone[2] in going from one fret to the fret immediately towards the bridge on the same string. The frets are numbered in ascending pitch, with the nut defined as the '0th fret'. The 12th fret produces an octave, theoretically half the length of the open string. However, due to end effects from the finite bending stiffness of the string, and the increase in tension, the string length is slightly less than half the open length[3]. The body meets the neck at the *body fret*. This occurs at the 12th fret on a *classical guitar*, but the

---

[1]TUSQ$^{\text{TM}}$ has become an industry accepted alternative to these animal products.

[2]ie: the frequency is multiplied by $\sqrt[12]{2} = 1.059463$.

[3]Because this effect increases with string diameter, the saddle is usually placed at a slight angle, with the third string sometimes displaced.

body fret is the 14th for most modern steel-string guitars.

By convention, the string with the highest pitch is called the first. The classical guitar has strings 1 to 3 made of nylon and 4 to 6 are metal wound around fibrous silk or nylon. The steel-string guitar has strings 1-2, and possibly 3, of a single wire and strings 3 (or 4) to 6 with additional wire coiled around a single wire core.

Because the longitudinal grain direction is always in the direction of the long axis of the guitar, this will be denoted the *longitudinal axis* of the guitar without confusion. For the same reason, the axis in the plane of the soundboard, but perpendicular to the longitudinal, will be called the *transverse axis*. The axis orthogonal to both the longitudinal and the transverse axes will be called the *depth axis*.

The tension in the strings tends to rotate the bridge and deform the soundboard. To make the instrument relatively loud, the soundboard must be thin and span a relatively large area (§3.4). Hence structural reinforcement is required. This is usually in the form of wooden braces. The bracing system—especially that of the soundboard—plays an important role in sound production [Ramirez, 1986, Ross and Rossing, 1979, Rossing, 1982, Richardson, 1998, 1982, Marty, 1987b] . This is examined further in §2.2 and §3.4. The back is also braced to make it more robust but the effects of this bracing system is not studied here.
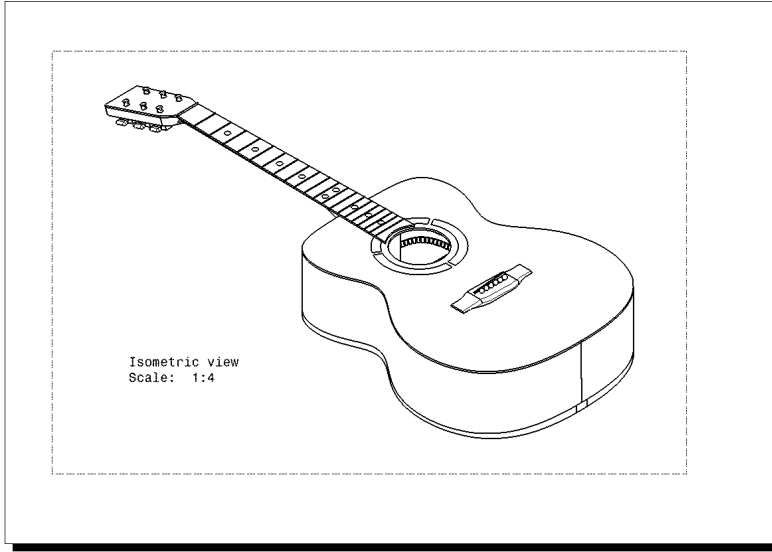
Figure 2.2: Isometric view of the OOO guitar used here. The axis conventions used here are shown. [Figure courtesy of Davy Laille and Matthieu Maziere]

2.2 Specialised anatomical features

Largely because of the various demands of musicians, there is much variation in the design parameters of different models. It is the aim of the present work to investigate how the guitar performs on a technical level, rather than to give a definitive report on various guitar designs. The guitar model studied here is a variant of the Martin Guitar Co. OOO steel-string acoustic, a popular model, with a standard bracing system, although there are some minor proprietary design features unique to the Gilet workshop. A schematic of this particular model is shown in Figure 2.2. Distinguishing features include an enlarged lower bout with an upper bout shaped similarly to the more common 'Dreadnought' model.

The soundboard bracing system

One of the most important design features of the OOO steel-string models made here is the Martin Guitar Co. style cross bracing system, shown in Figure 2.3, the distinguishing features being two wooden beams attached to the inside of the soundboard in an 'X' shape, covering most of the lower bout. This bracing system is made asymmetric by the two 'tone braces' extending from one of the 'X' braces. The bracing system is described in more detail in §3.4.
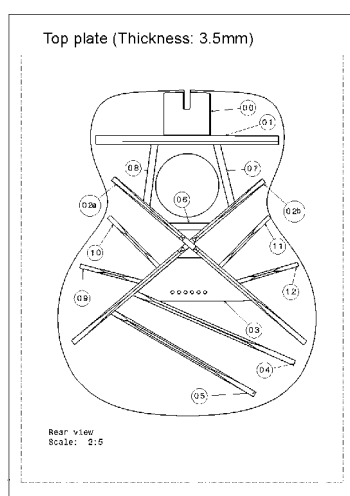
Figure 2.3: The soundboard bracing system used here (Gilet Guitars OOO Series, 2000.) [Courtesy of Davy Laille and Matthieu Maziere]

Figure 2.4: Photograph of one of the soundboards used here

The bridge

The bridge on a guitar is located in the middle of the soundboard. It fixes one end-point of the strings to the body such that energy from the vibrating string is

STEEL STRING GUITAR BRIDGE.
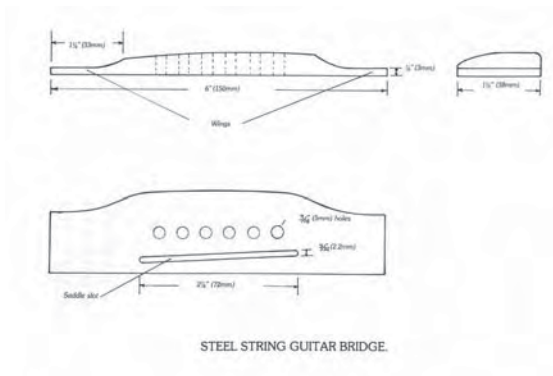
Figure 2.5: Schematic of bridge type used in steel string guitars (From [Williams, 1986a])

transmitted to the rest of the instrument and, ultimately, to the air. The design and material of the bridge varies much, especially between the steel-string and the classical guitar. Classical and steel-string guitars have similar saddles but differ in the way the strings are terminated and in the overall shape of the bridge. A plan of a typical bridge used in steel-string guitars is shown in Figure 2.5 [Williams, 1986a]. The bridge for a steel-string has six collinear holes to insert the strings (the strings on steel string and electric guitars have metal balls at one end for this reason.) The strings are held in place with conical wedges (*bridge pins*). The channel that holds the saddle is at an angle of about 4° from the base, because of a small length correction necessary due to the variation in string bending stiffness.

There is usually a piece of dense wood (usually maple) known as a *bridge-plate* forming part of the internal soundboard bracing (Figure 2.4) to provide strength and rigidity to the area directly under the bridge.

It is common for the soundboard to have some positive curvature. In this case

the underside of the bridge will need to be given the same curvature. The guitars made here have a curvature of a chord from a sphere of approximately 7.62 m (25 feet) in radius.

The neck

The neck is an important component of the guitar and has important low frequency interactions with some other major components of the instrument; modal analysis of the free guitar show that the neck forms part of a longitudinal bending mode along the axis of the instrument (*e.g.* [Alonso Moral and Jansson, 1982, French and Hosler, 2001, Russell and Pedersen, 1999]).

Although the vibratory modes of the guitar derived from the motion of the neck do not appear to affect greatly the sound of the instrument directly, they do have an effect on the tactile sensation of the instrument, having a significant effect on the 'feel' of the instrument [Bissinger and Hutchins, 2001, Hutchins, 1985, Askenfelt and Jansson, 1992], because humans are most sensitive at frequencies less than a few hundred Hertz [Brisben et al., 1999].

As is common, the necks used here contain internal steel rods (*truss-rods*) to control the amount of curvature the neck displays. However, unlike the traditional method of glueing a dovetail joint between the two, the necks are connected to the bodies of the instrument by a *bolt-on* neck system §3.4.

2.3   Excitation methods

The previous chapter highlighted some of the major design innovations made by luthiers. The changes to the design of stringed instruments in general have several physical constraints, *viz.* those regarding structural integrity, and those pertaining to the actual sound of the instrument. Mechanical vibrations in the instrument system require conversion into mechanical vibrations in the air. In normal playing conditions the strings are excited by either *plucking* with the finger (Figure 2.6), or 'picking' with a *plectrum* (a small, typically teardrop-shaped, piece of plastic, metal, shell or bone).

Either of these deforms the string, whose energy is then transferred to the guitar body *via* the bridge. Three dimensional simulations of the interaction between the finger and the string suggest that the friction and mechanical properties of the finger and the plucking direction are the most influential on the interaction between the string and the body and is affected to a lesser degree by the velocity of the finger-tip [Pavlidou, 1997].

There are other means of obtaining sound from the instrument by exciting the strings or the body, giving rise to a large range in timbre of the instrument and the number of playing techniques. The strings may be bowed, sustained magnetically (the e-Bow™ or Fernandez™ sustaining bridge) or mechanically (in the case of 'feedback'), scratched or struck with other objects. Also the body may be struck or rubbed, giving rise to particular sounds often exploited by musicians [Schneider, 1985].

Some of these excitation methods are used by researchers in the study of the instrument, although it is usually desirable to have more control over the excitation than in most of the methods described. Excitation of the strings excites the body at a number of frequencies, usually without explicit knowledge of the spectral energy distribution. It can thus be difficult to isolate the normal modes of the actual instrument (§2.9). Generally, the instrument is driven by external means, such as with an oscillating magnetic field acting on a permanent magnet attached to the instrument, a sound source (such as a loudspeaker) or mechanically, with some sort of shaker or impulse device. The body or strings may be given an impulse by being struck with an object. There have been attempts to make a device that plucks a string reproducibly (such as [Cass, 2003, Šali and Kopač, 2000]) but this has not been as successful as have the equivalent devices for bowed stringed instruments (a 'bowing machine' as in [McLennan, 2000].) A device such as this would be very useful, because it would provide excitation more like that associated with the usual sound of the guitar, but it would be more reproducible than the response obtained by using human players.

Interaction between the strings and the guitar body

The transverse modes of a vibrating guitar string are well studied and are generally better understood than the normal modes of the body of the instrument. Because the usual manner of excitation of the instrument is *via* the strings, it is important to understand the interaction between the two vibratory systems [Gough, 1981]. Mechanical properties of the strings used on the guitars studied here ('steel strings',

Figure 2.6: The action of plucking a guitar string. Shown are the relative positions of the finger-tip and the string, as viewed along the string axis, before, during and after the plucking action. The arrows represent the relative velocities, the dotted circles are the initial positions of the string.

Table 2.1) are different to those of the 'nylon string' sets typically used on the classical or flamenco guitar.

The coupling of string motion to a body mode of the instrument at the same frequency may be given by Equation 2.3.1 [Gough, 1981]:

$$[\mu \frac{\partial^2}{\partial t^2} + \mu \frac{\omega}{Q_S} \frac{\partial}{\partial t} - T \frac{\partial^2}{\partial x^2}] y(x,t) = f(x) e^{\hat{j}\omega t} \tag{2.3.1}$$

Here, x is the displacement along the axis of the string, t is the time and $y(x,t)$ is the amplitude of the string at right angles to the string axis and the angular frequency of the driving force is ω. The linear mass density of the string is represented by μ, Q_S is the Q-value of the particular string resonance and T is the (static) tension in the string. $f(x)$ is the distributed force per unit length, an arbitrary function of x. The second term represents the losses of the string, both radiative and mechanical. Taking the series solution $y(x,t) = (\sum_n a_n \sin k_n x) e^{\hat{j}\omega t}$, where $k_n = \frac{n\pi}{L}$, for a string of total length L. The a_n are the amplitude of the nth Fourier components:

$$a_n = \frac{2}{m} \cdot \frac{f_n}{\omega_n^2 - \omega^2 + \hat{\jmath}\frac{\omega^2}{Q_S}} \tag{2.3.2}$$

Where $f_n = \int_{x=0}^{L} f(x) \sin k_n x \cdot dx$.

The coupling strength between the string and the body normal modes is then [Gough, 1981]:

$$\alpha = \frac{2Q_B}{n\pi} \sqrt{\frac{2\mu L}{M_{eff.}}} \tag{2.3.3}$$

Where Q_B is the Q-value and $M_{eff.}$ is the effective mass of the guitar body mode (at the string-body interface) closest to the nth mode of the string of length L and linear string mass density μ. For $\alpha < 1$, the coupling is weak and the frequencies of normal modes are not significantly perturbed but the string motion is slightly damped by the coupling. For strong coupling, $\alpha > 1$, the resonance frequency of the closest normal mode is split symmetrically about the unperturbed frequency by the damping of both (by $\Delta f \simeq 2Q_B$). For $\alpha \gg 1$, the coupling is extremely strong and the mode frequencies are shifted significantly from their unperturbed values. Although the effects of this coupling have a profound effect on the timbre of the instrument [Pavlidou, 1997, Wright, 1996], it is difficult to isolate a string-body coupling region that is ideal for musicians: the coupling needs to be strong enough so that energy is transferred to the body and contributes to the loudness and high frequency component of the radiation (which relates to the musical concept 'brightness') but too strong coupling may lead to inharmonic and poorly sustained sound (contributing to the guitar *wolf-note*), as energy from the string is rapidly dissipated [Gough, 1981, Wright, 1996].

The string-finger interaction of both hands is important. The point where the finger forces the string onto the fret is not a perfect node for vibratory waves in the string with polarisations parallel to the plane of the fingerboard; the transmission coefficient of vibratory waves from the strings to the bridge having this polarisation is much lower than that for waves orthogonal to the plane of the soundboard [Richardson, 1982]. Transverse waves in the string with polarisations perpendicular to the plane of the soundboard have the strongest effect on the volume of air moved by the soundboard. Control of the initial polarisation of the vibrating string is most probably exploited by players, because it gives some degree of control over the longevity and timbre of a particular note. The polarisation cross-section (*i.e.* in the plane perpendicular to the longitudinal axis) of the string pulses describes an ellipse, depending on which direction the string is plucked in [Gough, 1981]. This is important to manufacturers. The master luthier, Gerard Gilet, often observes the right hand position players use on a new instrument; if they prefer to play too close to the bridge, the instrument requires enhancement at higher frequencies and requires a less bright sound if the player consistently plucks the instrument as close to the fingerboard as possible [Gilet, 2000]. Longitudinal and torsional string modes do not affect the radiated sound or store a great amount of the string's energy [Strutt, 1869].

Because the strings are important in determining the output sound of the instrument, the string properties contribute to the variation in measurable parameters in the characterisation of a particular instrument. For example, changes associated with the typical deterioration of the strings tend to increase the decay rate at high

frequencies and make the string more inharmonic [Hanson, 1987]. To simplify the measurements on the guitars studied here, we will be concerned with the physical properties of the instrument itself. String resonances and their interactions complicate these and, therefore, tests were conducted on the instruments without the strings attached. The guitar has been shown to be a linear system [Richardson, 1982], so the deformation due to the string tension should superpose, to first order.

2.4 The Helmholtz resonator

An important motion of the guitar that produces sound at lower frequencies is one in which the body enclosure acts as if it were a Helmholtz resonator coupled to the lowest vibratory mode of the soundboard. Neglecting the motion of the body, this motion may be treated as a simple harmonic oscillator with one degree of freedom, where the 'spring' is comprised of the air inside the enclosure, and the 'mass' is that of the air in the region of the soundhole. The frequency of an ideal Helmholtz resonator (a container with rigid walls, enclosing a relatively large volume of air, V, and a cylindrical throat[4] with length l, of small ($S \ll \pi l^2$) constant cross-sectional area S and assuming the wavelength is much longer than the largest single dimension of the container so that the pressure distribution is effectively uniform) may be expressed (Appendix A.1):

$$f_H = \frac{c}{2\pi}\sqrt{\frac{S}{Vl}} \tag{2.4.1}$$

---

[4]The term *throat* is used here to represent the length of an open pipe connected to the main body of the resonator. This is usually referred to as the 'neck' of the vessel, but is replaced here to reduce confusion with the neck of the actual guitar.
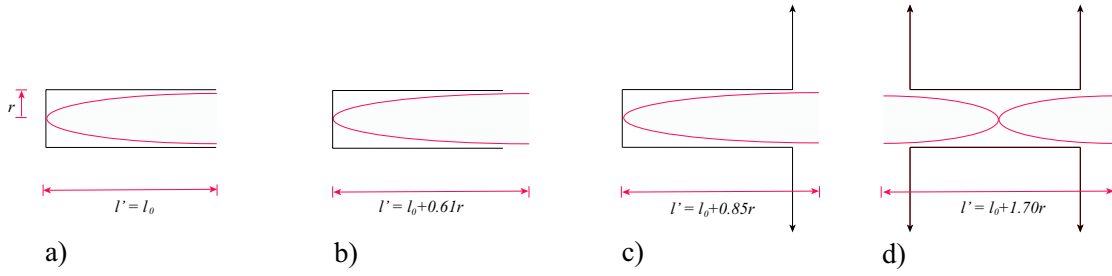
Figure 2.7: End corrections for the fundamental pressure standing waves in pipes with a) One end stopped and the other unbaffled, of negligible radius b) One end stopped and the other unbaffled, of radius r ([Strutt, 1869, Levine and Schwinger, 1948]) c) One end closed and the other with infinite baffle([Strutt, 1869, Fletcher and Rossing, 1998]) d) Pipe open and baffled at each end by an infinite plane.

where ρ is the density, and c the speed of sound, in air.

The geometry is complicated by the shape of the moving air mass, which may be quantified by an *effective length*, l_*. This results from the inertia of the air oscillating about the plane of the soundhole, which is dependent on the throat geometry (Figure 2.7). The application of the end correction to calculating the Helmholtz resonance is validated with a simple experiment in Appendix A.1. Of course there are limitations on the application of this simple treatment [Sacksteder, 1987].

For a lossless circular pipe of radius R, with an infinite baffle at one end the end correction is $l_* = 0.85R$ [Strutt, 1869, Fletcher and Rossing, 1998]. For a circular pipe with an infinite baffle at each end, the effective length is additive and therefore $l_* = 1.70R$. Although Figure 2.7 illustrates the velocity amplitude for a fundamental standing wave in a pipe, the end correction applies to the Helmholtz resonator for the same reasons, although the very long wavelength associated with the resonance of this example ($\simeq 3\ m$) means there is no node in the centre.

In the case of the guitar, the length of the circular 'pipe' (*viz.* the thickness of the soundboard, $\simeq 2.5$ mm) is small and the effective length of the 'pipe' at the soundhole is approximately equal to the end effects due to the large diameter and the conditions of both external surfaces of the soundboard around the soundhole. The effective length of the 'throat' of the body of a guitar considered as a Helmholtz resonator, with soundhole diameter $d = 2R$ and soundboard thickness at the soundhole, h, is given by:

$$l_* = h + 0.85d \qquad (2.4.2)$$

Typically, $h = 2.5$ mm and $d = 96.0$ mm, so $l_* = 2.5 + 0.85 \times 96.0 = 84.2$ mm.

Hence Equation A.1.12 may be simplified by substituting $l = l_*$:

$$f_0 = \frac{c}{2\pi}\sqrt{\frac{\pi d^2}{4V(h + 0.85d)}} = \frac{c}{4}\sqrt{\frac{d^2}{\pi V(h + 0.85d)}} \qquad (2.4.3)$$

and, because $h \ll l_*$,

$$f_0 \simeq \frac{c}{2\pi}\sqrt{\frac{\pi d}{3.4V}} \simeq 0.153 \cdot c\sqrt{\frac{d}{V}} \qquad (2.4.4)$$

Generally, for a modern guitar, the Helmholtz frequency tends to occur at about 100-150 Hz (Table 2.2) and this is recognised by luthiers as an important contribution to the radiated sound. The air resonance in this frequency region is not that of an ideal Helmholtz resonator because the walls of the enclosure are not rigid and are lossy. The requirement that the soundboard couple with the air cavity means that interaction between the vibrating plates and the air is not at all negligible so that

the frequency is altered by the coupling (§2.5). The term 'Helmholtz resonance' in the remainder of this thesis refers to the coupled motion between the ideal Helmholtz resonator and other components of the vibratory system. Also the plate is not an infinite plane and the spring constant of the Helmholtz resonator has some dependence on the height of the sides [Dickens, 1978] as well as the position of the soundhole [Meyer, 1974].

Consideration of this analogy between a Helmholtz resonator and the low frequency motion of the guitar provides an explanation why some makers sometimes introduce cardboard or brass tubes (a 'tornavoz' [Romanillos, 1987]) directly below (with the same diameter as) the soundhole, to lower the dominant radiating resonances of the instrument. This would increase the effective throat length of the Helmholtz resonator and thereby lower the frequency of the Helmholtz resonance and other air-coupled modes. This technique has also been useful in determining the extent of low frequency air/soundboard coupling in the instrument [Christensen and Vistisen, 1980]. Because of the typical frequency range of this resonance, if the soundhole is covered or restricted, the loudness of notes about A2 (110 Hz) is noticeably reduced.

2.5 Soundboard-air cavity coupling: the two-mass oscillator model

At low frequencies, the wavelength of sound in air is much longer than the characteristic dimensions of the guitar and the sound radiation may be modelled as

a simple monopole or piston source [Christensen and Vistisen, 1980, Christensen, 1984, Wright, 1996]. The simplest model to describe the mechanical nature of the guitar involves the two important low frequency vibratory components of the guitar system—the soundboard and the air cavity. The *two-mass oscillator model* here treats the soundboard of the guitar as a simple harmonic oscillator, coupled with the air enclosed by the body and the soundhole acting as another oscillator [Christensen and Vistisen, 1980, Caldersmith, 1978, Firth, 1977]. The relationship between the coupled and uncoupled frequencies of the resonators are (see Appendix A.2):

$$f_p^2 + f_H^2 = f_+^2 + f_-^2 \tag{2.5.1}$$

Where f_+ and f_- are the higher and lower coupled frequencies, f_p is the effective frequency of the soundboard (including air loading) and f_H is the frequency of the (uncoupled) effective Helmholtz resonator.

Assuming this simple model, mobility and sound pressure functions (measured at the soundboard) are obtained, with features similar to that in Figure 2.8 [Christensen and Vistisen, 1980] . Two local maxima ('peaks') are separated by a local minimum ('trough') at an intermediate frequency. The electromechanical (Force-Voltage) circuit diagram is given in Figure 2.9 [Fletcher and Rossing, 1998].

This model is limited to frequencies in the region of the coupled oscillators and assumes that the bandwidth of both elements is small enough so that no significant overlap occurs with other elements in the system. This is a valid assumption for the low frequency behaviour of the instrument and explains the three lowest frequency
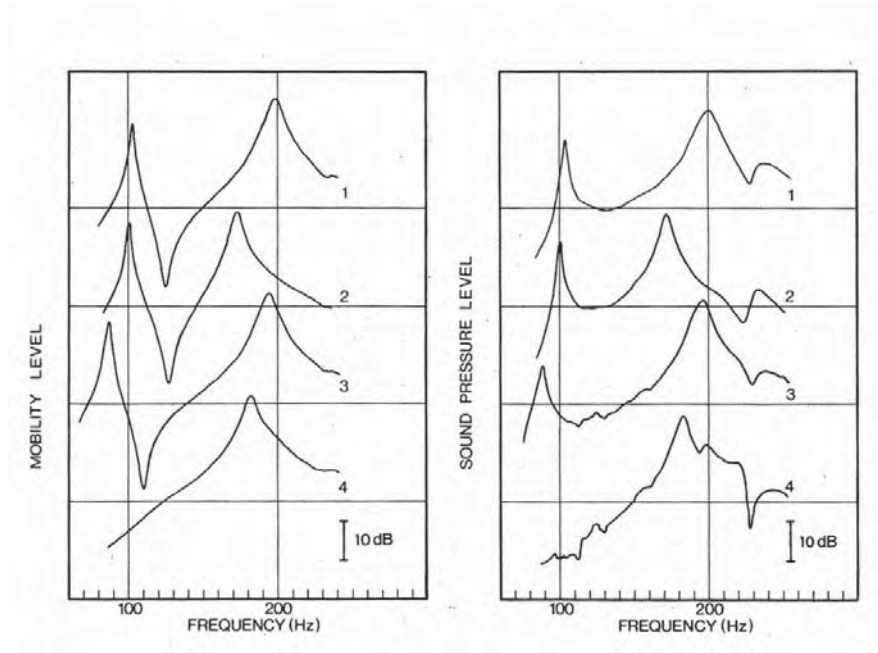
Figure 2.8: Mobility and pressure spectra investigating the extent of low frequency coupling between the soundboard and the air cavity. Curves (1) refer to the unperturbed guitar system. Curves (2) Represent mass loading effects (39.3 g added to soundboard). Curves (3) show the effects of increasing the effective length of the soundhole by the introduction of a tube with the same diameter of the soundhole. Curves (4) show effects of restricting air-flow through the soundhole. From [Christensen and Vistisen, 1980].

minima in the acoustic response of the instrument. Although the soundboard and internal air volume comprise a continuous coupled system, higher frequency behaviour could be modified to account for higher frequency soundboard vibrational modes by adding additional circuit elements to those in Figure 2.9 [Christensen, 1984].

At f_-, the air in the soundhole is almost 180° out of phase with the bridge of the guitar and is in phase at f_+, as shown in Figure 2.10.
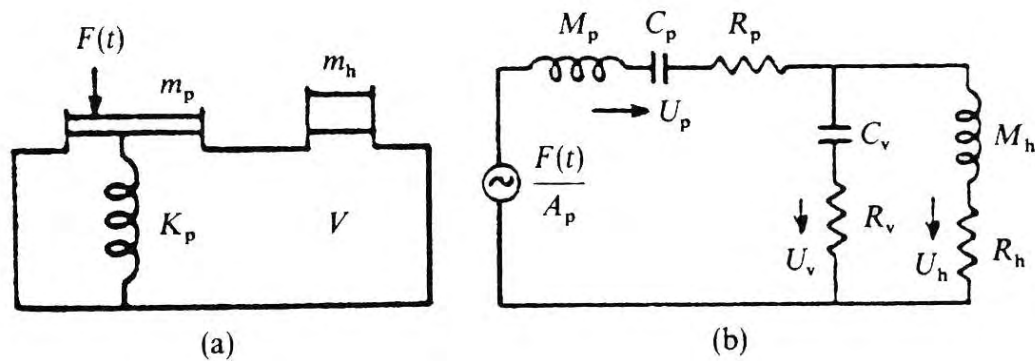
Figure 2.9: a) Schematic of the mass and stiffness interaction of a simple model guitar interaction between the soundboard, the air cavity and the air in the soundhole area treated as two coupled simple harmonic oscillators, and b) the electromechanical circuit analogue for the two-mass model of the guitar. The effective stiffness of the internal air cavity is not depicted in a) (From [Fletcher and Rossing, 1998].)
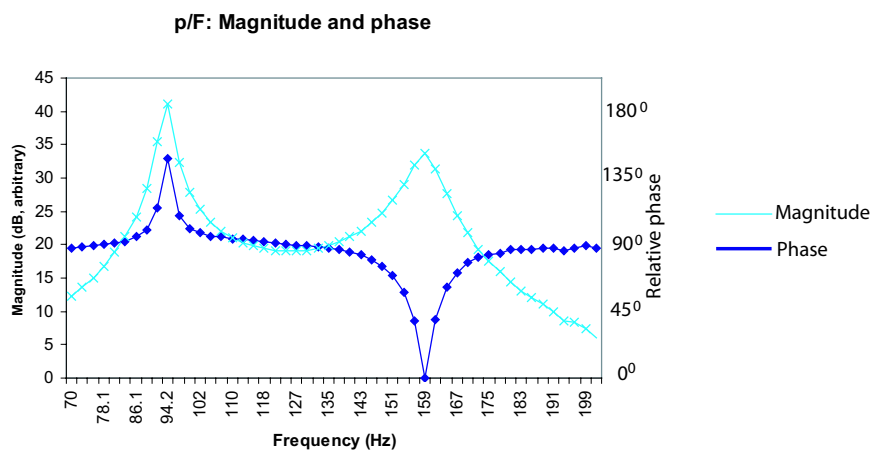
Figure 2.10: The low frequency phase relationship of pressure measured at the sound-hole in response to a force on the bridge of a guitar. For the low frequency mode, of frequency f_-, the motion of the air in the soundhole is almost 150° out of phase with the motion of the bridge. The next mode, of frequency f_+, is in phase with the motion of the bridge. (Measurement from Engelmann spruce guitar, 2 years after polishing.)

Free plate, membrane and coupling frequencies

These equations enable another means of characterising stringed instruments. The coupling between the soundboard and the air is of great importance. If the frequencies of the lowest three turning points in the mobility spectrum are measured, parameters derived using these equations might be applied in manufacturing instruments with greater consistency.

Rearranging Equation 2.5.1, the fundamental frequency of the soundboard loaded by the air in the cavity may be expressed as:

$$f_p = \sqrt{f_+^2 + f_-^2 - f_H^2} \tag{2.5.2}$$

From Equation A.2.11 the coupling frequency is:

$$f_{pH} = \sqrt[4]{f_H^2(f_+^2 + f_-^2) - f_+^2 f_-^2 - f_H^2} \tag{2.5.3}$$

By using this and Equation A.2.4 the frequency of the uncoupled soundboard is:

$$f_{p,0} = \frac{f_+ f_-}{f_H} \tag{2.5.4}$$

These expressions are simple combinations of the measurable low frequency turning points of the mobility spectrum. A basic prescription for measuring or characterising stringed instruments might then be:

1. Measure frequencies f_+, f_- and f_H from the acoustic frequency response spectrum

2. Obtain the air-loaded plate frequency $f_p^2 = f_+^2 + f_-^2 - f_H^2$

3. Calculate the free-plate frequency $f_{p,0} = \frac{f_+ f_-}{f_H}$

4. Calculate the coupling frequency $f_{pH} = \sqrt[4]{f_H^2(f_+^2 + f_-^2) - f_+^2 f_-^2 - f_H^4}$

It is also useful to express these quantities in terms of a normalised frequency, by division by f_H. Expressing such normalised frequencies using a $\mathcal{F}$, ($f_i :\rightarrow \frac{f_i}{f_H} \equiv \mathcal{F}_i$) the frequency relations can then be simplified to:

$$
\begin{aligned}
\mathcal{F}_p^2 &= \mathcal{F}_+^2 + \mathcal{F}_-^2 - 1 \\
\mathcal{F}_{p,0}^2 &= \mathcal{F}_+ \mathcal{F}_- \\
\mathcal{F}_{pH}^2 &= \sqrt{\mathcal{F}_p^2 - \mathcal{F}_{p,0}^2} = \sqrt{\mathcal{F}_+^2 + \mathcal{F}_-^2 - \mathcal{F}_+ \mathcal{F}_- - 1} \\
\mathcal{F}_a &= \mathcal{F}_{pH}^2 = \sqrt{\mathcal{F}_+^2 + \mathcal{F}_-^2 - \mathcal{F}_+ \mathcal{F}_- - 1}
\end{aligned}
\tag{2.5.5}
$$

Using data from several guitars with various configurations (such as altered bracing) from [Meyer, 1974], Ove Christensen and Bo Vistisen showed that the low frequency soundboard/air coupling parameter, $\mathcal{F}_{pH}$, for classical guitars measured by them and [Meyer, 1974], ranges from 0.7 to 0.9. Because the soundpost transmits energy from the soundboard to the back plate, we should not expect high values for low frequency soundboard/air coupling in violin family instruments, with a slight correlation between soundboard frequency and coupling [Christensen and Vistisen, 1980]. From a violin in [Firth, 1976/77], this was calculated to be 0.63 [Christensen and Vistisen, 1980]. A meta-study of these results and others from measurements made by previous authors [Hutchins, 1989, Christensen and Vistisen, 1980, Firth,

Guitar				
Study (instrument)	Resonance frequency (Hz)			Coupling parameter
	f_-	f_H	f_+	F_{pH}
[Christensen and Vistisen, 1980]	100	123	214	0.91
[Firth, 1977] (Levin LG-17)	90	112	179	0.86
[Erndl, 1999]	108	150	205	0.80
(Gilet OO (1998))	108	140	180	0.72
(Gilet MJ (1998))	80	115	160	0.83
[Le Pichon et al., 1998]	121	152	216	0.78
(ES, finished)	91.5	126.5	158.8	0.72
(Aria 'WO-RN')	94.2	126.5	156.1	0.69
(Gilet OO)	115.7	172.3	274.5	0.96

Table 2.2: Meta-study of low frequency coupling in guitars.

Violin					
Study	Instrument	f_- (Hz)	f_H (Hz)	f_+ (Hz)	F_{pH}
[Hutchins, 1989]	V1	278	375	474	0.72
	V2	272	368	485	0.76
	V3	267	354	447	0.71
	V4	276	389	476	0.70
	V5	272	334	461	0.74
[Firth, 1976/77]		278	295	457	0.63

Table 2.3: Meta-study of low frequency coupling in violins.

1977, Erndl, 1999, Le Pichon et al., 1998] (Tables 2.2 and 2.3) show F_{pH} to range from 0.69 to 0.96 for the guitar and 0.63 to 0.76 for the violin.

Effective masses and stiffness of plates at resonance

Because of the complicated nature of the structures being studied, many of the parameters examined are effective values. The value of an effective variable may depend on how the measurement or calculation was performed. The following calculations
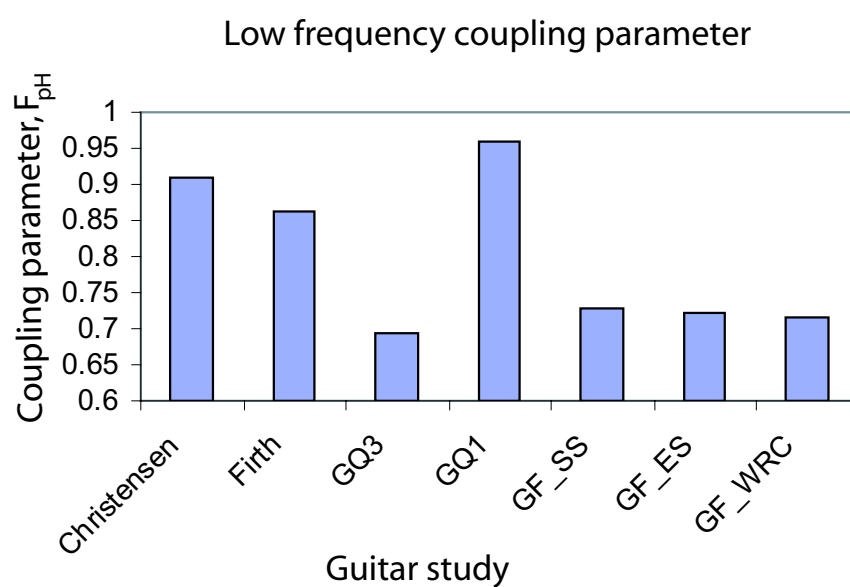
Figure 2.11: 'Christensen' refers to the guitar studied in [Christensen and Vistisen, 1980], 'Firth' refers to the Levin guitar LG-17 in [Firth, 1977]. The remainder are the guitars studied in this thesis.

are valid in the vicinity of a resonance mode and we might expect different values obtained from different resonances. The particular resonance is labelled with a subscript i but we shall mostly be concerned with the lowest, $i = 1$.

At low frequencies, approximating the free soundboard as a simple harmonic oscillator, and, knowing the mass of the plate and the resonance frequency of the ith normal mode, an effective stiffness may be defined:

$$f_i = \frac{1}{2\pi} \sqrt{\frac{K_{p*}}{m_p}} \tag{2.5.6}$$

Differentiating this with respect to the mass m_p, the effective mass, m_{p*} is [Schelleng, 1963]:

$$m_{p*} = -\frac{f_i}{2} \frac{1}{\frac{\partial f_i}{\partial m_p}} \tag{2.5.7}$$

This may be re-arranged to obtain the effective stiffness, K_{p*}:

$$K_{p*} = 4\pi^2 f_i^2 m_{p*} = -2\pi^2 f_i^3 \frac{1}{\frac{\partial f_i}{\partial m_p}} \tag{2.5.8}$$

The term $\frac{\partial f_i}{\partial m_p}$ may be measured by observing the frequency perturbation of the ith resonance frequency by adding a range of masses at the excitation point. If the amount of mass added is small, the effect is approximately linear. This is shown, for example, on the violin (Figure 2.12).

However these measurements are from the coupled resonance at f_+ (an example of similar measurements on the guitar are shown in Figure 2.13). Because f_+ is associated with coupled modes, using measurements of $\frac{\partial f_i}{\partial m_p}$ for this resonance alone leads to an overestimation of the effective stiffness of the guitar soundboard [Christensen

Mass Perturbation of f+ (violin)
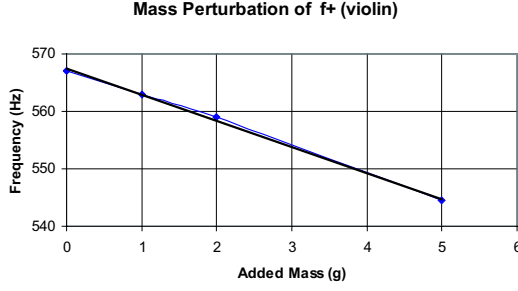
Figure 2.12: Mass perturbation of the f_+ resonance of a violin. ($\frac{\partial f_+}{\partial m} = $ const. $= -4500$ Hz·kg^{-1}, The value of the least-squares fit parameter, ($R^2 = 0.9977$, for 4 data points) indicates the change in frequency is linear for this mass range. Measurements by John McLennan in [McLennan, 1993].)

and Vistisen, 1980]. Similarly, measurement of the effect of mass-loading on the f_- frequency leads to an underestimation of the stiffness (Figure 2.14).

Mass Perturbation of f+ (guitar)

Mass Perturbation of f- (guitar)
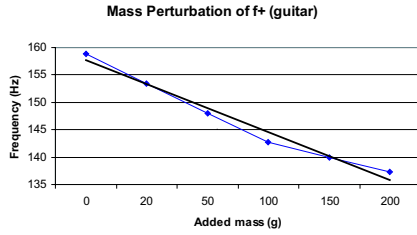
Figure 2.13: Mass perturbation of the f_+ resonance of a guitar. Here, $\frac{\partial f_+}{\partial m} \simeq -4400$ Hz $\cdot$ kg^{-1} ($R^2 = 0.9771$, for 6 data, measurements made on ES guitar).
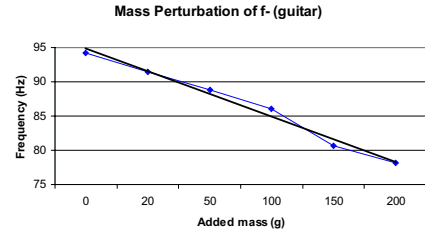
Figure 2.14: Mass perturbation of the f_- resonance of a guitar. Here, $\frac{\partial f_-}{\partial m} \simeq -3300$ Hz $\cdot$ kg^{-1} ($R^2 = 0.9845$, for 6 data, measurements made on ES guitar).

Further, because the resonances f_- and f_+ are coupled, especially for large loads, neither resonance is well approximated by a simple harmonic oscillator, *i.e.* with resonance frequency proportional to $\frac{1}{\sqrt{m_p}}$ (Equation 2.5.6).

Nevertheless the free-plate frequencies $f_{p,0}$, calculated from Equation 2.5.4, agree

well with Equation 2.5.6 (Figure 2.15). The solid lines in Figure 2.15 are calculations of the frequency dependence on mass loading for a simple harmonic oscillator with constant stiffness which is determined from the measurements with mass loads of 50 g. This gives a *post hoc* justification for the approximation of a simple oscillator, Equation 2.5.6. Results of calculations of the effective stiffness values of soundboards of the guitars studied in this thesis, and for the completed instruments, are presented in §7.7.

Graham Caldersmith derived from first principles an approximation to calculate the effective stiffness of a guitar soundboard by knowing the distribution and material properties of the bracing and the dimensions and approximate mean displacement of the soundboard at resonance [Caldersmith, 1978]. This is in good agreement with experiment and the analysis shows the stiffness contribution from the bracing system (in a classical guitar) to be of the same order of magnitude as that of the soundboard itself.

2.6 Three-mass oscillator model

The two mass oscillator model may be extended to incorporate the motion of another important component, the back-plate, as a third harmonic oscillator [Meyer, 1974]. There are two possibilities [Fletcher and Rossing, 1998]:

(i) $f_p > f_b$, *ie* the fundamental resonance frequency of the soundboard is *higher* than that of the back-plate. This will *increase* the value of f_+; or
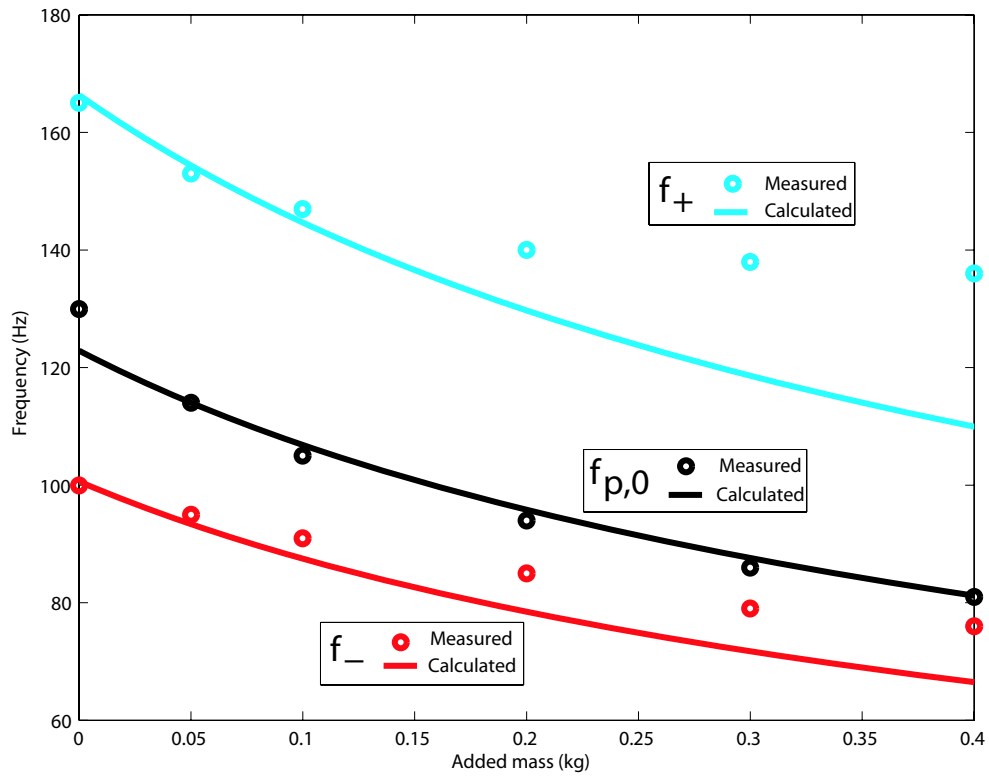
Figure 2.15: Mass perturbation of the $f_{p,0}$ compared to the f_+ and f_- resonances of a guitar. Note that the calculated free-plate frequencies, $f_{p,0}$, are better approximated by a simple harmonic oscillator model than those of the coupled resonances f_+ or f_- alone. Measurements made on ES guitar.

(ii) $f_p < f_b$, the fundamental resonance frequency of the soundboard is *lower* than that of the back-plate. This will *decrease* the value of f_+.

Most guitars have a lower soundboard fundamental frequency than that of the back-plate, $f_p < f_b$, hence the effect of back-plate coupling is generally a lowering of the frequency of the two peaks f_- and f_+ in the mobility or dynamic mass spectra. If the coupling is strong enough, there will also be a bifurcation of the f_+ peak. This is not usually the case with the guitar but may occur with the violin because the latter has a soundpost connecting the two plates (Figure 2.16).

2.7 The importance of bracing

The primary function of the bracing used on the plates of the guitar is to maintain the structural integrity of the instrument. However the choice of soundboard bracing also has a large effect on the sound produced, and much of the recent innovation in guitar design has been to do with this [French and Hosler, 2001]. The bracing of the modern classical guitar is largely due to the famous luthier, Antonio de Torres Jurado (1817-1892) who pioneered the symmetric bracing system still commonly used on modern classical guitars [Romanillos, 1987]. The C. F. Martin Guitar Company introduced an asymmetric 'X' bracing system in the 1850's, which is the most widely used bracing system in modern steel-string guitars and is the system used on the guitars studied in this thesis [Longworth, 1975].

p/F: Magnitude and phase
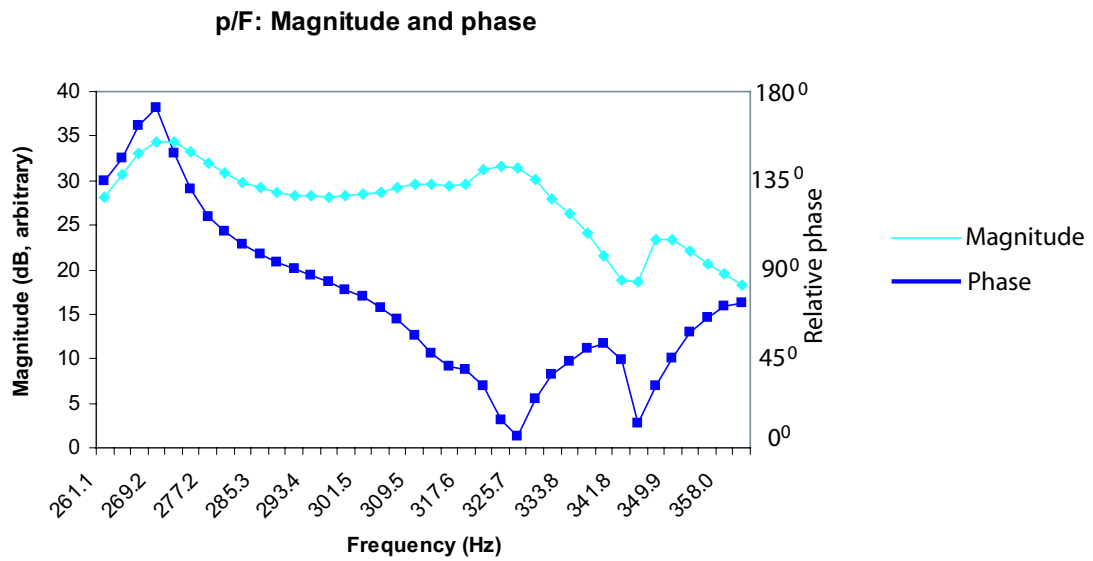
Figure 2.16: The low frequency phase relationship between pressure at one of the 'f'-holes and force on the bridge of a violin. Measured from Powerhouse Twin Violin 1 [Inta et al., 2005]. The two higher peaks close to being in phase are most probably generated by coupling with the back-plate.
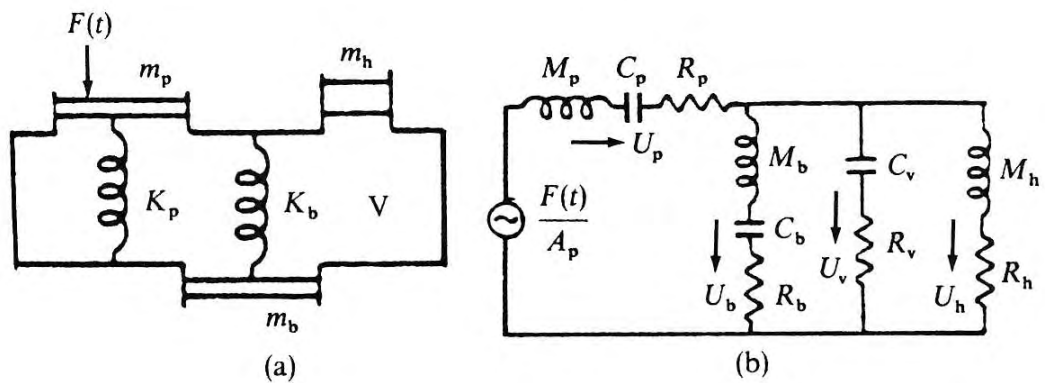
Figure 2.17: Electromechanical diagram of the mechanical elements comprising the three-mass oscillator model, as applied to the guitar; the back-plate is introduced in addition to the two mass model in §2.5. From [Fletcher and Rossing, 1998].

In an investigation on the effect of a number of soundboard bracing configurations on the response of classical guitars, Jürgen Meyer found that the traditional Torres 'fan-bracing', with between five and seven braces were optimal [Meyer, 1983a]. Bernard Richardson found that braces running across the grain of the soundboard had more influence on the soundboard modes than those aligned with the grain [Richardson, 1982, 1983] but were not as influential on the mechanics of the soundboard as its thickness distribution [Richardson and Roberts, 1985]. M. J. Elejabarrieta *et al.* looked at the effects of bracing on a classical guitar during construction, showing the addition of braces around the soundhole reduced a number of modes and greatly altered the admittance response of the free soundboard [Elejabarrieta et al., 2000, 2001] . Thomas Rossing and Gila Eban examined the low frequency modes of a soundboard with a novel bracing system, which showed little difference to the more conventional classical guitar bracing system [Rossing and Eban, 1999].

Cross-bracing alters the coupling between the air cavity and the soundboard modes: the phase change at the lowest resonance (A0) between the air cavity and the soundboard is lower for cross-braced instruments than that for fan-bracing, where the phase difference is very close to 180° [Ross and Rossing, 1979, Firth, 1977]. For example, in §2.5 I measured the relative phase change as slightly less than 150° for the Engelmann spruce guitar (Figure 2.10). The dipolar soundboard modes are often not strong radiators for guitars with symmetric bracing [Christensen, 1984]. The symmetry of these dipoles may be broken by the use of asymmetric bracing (such as cross-bracing) and may improve radiation from dipolar as well as higher frequency modes. Technical details of the cross-bracing system studied in this thesis are given in §3.4.

Vibration of a cantilever beam

The bracing system of the plates of the guitar is a system of slender beams. Slender beams are simple enough systems to measure the Young's modulus of the beam material using resonance methods [Schlägel, 1957, Dunlop and Shaw, 1991, Harjono, 1998]. Hence the vibratory behaviour of beams is a useful means of characterising this important material property of the components used in guitars as well as in determining the vibratory behaviour of the actual bracing components.

For a simple, slender beam with Young's modulus E, moment of inertia I and mass m [McLachlan, 1951, Sokolnikoff, 1946]:

$$\frac{\delta^2}{\delta x^2}(EI \cdot \frac{\delta^2 \xi}{\delta x^2}) = -m\frac{\delta^2 \xi}{\delta t^2} \tag{2.7.1}$$

where δ denotes a small change in a variable, x is the distance along the axis from one end of the beam and ξ is the perpendicular displacement, at time t.

The general solution for the displacement of a uniform beam is [Boas, 1983]:

$$\xi(x) = A\cosh(kx) + B\sinh(kx) + C\cos(kx) + D\sin(kx) \tag{2.7.2}$$

The boundary conditions for a homogeneous cantilever beam of length L, with perpendicular displacement ξ as a function of position on the beam axis, x, are:

$$\xi(0) = 0 \qquad \frac{d\xi(0)}{dx} = 0 \qquad \frac{d^2\xi(L)}{dx^2} = 0 \qquad \frac{d^3\xi(L)}{dx^3} = 0 \tag{2.7.3}$$

Indicating there is no vertical displacement or slope at the fixed point $(x = 0)$, and zero bending moment and shearing force at the beam's extremity $(x = L)$.

The coefficients $s_i = \{1.194, 2.988, 5.000, 7.000, ...\}_{i=1}^{\infty}$ are dependent on the boundary conditions in Equation 2.7.3, and are computed by solving relation 2.7.4.

$$\cos(k_i L) \cdot \cosh(k_i L) = -1 \tag{2.7.4}$$

Where $k_i \equiv \sqrt[4]{\frac{\mathbf{m}\omega_i^2}{E_Y I}}$ is the wavenumber for the ith resonance mode.

For an isotropic, homogeneous beam, with constant cross-section and length L much longer than any other dimension, we can find the frequency of vibration of the ith resonance mode at low amplitudes:

$$f_i = \frac{\pi c \kappa}{8L^2} \cdot s_i^2 \tag{2.7.5}$$

Where κ is the radius of gyration of the beam in the plane perpendicular to the longitudinal beam axis and $\pi = 3.14$ and c is the speed of sound in the material.

The apparatus used to measure the frequency of the wooden beams is a clamp system similar to [Harjono, 1998] (§5.2), and the measured response is that of a two mass system (see Appendix A.3).

2.8 General behaviour in various frequency regimes

The guitar responds and radiates differently at different excitation frequencies. Although the frequency range of the fundamental of the notes able to be played on a steel-stringed acoustic guitar tuned to concert pitch and standard tuning is

$82 \rightarrow 1050$ Hz (Table 2.1). Although excitation outside this frequency range is induced through higher harmonics of the strings or beating between strings, Ove Christensen showed that most of the radiated acoustic energy in classical guitar music occurs between 200 Hz and 800 Hz in the time-averaged output spectrum [Christensen, 1983]. However, considering that the human ear is most sensitive in the range of $1000 \rightarrow 5000$ Hz, the importance of higher modes should not be neglected. For example, it is likely that the sensation of 'brightness' is determined largely in the frequency range $1 - 3$kHz [Jansson, 2002]. The frequency ranges given below are approximate values and are dependent on the particular instrument being studied.

An illustration of the progression and shape of the low frequency soundboard modes is given in Figure 2.18. At very low frequencies ($\approx 0 \rightarrow 90$ Hz) vibratory modes involve the bending of the entire guitar, including the neck. At low frequencies ($\approx 90 \rightarrow 250$ Hz) the bulk motion of the body is important, and this is where most interaction with the soundboard and the Helmholtz motion of the internal air cavity (§2.4). Moderate frequencies ($\approx 200 \rightarrow 600$ Hz) involve large movement of the soundboard and, consequently, this is where most of the studies of the finished guitar using the technique of Chladni figures (§2.9) are performed. Some resonances in this frequency range are due to coupling between fundamental plate resonances and higher internal air cavity modes [Jansson, 1977]. Higher frequencies ($\approx 600 \rightarrow 1200$ Hz) correspond to fairly localised motion of the soundboard. High frequencies ($\approx 1200 \rightarrow 10000$ Hz) involve rather more complicated interactive motions involving the soundboard, bridge and other elements. A summary of this is
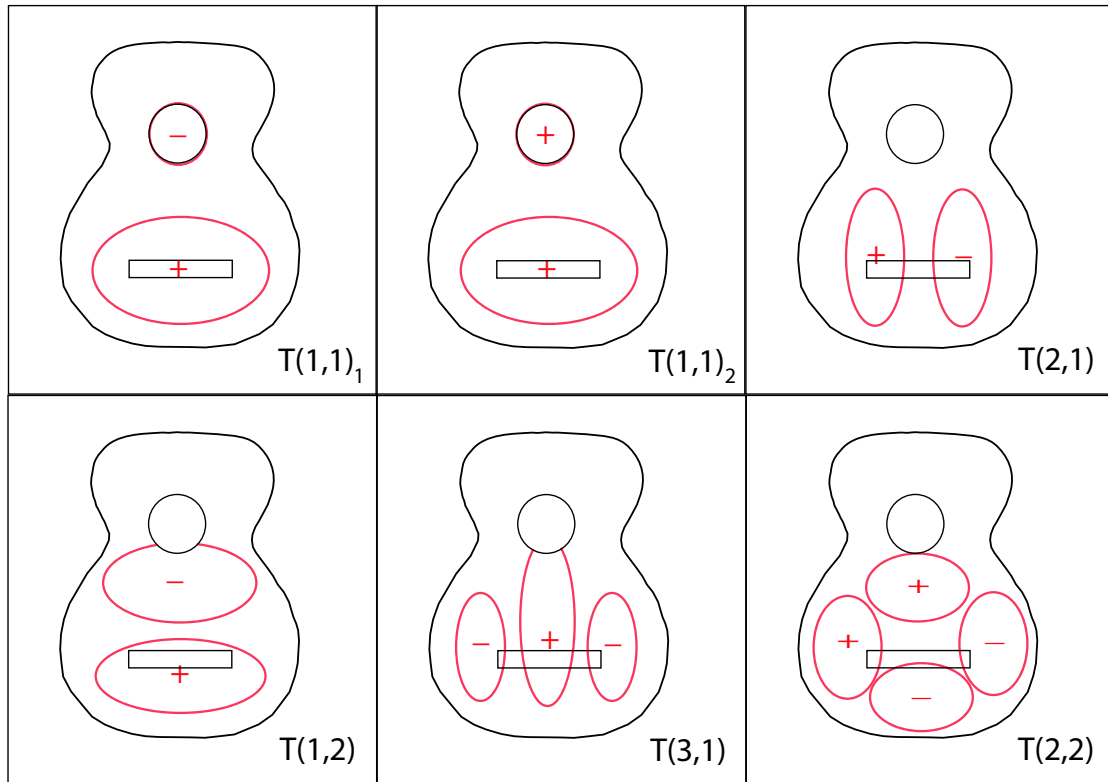
Figure 2.18: The first six modes of a guitar soundboard. The relative phase of the air in the soundhole is given in the $T(1,1)_1$ and $T(1,1)_2$ modes to distinguish the two modes. The $T(2,2)$ mode is often referred to as the $T(4,1)$ mode in other works.

Description	Frequency range (Hz)	Main vibratory components
Very low	$0 \rightarrow 70$	Entire instrument, including neck
Low	$70 \rightarrow 150$	Body/air
Moderate	$150 \rightarrow 600$	Large soundboard/air
High	$600 \rightarrow 1200$	Small soundboard
Very high	$1200 \rightarrow 10000$	Bridge/soundboard

Table 2.4: Important guitar components as a function of frequency. 'Large soundboard' refers to bulk motion of the soundboard with a simple nodal topology (able to be unambiguously characterised with a pair of integers). 'Small soundboard' denotes relatively local movements of portions of the soundboard and more complicated topology of the nodal lines.

given in Table 2.4.

2.9   Resonant modes of the guitar

The guitar may be viewed as a system of coupled oscillators, and the efficient transfer of energy from the strings to sound in the air is dependent on the exploitation of resonances. To characterise the vibratory behaviour of the guitar, it is necessary to study the modes of individual components and how the components relate to each other.

Assuming the important components are well coupled mechanically (such as the soundboard/sides, bridge/soundboard bonds and the neck/body joint), and that and the strings are coupled optimally to the body (§2.3 and §3.4), the most important vibratory element of the guitar system is the soundboard [Caldersmith, 1978]. Some work has gone into finding a relationship between the frequency response of the 'free'

soundboard (*i.e.* not bound to the back and sides) and that of the plate attached to the back and sides, so far with only limited success [Schleske, 2000]. One reason for this is that the boundary conditions imposed on the soundboard by the attachment to the back and sides is undetermined. This 'hinge joint' between the soundboard and the sides is usually reinforced with strips of wood (*linings*) with a triangular cross-section (§3.4). The linings strengthen the joint by increasing the area of the bonding surfaces. There have been attempts to determine the effect of this joint, such as by using a reversible clamping system [Meyer, 1983a] but it is difficult to determine how closely this resembles the completely glued joint. There are also complications introduced by interactions with the enclosed air cavity [Caldersmith, 1985, Christensen and Vistisen, 1980, Fletcher and Rossing, 1998] and other components.

Vibratory modes of rectangular and circular plates

The most important components contributing to the sound radiated from the guitar (*viz.* the soundboard and back-plates and the sides) are in the form of plates.

Consider the simplest case *i.e.* that of a membrane (a perfectly flexible, infinitely thin, uniform solid under a constant tension great enough to not be affected by vibrations of small amplitude). The motion is described by [Strutt, 1869]:

$$\ddot{w} - c^2 \nabla^2 w = 0 \qquad (2.9.1)$$

where w is the transverse displacement of the membrane.

This is similar to the ideal string except that the transverse amplitude is a function of two spatial dimensions. In the case of a rectangular membrane, it is convenient

to express in terms of rectangular Cartesian co-ordinates with x and y axes parallel to the edges of the rectangle: $w :\rightarrow w(x, y, t)$. To maintain the tension, the edge conditions of a membrane are clamped, *i.e.* $w(0, y) = w(a, y) = w(x, 0) = w(y, b) = 0$, a and b being the length of the rectangle in the x and y directions, with one corner as the origin, (0,0). So, analogously to the ideal string, a solution to Equation 2.9.1 is:

$$w = \sin\left(\frac{m\pi x}{a}\right) \sin\left(\frac{n\pi y}{b}\right) \cos\left(\omega t\right) \tag{2.9.2}$$

Where m and n are integers and $\omega^2 = c^2 \pi^2 \left(\frac{m^2}{a^2} + \frac{n^2}{b^2}\right)$. The nodal system ($w(x, y) = 0$) is therefore in the form of straight lines, parallel to the edges, with the equations $y = \frac{b}{n}, \frac{2b}{n}, ..., \frac{(n-1)b}{n}$ and $x = \frac{a}{m}, \frac{2a}{m}, ..., \frac{(m-1)a}{m}$ respectively.

For a circular membrane of radius a, it is convenient to solve Equation 2.9.1 using polar coordinates (with origin (0,0) at the centre of the membrane):

$$w = J_n(kr) \cos n\theta \cos \omega t \tag{2.9.3}$$

The edge condition is $J_n(ka) = 0$, where $J_n(x)$ is the nth order Bessel function. So the nodal distribution can be represented as:

$$J_n(kr) \cos n\theta = 0 \tag{2.9.4}$$

So there is a series of concentric circles, described by $J_n(kr) = 0$, and diameters, distributed with the angles $\theta = \frac{(2m+1)\pi}{2n}$.

A plate is more complicated because it has a finite compliance; the restoring force of a plate with no applied stresses is internal. This introduces a term dependent on

the bending stiffness into the differential equation of motion.

Assuming a thin isotropic plate of thickness h, Poisson's ratio ν, mass density ρ and Young's modulus $E_L = E_T \equiv E$, with no externally applied force, and small amplitudes of vibration, the equation of motion becomes [Strutt, 1869]:

$$\ddot{w} + c^4 \nabla^4 w = 0 \qquad (2.9.5)$$

Where $c^4 = \frac{Eh^2}{12\rho(1-\nu^2)}$. If $w \propto \cos \omega t$, then, by taking $k^2 = \frac{\omega}{c^2}$, Equation 2.9.5 becomes:

$$(\nabla^4 - k^4)w = 0 \qquad (2.9.6)$$

The solution of Equation 2.9.6 for a rectangular plate with clamped edges may be expressed as [Skudrzyk, 1968]:

$$w = A_{m,n} \cdot \sin(\frac{m\pi x}{a}) \cdot \sin(\frac{n\pi y}{b}) \cdot \cos(\omega_{mn}t) \qquad (2.9.7)$$

where $A_{m,n}$ is the amplitude and

$$\omega_{mn} = \omega_{np}m^2 + \omega_{bp}n^2 = \frac{c^2\pi^2}{a^2} \cdot m^2 + \frac{c^2\pi^2}{b^2} \cdot n^2 \qquad (2.9.8)$$

and m and n are integers. For example, the (1,2) mode (*i.e.* $m = 1$, $n = 2$):

$$w = A_{1,2} \cdot \sin(\frac{\pi x}{a}) \cdot \sin(\frac{2\pi y}{b}) \cdot \cos((\frac{c^2\pi^2}{a^2} + \frac{4c^2\pi^2}{b^2})t) \qquad (2.9.9)$$

Similarly to the membrane, the solution for the case of the circular plate is found by solving Equation 2.9.6 in polar coordinates. For a free edge, the solution becomes:

$$w_n = P \cos n\theta - \alpha(J_n(kr) + \lambda J_n(\hat{\jmath}kr)) \cos \omega t \qquad (2.9.10)$$

Also similarly to the membrane, the nodal system has n diameters symmetrically distributed as $\cos n\theta - \alpha$ and concentric circles in the form of $J_n(kr) + \lambda J_n(\hat{\jmath}kr) = 0$, where λ and k are to be determined by the boundary conditions. For example, for free edges and $n = 0$:

$$2(1 - \nu) + \hat{\jmath}ka\frac{J_0(\hat{\jmath}ka)}{J_0'(\hat{\jmath}ka)} + ka\frac{J_0(ka)}{J_0'(ka)} = 0 \qquad (2.9.11)$$

where $J_n'(x) = \frac{dJ_n(x)}{dx}$.

Because of its basic overall geometry, at lower frequencies the guitar soundboard acts similarly to a simple rectangular plate if the orthotropic nature of the plate is taken into account (Table 6.2). The similarity diverges at higher frequencies, because the overall shape is not exactly rectangular and the bracing system locally alters the properties of the plate.

Vibratory modes of the guitar soundboard

The most important sound producing component of the guitar is the soundboard [Caldersmith, 1978]. At low frequencies, the soundboard of the guitar has vibratory modes qualitatively similar to that of isotropic rectangular or circular plates, although the braces influence the nodal distributions. The simple vibratory modes in Table 2.6 are deemed important by many luthiers and occur in the frequency range $80 \rightarrow 600$ Hz. At higher frequencies ($\gtrsim 600$ Hz), multipole (*i.e.* spherical radiation modes greater than a dipole) vibrational modes occur, and at frequencies $\gtrsim 1000$ Hz

Mode description	Label
Air	Ai
Soundboard	$T(m,n)_i$
Body	Bi

Table 2.5: Nomenclature of specific modes used on stringed instruments. Note that the mode labels for the guitar soundboard, once attached to the back and sides denote the number of *antinodal regions*, as in [Wright, 1996], in contrast to that used to denote the number of nodes on a free or simply supported simple plate.

there is significant overlap of various spherical radiation modes, the so-called 'resonance continuum' [Caldersmith, 1986, Christensen, 1984]. The pressure amplitude of the radiated sound from the first soundboard mode of the guitar is almost an order of magnitude larger than any higher normal modes [Christensen, 1984] and most of the energy radiated from the instrument is at frequencies below 1 kHz [Christensen, 1983].

There is some confusion regarding the labels denoting resonance modes of plates of stringed musical instruments: the (m,n) terminology used in §2.9 describes the normal modes of simple rectangular (or circular) plates, where n is an integer describing the number of nodal lines in the x (angular) direction, and m describes the number of nodal lines (concentric rings) in the y (radial) direction.

To differentiate among air, soundboard, back-plate and other vibratory modes, many authors use the convention of a letter and a set of integers, as in Table 2.5 ([Alonso Moral and Jansson, 1982, Jansson, 1971, Hutchins, 1989] and developed for the guitar in [Wright, 1996]). Note that here the numbers refer to the number of *antinodal* regions, in contrast to the labelling system used in Table 2.6.

Mode Label	Description used by luthiers
$T(1,1)_1$	Monopole
$T(1,1)_2$	Monopole
$T(1,2)$	Cross dipole
$T(2,1)$	Long dipole
$T(1,3)$	Tripole

Table 2.6: Nomenclature for normal vibratory modes on a plate (usually associated with the back and sides of a stringed instrument).

Table 2.6 gives alternative descriptive terms for various resonances, in terms of their radiative (multipole) nature [Caldersmith, 1985]. Luthiers commonly describe soundboard modes in terms of the multipole.

This convention is convenient for low frequency modes, but it is impossible to discriminate among higher frequency modes using a single pair of integers because of the more complicated geometry and mechanical anisotropy (*e.g.* Figure 2.19).

Some modes occur at multiple frequencies. The $T(1,1)$ mode is measured at two different frequencies due to coupling with air motion at the soundhole (§2.5) and may be measured at a third frequency if the back plate is made to couple with other air modes [Caldersmith, 1985]. This appears as multiple peaks in the corresponding pressure response spectrum, but appears topologically as the same $T(1,1)$ standing wave configuration.

The $T(1,1)_i$ and $T(1,3)$ modes involve a large net movement of air and, consequently, dominate sound production at lower frequencies. The design of the guitar is such that as the excitation frequency is increased above the $T(1,1)_i$ modes there is a constructive contribution to sound production from the $T(1,3)$ mode [Caldersmith, 1985].

The vibratory modes of an isotropic plate with simple geometry (§2.9) are a series of normal modes (*i.e.* $\int \int (w_a w_b) dx dy = 0$). Most of the vibratory modes of the soundboard attached to the back and sides involve coupling with other components of the instrument, as well as the air. The experiments in this thesis do not attempt to decouple these elements on the measured instruments and therefore normality of the observed vibratory modes cannot be guaranteed. The resonances of the plates will be referred to as vibratory modes, but are not necessarily *normal* vibratory modes; in very important cases they will refer to coupled modes.

Figure 2.19: Example of a high frequency (8452 Hz) Chladni mode of a guitar soundboard. It would be impossible to characterise this with a simple integer pair.

Methods used in determining plate resonances

There are many ways to determine the normal modes of vibratory systems. The simplest methods involve the human sensory system: the visual, hearing and tactile systems can be fairly good at detecting the relative amplitude of resonances, although this is hard to communicate objectively. Another simple method is that employed originally by Ernst Chladni in 1787 [Chladni, 1787]. Most of the spatial information

on soundboard modes of the guitar in this thesis will be derived from the analysis of Chladni figures.

Chladni figures

If a plate is continuously excited at a frequency of a vibratory mode the spatial positioning of maxima and minima of vibration become time-independent. Because of the two-dimensional geometry of the plate, the loci of the nodes form lines instead of points as they would for a one dimensional string (§2.9). If a fine particulate material is evenly distributed over the upper surface of the plate the particles will tend to settle into the nodal positions (although in the case of very light particulates, the opposite may be true, as observed by Savart with lycopodium powder [Strutt, 1869]). The nodes are not necessarily areas of zero vibration; rather they comprise local vibratory minima. Some of the lower frequency Chladni modes of the guitar soundboard are not standing waves of the plate but are the central area of the soundboard undergoing a 'membrane' motion (§2.5). In this case the particulate material is cleared from the central region, but the boundary of aggregated particulate material is altered if the amplitude of excitation is changed.

A disadvantage of this technique is that the plates have to be supported horizontally, and only relatively flat objects may be measured, but is readily applicable to instruments with flat plates such as the guitar [Erndl, 1999], and plates with a limited amount of simple curvature in the vertical direction, such as a free violin plate [Bossy and Carpentier, 1998].

A related technique, holographic interferometry [Jansson, 1971, Richardson, 1988],

extracts similar vibratory information on the spatial distribution of the vibratory modes, from the interference of coherent monochromatic light sources, but is not restricted by the same gravitational constraints or strong surface curvature and imperfections [Rossing, 2000]. Some information about the relative amplitude of vibration is also gained through this method. A disadvantage of holographic interferometry is that it requires relatively sophisticated and expensive apparatus and often takes a long time to prepare correctly, which makes it prohibitive for most luthiers to use routinely in the workshop.

Because of the simplicity of the Chladni figure method, it is used extensively by many luthiers in the determination of plate properties of the instrument during and after construction. However, there is demand from a group of luthiers to make more quantitative measurements of their instruments (for example [Richardson, 1995b, Hutchins, 1962, Brune, 1985b]). This is made difficult because there is not yet a widely accepted measure to use in evaluation of an instrument. Consequently, for any novel measure to be acceptable, it is important to relate this to the traditional Chladni method.

2.10 Interpretation of response curves

The various vibratory modes of the guitar soundboard produce particular spectral features as a response to excitation of the instrument, which are, in turn, dependent on the relative characteristics of the plates and other components. Therefore, to characterise the effect of these components and, hence, to improve the reproducibility of manufacture of a particular instrument, it is most useful to look at the spectrum of

an appropriate ratio, commonly involving pressure, acceleration, velocity or force. The most usual of these frequency dependent ratios are *dynamic mass* ($\frac{\text{force}}{\text{acceleration}}$), *mobility* ($\frac{\text{velocity}}{\text{force}}$), (respectively the reciprocals of *accelerance* and the *mechanical impedance*) and the *pressure force ratio* ($\frac{\text{pressure}}{\text{force}}$), expressed as the Fourier transform of the time-varying quantity in question, with the numerator being the output resulting from the input in the denominator known as a *transfer function*.

Measurements of vibratory quantities made at the same position as the excitation are called *driving point* functions, although are sometimes also referred to as transfer functions. Some features of the transfer function, in principle, enable a particular instrument to be characterised. This might have many practical applications, such as in the quality control of production instruments.

The data presented in this thesis on the characterisation of materials (Chapter 5) relies on the interpretation of the dynamic mass spectra of samples. The data used in Chapter 6 and Chapter 7 is in the form of dynamic masses and pressure force ratios. Chladni modes are most often obtained at the points of steepest gradient in the dynamic mass (Figure 2.20). In this thesis, the dynamic masses (and mobilities) are driving point measurements made at the bridge, and the pressure force ratios are transfer functions from a force applied at the bridge and the sound pressure is measured at the soundhole (or f-hole in the case of the violin). Dynamic mass is an effective parameter, and represents the phase difference between the applied force and the resulting acceleration of a body. The dynamic mass spectrum has a large range in magnitude around resonances and so it is conventional to express the dynamic mass spectra on a decibel (dB) scale.
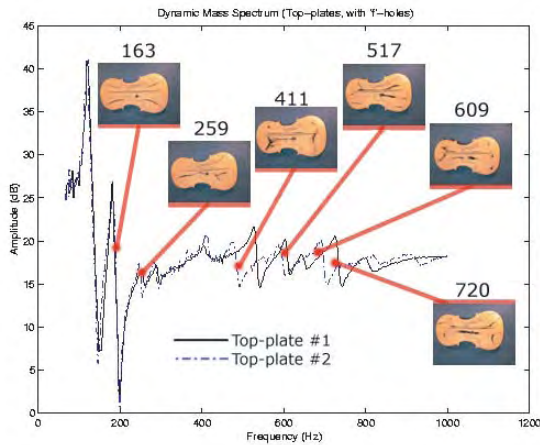
Figure 2.20: The relationship between Chladni modes of a free plate and the dynamic mass spectra. Measurements of Powerhouse Twin violins 1 and 2 [Inta et al., 2005].

Many studies have been comparisons of theoretical models with experiment [Calder-smith, 1985, 1978, 1977, Firth, 1977, Le Pichon et al., 1998, Griffen et al., 1998, Christensen and Vistisen, 1980, Christensen, 1984, Marshall, 1985, Schelleng, 1963]. However some attempts have been made to compare detailed spectral features, or similarly measurable parameters, between various instruments to obtain a 'quality map' [Ross and Rossing, 1979, Jansson, 1997, Richardson, 1995a, Hutchins, 1989]. The success of this approach has been limited because of the lack of an agreed measure of the 'quality' of an instrument. The best results with this goal have incorporated a component of psychoacoustic evaluation of the instrument [Wright, 1996, Rosen, 1995, Wright and Richardson, 1995, Meyer, 1983b, Boullosa et al., 1999] although tests of this nature have yet to be constructed in such a way that convincingly relates to conditions outside of the well-controlled environment of these tests.
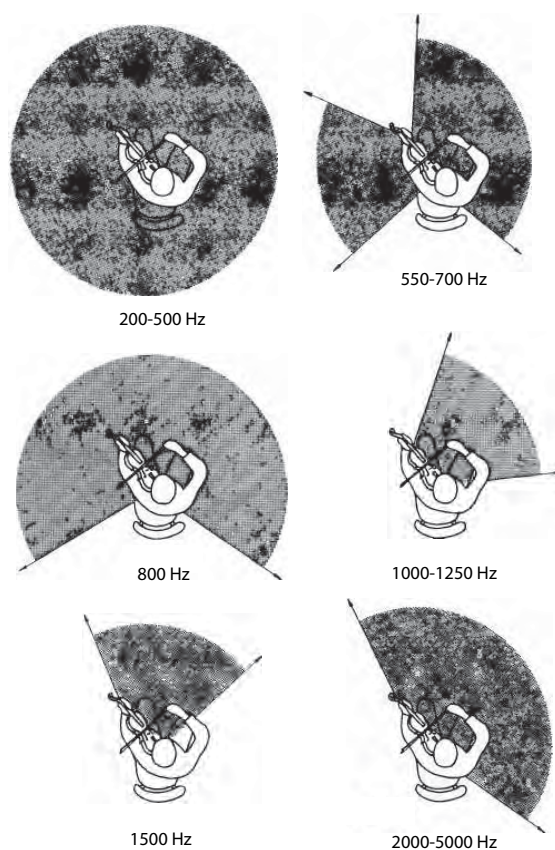
Figure 2.21: Principal radiation directions for a violin. From [Meyer, 1972].

2.11 Acoustic radiativity of the guitar

At lower frequencies ($<$ 350 Hz) the guitar essentially radiates sound spherically, with increasingly complex spatial configurations at higher frequencies [Le Pichon et al., 1998], similarly with other stringed instruments, such as the violin in Figure 2.21 [Meyer, 1972].

For the guitar, the majority of the radiated energy is in the monopole form [Christensen, 1984], where the entire body is able to flex, producing a large net volume

change [Caldersmith, 1985].

If the instrument is assumed to be a simple point source radiator, a result of driven by a sinusoidal force with amplitude F, at an angular frequency of ω, the air pressure at a distance r from a single (uncoupled) mode with resonant frequency ω_0, damping γ, and effective mass m and effective area A may be expressed as [Christensen and Vistisen, 1980]:

$$p = F \frac{A}{m} \frac{\rho}{4\pi r} \frac{\omega^2}{(\omega_0^2 - \omega^2) + \hat{\jmath}\gamma\omega} \tag{2.11.1}$$

where ρ is the density of the air. Thus the pressure amplitude is greater for a low effective mass and high effective radiating area.

However, for a constant excitation force the intensity of acoustic radiation from the guitar, in general, not only a function of distance from the instrument but also has an angular dependence, especially at higher frequencies. This distribution of acoustic intensity in space can be represented by radiative contributions from each resonance mode, which can be modelled using spherical harmonics [Derogis et al., 1995].

$$P_n^m(x) = (1 - x^2)^{\frac{m}{2}} \frac{d^m P_n(x)}{dx^m}, \; P_n(x) = \frac{1}{2^n n!} \frac{d^n (x^2 - 1)^n}{dx^n} \tag{2.11.2}$$

For the nth degree spherical harmonic:

$$Y_n(\phi, \theta) = a_{n0} P_n(\cos\phi) + \sum_{m=1}^{n} (a_{nm} \cos m\theta + b_{nm} \sin m\theta) P_n^m(\cos\phi) \tag{2.11.3}$$

The solution of Laplace's equation ($\nabla^2 T = 0$) in a sphere ($r = a = $ constant $a \geq 0 \, \epsilon \, \mathbb{R}$) which is dependent only on the angle as $r \to a$ and is finite at $r = 0$ is of the form:

$$T(r, \phi, \theta) = \sum_{n=0}^{\infty} (\frac{r}{a})^n Y_n(\phi, \theta) \qquad (2.11.4)$$

Taking $\theta = 0$:

$$
\begin{aligned}
T(r, \phi, 0) &= \sum_{n=0}^{\infty} (\frac{r}{a})^n Y_n(\phi, 0) \\
&= \sum_{n=0}^{\infty} (\frac{r}{a})^n [a_{n0} P_n(\cos \phi) + \sum_{m=1}^{n} (a_{nm} + b_{nm}) P_n^m(\cos \phi)] \\
&= \sum_{n=0}^{\infty} (\frac{r}{a})^n [a_{no} \frac{1}{2^n n!} \frac{d^n (\cos^2 \phi - 1)^n}{dx^n} + \sum_{m=1}^{n} (a_{nm} + b_{nm}) \sin^m \phi] \quad (2.11.5)
\end{aligned}
$$

Or by taking $\phi = 0$:

$$
\begin{aligned}
T(r, 0, \theta) &= \sum_{n=0}^{\infty} (\frac{r}{a})^n Y_n(0, \theta) \\
&= \sum_{n=0}^{\infty} (\frac{r}{a})^n [a_{n0} \frac{1}{2^n n!} \frac{d^n \text{const.}}{dx^n} + \sum_{m=1}^{n} [a_{nm} \cos m\theta + b_{nm} \sin m\theta P_{n0}^m]] \\
&= 0 \qquad (2.11.6)
\end{aligned}
$$

The angular, radial and frequency dependence of the acoustic radiation from the instrument is then:

$$H_n(r, \theta, \phi, \omega) = h_n^{(2)}(jkr) P_n(\cos \theta) \qquad (2.11.7)$$

where the $h_n^{(2)}(jkr)$ are the spherical Hankel functions, and $P_n(\cos\theta)$ represent the nth order Legendre's polynomial in $\cos(\theta)$.

The former can be expressed as:

$$h_n^{(2)}(jkr) = J_0(jkr) - iY_0(jkr) \tag{2.11.8}$$

Where $J_0(x) = 1 - \frac{x^2}{2^2} + \frac{x^4}{2^4(2!)^2} - \frac{x^6}{2^6(3!)^2} + ...$

and the latter, $Y_0(jkr)$, are the Taylors' series solutions to the differential equation

$$(1-x^2)y'' - 2xy' + n(n+1)y = 0 \tag{2.11.9}$$

with $x = \cos\theta$ [Boas, 1983].

With the requirement that $P_n(1) = 1$, the first few Legendre polynomials are:

$P_0(x) = 1$, $P_1(x) = x$ and $P_2(x) = \frac{1}{2}(3x^2 - 1)$.

2.12 Conclusion

A quantitative description of how important elements contribute towards producing the sound of the guitar has been developed, after the definition of important components of the guitar. Some methods have been developed to characterise vibratory modes of the instrument, such as through plate resonances and the effect of the low frequency air cavity (Helmholtz) resonance. Simple models of important coupled systems, such as the string/body and soundboard/air cavity were presented. Some possible measures were derived to characterise a particular instrument so that the

probability of reproducing a particular instrument may be improved. The next chapter examines the properties of the common materials and methods used in making guitars.

Chapter 3

The Construction of the Guitar

"The art of making a good instrument is a complex marriage between 'sound quality', playability and visual æsthetics—with a little bit of whim and luck thrown in for good measure." —Bernard E. Richardson [Richardson, 1995b]

The physical models, as presented in the previous chapter, help illuminate many of the instrument design and construction decisions made by luthiers. However, a large part of this illumination is given through the clarity of hindsight. If a maker experiments with a variation in design, they usually have some idea of the outcome, and is not often done in a quantitative manner. The lack of objective measures of the 'sound quality' of a particular instrument means that design innovations and testing methods applied by makers are usually performed in an *ad hoc* fashion and, in this environment, trial-and-error experiments have provided the most satisfactory results. The lack of controlled scientific experiments in this area means that the consistency of high quality instruments is not assured—even among expert makers [Richardson, 1988]. This chapter examines necessary technical details on important construction processes. The details of techniques described here are those carried

out in the Gilet workshop.

3.1 Introduction

Modifications to the design of the guitar are not dictated solely by acoustic considerations. A particular instrument may well have what is agreed upon as a 'good' sound but if it is not appealing in an æsthetic, economic and ergonomic sense it will be very hard to sell such an instrument. The ergonomic and visually æsthetic attributes of the guitar are recognised as important but are beyond the scope of the present work. Most components serve structural, acoustic and æsthetic functions simultaneously. However, only modifications relevant to the acoustic and vibratory behaviour of the guitar will be addressed in this thesis.

An important trend in the last two hundred years has been for an increased soundboard area, in response to demand for a louder instrument [Morrish, 1997, McIntyre and Woodhouse, 1978]. This requires thicker and more rigidly braced soundboards with stronger materials to retain structural integrity, and to efficiently couple with the air.

The other variations that affect the timbre are not obvious. Historically, many changes in construction techniques are a result of technological advances (such as the adoption of aliphatic resins instead of animal hide glue) or the availability of materials. The species of wood used on the soundboard has a great effect on the tone. A range of timbers are used for this purpose [Richardson, 1998, Gerken, 2001,

Morrish, 1997, Belair guitars, 2002, Worland guitars, 2004]. For instance the North American timber, Sitka spruce (*Picea sitchensis*), is now accessible to most luthiers, whereas the decline in stock of the popular Brazilian Rosewood (*Dalbergia nigra*) now makes it extremely difficult to obtain legally in most countries.

3.2 Material used in construction

Wood is the most widely used building material in the world: the word 'material' itself derives from the Latin word for timber, *materia*. Wood is by far the most widely used material in manufacturing stringed instruments. Despite the variety of construction materials currently available (such as synthetic polymers and carbon fibre composites [Besnainou, 1995]), luthiers have usually continued using wood. Do damping and elastic properties of wood appear to be preferred by players and listeners? Many luthiers have experimented with other materials but it appears there is difficulty accepting an instrument whose sound is unlike that produced by a natural timber. The manufacture of stringed instruments requires some knowledge of the engineering properties of the wood species used.

The structure of wood

There are several works on how the bulk properties of wood relate to the cellular and microscopic nature of the material [Bucur, 1995, Gibson and Ashby, 1997, Haines, 2000, Bodig and Jayne, 1982, Forest Products Laboratory, 1999]. Wood is a complicated composite of hard-celled cellulose microfibrils (organic cells known

as *tracheids*) embedded in a *lignin* (phenyl propane based polymer) and *hemicellulose* resin matrix. Wood exhibits great variation in its mechanical properties [Forest Products Laboratory, 1999, Chomcharm and Skaar, 1983, Caldersmith and Freeman, 1990] . The seasonal variation in the cell wall density of a tree is evident, when looking at the end of the cut log, as a concentric ring structure known as *growth rings* formed by the walls of the long slender tracheids. The orientation parallel to the axis of the tracheids is known as the *grain direction* (Figure 3.1.) The tracheids are cellulosic polymers (based on the mer $C_5H_{10}O_5$), as is hemicellulose. However, the tracheids exhibit a very high degree of polymerisation ($5000 \rightarrow 10000$) compared to the hemicellulose ($150 \rightarrow 200$) [Flinn and Trojan, 1975]. Because the microstructure of wood is composed of these long polymer chains embedded in a resin, the mechanical properties of wood are highly anisotropic. This is illustrated in Table 3.1, which also illustrates some of the variation found in the density and elastic moduli in some commonly used timbers [Kaye and Laby, 1973]. However a table such as this one is inadequate for determining high quality wood to be used for constructing elements of a guitar; the quantities shown here are a rough illustration of typical properties of common species. The material properties within a log vary because of the grain distribution, and show massive variations at the cellular level in the growth ring plane (about $1 \rightarrow 10\mu m$) [Gibson and Ashby, 1997]. To some extent the material properties are less variable on larger scales, because of the effect of averaging over many cells. The wood used in guitar soundboards is always cut such that the long axis is parallel to the long axis of the tree (§3.2). In doing this, the speed of sound is higher and the values of damping lower than for wood cut at an angle to the grain [Schleske, 1990].

Taking the tree trunk as a series of concentric cylindrical shells, and, cutting thin enough rectangular prisms, the growth ring curvature is negligible and occurs in straight parallel lines orthogonal to both the longitudinal and the tangential axis. The wood specimens examined in this thesis are generally such that dimensions in the growth ring plane are small enough ($\lesssim$ 12 mm), so the properties are essentially orthotropic, as shown in Figure 3.1. The principal axes are denoted by the following subscripts:

$$i = \begin{cases} L & (longitudinal) & \text{parallel to the grain;} \\ R & (radial) & \text{in the radial direction;} \\ T & (tangential) & \text{orthogonal to } L \text{ and } R. \end{cases}$$

Figure 3.1: The principal axes useful for modelling wood as an orthotropic material. From [Schleske, 1990].

A piece of timber that is cut from a log as a rectangular prism, so that the long axis is parallel to the grain fibre orientation, and so the width of the prism is in the radial direction, is said to be *quarter-sawn*. Most woods used for the top, back and side plates, and the braces of the guitar, are of quarter-sawn timber. As Table 3.1 suggests, there is a direct relationship between the speed of sound and the angle to the grain, along the length of a given specimen of wood [Schleske, 1990].

In addition to being quarter-sawn, the timber used for the two halves of the soundboard (and sometimes the back) is *book-matched*, where the material is two

Wood Species	Relative density	Young's modulus			Anisotropy ratio
		Longitudinal E_L(GPa)	Radial E_R(GPa)	Transverse E_T(GPa)	$\frac{E_L}{E_R}$
Ash	0.7	16	1.6	0.9	17.8
Balsa	0.2	6	0.3	0.1	60.0
Beech	0.7	14	2.1	1.1	12.7
Birch	0.6	16	1.1	0.6	26.7
Mahogany	0.5	12	1.1	0.6	20.0
Oak	0.7	11	—	—	—
Walnut	0.6	11	1.2	0.6	18.3
Teak	0.6	13	—	—	—
Douglas Fir	0.5	16	1.1	0.8	20.0
Scots Pine	0.5	16	1.1	0.6	26.7
Spruce	$0.4 \rightarrow 0.5$	$10 \rightarrow 16$	$0.4 \rightarrow 0.9$	$0.4 \rightarrow 0.6$	$11.1 \rightarrow 40$

Table 3.1: Some examples of the range of material properties exhibited by different species of wood. Notice that many wood species, including spruce, are highly anisotropic in their elasticity (*i.e.* $\frac{E_L}{E_R} \gg 1$). From [Kaye and Laby, 1973].

plates from directly neighbouring cuts (Figure 3.2) and the grain features and density distribution are symmetric about reflection along the L axis, much like a book.

The complexity of wood structure means that a great variation in physical properties occurs not only amongst individuals within a species, but even among neighbouring pieces *extracted from the same tree* (§5.5 and Table 5.5, [Caldersmith and Freeman, 1990]). This makes the processes of timber selection and quality control important for optimising the mechanical properties of components for an instrument and in improving the rate of replication of a particular instrument. In general the mechanical properties vary the most between the grain (L) direction and the other two (R,T) directions. For Sitka spruce, the Young's modulus in the grain direction is often more than twenty times that in the other directions [Forest Products Laboratory, 1999, Harjono and Dunlop, 1998].
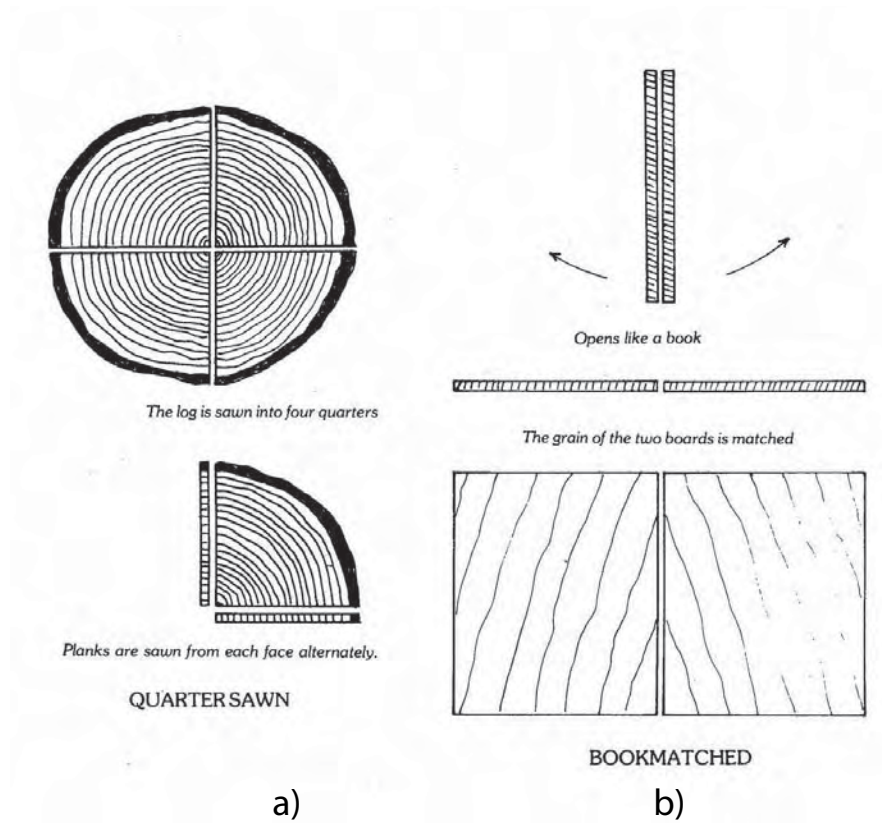
Figure 3.2: Schematics of the process of a) quarter-sawing and b) book-matching wood from raw log form. Most high quality sound boards are of book-matched quarter-sawn timber. From [Williams, 1986a].

Bulk properties and the use of wood

Aside from the variation in mechanical properties with direction, wood also varies in mechanical properties as a function of other parameters. One of the most important of these is the internal moisture content of the wood. Wood is *hygroscopic*, interacting with the moisture in the ambient atmosphere to reach an equilibrium of the mass proportion of internal water. The *moisture content* is defined as the mass fraction of free water in the wood:

$$\Upsilon = \frac{m_{inital} - m_{dry}}{m_{dry}} \tag{3.2.1}$$

where $m_{initial}$ is the initial mass and m_{dry} is the mass of the sample with all of the free water removed. The process used in this thesis to obtain the dry mass is the *oven-dry method* [Forest Products Laboratory, 1999] and the technique used is detailed in §5.3.

Significant seasonal differences in the equilibrium moisture content (EMC) [Simpson, 1998] give changes in the mass density and the elastic moduli (§5.3). It is therefore important to control, or at least measure, the moisture content of the wood when making other measurements of the properties of woods. All high quality wood used in stringed musical instruments undergoes a period of *seasoning*, where the wood is stored in an environment with a controlled humidity and temperature for an extended period of time (often for many decades) to allow the wood to equilibrate. The most well understood and important equilibrium process here is that of the internal concentration of water in free liquid form. Although there is believed to be an

amount of chemical equilibration (including the varying degree of polymerisation) which has a complicated relationship with the moisture content of the wood, the seasoning process results in greater mechanical stability of the material. Differences in mechanical properties have been observed between a well seasoned and a 'merely' dry piece of wood [Manno, 1988].

Some seasoning processes involve steeping the freshly cut wood in a body of water to remove the more volatile matter in the sapwood [Hamlin, 2004] and there is one account that the wood used for making the Cremonese violins were stored in the same housings as livestock and the urea, from the urine of the animals, accelerated the seasoning process [Lolov, 1984].

The equilibrium moisture content (EMC) of a live (or recently felled) tree is generally about $30 \rightarrow 200\%$ [Forest Products Laboratory, 1999], whereas the nominal EMC of a piece of wood in typical atmospheric conditions where the work of this thesis was done (*viz.* values given in a table of material property data for Sydney, Australia) is at 12% [Simpson, 1998].

Luthiers often fabricate the soundboard and bracing in an environment that is conducive to the adsorption of adhesives: as dry as practical, without damaging the microstructure. The soundboards constructed here were made in a controlled environment with a relative humidity of $43 \pm 2\%$ within the Gilet workshop.

Although the wood specimens used in the manufacture of high quality stringed instruments is usually of very high quality, they may have many inhomogeneous features or *defects*, as a result of natural processes occurring while the tree is growing.

The grain density may often be irregular, so that the growth rings are not parallel. An extreme defect of this nature is when a branch or other growth is encountered, producing a *knot*. There may also be disconnected regions of volatile material (*pitch-pockets*). Invariably, the elastic moduli and strength of a piece of timber is strongest when there are no defects (*clear wood*) [Forest Products Laboratory, 1999].

Elastic moduli and densities

The simplest non-trivial stress-strain relation for solid materials is Hooke's law. If σ_i represents the stress (applied force in the ith direction per unit area in the plane perpendicular to i) then, for an ideal elastic material, there exists a corresponding strain in the ith direction, ξ_i, according to the following relationship:

$$E_i = \frac{\sigma_i}{\xi_i} = \text{elastic modulus for the material} \qquad (3.2.2)$$

Where E_i is the relevant elastic modulus in the ith direction. One would expect that the most reliable method for determining this in a specimen would be to directly measure the resulting strain from a given applied stress, but this so called *static measurement method* can be difficult to apply in practice and may not accurately represent the dynamical behaviour of the sample because of time dependent effects such as mechanical hysteresis (*e.g. creep*) [McIntyre and Woodhouse, 1986]. Pulsed ultrasonic vibrations are used for material characterisation for more isotropic materials [McMaster, 1959] but, because of scattering within the grain layers, a natural filtered bandpass system is set-up, making the measurements dependent on the band frequencies, although Voichita Bucur has done much work in this area [Bucur,

1995]. A reliable method for determining the elastic and damping properties of samples at the frequencies of interest is by vibrating the beam at audio frequencies and analysing the subsequent behaviour under certain restraints (a *dynamic measurement method* [Schlägel, 1957, Dunlop and Shaw, 1991, Harjono and Dunlop, 1998]). This has the advantage of accurately measuring the damping and determining the elastic properties. There is also a difference in dynamic E_L and damping compared to static measurements [Ouis, 2002]. The group velocity of vibratory waves in a large solid ('speed of sound') in the ith direction of the material, c_i, is dependent on the appropriate elastic properties and density of the material in question. In this case the lateral vibrations of a slender beam are measured, and it is necessary to know the speed of longitudinal compression waves through the beam. In this case the important elastic constant is the longitudinal Young's modulus E_L and the relevant inertial property is the bulk mass density, ρ. So the speed of sound is then:

$$c_L = \sqrt{\frac{E_L}{\rho}} \tag{3.2.3}$$

A simplifying assumption is that the elasticity of wood is *homogeneous* (the elastic properties are independent of any particular point under consideration) thereby ignoring the obvious variability of wood on a microscopic scale (§3.2). It is inadvisable to extrapolate the following treatment to wood with linear dimensions much different to what is presented in this thesis. If a typical sample of spruce is much larger than about 5 mm in the tangential direction, the assumption of orthotropy becomes unreasonable, and if the sample is too small the detailed microscopic nature of the wood is significant [Gibson and Ashby, 1997].

Wood species	Mass density	Radiation Ratio $\frac{c_L}{\rho}$	Modulus Ratio $\frac{E_L}{E_T}$	Logarithmic decrement $\delta \times 10^2$
	$(\mathrm{kg} \cdot \mathrm{m}^{-3})$	$\left(\mathrm{m}^4 \cdot \mathrm{kg}^{-1} \cdot \mathrm{s}^{-1}\right)$		
Western Red cedar	305-380	14.4-16.4	11.1-25.0	2.1-4.4
Sitka spruce	405-475	11.5-14.0	16.7-33.3	2.7-4.6
Californian Redwood	390-400	10.8	2.9-3.7	2.5-3.1
Norway spruce	450-490	8.7-11.0	7.1-12.5	2.7-4.4
European maple	570-670	6.0-7.0	4.2-5.6	3.2-4.2

Table 3.2: Measurements of physical properties of representative specimens of clear wood from species important for use in stringed musical instruments [Dunlop and Shaw, 1991].

3.3   Damping

Damping is a measure of the loss of energy of a dynamic system to the environment, resulting ultimately in the form of heat. There are a few accepted measures to quantify damping, each with a slightly different purpose. The most useful expressions of damping describe how the system loses energy over time. For a linear vibratory system with viscous losses, this can be expressed most conveniently by the amount of energy lost per vibratory cycle, which is easily translated to the frequency domain.

Radiative damping can be measured by looking at the *decay time* of the system. If a linear oscillatory system is excited by a relatively large initial impulsive force (*ie*: occurring over a relatively short time) and is then left free of external influences, a global maximum occurs within the first cycle, directly after the impulse, and will have progressively smaller amplitudes. The decay time is the time taken for the amplitude (the displacement at the same phase angle) to become $e^{-1} = 0.37$ of the initial value.

The damping or loss factor, d, of a particular resonance is the reciprocal of the quality factor, Q, of that resonance. If f_1 and f_2 represent the lower and higher frequencies directly surrounding the resonance frequency f_0 where the spectral power has dropped to half the local maximum, then $f_2 - f_1 \equiv \Delta f$ is the bandwidth of the resonance. The damping can then be expressed as in Equation 3.3.1.

$$d = \frac{1}{Q} = \frac{f_0}{\Delta f} \tag{3.3.1}$$

In practice, this method is experimentally expedient for $d \simeq 0.001 \rightarrow 0.6$. If $d \gg 0.6$, no standing waves are able to form, making amplitude measurements impossible, while if $d \ll 0.001$, the resonance peaks become too narrow, making measurement of the bandwidth, Δf, difficult [Schlägel, 1957].
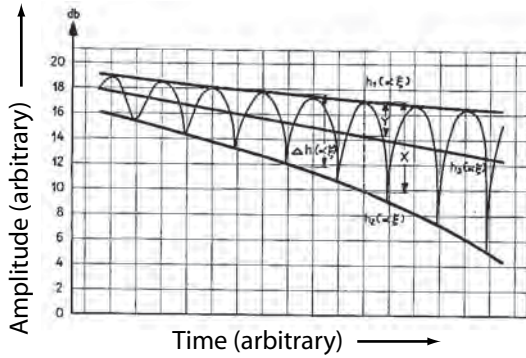
Figure 3.3: Theoretical damping for a material with low damping constant (From [Schlägel, 1957]).

Another, related, measure of damping is the *logarithmic decrement, δ*. This is the ratio of any two consecutive displacement amplitudes. This measure is useful if the damping is effectively viscoelastic (*ie* strictly proportional to velocity only; the substance is both viscous and elastic when experiencing deformation) and therefore would expect the displacement envelope to decrease exponentially over time.

It may also be convenient to analyse a system in terms of the phase shift between stress and strain produced by damping. If we introduce the concept of a *Dynamic Elastic Modulus* [Schlägel, 1957]:

$$E^* = E' + \hat{j}E'' = E'(1 + \hat{j}d) \tag{3.3.2}$$

Where E^* is a complex quantity and d, the loss factor from Equation 3.3.1, is a function of the *loss angle*, δ:

$$d = \tan\delta = \frac{E''}{E'} = \frac{\mathbb{I}(E^*)}{\mathbb{R}(E^*)} \tag{3.3.3}$$

and the conventional elastic modulus may be obtained by taking $E = E' = \mathbb{R}(E^*)$.

The loss factor of the ith resonance may be found by examining the time taken for the peak amplitude of the system to fall to 60dB below the maximum (the *reverberation time*, $T_{\text{rev.}}$) and the frequency of that resonance:

$$d_i = \frac{log_e(10^3)}{\pi T_{\text{rev.}} f_i} = \frac{2.199}{T_{\text{rev.}} f_i} \tag{3.3.4}$$

These damping measures may be related to the Q-value of the appropriate resonance by:

$$d = \frac{1}{Q} = \tan\delta \tag{3.3.5}$$

Damping in wood

Because of the complicated nature of wood, there are several different mechanisms responsible for losses in the acoustic and mechanical vibration of wooden components. The largest internal source of damping is in the lignins, because the structure of the cellulosic microfibrils are fairly crystalline.

Internal damping is an important vibratory characteristic of wood that has been largely overlooked in previous works, partly because of the difficulty of measurement. A reliable method of determining it is through low audio-frequency vibration [McIntyre and Woodhouse, 1986]. Measurements of Sitka spruce give a nominal damping factor of $d \sim 0.02$ [Haines, 2000]. However there is a great variation in damping between specimens, making it difficult to guarantee the accuracy of a general value for a particular piece of wood. There is also some variation of damping with frequency [McIntyre and Woodhouse, 1986].

The anelasticity of wood

Calculation of the Young's moduli of wood samples from the lowest resonance frequency assumes that damping is a constant of the material. However there is some dependence on frequency of the elastic moduli and damping measured here, as well as in other studies on the vibroelastic properties of wood [Ouis, 2002, Haines, 2000].

If the effect is significant, this compromises the assumption of ideal elasticity (Hooke's law, Equation 3.2.2). Assuming the dynamic behaviour is non-plastic (*i.e.* no mechanical hysteresis occurs), this phenomenon is known as *anelasticity*. It is

not clear if there is significant mechanical hysteresis at stress amplitudes normally encountered in the stringed musical instruments.

The damping of musical instrument wood is noticeably frequency dependent. It would hence be appropriate for the present application to use values obtained in the frequency range of interest, $0 \rightarrow 1200$ Hz.

There is evidence for this frequency dependent nature of damping of materials other than wood, for example in Figures 3.4 and 3.5, where relaxation processes occur on the lattice level between atoms of various elements in alloy form.
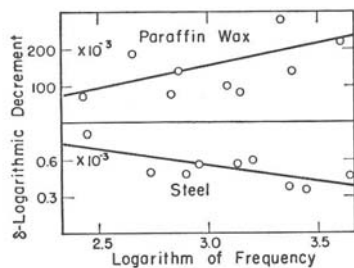
Figure 3.4: The dependence of damping (logarithmic decrement) on frequency is different for paraffin and steel (From [American Institute of Physics, 1972]).
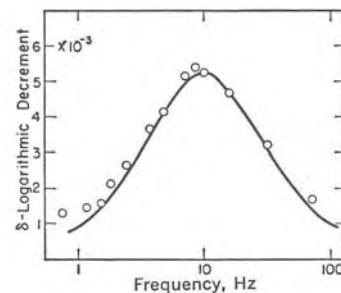
Figure 3.5: An example of the frequency dependance of damping (in this case, the logarithmic decrement) for a metallic alloy. 'German silver' is an alloy of copper, zinc and nickel (nominally $Cu_{0.5}Zn_{0.2}Ni_{0.3}$) (From [American Institute of Physics, 1972])

The relationship between stress and strain is more complicated than that in Equation 3.2.2, due to the introduction of linear independence of the rates of change of both stress and strain, giving the *relaxation equation*[Skudrzyk, 1968]:

$$\xi + \tau_\xi \dot{\xi} = K(\sigma + \tau_\sigma \dot{\sigma}) \tag{3.3.6}$$

Here τ_ξ and τ_σ are constants (the *relaxation times*) for the strain and internal stress of the material respectively. These quantities represent the time the compliant elements take to return to equilibrium after some deformation, and the time taken for the corresponding internal stresses to equilibrate. If the vibrations are periodic, the time derivative operator can be replaced: $\frac{\partial}{\partial t} :\to \hat{j}\omega$. So, putting Equation 3.3.6 into Equation 3.2.2, the complex Young's modulus becomes:

$$E = \frac{\sigma}{\xi} = \frac{1 + \hat{j}\omega\tau_\xi}{K(1 + \hat{j}\omega\tau_\sigma)} = \frac{1}{K}[\frac{(1 + \omega^2\tau_\xi\tau_\sigma) + \hat{j}\omega(\tau_\xi - \tau_\sigma)}{1 + \omega^2\tau_\sigma^2}] \tag{3.3.7}$$

and the usual expression for the Young's modulus is obtained by taking the real part of Equation 3.3.7:

$$E_Y = \mathbb{R}(E) = \frac{1}{K}[\frac{1 + \omega^2\tau_\xi\tau_\sigma}{1 + \omega^2\tau_\sigma^2}] \tag{3.3.8}$$

So, for relaxation processes, the elasticity is a constant for very low frequencies (relaxation times are very much quicker than the forced vibrations) and for very high frequencies (the material stiffens because it does not have a chance to relax to equilibrium) and increases to a maximum at intermediate frequencies, determined by the relative magnitudes of τ_ξ and τ_σ. Some solids, such as rubbers, have a fairly large range of relaxation times and some metals, such as iron and brass, also exhibit characteristic relaxation spectra because of internal heat conduction on a microscopic level. A nominal value for the relaxation time in wood is $\tau \simeq 10^{-7}$ s [Ouis, 2002].

It is conceivable this would occur in wood because of its microscopically complex

composition and structure, although the extent of this effect is unknown. There has been some investigation into the microscopic phenomena responsible for this behaviour in wood, which shows that links between long polymer chains are broken and reformed in a different configuration, resulting in a time-dependent stress-strain relation similar to that of velcro [Keckes et al., 2003]. It is also possible that relaxation on a molecular and macromolecular level in important wooden components of stringed musical instruments may be responsible for the 'playing in' effect of these instruments, as studied in the work of Carleen Hutchins, among others [Hutchins, 1998, Turner, 1997].

Because the measurement of damping in wood is frequency dependent, it is important to qualify the frequency region a damping parameter was obtained from. For the soundboard braces, the frequency range of interest is quite low ($\lesssim 1000$ Hz).

3.4 Traditional techniques of construction

The manufacture of stringed musical instruments has a long tradition and history and many techniques have been developed for particular instruments that are readily applicable to others. Many of the techniques used in making guitars are derived from other, more established, instruments such as the violin. An example of this is the selection of materials using the tap-tone method. However, over time, the manufacturing philosophies of guitar makers have diverged from those of makers of other stringed instruments. For example most makers of violins only use sharp blades to shape the plates of the instrument, whereas guitar makers generally use a range of

blades, power tools and abrasives. Novelty is considered acceptable, both in design and in manufacturing techniques.

One of the principles in making guitars has been of increasing simplicity, with an emphasis on pragmatism. The guitar is a simple instrument to build compared to most other stringed instruments. It is essentially a system of flat plates[1] and is relatively easy to prepare and to assemble.

Testing and quality control is necessary for establishing a luthier's reputation. The practised luthier builds up a vast database of various physical characteristics important to the construction of a good instrument. There is usually a great reliance on direct sensory measurement. Useful information may be gained through visual, tactile, auditory and even olfactory cues. Often the assessment is done intuitively or subconsciously, and the maker is said to have a 'feel' for the technique in question [Morrish, 1997].

A common mechanical device constructed for a particular task, but not incorporated into the final instrument, in order to save labour, alleviate tedious activity or improve safety, is known as a *jig*. For example, the sides of the instrument are held together in a jig to retain them in a bent form while the soundboard and back are glued on. The bridges used on the guitars studied in this thesis are held in a jig so that the shape is well controlled, enabling a high probability of replication.

It is very difficult to reverse the result of removing too much material from a wooden component, without compromising or altering the properties. For this

---

[1]The sides are initially flat plates that are bent to shape under high temperature and humidity.

reason most components are made larger than the final product. This tends to reduce the probability of reproducing a particular instrument. Consequently, for the three guitars studied in this thesis, the dimensions of all important components were made to be those of the smallest member of the set. For example, a common method of altering the output of the instrument is to remove wood from the soundboard. In the present study, the soundboards of three guitars were thinned after glueing to the rest of the body. Each was thinned to an acceptable level, according to the prescription outlined below, and then the thickness distribution of each was measured. The portion of each soundboard was made as thick as the thinnest point for each of the three soundboards.

Tap-tones

One of the most well known traditional methods of appraising wooden components for use in stringed instruments is the 'tap-tone'. The luthier holds the piece of wood at the appropriate position (depending on the geometry; for a slender beam this is usually at the nodal position of the fundamental free-free mode, *viz.* 22.4% of the length of the beam) and strikes the wood percussively. The material properties of the wood—especially any bulk defects—affect the vibratory properties of important sound-producing components of the guitar [Ezcurra, 1996]. A considerable amount of useable information may also be gained from the tactile response of the sample [Romanillos, 1987]. The extent to which the tap-tone method is useful depends on the experience of the luthier. It is difficult to articulate the results of a tap-tone test objectively without some instrumentation. The techniques used in this study to measure the properties of wood (§5.2 and Appendix C) do so by objective and

accurate means which are able to be communicated effectively.

The soundboard

The soundboard is a thin, initially flat, wooden plate. It is composed of two book-matched plates joined such that the regions with denser growth ring structure (*i.e.* that which was closer to the heart of the original tree) are along the central axis of the guitar. Apart from the æsthetic appeal, this is so that the soundboard is structurally reinforced toward the centre of the plate. The stiffness distribution of the soundboard is therefore inhomogeneous by design.

The soundboard is made thin so that it has a relatively small mass for a relatively large area enabling the efficient transmission of vibrations to the surrounding air. However it must be strong enough to withstand the tension load on the soundboard produced by the strings. Furthermore, if sound is transmitted too efficiently from the string, there is less energy in the string to sustain the notes being played on the strings, which is partly responsible for the 'play-off between loudness and tone' [Gerken, 2001].

The famous luthier Antonio de Torres Jurado demonstrated the importance of the soundboard in the production of sound from the guitar [Romanillos, 1987]. The soundboard is usually made of spruce or cedar because of their high stiffness to mass ratio, as well as their desirable damping and anisotropic material properties [Dunlop and Shaw, 1991].

Thinning the soundboard

Some higher quality guitars have their soundboard thinned after being glued to the sides and back. Usually the edges of the lower bout are thinned, leaving the central region in the lower bout and all of the upper bout untouched. This increases the radiation output at middle frequencies ($300 \rightarrow 700$ Hz) [Krüger, 1982]. The edges are made more flexible and less massive.

The luthier marks the thickness on points at the edge of the soundboard, going from the edges just below the soundhole and smoothly reducing to the thinnest portion near the butt at 1.5 mm. In this area, the soundboard is marked with a pencil in a line approximately 80 mm from the edge, following the boundary of the edges of the soundboard, as in Figure 3.6.

The two tools used to thin the soundboard are a flat carpenter's plane and sandpaper glued to the large face of a flat block ($175 \times 75 \times 25$ mm) of Teflon®(polytetrafluoroethylene (PTFE)) in order to give a flat abrasive surface. Therefore, in conjunction with the thinning prescription, the profile of the soundboard *should* be rectilinear. We would not expect much localised variation of the thickness gradient on scales below about 40 mm in the longitudinal or lateral directions.

During this process, the experienced luthier often listens for the change in acoustic response when removing soundboard material; the act of sanding or rubbing hands over the soundboard [Williams, 2003] provides a source of a broad band vibratory signal over the appropriate frequency range. This is compared with a response remembered from past experience. Hence this method does not explicitly depend on the soundboard thickness distribution *per se*. However for the purpose of controlling
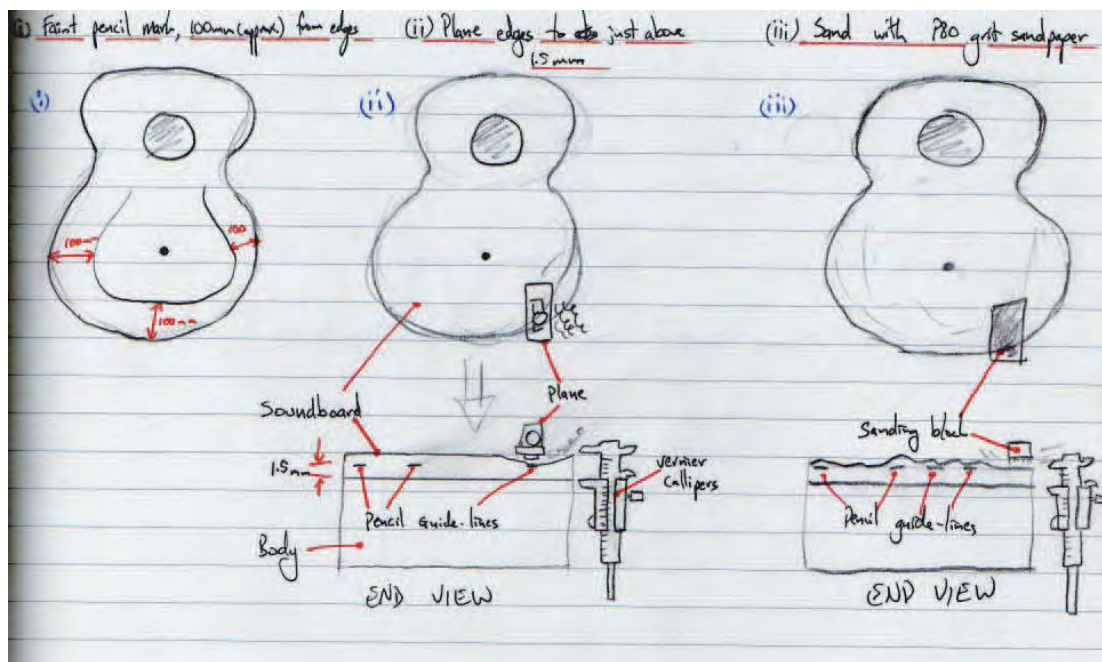
Figure 3.6: Working diagram of soundboard thinning procedure, as explained by Gerard Gilet to the author.

the three guitars in this thesis, it was necessary to have similar thickness distributions for all three soundboards. Measurement of the thickness variation of the soundboard at this point is quite difficult; a solution to this problem is given in §6.5.

The back and sides

Ideally the back and sides provide a stiff enclosure so that much of the sound is radiated from the front of the instrument. This is more of a priority for the classical guitars than for steel-string instruments because of the necessity of the instrument to 'project' sound in a concert environment (*i.e.* to strongly radiate sound towards an audience). Consequently the materials for the back and sides need to have a high mechanical impedance, such as is found in rosewood or mahogany. The back and sides of the guitars studied in this thesis are of Sapele mahogany (*Entandrophragma cylindricum*).

The sides are made from two initially flat plates and are bent into shape by a process of heating, at a high moisture content, over a side-jig having springs to force the sides to the contour of the final instrument. The back-plate is a system of two plates glued together in a similar way to the soundboard. The back and the sides are reinforced with a simple bracing system. In addition, the back-plate has a piece of spruce about 20 mm wide and 3 mm thick (a *marriage-strip*) to reinforce the joint between the two plates.

Bracing in the OOO steel string guitar

The asymmetric cross-bracing system is the most commonly used in reinforcing the soundboards of steel string guitars. This style of bracing was adopted after development by the C. F. Martin Co. in the late 1890's [Longworth, 1975]. This bracing system would be symmetric about the longitudinal axis if it were not for the two 'tone-braces' extending through the central region of the soundboard (Figure 3.7). The tone-braces extend through much of the lower bout and strongly influence the output sound of the instrument. The large uppermost brace in the upper bout, the *transverse bar*, is the largest brace of the system. This and the *bridge-plate*, which covers the internal region of the soundboard directly underneath the bridge, are the only braces not made from Stika spruce. The former is made of Amoora (*Amoora cucullata*) and the latter is of Sugar maple (*Acer saccharum*).

Sitka spruce is the preferred brace material for the back and soundboard because it has a high stiffness-to-mass ratio ['the Doc', 2005, Sheppard, 1997]. However, Engelmann spruce is occasionally used for the 'tone-braces' in the lower bout of the X-bracing system, and it is thought this has some effect on the output sound [Sheppard, 1997].

Profiling braces

Once the brace-wood has been selected and made into rectangular beams, it is common to shape the cross-section so that it resembles an isosceles triangle atop a rectangle, with the length of the base of the triangle being the same as the adjoining
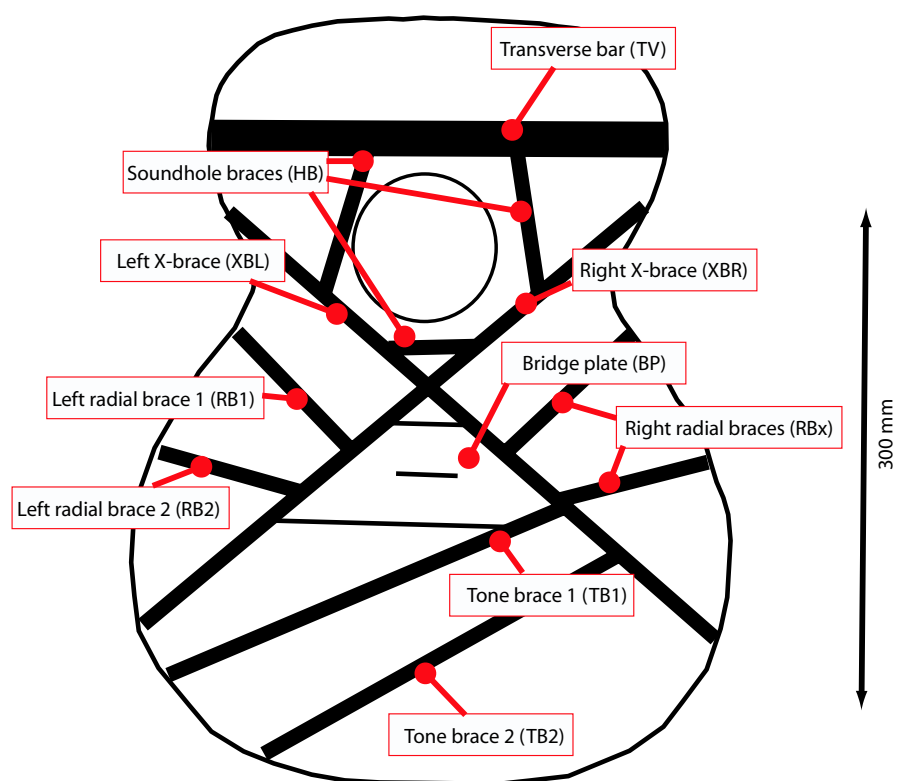
Figure 3.7: The Martin X bracing system used on the guitars studied here. Note the asymmetry of the bracing system is due to the two 'tone-braces,' covering a significant area of the lower bout.

108
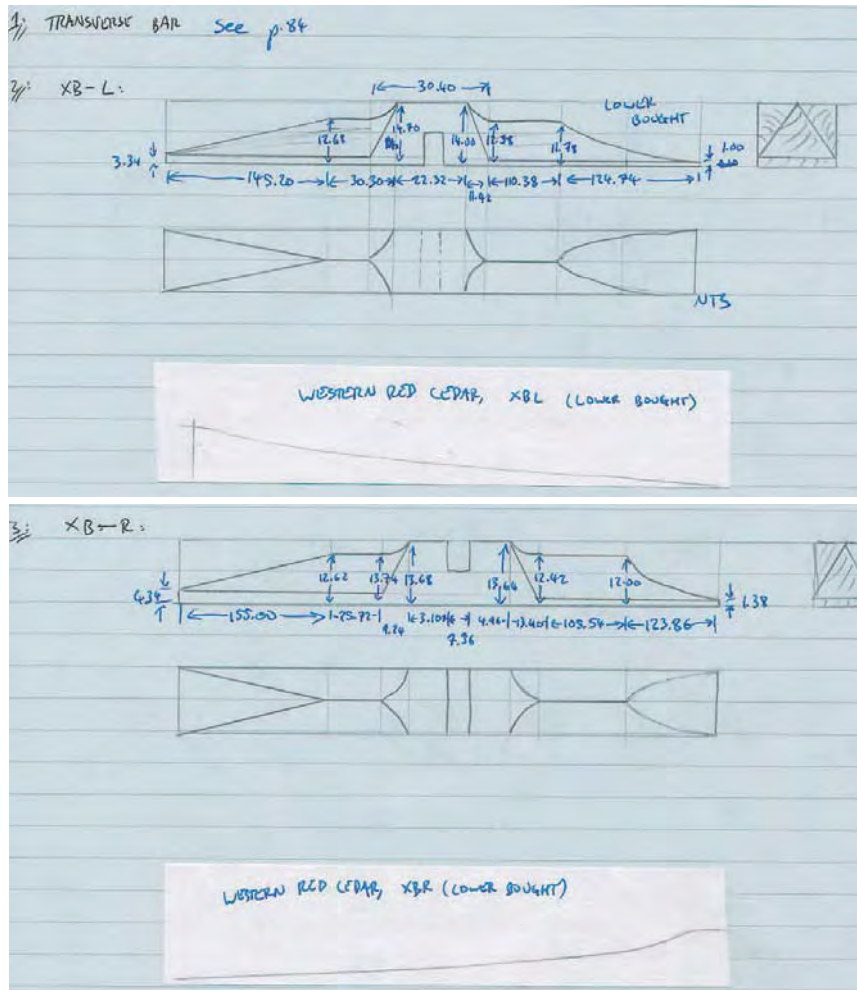
Figure 3.8: Working diagram showing measurement of dimensions of left and right cross braces, including measurements of brace dimensions. Braces shown are WR-CXBL and WRCXBR, the main cross-braces for the Western Red cedar soundboard.
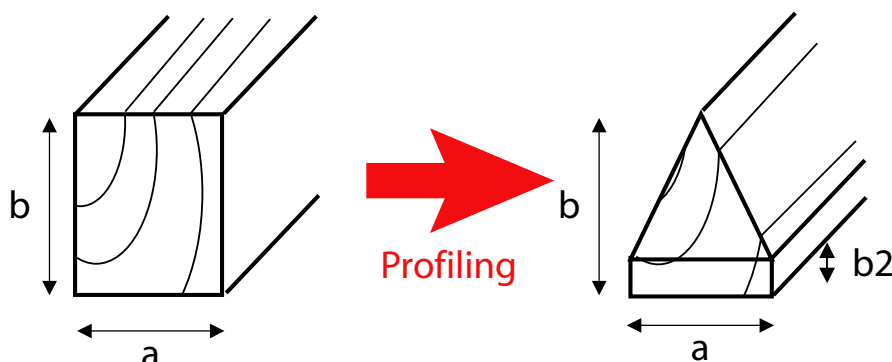
Figure 3.9: The initial brace cross-section is a simple rectangle. This is modified to an isosceles triangle atop a rectangle with a common edge. The apices are further modified in the scalloping process such that the cross-section is no longer constant. Figure after [Vernet, 2001].

side of the rectangle (Figure 4.3). The effect of brace profiling is simulated for a simple brace/plate system, using a finite element model, is presented in §4.3, and the theoretical effect of this on the normal modes of a slender beam was given in §2.7.

Considering the requirement to retain a large gluing surface, this profiled cross-section is more optimal for a bracing beam than a simple rectangle because the stiffness is a function of the cube of the thickness and only linear with width. Therefore much of the mass of the brace is reduced with little reduction in stiffness. Some luthiers have extended this treatment to a parabolic cross-section to further optimise the function of the braces [van Linge, 1996]. Another example of a brace optimisation technique is the carbon fibre/balsa composite braces used in *e.g.* Smallman guitars, which are effectively a type of I-beam.

The main X braces both have a small (roughly 20 mm long) length retaining the rectangular section (the *knuckle*) to fit the braces together.

One important modification to brace geometry is the process of profiling, a technique used by luthiers to optimise the stiffness to weight ratio of beams by altering their cross-section from that of a rectangle to a pentagon. While having the same total height, a sharp apex is formed, by an isosceles triangle on top of a rectangle with a width equal to the base of the triangle. Because the geometry is different, there is some divergence from the vibratory behaviour of a simple beam with rectangular cross-section, due to the change in the radius of gyration, κ, in the direction of the applied excitation force. Because the resonant frequencies of a simple beam are proportional to its cross-sectional radius of gyration, κ (see Equation 2.7.5), altering the cross-sectional geometry of the beam will result in a corresponding shift in frequency. Denoting the changed state as primed variables in Equation 2.7.5 and the original geometry with unprimed variables, the frequency ratio for the ith mode is:

$$\frac{f_i'}{f_i} = \frac{\frac{\pi c \kappa' s_i^2}{8L^2}}{\frac{\pi c \kappa s_i^2}{8L^2}} = \frac{\kappa'}{\kappa} = \sqrt{\frac{I'}{I}}$$

For a rectangular cross-section, height a (in the plane of vibration), $I_{CM} = \frac{Ma^2}{12}$, and, for an isosceles triangle of height h, the rotational moment of inertia is $I_{CM}' = \frac{Mh^2}{18}$. The change in resonance frequencies is thus:

$$\frac{f'}{f} = \sqrt{\frac{12h^2}{18a^2}}$$

$$= \frac{h}{a}\sqrt{\frac{2}{3}}$$

Thus the frequency ratio becomes:

$$\frac{f'}{f} = \frac{\sqrt{2}h}{\sqrt{3}a}$$

Finally, if the new height is identical to the original, $h = a$, then the frequency ratio is simply:

$$\frac{f'}{f} = \sqrt{\frac{2}{3}}$$

Hence the resonant frequency of a given lateral mode of a cantilever, whose cross-sectional shape has been made into an irregular pentagon, symmetric upon reflection about the vertical axis, from a rectangle of identical height, is shifted lower, to about 82% of the original. Therefore the practice of profiling braces significantly reduces the mass of the brace with little corresponding loss in stiffness in the vertical direction. This enables more efficient impedance matching between the vibrations of the braced soundboard and the air because the braces give similar reinforcement with less mass. The frequencies of the normal vibratory modes are approximately 82% that of the original brace.

Scalloping braces

The alteration of the cross-section of the braces, so that they are no longer constant ('scalloping', Figure 3.10) was first widely introduced by the Martin Guitar Co. in the early 1900's [Longworth, 1975].

This technique is commonly used to alter instruments to produce a more 'mellow' tone [Ford, 2005] but the effect has not been well studied mechanically. Scalloping

112

Unscalloped brace   Brace with sides scalloped   Fully scalloped brace
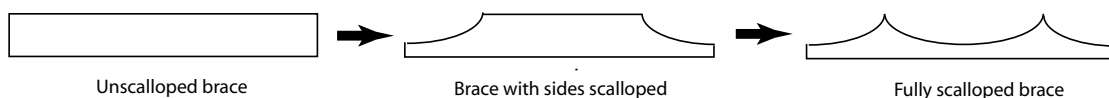
Figure 3.10: Side view of the scalloping processes of a wooden brace. A beam of constant, rectangular, cross-section is shaped such that the edges are tapered with a concavity (partially scalloped) and the middle of the brace is also made concave (fully scalloped brace.)

cannot be performed on some instruments because of the resulting decrease in structural integrity.

In the present study, important braces on the soundboard (those occupying the central position on the soundboard: the lower bout portion of the X-braces, and the larger of the two 'tone-braces') went through an intermediary stage of scalloping where not as much material was removed (§7.6) compared to the completely scalloped instruments (§7.6.)

Because it is relatively difficult to scallop braces on a soundboard attached to the back and sides, this process is usually performed before the soundboard is glued to the rest of the body. It is, however, sometimes required in order to alter the sound of a fully constructed instrument, in accordance with the wishes of the musician. Therefore it is useful to examine the changes induced by scalloping the braces of the finished instruments. Because it was planned *ab initio* to scallop the braces in the guitars studied, a template (*i.e.* a simple shape designed to fit into place inside the guitars, providing a solid boundary) was constructed from Perspex™ sheet (2 mm thick) for each tone-brace at both stages of scalloping (Figure 3.11.) The outlines of the two stages were marked in pencil on both the braces in each guitar when the soundboard was being worked on, before attaching it to the back and sides. The

templates were used during the scalloping procedure to judge the proximity to the wanted brace geometry.

A small thumb-plane, some pieces of sandpaper, a small plane mirror and a portable light-source (Figure 3.12) were used to scallop the braces in accordance with the markings on the braces and the scalloping templates in Figure 3.11. The template was sometimes bonded to the inside of the braces with plasticine and all the work was performed by hand, using the soundhole for access.

Also, a finite element model was constructed to investigate the effects of brace scalloping in §4.3.

The bridge and saddle system

The bridge/saddle system (§2.2) is the most important element in the conversion of the vibratory energy of the string to acoustic radiation. Its central position on the soundboard means that the bridge/saddle system contributes a significant amount of mass and stiffness to the soundboard, influencing the vibratory modes of the instrument at all frequencies (§7.2).

The analogy between the bridge and an impedance transformer is very useful. To interact efficiently with the air, it is desirable to have a soundboard with a relatively low mechanical impedance. However, the relatively high impedance of the strings (*i.e.* a relatively large amount of force is concentrated over a small area at the saddle) means that an impedance interface is required to transform the vibration. Because of this, the wood used for bridges is generally very dense, with relatively high Young's moduli, such as ebony or rosewood.

X-brace template 1

X-brace template 2

Tone-brace template 1

Tone-brace template 2

Material: 2mm Perspex sheet
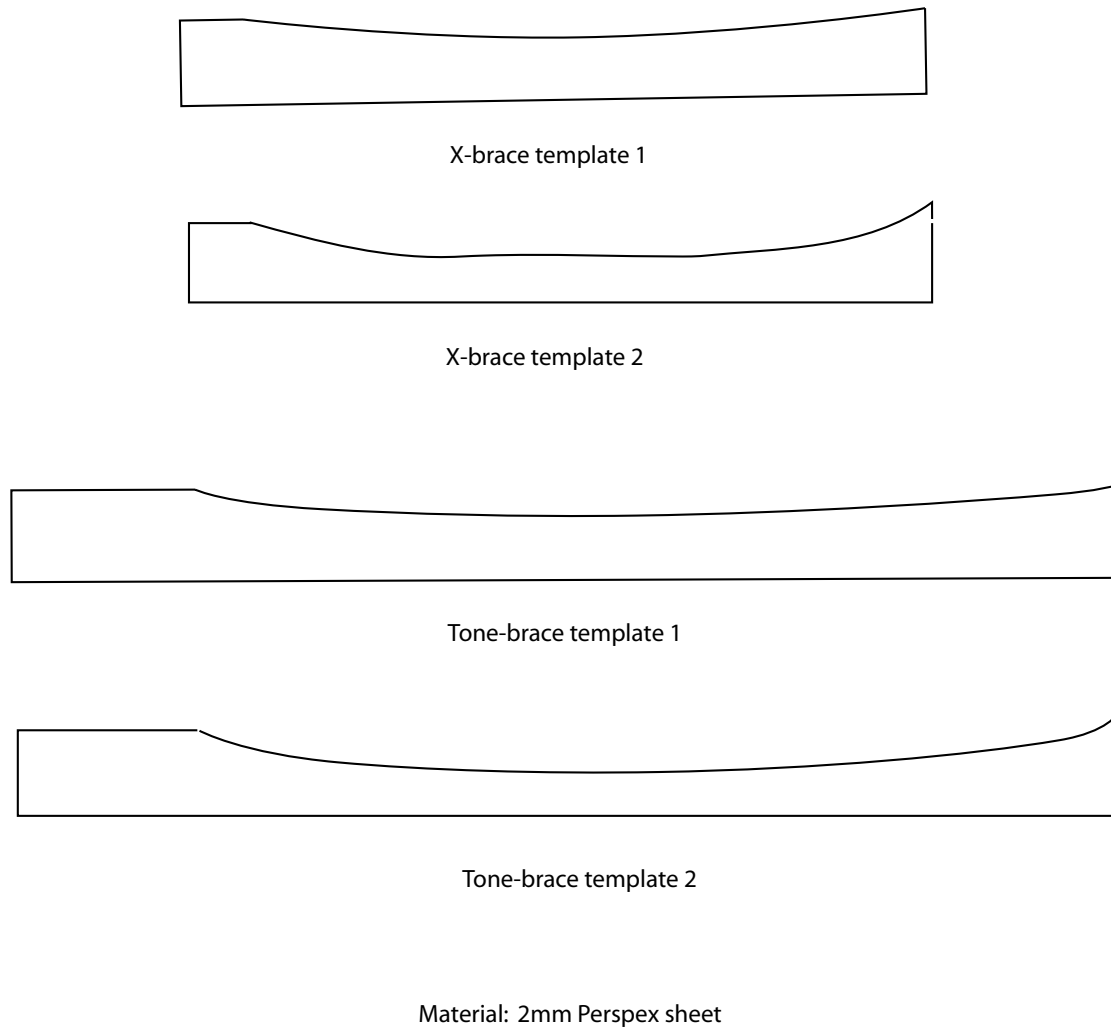
Figure 3.11: Outline of the templates used for scalloping the tone-braces in the guitars.

Figure 3.12: The tools used in scalloping the tone-braces.

Figure 3.13: Photograph of the set-up for the scalloping procedure after the soundboard has been attached to the back and sides.

Figure 3.14: A luthier scallops the braces with a small thumb-plane, working from inside the sound-hole.

The bridge is cut from a flat plate of wood (Figure 2.5), and is made with the aid of a jig, so that bridges are able to be reproduced with a relatively high degree of precision. The bridges of the guitars studied here are of 'Indian' rosewood (*Dalbergia laterfolia*). Measurements of the effect of the bridge on the vibratory characteristics of the guitars studied in this thesis are given in §7.2.

Break angle and string correction

The strings of a steel-string guitar are held in by the bridge pins (§2.2) which are some distance ($\approx$ 10 mm) behind the saddle. Hence the strings in this region are bent over the saddle, making an angle to the plane of the soundboard. This angle is known as the *break angle* (the term also applies to the strings terminating at the nut). A small break angle allows relative motion between the string and the saddle (or nut), contributing to unpleasant 'buzzing' sounds [Ford, 2005]. A high break angle creates excessive mechanical stress at the saddle and may contribute to the strings breaking at this point. The optimal break angle is said to be $20° \rightarrow 25°$ [Fishman Transducers, 2004]. Also the saddle is aligned at an angle to the rest of the bridge, in the plane of the soundboard, because of the *string compensation* mentioned in §2.1 [Fletcher and Rossing, 1998].

Linings

The joints between the sides and the soundboard and the back plates are important for the structural integrity and function of the guitar. To increase the strength of these bonds, strips of wood (*linings*) are introduced to the internal interface between

the plates and the sides. Because the linings are constrained to follow the curvature of the sides, the linings are usually made more flexible in the lateral direction through a series of regular thin cuts (*kerfs*).

The bindings

The *bindings* are pieces of timber used to reinforce the boundary formed at the soundboard and the sides of the guitar. The guitars studied in this thesis also have a *herring-bone*, which is a strip of wood joined to the binding material, extending about 5 mm toward the centre of the soundboard. The effect of the bindings on the vibration of the guitar soundboards studied here is examined in §6.6.

The neck joint

The neck is the structural member of the guitar that supports the fingerboard, and is roughly as long as the body of the guitar. The joint between the body and the neck needs to be strong enough to withstand the tension of the strings in the longitudinal direction as well as any lateral forces on the instrument. Hence the top portion of the body usually has a solid block of wood (the *neck-block*) to enable a strong mechanical coupling. Traditionally, the neck is joined with adhesives and a dove-tail joint. However, the guitars studied in this thesis make use of a neck-joint relying on bolts (a *bolt-on neck system*), developed initially by Robert Taylor of the Taylor Guitar Co. This system allows easier access to the neck for maintenance than does the traditional system, and there is no vibratory disadvantage if the mechanical coupling is made well [Ford, 2005].

Schematics of the necks used here are given in Figure 3.15. The vibratory effects of the addition of the neck to the body are examined in §7.1.

The surface polish

The process of *polishing* the guitar involves the application of protective material onto the outer surface of the exposed plate areas. This process enhances the æsthetic quality of the instruments, helping to protect the exterior, and provides a buffer against humidity and thermal changes to the wooden components.

A range of polishes are used on guitars. All require some solvent, most of which evaporates over time. Once the solvent has disappeared, the polish becomes harder and is said to be *cured*.

There is debate on the effect of the polish on the sound of stringed instruments in general, especially in the case of the violin [Schleske, 2000, Barlow and Woodhouse, 1989, Schelleng, 1968, Fryxell, 1984]. However, it is widely asserted among luthiers that the best resulting finish is one that is applied as thinly as possible. Nevertheless, the polish must be sufficient to seal the surface wood cells such that sweat and other foreign matter does not penetrate the protective barrier [Williams, 1986a]. Before the application of the actual polish, some alteration of the surface properties of the guitar occurs. A progression of finer sandpaper is used over all surfaces to be polished, to P1000 grade (1000 abrasive particles per square centimetre) such that no scratches larger than ~ 0.3 mm are visible and there are no sharp discontinuities in the surface gradient.

Neck

44.09

26.01

Bottom view
Scale: 1:5

Isometric view
Scale: 1:5

65.88

116.95

27.28

44

359.3

5 5

Front view
Scale: 1:5

17

16

161°31'7.07"

32

26.12

118.5

Left view
Scale: 1:5

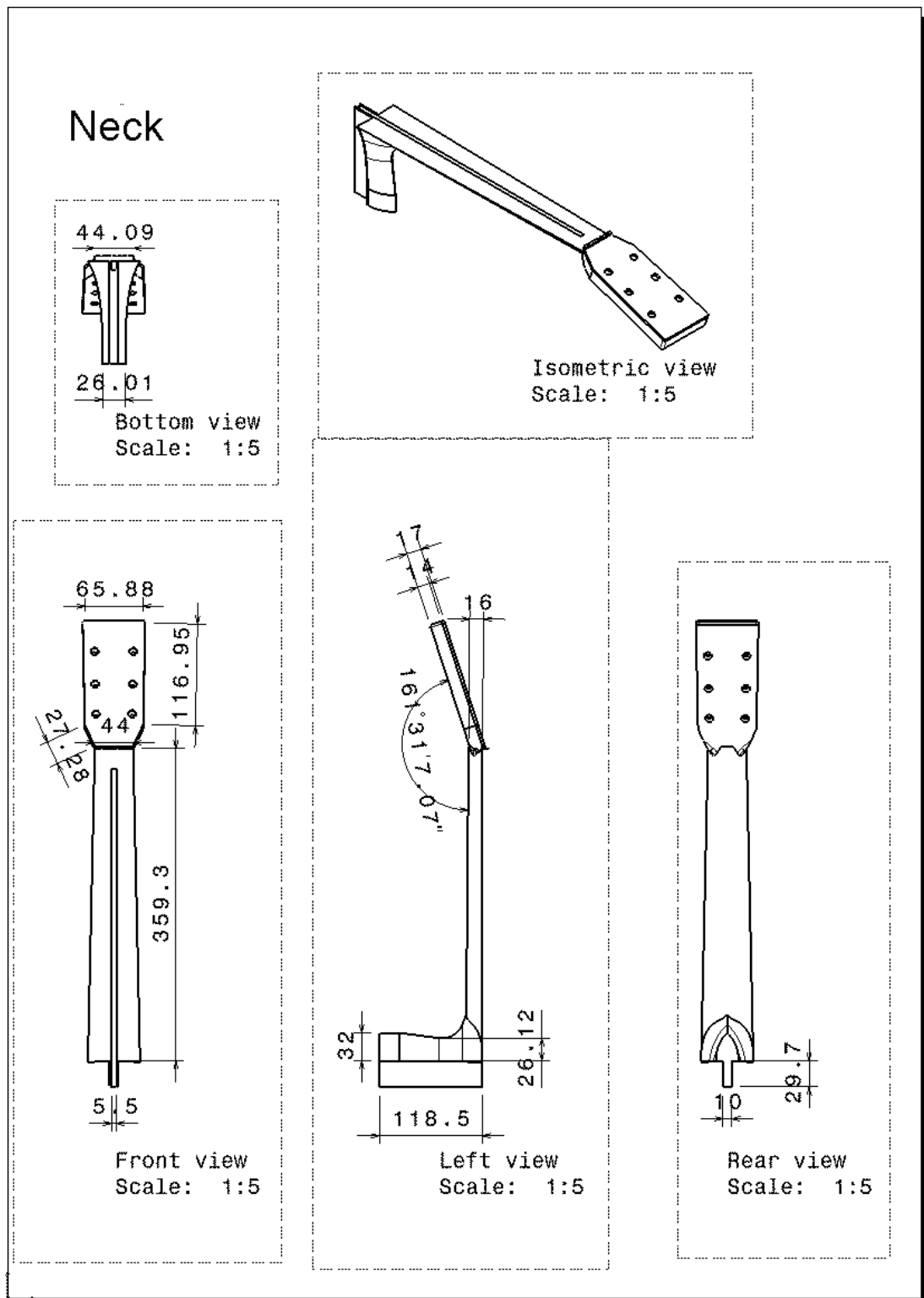29.7

10

Rear view
Scale: 1:5

Figure 3.15: A schematic and dimensions of the neck used here. Dimensions in millimetres. The scales do not apply to this reproduction. Image courtesy of Mattheiu Maziere and Davy Laille.

The polish used on the guitars studied here is a nitrocellulose lacquer, applied with a pneumatic spray-gun. The effects of the application of polish to the guitar on the vibratory response of the soundboard is given in §7.3. The effects of allowing the polish to cure for a period of 63 days are examined in §7.4.

Aesthetic elements

As well as being an engineering structure, a good quality guitar is often a work of art. There are many elements that serve a primarily æsthetic function. Decoration of the instrument was reduced to a minimum through the influence of de Torres Jurado [Romanillos, 1987]. However, some elements of the guitar are purely cosmetic. The rosette (§2.1) is an annular structure enclosing the soundhole, and is embedded in the surface of the soundboard. It is usually made from small pieces of various timbers or mother-of-pearl (the interior layers of the shell of the oyster *Pinctada maxima*). The rosette may also protect the soundboard from crack propagation near the soundhole.

The most prominent and intricate cosmetic feature of the (steel-string) guitar is usually the *inlay*. The inlay is made of attractive material, commonly mother-of-pearl or abalone, although semi-precious gemstones have also been used. The inlay is generally found as position markings on the fingerboard and a motif (often the luthier's trademark) is commonly found on the head-stock. Some instruments have inlay figures on the rosette and the bindings.

The rosettes used on the instruments in this study are a mixture of ebony, spruce and a rosewood arranged in a ring formation. The butt-strips are of the same material as the bindings (rosewood and spruce). The inlays on the fingerboards are small thin

discs of mother-of-pearl and the fret markers on the uppermost side of the neck are of high density polyethylene. There are no inlays on the head-stocks.

The *butt-strip* is a small decorative plate to cover the line formed by the joining of the sides at the butt of the guitar. The material used for the butt-strips in the guitars studied in this thesis is the same material used for the bindings.

3.5   Recent innovations

The design of the guitar is still evolving. Improvements are made due to the innovation of the instrument makers and their collaborators. Much inspiration and many design ideas are borrowed from other instruments. For example, there have been attempts at installing a soundpost into the instrument, similar to that in the violin, such as that by Joël Laplane [Laplane et al., 1995]. Laplane also made instruments with internal bridges and multiple soundholes in various positions, and physical attributes of the instruments, such as the resonance modes, were measured [Chaigne and Rosen, 1999]. There has been experimentation with the bracing system to address particular issues, such as the common occurrence of a nodal line on or near the third string at the $T(2, 1)$ (see mode nomenclature in Table 2.5) soundboard mode (at a frequency of about $200 \rightarrow 300$ Hz) producing a large 'dead area' on the lower notes of this string. It is recognised by luthiers and researchers that an approach using physical principles would be beneficial to the guitar industry as a whole (but not without some resistance [Kasha, 1995, Brune, 1985b, Wyszkowski, 1985, Hampton, 1985, Eban, 1985, Brune, 1985a, Williams, 1986b, Wyszkowski, 1986, Margolis, 1986, Brune, 1986]). An oft-quoted success of innovative guitar manufacture is that

made by Greg Smallman, in using a lattice-style soundboard bracing system made of a carbon fibre/balsa composite [Atherton, 1990]. This enabled a great reduction in mass of the soundboard, creating a much louder instrument.

Because of the novelty seeking nature of many guitar players, and the economic benefits associated with innovation, it is likely that luthiers will continue to experiment with design features to remain competitive with their peers.

3.6   Phases of construction examined in this thesis

Dynamic mass and pressure force ratio spectra, as well as Chladni figures were measured at ten stages of construction on the three guitars: the braced soundboards, the bodies directly after the soundboard was glued to the back and sides, after applying the bindings, after thinning the soundboard, after putting the bridge on, after polishing, after allowing to cure and then to age for almost two years, and then partly and then fully scalloping the cross- and tone-braces. It is inconvenient to include the full name of each construction stage with the measurements, so the construction phases will be referred to by the abbreviations in Table 3.3.

Construction stage	Abbreviation
Free soundboard	SB
Bodies only	BDY
After binding	BB
After thinning	BTT
Without neck	WON
With bridge	GB
After polishing	GF
Allowing polish to dry	GH
Ageing two years	2yr
Braces partly scalloped	SCL50
Braces fully scalloped	SCL100

Table 3.3: Abbreviations for the construction stages investigated throughout the study of the three guitars in this thesis.

Chapter 4

Applications of the Finite Element Method to instrument construction

"It is nice to know that the computer understands the problem. But I would like to understand it too"—Eugene Wigner (1902-1995)

The speed and processing capability of modern computing systems, and the wide range of software written for them, enables the mechanical modelling of vibratory systems to be performed easily. The Finite Element Method (FEM) has been applied in a wide range of problems in mechanical and more specialised types of engineering. Systems previously modelled range from nuclear reactors [Campbell, 1995] to novel aerospace transportation vehicles [Abdul-Aziz, 1996].

This chapter summarises some of the work done in collaboration with three undergraduate students from the École Normale Supérieure in France working on this project at The University of New South Wales: David Vernet in 2001 [Vernet, 2001],

Davy Laille and Mathieu Maziere (both in 2002) [Laille, 2002, Maziere, 2002]. Motives and methods for using the FEM are given in §4.1. Selection of the appropriate model and values of material properties and boundary conditions are given in §4.2. This is followed by applying this method to the problem of scalloping braces on the guitar soundboard (§4.3) and to the soundboard (§4.5) and the finished guitar (§4.6) after preliminary study is made on the influence of glue bonds between important elements (§4.4). Finally, there is discussion of the application of finite element methods to the manufacture of guitars (§4.7).

4.1 Methods and motives for using finite element calculations

Although most of the work in this thesis is of an empirical nature, it is useful to compare the results of these experiments with numerical simulations based on known geometry and material properties. This enables interpretation of the experimental results and also provides, in principle, a tool for the luthier in the diagnosis and design of instruments, without performing the costly procedure of constructing or modifying existing instruments. It is convenient to perform these numerical simulations using available and relatively inexpensive computers. The contents of this chapter rely on two finite element software packages: CASTEM 2000 and Catia V5R7. The computer used to model using the CASTEM program was a single desktop PC with a Pentium III™ processor rated with a clock 'speed' of 800MHz and RAM of 512MB capacity. The computer system used to run the Catia package was a member of a cluster of undetermined processing rate, although it is estimated it normally would

not process calculations much faster than the machine just mentioned.

The prescription for constructing an FEM of a dynamical system involves the division of a system into many localised *elements*, where each element has the mechanical parameters in the linear differential equation for a simple harmonic oscillatory system, assuming simple viscous damping:

$$m\ddot{\xi} + R\dot{\xi} + k\xi = F(t) \qquad (4.1.1)$$

where ξ is the time-dependent displacement, m is the mass of the element, R the viscous damping coefficient, k the stiffness of the element and $F(t)$ the resultant of the external force on the element, which is dependent on the imposed constraints or boundary conditions, and the neighbouring elements. Solutions to the dynamical system are obtained numerically for each element.

Previous FEM work done on the guitar

A good overview of numerical models relating to the guitar is given by Antoine Chaigne [Chaigne, 2002]. Oliver Rogers used an FEM to calculate modal frequencies on free violin plates after the removal of wood at various parts [Rodgers, 1990]. Ove Christensen and Bo Vistisen [Christensen and Vistisen, 1980, Christensen, 1984] presented a simple model of the sound output of the guitar and the coupling effect of the air by assuming the soundboard and back-plate and the internal air cavity were simple (point) radiators. Elejabarrieta, Ezcurra and Santamaría [Elejabarrieta et al., 2001] modelled the guitar soundboard at various stages of construction, comparing

it with a soundboard being constructed by a luthier. The model was modified to include the hinged boundary properties introduced by joining the soundboard to the sides (§2.9).

A model, initiated by Bernard Richardson and Gordon Walker [Walker, 1991] and refined by Bernard Richardson and Howard Wright [Wright and Richardson, 1995, Wright, 1996, Wright and Richardson, 1997], used the methods outlined in [Christensen and Vistisen, 1980, Christensen, 1984] to simulate the sound output by the complete guitar and performed psychoacoustic tests using tones synthesised from this model. It was found that the effective mass and monopole areas of each mode contributed more to the perception of tone quality than the frequency or Q-value of the mode nearest in frequency to that considered.

A model of the sound radiation field of the guitar was created, and compared with experiment, by Alexis Le Pichon, Svein Berge and Antoine Chaigne [Le Pichon et al., 1998].

Gregoire Derveaux, Antoine Chaigne, Patrick Joly and Elaine Bécache [Derveaux et al., 2003, Bécache et al., 2005] presented a model of the guitar with a high degree of sophistication and completeness. This work models the motion of the plucked string through to the field of the sound radiated by the instrument. This work involved collaboration of a group of engineers and guitar-makers.

The models presented below are detailed simulations relating specifically to the vibratory properties of the steel-string acoustic guitars studied in this thesis. However, to achieve sufficient accuracy, it is necessary to investigate some aspects of similar systems to observe the calculated effects of brace scalloping and adhesive coupling.

The FEM software packages

CASTEM 2000 was initially developed by the Mechanical Department of Technology (DMT) of the French Police Station and Atomic Energy, for modelling thermal activity in nuclear reactor vessels, and was further developed to model vibratory systems numerically. In CASTEM, the mesh has to be programmed and each component has to be explicitly entered as a set of vector co-ordinates.

Using Catia, it is easy to define relatively complicated mesh geometries because the more limited options allow means of programming *via* a graphical user interface.

CASTEM gives the user more precision and control over the program structure, as well as having a broader range of commands and analysis tools, such as the options of orthotropy and of the output of transfer functions, but is time-consuming to program. Calculations of a reasonable mesh size can take a long time to perform on a typical desktop personal computer. Using Catia, on the other hand, it is very difficult to control the mesh size and geometry, which makes it harder to compare results to experiment. Occasionally small changes in input parameters can result in large differences in the output [Maziere, 2002]. It is convenient to construct structures with complicated geometry in Catia and it is capable of producing sophisticated animations or rendered drawings of the results.

4.2 Inputs for the model

The accuracy of the simulation of vibratory systems depends on the precision of the boundary conditions and material properties of each component, which are derived empirically. Also important are the assumptions made about the overall model. For example, the assumption of isotropy would make computation faster and more efficient, but is of course inappropriate for wood (§3.2).

The assumption of homogeneity is also not appropriate here. The soundboard of an acoustic guitar is generally made of two plates glued together so that the grain features and grain density are symmetric about the main axis of the instrument (*i.e.* 'book-matched' §3.2, §3.4). Because the thickness of the plate is small in the tangential (T) direction, there is negligible variation in properties in this direction. However, we should expect the material properties to vary considerably in the radial (R) direction (§3.2).

Measurements of the spatial variation of Young's modulus (using the nondestructive methods described in §5.2) from 11 samples of wood material directly surrounding the simple square plates modelled in §4.3, distributed according to Figure 4.1, showed there were some substantial differences in the resonant frequencies, with discrepancies of up to 25%, in the case of the fundamental free-plate mode (0,2) [Vernet, 2001]. Hence the assumption of homogeneity is inappropriate for models of the guitar soundboards in §4.5 and §4.6.

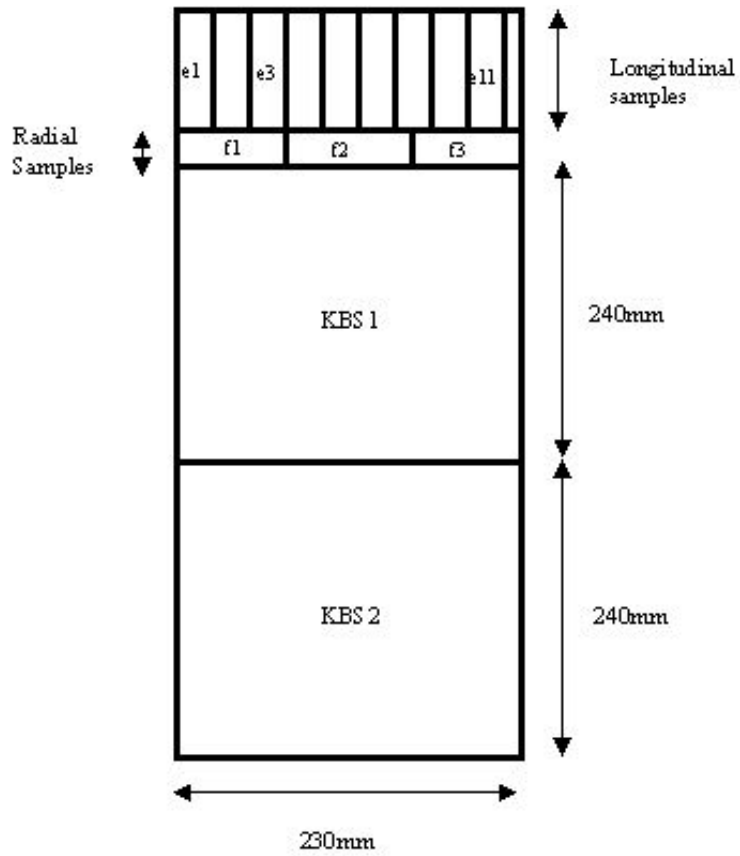Measurement of the Young's modulus in the transverse and radial directions, the

Figure 4.1: Illustration of the spatial position of samples taken from wooden material surrounding the rectangular plates modelled in §4.3. From [Vernet, 2001].

shear moduli G_{ij} or the Poisson's ratios ν_{ij} (where i, j are the principal axes L, R and T) is more difficult. This is partly because of the relatively small size of the samples ($\lesssim 100$ mm long, $\simeq 20$ mm wide and $\simeq 3$ mm thick). All the plates considered here are thin (*i.e.* the thickness is no more than 1% of the smallest lateral dimension) so the value of the Young's modulus in the direction parallel to the radial axis, E_R, is not important at lower frequencies. For long thin beams, such as the brace material, the Young's moduli E_R and E_T are not as important. Nevertheless, parameters are required as input for the simulation. Nominal values of the remaining elastic properties that were not measured were taken from [Forest Products Laboratory, 1999].

The models in §4.6 are performed on Catia, which does not explicitly support orthotropic input. In this case, orthotropy was simulated by introducing an array of identical reinforcing rods into the soundboard, of negligible mass and with magnitudes of Young's moduli necessary to produce the anisotropy found in wooden soundboards [Laille, 2002, Maziere, 2002].

Hence the wooden components modelled here are assumed to be orthotropic and the soundboards are assumed to be inhomogeneous along the transverse axis (the orthotropy is important because the soundboard of the guitar is designed actively to exploit the innate anisotropy and inhomogeneity of wood [Locke, 2005]).

4.3   Brace scalloping

The process and purpose of brace scalloping is described in §3.4. It may be possible to relate the change in timbre ascribed to scalloping to the appropriate transfer function

characterising the plate. However, the changes to the geometry are complicated, making it difficult to predict the result. The FEM makes it possible to model the effects of scalloping on the vibratory behaviour of a plate with bracing. The model results are first compared with those of two simple thin wooden plates, both in the shape of a square, with a single diagonal brace, after which the complete guitar soundboard is analysed. Experiments involving the scalloping of important braces on the soundboards of finished guitars are presented in §7.6.

Simple plates

The single most important contribution to the sound of the guitar is thought to be that of the braced soundboard [Meyer, 1983a, Richardson, 1982, Elejabarrieta et al., 2000, 2001, Rossing and Eban, 1999] . Studying the vibratory behaviour of the free guitar soundboard is complicated by the details of the bracing structure. It is useful to compare the vibratory behaviour of a guitar soundboard with a FEM simulation to understand the important dynamics, but, to be confident of the model, it is helpful to compare to a plate of simpler geometry and bracing configuration.

Because the wood is inhomogeneous and orthotropic, the mesh has to be divided into regions of different properties. Laminar shell elements were used to model soundboard and braces, both before and after scalloping the braces.

The model was compared to experiments using the Chladni figure technique (§2.9). Figure 4.2 shows a comparison between Chladni figure experiments on two simple wooden plates, KBS1 and KBS2, and modal analysis using an FEM [Vernet, 2001].
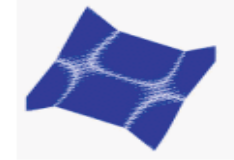
Fem		KBS1 Chladni Patterns		KBS2 Chladni Patterns	
FEM shape	FEM fqv (Hz)	C. P. fq (Hz)	$\dfrac{f_{cp} - f_{fem}}{f_{fem}}$ (%)	C. P. fq (Hz)	$\dfrac{f_{cp} - f_{fem}}{f_{fem}}$ (%)
	252.8	248.9	-1.54	241.7	-4.39
	324.4	307.4	-5.24	299.2	-7.77
	375.73	375.5	-0.06	382.6	1.83
	429.5	444	3.38	507.4	18.14

Figure 4.2: Comparison between predictions made by FEM and measurement of mode shapes and frequencies for two simple wooden plates, KBS1 and KBS2. From [Vernet, 2001].

Figure 4.3: The initial brace cross-section was a simple rectangle, measuring 12×8mm. This was modified to an isosceles triangle atop a rectangle with a common edge. The apices were further modified in the scalloping process such that the cross-section was no longer constant. Figure after [Vernet, 2001].

Braces with constant cross-section
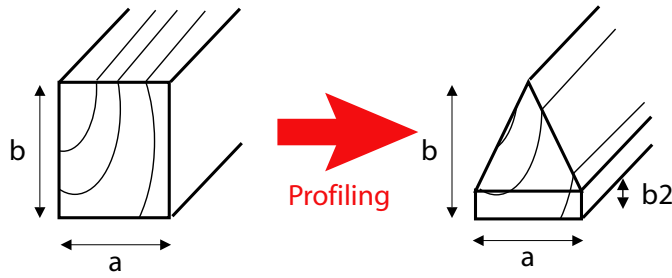
The longitudinal Young's moduli E_L and the mass densities ρ of 11 candidates for wooden braces having rectangular cross-section (12×8mm) made of Stika spruce were measured. The two most similar in E_L (*ca.* 12 GPa) were retained. Then one of these was cut longitudinally to give a constant pentagonal cross-section of the same height as the original (Figure 4.3). The rectangular brace was altered in height so that it had the same moment of inertia (in the plane perpendicular to the base of the strut). Both braces were glued diagonally to the simple plates (KBS1 for the pentagonal and plate KBS2 for the rectangular brace) in the same way a brace is glued to a guitar soundboard.

The results of Chladni figures on these simple plates are given in Figure 4.4. The amplitudes of some of the peaks in the transfer functions are of greater magnitude for the plate with the triangular brace configuration, compared to the rectangular bracing. The agreement in the measured modal frequencies between the two plates was within 4%, the greatest difference being at the fifth mode (*ca.* 450 Hz) where the brace is a node.
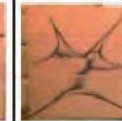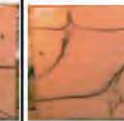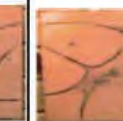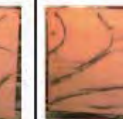
Figure 4.4: Comparison of Chladni figures of simple rectangular wooden plates, each with a single diagonal brace with rectangular (KBS2) and triangular cross-section (KBS1). The solitary dark point appearing in each image is the position of the small rare-earth magnet used to drive the plate, in combination with a solenoid. From [Vernet, 2001].

The simulation predicts more distinct modes than are detected experimentally. In the frequency range $0 - 1000$ Hz, 12 modes were identified in the FEM; seven distinct modes were found experimentally.

Simple rectangular wooden plates having a single scalloped brace The scalloping process (§3.4) begins with removal of material from both ends of the brace ('partly scalloped') and then from the middle ('fully scalloped').

Numerical simulation of the motion of each rectangular plate predicts a lowering in modes 1, 2 and 3 with little change in mode 5, in response to scalloping the single diagonal brace. This is confirmed by experiment (Figure 4.5). Agreement with the measured modal frequencies is good. Experimentally, the sixth mode is lowered in frequency (from 650 Hz to 580 Hz). This mode has a large number of nodal and

FEM calculations

| mode | Unscalloped strut | | half-scalloped strut | |
	FEM	fq	FEM	fq
1		104		91
2		220		208
3		234		236
4		290		
5		481		480

Chladni figure measurements

| mode | Unscalloped strut | | Half-scalloped strut | |
	Chladni Patterns	fq	Chladni Patterns	fq
1		100		91
2		221		213
3				
4		279		265
5		479		478
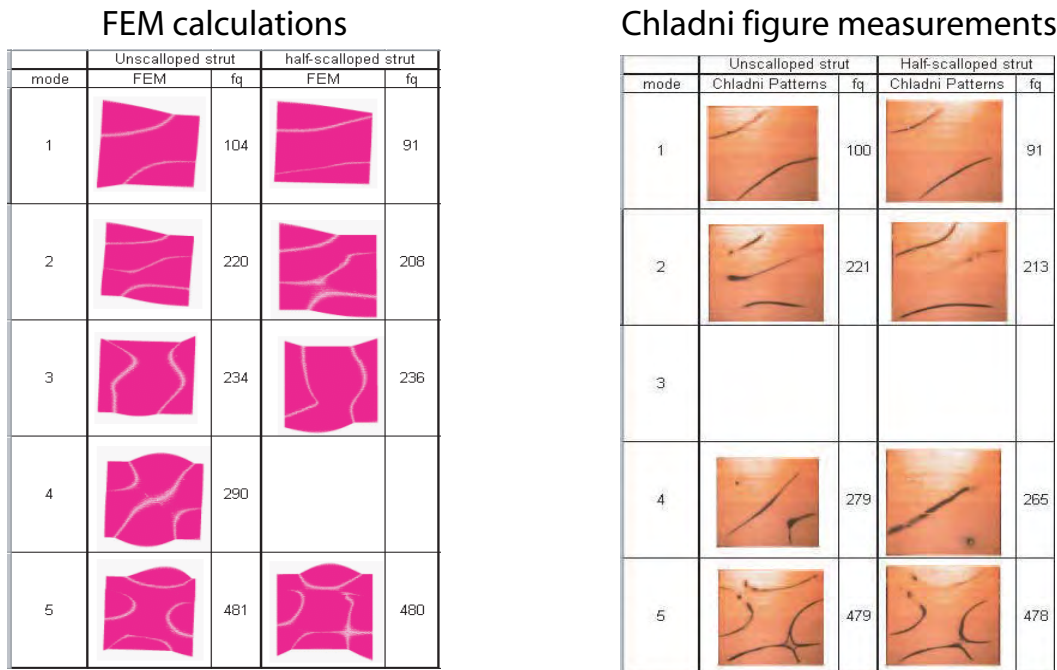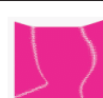
Figure 4.5: Comparison of FEM calculations with measurements of Chladni figures of simple rectangular plates with single braces partly scalloped. From [Vernet, 2001].

antinodal lines crossing the brace.

Comparison of the partly scalloped plate system to that with a fully scalloped brace show a 13% increase in the frequency of the second mode, a 8% decrease in the third mode and little differences in the fourth and fifth mode frequencies (Figure 4.6). Again, this agrees well with experiment (Figure 4.7). Modes with nodal lines near the region of the brace are affected the most, notably mode four (*ca.* 280 Hz).

Some differences in the dynamic mass spectra are noticeable at higher frequencies $(30 \rightarrow 20,000$ Hz, Figure 4.8). However the apparatus used for excitation (Brüel and Kjær 4809 shaker) and detection (Brüel and Kjær 8001 impedance head) are

Figure 4.6: Comparison of FEM calculations with measurements of Chladni figures of simple rectangular plates with single braces fully scalloped. From [Vernet, 2001].
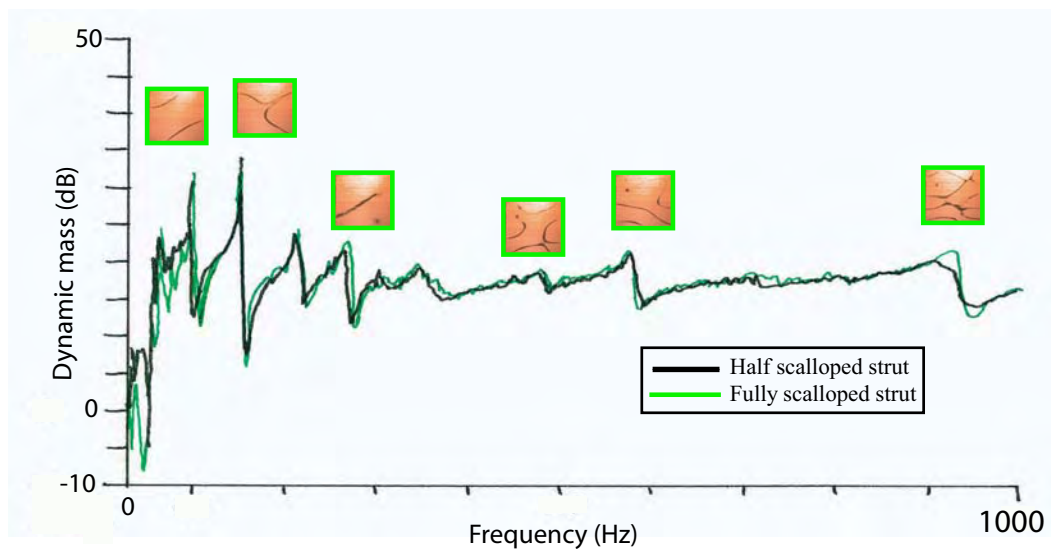
Figure 4.7: Comparison of dynamic mass measurements of simple wooden plates with a single brace after scalloping the edges of the braces and after scalloping the middle part of the brace also. From [Vernet, 2001].
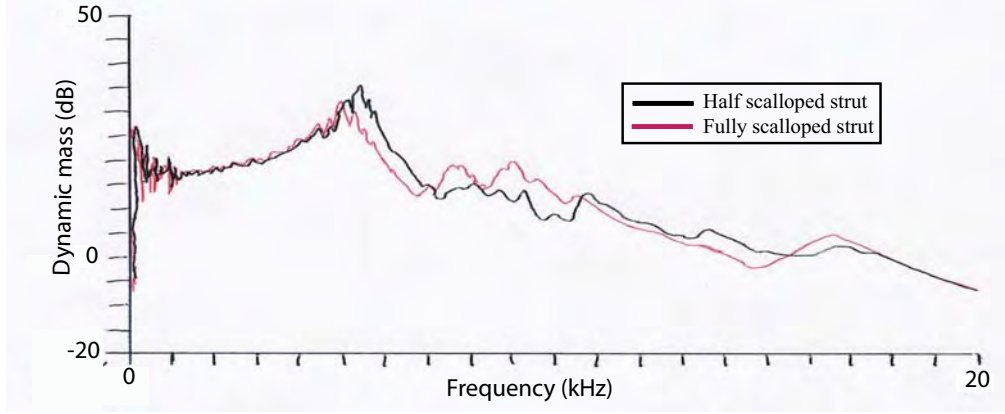
Figure 4.8: Higher frequency response function of plate with a single diagonal brace. The two plots are that with and without brace scalloping. From [Vernet, 2001]

linear only in the frequency range $0 \rightarrow 6$ kHz. There are some obvious large relative differences in the magnitudes of the dynamic mass between the plates at about 5, 7.5 and 9 kHz. The peaks are broadened and the peaks are also slightly lowered in frequency.

The FEM models used here simulate the motion of the plates with the condition of a free edge. The mass load of the magnet and the sand used to create the Chladni figures tend to decrease the frequencies of most of the normal modes compared to free-free conditions by $\lesssim 5\%$. There is good agreement between the FEM and experiment with the frequency and nodal distribution of low frequency vibratory modes, both before and after brace scalloping of the simple plates. At these frequencies, little difference is seen in modal frequencies and geometries between the scalloped and the

unscalloped plate systems. However both the Q-value and the amplitude of higher frequency peaks in the dynamic mass spectra increase after scalloping.

4.4 Glue bonds

Because all of the important components in a guitar are joined by an adhesive, it is important to determine whether this bond affects the vibratory properties of the guitar under the conditions considered here. The mass due to the relatively small amount of glue required to form a good bond is small in comparison with the brace itself, so the effect due to mass loading is probably small. However it is conceivable the bond would damp and either stiffen or weaken the bonded area, depending on the type of adhesive used.

The comparison of an FEM model with an experiment of the coupling between a single wooden brace and a simple plate was performed using the simply braced rectangular structures in §4.3 [Maziere, 2002, Laille, 2002].

For the three lowest frequency modes, the agreement between modelled and experimental mode frequencies were very similar. However, this agreement diverges at higher frequencies and it is difficult to determine whether the differences are because of inhomogeneity of the wood or the coarseness of the FEM mesh. To simplify the analysis of the influence of glue on interactions between vibrating wooden members, the interaction between two slender beams, glued together, was studied.

Modifying the simple beam equation (Equation 2.7.1) to obtain a system of two beams coupled by a glue bond, Maziere and Laille found that the two beams are essentially co-moving until the glue begins moving at $f = f_{\text{crit.}}$. However, even if the Young's modulus of the adhesive were very small, the critical frequency is quite high ($f_{\text{crit.}} > 20$ kHz). Therefore the experimental apparatus used for examining
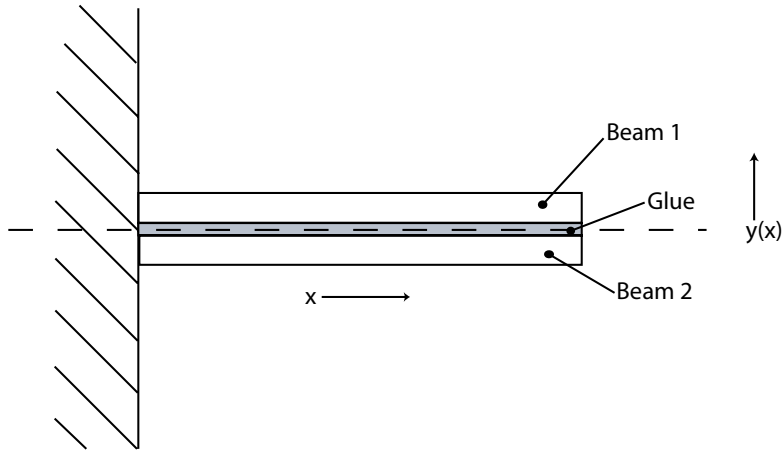
Figure 4.9: Geometry of a two-beam cantilever with beam elements coupled by an intermediary adhesive. After [Laille, 2002].

the vibratory behaviour of beams in §5.2 would not be capable of experimentally verifying any plasticity of the glue bond.

This does not mean that there is no effect of the coupling adhesive on the dynamics of two coupled beams below 20 kHz, but it shows there is no tendency for any in-plane relative motion of two adhesively-coupled beams within the frequency range of interest. It is therefore appropriate to assume that the wooden braces glued to the main soundboard may be modelled as if they were joined with no means of relative displacement.

4.5　The free guitar soundboard

A model was created in CASTEM of the OOO guitar soundboards studied in §6.3, using a mesh containing approximately 9000 elements [Vernet, 2001]. A larger mesh

Figure 4.10: Comparison between experiment and FEM calculation of the first four modes of a steel-string guitar soundboard. The numbers given are the frequencies (Hz) that the particular mode occurs. From [Vernet, 2001].

size was not possible because the displacement matrix to be solved has an immutable size limit. The results were then compared to the modes identified experimentally in §6.3.

The FEM predicted 12 possible normal modes in the frequency range $50 \rightarrow 800$ Hz. Experimental techniques such as Chladni figures (§6.3) or laser holography [Jansson, 1971, Richardson, 1982] do not indicate there are this many distinct vibratory modes in this frequency range. Although the Chladni figure method indicates up to 14 figures in this frequency range (Figure 6.7), these are not all distinct modes; there are more likely a total of seven. Experimental Chladni figures and calculated normal modes from the FEM model on the free soundboard of a steel-string guitar for the first four modes compare well (Figure 4.10).

At higher frequencies the areas bounded by nodal lines are usually smaller and local inhomogeneities in the elastic properties of the wood, which the model is not able to resolve, become more important. Further, the spatial distribution of the nodes becomes more complicated so discretisation errors in the mesh become much more important. Finally, the model used here does not account for the load on the soundboard surface due to the surrounding air. The mass loading and mode damping effects of the experimental excitation apparatus and the sand used in visualising the Chladni figures also affect the vibratory behaviour of the soundboard and this method gives no direct means of determining the amplitude distribution on the soundboard surface, unlike the FEM model in [Vernet, 2001].

Scalloping braces on the soundboard

Figure 4.11 shows the results of the FEM calculation presented here for the OOO steel-string guitar soundboards with a standard Martin cross-brace system with scalloped cross-braces. Scalloping of the middle of the cross-braces and the upper tone-brace was not performed on these soundboards until the guitar was completely finished (§7.6) hence there is no experimental data in Figure 4.11. Figure 4.12 shows a calculation for the same soundboard, similar except that only the upper tone-brace was scalloped. Figure 4.13 shows the results of FEM calculation of a steel-string guitar having both the cross and the tone braces scalloped.

Again, the two lowest frequency modes are not affected by scalloping the cross-braces because, in both cases, their central region is not a node at these frequencies. The third mode is decreased by 33 Hz (25%) and the fourth mode decreased in frequency by 7 Hz.

Figure 4.11: Calculation of normal modes of a free soundboard of a steel-string acoustic guitar with standard Martin cross-bracing, after scalloping the cross-braces only. From [Vernet, 2001].
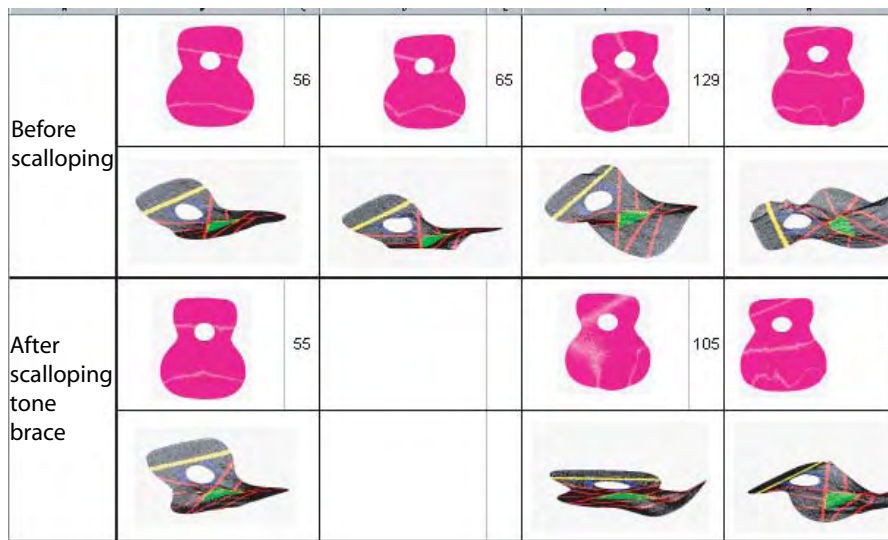
Figure 4.12: Calculation of normal modes of a free soundboard of a steel-string acoustic guitar with standard Martin cross-bracing, after scalloping the upper tone-brace only. From [Vernet, 2001].
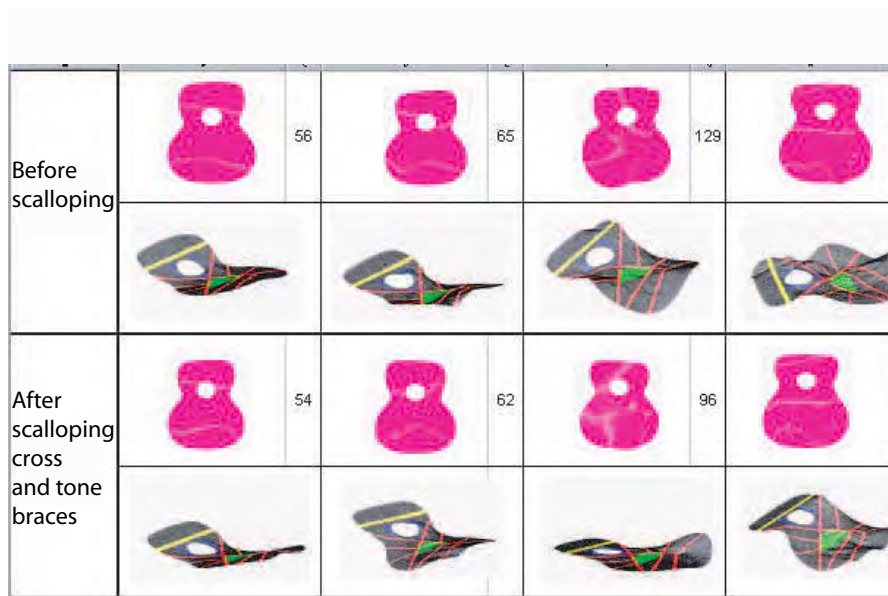
Figure 4.13: Calculation of normal modes of a free soundboard of a steel-string acoustic guitar with standard Martin cross-bracing, after scalloping the cross-braces and the upper tone-brace. From [Vernet, 2001].

Although the experiments on scalloped bracing on the guitar soundboard §7.6 are of the plate attached to the back and sides, and are therefore altered by the interaction with the air and the back and sides, the results compare well with the model (Figure 4.11). Differences are only large for the third and fourth soundboard modes, T(2,2) and T(3,2) (Figure 7.39), where there is a slight lowering of frequency and a broadening of the peak at these modes. There is a slight lowering of the first soundboard mode frequencies (Table 7.6).

4.6   Guitar body

Using the model of the free soundboard (§4.5) and geometric measurements of steel-string guitars, an FEM of a complete guitar was constructed, including the strings. The complete guitar is required to withstand the considerable tension placed on the soundboard and neck by the strings (> 700N with standard tuning.) The properties of standard guitar strings were measured, and the results were used to model strings on the complete guitar. Although the strings add a significant amount of tension to the soundboard, they contribute little to the dynamic motion of the soundboard [Laille, 2002, Maziere, 2002]. The model was used to construct an animation showing the vibratory modes of the soundboard [Laille and Maziere, 2002]. An important limitation of this model is that Catia is not able to model interactions of the guitar plates with the air, which is being frequency dependent (§2.8), and has a significant effect on the mode frequencies (§2.5).

The neck is an important element of the guitar at low frequencies. The two

MODES	Experimental model	Isotropic model	Orthotropic model
	59 Hz	54 Hz	57 Hz
	188 Hz	393 Hz	260 Hz

Figure 4.14: Low frequency modes of the complete guitar incorporating the neck of the instrument. From [Laille and Maziere, 2002].

first modes of vibration of the entire guitar that involve interaction with the neck, are given in Figure 4.14. Measurements of the pressure force ratio spectra after the addition of the neck show features occurring close to these frequencies, but not without the neck (§7.1). Similar motion is displayed in modal analysis studies of the low frequency modes of guitars [Russell and Pedersen, 1999, French and Hosler, 2001].

4.7 Conclusion: Applications of finite element simulations to instrument construction

The advantage to manufacturers of a reliable model of the vibratory behaviour of the guitar is that it would be possible to trial novel design modifications without constructing the instrument. Detailed modelling of the vibratory behaviour of the guitar is useful for predicting the effect of particular techniques used by luthiers in the manufacture of guitars. It is shown here that accurate determination of the geometry, density and Young's moduli is necessary. Such measurement is possible using techniques described in §5.2, if nominal values for E_R and ν_{ij} are assumed for the appropriate wood species.

For example, modelling of brace scalloping on a simple rectangular wooden plate with a single wooden diagonal brace shows there is very good agreement with Chladni figure measurements, both in modal shape and frequency for the lowest five modes. The modes affected the most are those with a nodal lines near the position of the brace, especially those with a number of phase changes along the length of the brace. Measurement shows that the Q-factor of high frequency peaks in the dynamic mass spectrum of simple plates with a scalloped brace is increased, and there is a general lowering of peak frequencies. An instrument with a soundboard modified in this way should thus have less variation in radiated output with excitation frequency.

These conclusions for the simple braced plate systems apply for the model of the free guitar soundboard; the third soundboard mode is affected most by the scalloping

of both the lower part of the cross-braces and the tone-brace.

The model of the free soundboard was then used to model the complete guitar [Laille and Maziere, 2002]. Coupling effects from the neck contribute to very low frequency modes (*ca.* 60 Hz) of the guitar (*qv* §7.1).

Future calculations

Some of the data in chapters 5, 6 and 7 could be further applied to numerical simulation of the guitar. However, it would be more useful if the models in this chapter were improved by addressing some of the challenges raised.

Further, while CASTEM 2000 is able to produce transfer functions of the modelled system, it is more difficult to program the detailed geometry required in modelling a guitar and it has a limited mesh size. Catia is more convenient to program complicated mesh geometries, but does not directly support the modelling of orthotropic materials. Neither package is currently able to model the interactions of plates with the surrounding air.

Modelling the effect of these changes on the overall sound produced by the guitar would be more complicated and is not performed here.

Chapter 5

Experimental: Selection of Materials

"While felling three spruce trees with a fellow violin maker at an altitude of 1700 metres, we were amazed by the differences in sound that were produced when the segments of the trunk came crashing down in the steep mountain terrain: One would make a dull sound while the other would be bright and clear as a bell."—Martin Schleske (1965-)

To produce wooden musical instruments with consistent mechanical properties, one must characterise the material properties of its components before construction. This chapter presents some techniques used to determine the important material properties, according to the luthier, of components incorporated into the steel-stringed acoustic guitars studied in this thesis. The Young's modulus in the longitudinal direction E_L is important for braces. This is also true for the soundboard, along with the Young's modulus in the transverse direction, E_T, and the mass density ρ. There may be some sensitivity of vibratory modes involving a large amount of

torsion to variation in the shear modulus G_{LR}, but the shear modulus G_{LT} and the Young's modulus in the radial direction, E_R, are not as important for determining the vibratory properties of thin plates [Ezcurra, 1996]. For thin beams and plates, the variation in Poisson's ratio for wood has little effect on the resulting dynamics.

The important soundboard braces are characterised by driving point dynamic mass measurements (§5.2). For the soundboards, the driving point dynamic mass at the bridge point, the damping of important resonances, and the spatial distribution of the normal vibratory modes by use of Chladni patterns (§6.3) are measured. Other components have less stringent vibratory and acoustic requirements [Meyer, 1983a].

The choice of wood species used for the various components of the guitars studied here are described in §5.1. The method used in measuring the elastic properties of wooden samples are given in §5.2, and some alternatives to this are presented in Appendix C. Desirable properties of the important components of the guitar are presented in §5.4, including measurements of the components incorporated into the guitars studied here. Internal damping of the components are given in §5.11 and the results are summarised in §5.12.

5.1 Timber used in the guitars studied

The great variety of species used in the manufacture of any individual guitar illustrates the level of exploitation and optimisation of the mechanical and æsthetic properties a luthier requires in order to produce a high quality instrument. A list

of the timbers used in manufacture of the components of the guitars studied here is given in Table 5.1. Not only is Sitka spruce sought after for brace material (§5.5), it is also used commonly for soundboard timber in steel-string guitars, giving a generally 'bright' sound (*i.e.* radiating relatively high power at high frequency [Schubert et al., 2004]). Engelmann spruce soundboards also give a relatively 'bright' sound but they are more 'mellow' than Sitka spruce soundboards. Western Red cedar is said to give even greater 'mellowness' [Belair guitars, 2002, Worland guitars, 2004, Alaska specialty woods, 2005]. Cedar is used more commonly in classical guitars. The three timbers mentioned here are commonly used for making soundboards and it is for this reason that these three timber species have been chosen for the present work. The other materials used in the construction of these instruments are used on production instruments made in the Gilet Guitars workshop.

Mahogany or rosewood is commonly used for back and side materials because of their visual beauty [Romanillos, 1987], but these timbers are also dense and provide a stiff enclosure so that more sound energy is radiated through the top of the instrument. The neck and neck-block are made from Amoora (*Amoora culcullata*), a dense timber with a high surface hardness. The fingerboard is of 'African' rosewood [1] (*Dalbergia holideria*) and the bridge is made of 'Indian' rosewood[2] (*Dalbergia laterfolia*) which are both visually attractive and also very dense, hard and resistant to moisture induced degradation. The tail-block is made of high quality hardwood ply (to reduce cracks forming along the grain) and is a combination of timbers. The

---

[1]This common term applies to a number of similar timber species originating in Africa.
[2]This common term applies to a number of similar timber species originating in India.

linings of the instrument (§3.4) help the glueing of the top soundboard and back plate to the sides and, depending on the style of lining, need to have a high grain density to prevent splitting due to the enforced curvature. The rosettes (§3.4) used here are manufactured from a combination of rosewood, ebony and maple cut into small square cross-sections ($\simeq 4$ mm^2) approximately 2 mm high. These are glued in a series of concentric rings. The butt-strip (§3.4) is made of a rectangular plate of rosewood with a small border of maple, the same thickness and type as the maple used in the bindings. The inlays (§3.4) have a purely decorative purpose and are made of mother-of-pearl. The nut is made of cattle bone. The saddles are made of a hard polymer (TUSQ$^{\text{TM}}$) and the bridge pins are also of a durable polymer. The frets and the machine (tuning) heads are made primarily of stainless steel.

5.2   Measurement techniques

A beam resonance measurement technique similar to that used by John Dunlop, M. Shaw and Redes Harjono [Dunlop and Shaw, 1991, Harjono, 1998], is used to measure the Young's modulus of wooden beams. The specimen to be tested is placed in the jaws of an aluminium clamp, as in Figure 5.2, so that the jaws firmly hold the beam halfway along its length. A time-varying force is applied to the base of the clamp by a shaker/vibrator (Brüel & Kjær 4809), with an impedance head (Brüel & Kjær 8001, force sensitivity: 379 mV/N Acceleration sensitivity: 3.12 mV/ms^{-2} Linear frequency range: $0 \rightarrow 6500$ Hz)). This enables measurement of the time-varying force and acceleration at this point. The dynamic mass (the ratio of these quantities) of the system is then analysed; the normal modes of the system are identified

Component	Wood Type	
	Botanical Name	Common name
Soundboard 1	*Picea sitchensis*	Sitka spruce
Soundboard 2	*Picea engelmannii*	Engelmann spruce
Soundboard 3	*Thuya plicata*	Western Red cedar
Back	*Entandrophragma cylindricum*	Sapele mahogany
Sides	*Entandrophragma cylindricum*	Sapele mahogany
Neck	*Amoora cucullata*	Amoora
Neck block	*Amoora cucullata*	Amoora
Soundboard bracing	*Picea sitchensis*	Sitka spruce
Back bracing	*Picea sitchensis*	Sitka spruce
Marriage strips	*Picea sitchensis*	Sitka spruce
Transverse bars	*Amoora cucullata*	Amoora
Fingerboard	*Dalbergia holideria*	African rosewood
Bridge	*Dalbergia laterfolia*	Indian rosewood
Bridge-plate	*Acer saccharum*	Sugar maple
Top linings	*Elaeocarpus grandis*	Blue fig
Back linings	*Entandrophragma cylindricum*	Sapele mahogany
Bindings	*Dalbergia laterfolia*	Indian rosewood
	Acer saccharum	Sugar maple
Tail block	various	various
Rosette	various	various
Butt-strip	various	various

Table 5.1: Woods used in manufacture of the three Martin OOO style guitars made and studied in this thesis.

by resonance features on the dynamic mass spectra.

Assuming a wooden beam held in this manner is a transversely vibrating cantilever, the Young's modulus E_i (in the direction parallel to the beam axis) may be obtained by measurement of the frequency of the ith mode of vibration, f_i:

$$E_i = \rho(\frac{8f_iL^2}{\pi s_i^2\kappa})^2 \tag{5.2.1}$$

where κ is the radius of gyration of the beam in the direction of the applied excitation. For beams with a constant rectangular cross-section, of height t, $\kappa = \frac{t}{\sqrt{12}}$. Here, L is the half-length and ρ is the mass density of the sample. By solving Equation 2.7.4 the coefficients for the cantilever beam system, s_i, are:

$$s_i = 1.194, 2.988, 5, 2.000j - 1.000 \tag{5.2.2}$$

for $i = 1, 2, 3, ...$ and $j \geq 3$.

An example of a typical dynamic mass driving point function for a wooden beam is shown in Figure 5.1. This gives the frequency of each normal mode of the beam, f_i.

One of the advantages of this clamping system is that the clamp has a relatively small contact area with the wood samples, which minimises mechanical interference. Most importantly, the measurements are nondestructive. The results of measurements made on wood material suitable for soundboard braces, from a single large block of wood, are presented in Table 5.6. Some alternative measurement techniques are presented in Appendix C, which could be of use to a luthier in the characterisation of materials.
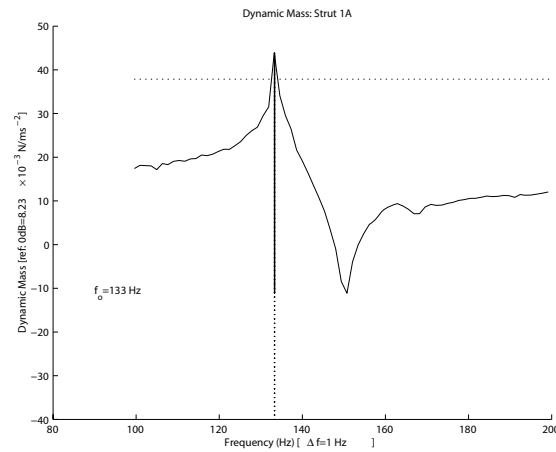
Figure 5.1: Dynamic mass driving point function for a typical wooden beam sample, used for soundboard bracing, held in the clamping system used here.
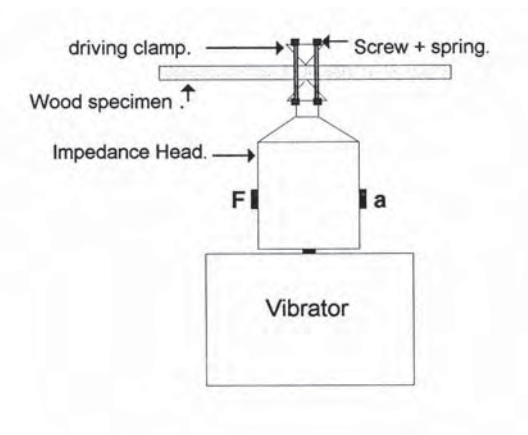
Figure 5.2: Clamping system used for measurement of vibratory behaviour of wooden beam samples (From [Harjono, 1998]).

Component	Mass (g)
B&K8001 impedance head	30.7
Holding shaft	17.2
Clamp	21.9
Mica washers	1.0
Total mass	70.6

Table 5.2: Masses of apparatus used in clamping system used to measure E_L for wooden beams. The mass in front of the impedance head is 40.1 grams.

The cantilever behaviour of the system

The assumption that the vibrational behaviour of long beams held in the clamp used here can be effectively modelled as a cantilever is based on the assumption that the clamp sufficiently ensures no relative rectilinear or rotational motion is allowed. Is this assumption appropriate? The frequency ratios of consecutive normal modes of a cantilever are calculated (for example [Timoshenko, 1934, Sokolnikoff, 1946, McLachlan, 1951, Skudrzyk, 1968, Landau and Lifshitz, 1970]).

Because $E_i \propto \frac{f_i^2}{s_i^4}$ (Equation 5.2.1) and, for a viscoelastic solid, $\frac{E_{i+1}}{E_i} \simeq 1$, (*i.e.* the Young's modulus is independent of the mode of vibration) the progression of the mode frequencies should then be:

$$\frac{f_{i+1}}{f_i} = (\frac{s_{i+1}}{s_i})^2 \qquad (5.2.3)$$

Comparisons between the theoretical frequencies and measurements of a single aluminium rod with a circular cross-section are shown in Table 5.3. For this experiment the nodal and antinodal positions were found by touch: the tip of the author's index finger was lightly touched to the surface of the beam and moved slowly along the length until the maxima/minima were detected. This method is effective at frequencies below about 1 kHz, after which human tactile sensitivity is very limited for small amplitudes [Brisben et al., 1999].

The aluminium beam used here has a mass of 25.0 ± 0.5 g, a diameter of 6.00 ± 0.02 mm, and a total length of 1.022 ± 0.002 m. The uncertainty in the exact position of the anitnodes is much higher than that for the nodes (± 13 mm, compared to ± 2 mm at 560 Hz, the frequency of the mode $i = 4$.) The measured vibratory
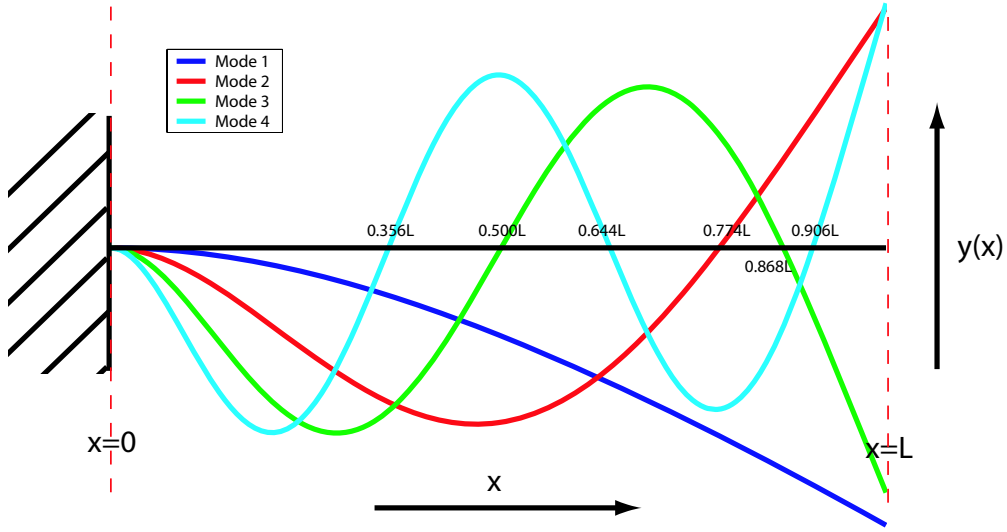
Figure 5.3: Theoretical motion of a cantilever beam for the first four normal modes. Numbers indicate nodal positions as a fraction of total length.

behaviour of this beam is in good agreement with what we would expect from a cantilever.

The relation $c_L = \sqrt{\frac{E_L}{\rho}}$ is used without concern for any other type of wave. In fact, this is valid only if the length of the beam, L, is much more than the largest lateral dimension, d (*viz.* $\frac{L}{d} \gtrsim 18$) [Štubňa and Liška, 2001], after which the analysis of the motion becomes more involved. The braces to be tested here have dimensions $8.0 \times 13.5 \times 460.0$ mm, so $\frac{L}{d} = 34.1$. For smaller $\frac{L}{d}$, shear deformations are not negligible and a proper treatment would require an application of the Timoshenko beam equation [Timoshenko, 1934].

Mode, i		Frequency ratio	Nodal positions, $\frac{x}{L}$			
1	(Theoretical)	1	0	-	-	-
	(Aluminium beam)	1	0	-	-	-
2	(Theoretical)	6.26	0	0.774	-	-
	(Aluminium beam)	6.05	0	0.788	-	-
3	(Theoretical)	17.54	0	0.500	0.868	-
	(Aluminium beam)	16.94	0	0.511	0.881	-
4	(Theoretical)	34.37	0	0.356	0.644	0.906
	(Aluminium beam)	32.94	0	0.364	0.654	0.902

Table 5.3: Comparison of nodal positions for normal modes of a theoretical cantilever beam and experiment on an aluminium beam with a constant cross-section, using the system described here. The frequency ratio is the frequency of the mode divided by the frequency of the fundamental mode ($i = 1$). The nodal positions are expressed as a fraction of the total length of the beam.

5.3   Measuring and controlling the moisture content of wood

The moisture content of all important wood samples used was measured. For example, the large block of Sitka spruce used to select brace wood for the three guitars studied here (§5.5) had been seasoned for two years but, immediately after processing to produce brace stock, the moisture content of some of the brace-wood from the interior of the block was above the approximate 12% that should be expected for equilibrium with the humid Sydney environment. For example, strut 4B was initially at 14.4%. After 63 days, it had equilibrated to 11.5%.

There are various means of measuring the moisture content of wood, involving electrical resistance, capacitance, x-ray, or ultrasonic methods, but the most accurate is that of measuring the mass loss after completely drying a specimen, the *oven-dry*

method [Forest Products Laboratory, 1999]. With this method, care must be taken to not use such a high temperature that will result in moisture sorption hysteresis, (*e.g.* by the release some of the more volatile matter) thereby decreasing the mass of the sample in addition to the actual water loss. Although there is a small amount of sorption hysteresis in any sample of wood dried to a very low moisture content, because of permanent changes to the microstructure, it is a relatively small effect if performed gradually [Forest Products Laboratory, 1999]. The process of achieving ambient equilibrium moisture content is at a higher rate in drying from a very humid environment than that of absorbing water when going from a very dry environment [Fryxell, 1990]. As a rule of thumb, to reach the equilibrium moisture content of the environment, the ratio of the water absorbtion rate to the desorption rate, for the same mass of wood, is approximately 0.85 [Forest Products Laboratory, 1999].

A thermostatically controlled oven with an air cavity of 0.07 m^3 was used to oven-dry the wooden samples. The drying temperature was set to 101 ± 2°C (some tests were performed at lower temperatures) and the mass of the sample (having the same initial mass and dimensions as the specimens to be incorporated into each instrument) was checked periodically until no variation of mass with time was measured. Care was taken so that measurement of the mass of the sample, taken in the ambient environment, was made over the smallest time possible (approximately 90 seconds) because absorbtion of moisture is very rapid at low moisture levels. Cotton gloves were worn to minimise moisture and oils being adsorbed into the wood during handling.
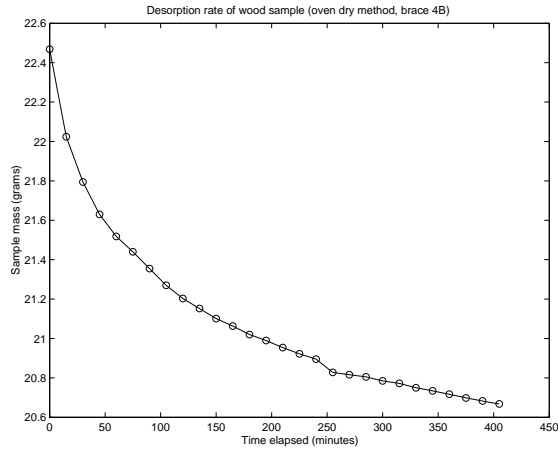
Figure 5.4: Measurement of the desorption of a wooden brace sample in an oven at constant temperature (Temperature: 80°C).

An example of the rate of moisture loss for samples of brace wood in this oven is given in Figure 5.4. The moisture content, Υ, of an oven-dried sample is defined as:

$$\Upsilon = \frac{m_{\text{inital}} - m_{\text{dry}}}{m_{\text{dry}}} \tag{5.3.1}$$

where m_{initial} is the initial mass and m_{dry} is the mass after the oven-drying process. This (*oven dry*) mass is determined when the sample mass is no longer decreasing with time in the drying oven and is a function of the required accuracy of measurement and the limit of precision of the mass balance, as well as exposure to the ambient humidity during measurement.

The results of measurements of the Western Red cedar sample WRC0 gave $m_{\text{initial}} = 2.327$ g and $m_{\text{dry}} = 2.135$ g, hence the moisture content was 9.0% . The uncertainty in the moisture content values, $\Delta\Upsilon$, may be derived from the masses and the uncertainty in the mass measurements thus:

$$\Delta\Upsilon = \frac{(3m_{\text{dry}} - m_f)\Delta m}{(m_{\text{dry}} + \Delta m)m_{\text{dry}}} \tag{5.3.2}$$

where m_{dry} is a constant, m_f is the mass of the specimen when measured, and Δm is the uncertainty in the mass measurement of both masses.

As an example, brace 4B had a dry mass of $m_{\text{dry}} = 20.2$ g. At an equilibrium moisture content of 11.4%, $m_f = 22.5$ g and $\Delta m = 0.05$ g, and therefore $\Delta\Upsilon = 0.47\%$. For $m_f = m_{\text{dry}}$ (*i.e.* $\Upsilon = 0\%$) with the same brace, $\Delta\Upsilon = 0.49\%$. These values are typical for the braces measured here, so the uncertainty in the equilibrium moisture content will be taken as being $\Delta\Upsilon = 0.5\%$ for the brace wood samples.

The above treatment is an example of how to accurately determine the moisture content of a sample of wood. Because wood is so hygroscopic, it is important to know the moisture content in order to control for quality and measurement of properties. The oven-dry method, although an accurate method of measuring moisture content, is rather time-consuming. There are quicker methods available that use devices to measure the change in electrical properties (the conductivity or the dielectric constant) due to the presence of moisture but they are often less accurate, species dependent, and are often constrained in their effective measurement range [Simpson, 1998].

Variation of E_L with moisture content

Measurements of the Young's modulus in the longitudinal direction on soundboard and brace samples are given in Table 5.4 as a function of the moisture content.

Naïve calculation suggests the changes in speed of sound of the material are not merely from mass loading effects of the additional water. If this were the case, for

Sample	Density $\mathrm{kg \cdot m^{-3}}$	f_1 Hz	E_L GPa	Moisture content %
WRC0	300.58	1199	6.49	8.99
WRC0	297.35	1213	6.58	7.8
ES0	390.23	1280	10.44	8.99
ES0	389.71	1284	10.22	8.8
Strut 4B	(20.2)	157.6	17.4	0.0
Strut 4B	(20.8)	148.6	15.9	3.3
Strut 4B	(21.4)	148.1	16.2	6.0
Strut 4B	(21.6)	145.4	15.8	6.9

Table 5.4: The variation of Young's modulus in the longitudinal direction, E_L, with moisture content for small samples of wood. Values of E_L were obtained through measurement of the vibration of a long cantilever beam of a sample of wood, after the oven-dry mass of the sample was measured, allowing determination of the moisture content.

the cantilever beam, $f_1 \propto \frac{\kappa c_L}{L^2}$, where f_1 is the frequency of the first mode of the cantilever, κ is the moment of inertia in the axis of the lateral bending. c_L is the speed of sound, in the longitudinal direction, within a beam of length L. Denoting moisture content dependence with a subscript Υ:

$$f_{1,\Upsilon} \propto \frac{t_\Upsilon c_{L,\Upsilon}}{L_\Upsilon^2} \tag{5.3.3}$$

In general, the change in dimensions of a piece of wood are dependent on the moisture content, and these changes differ along the principal axes. The change in the longitudinal direction is negligible for spruce [Forest Products Laboratory, 1999], and the changes in the volume and in length in the tangential direction, in drying from the green state to some moisture content Υ (below 30%), are given approximately by the shrinkage rates, $S_{V,\Upsilon}$ and $S_{T,\Upsilon}$, in equations 5.3.4 and 5.3.5:

$$S_{V,\Upsilon} = 0.115\frac{0.3 - \Upsilon}{0.3} \tag{5.3.4}$$

$$S_{T,\Upsilon} = 0.075\frac{0.3 - \Upsilon}{0.3} \tag{5.3.5}$$

Taking the ratio at $\Upsilon = 0\%$ and using the definition of moisture content, Equation 5.3.1:

$$\begin{aligned}
\frac{t_\Upsilon}{t_0} &= \frac{S_{T,\Upsilon}}{S_{T,0}} \\
\frac{V_\Upsilon}{V_0} &= \frac{S_{V,\Upsilon}}{S_{V,0}} \\
\frac{m_\Upsilon}{m_0} &= 1 + \Upsilon
\end{aligned} \tag{5.3.6}$$

Expressing the speed of sound as $c_{L,\Upsilon} = \sqrt{\frac{E_{L,\Upsilon}}{\rho_\Upsilon}}$ and using Equation 5.3.3, the ratio of the frequency of the first mode of the beam at moisture content Υ, $f_{1,\Upsilon}$ to the frequency of the same mode at $\Upsilon = 0$ %, $f_{1,0}$ is:

$$\begin{aligned}
\frac{f_{1,\Upsilon}}{f_{1,0}} &= \frac{t_\Upsilon}{t_0}\sqrt{\frac{\rho_0}{\rho_\Upsilon}}\sqrt{\frac{E_{L,\Upsilon}}{E_{L,0}}} \\
&= \frac{S_{T,\Upsilon}}{S_{T,0}}\sqrt{\frac{S_{V,\Upsilon}}{S_{V,0}}\frac{1}{1+\Upsilon}}\sqrt{\frac{E_{L,\Upsilon}}{E_{L,0}}} \\
&= \sqrt{\frac{(0.3 - \Upsilon)^3}{0.3^3(1+\Upsilon)}}\sqrt{\frac{E_{L,\Upsilon}}{E_{L,0}}}
\end{aligned} \tag{5.3.7}$$

Using the data from Table 5.4 for strut 4B at $\Upsilon = 6\%$, the frequency ratio becomes $\frac{f_{1,0.06}}{f_{1,0.00}} = 0.940 \pm 0.007$. But if the Young's moduli are independent of moisture content ($\sqrt{\frac{E_{L,\Upsilon}}{E_{L,0}}} \simeq 1$), as is the case with viscoelastic solids [American Institute of Physics, 1972] , then from Equation 5.3.7 $\frac{f_{1,0.06}}{f_{1,0.00}} = 0.6950 \pm 0.005$. Therefore there are changes to the magnitude of E_L with moisture. Although this treatment is probably a little simplistic, it is plausible that this behaviour could be explained by stronger hydrogen and other intramolecular bonds as a result of the rehydration process. These microscopic quantities have a great influence on the properties of the material [Gibson and Ashby, 1997, Gibson, 1989].

5.4   Selection criteria

The selection of appropriate materials requires much 'hands-on' experience to master. With practice, assessment of some properties of timber may be carried out without the aid of measuring tools. However this is limited to a few properties and takes many years to become proficient (§3.4).

For bracing (§5.5), it is desirable to possess a high elastic modulus. This, for beams of the same height and cross-section, is proportional to the *stiffness-to-mass ratio*[3], a quantity luthiers value highly in determining brace material [Gilet, 2000]. The fingerboard(§5.9), neck(§5.8) and head-stock material need to have a high surface hardness and moisture resistance. Depending on the type of guitar, the back and sides(§5.10) should be made of a stiff, dense wood. It is less clear what is most

---

[3] $hE_L(\frac{\kappa}{M})^2$, where h is the height of the brace, E_L the longitudinal Young's modulus, κ the radius of gyration and M the total mass of the brace.

desirable for wood on the bridge (§5.7) and soundboard(§5.6). It has been conjectured that the quantity $\rho c_L = \frac{E_L}{c_L} = \sqrt{E_L\rho}$ or the radiation ratio, $\frac{c_L}{\rho} = \sqrt{\frac{E_L}{\rho^3}}$ are desirable parameters to 'optimise' (in this case to emulate known values for desirable instruments) for plate material [Schelleng, 1963]. However optimising this quantity alone is unlikely to result in a consummate component. For example, the internal damping of these components have a great, but largely unquantified, effect on the vibratory and acoustic behaviour of the guitar [Haines, 2000, Schleske, 1990].

5.5   Bracing material

Despite their important structural and acoustic function (§2.1), braces are probably the simplest components to optimise in terms of mechanical properties: a luthier desires a brace with a high E_L. However it is difficult to compare the effect of this to existing instruments because measurement of the brace material is not commonly carried out, nor controlled experimentation on the effects of braces with variable E_L. As a species, Sitka spruce tends to have a high E_L, and thus is commonly used for braces [Bourgeois, 1994].

Grouping brace material by similarity of elasticity

Because the purpose here is to obtain three similar guitars, it is required to obtain three sets of brace material that have the most similar E_L. I took a sample of 20 braces from the same seasoned and quarter-sawn block of Sitka spruce aligned so that the length of the block was parallel to the grain. These were labelled in three
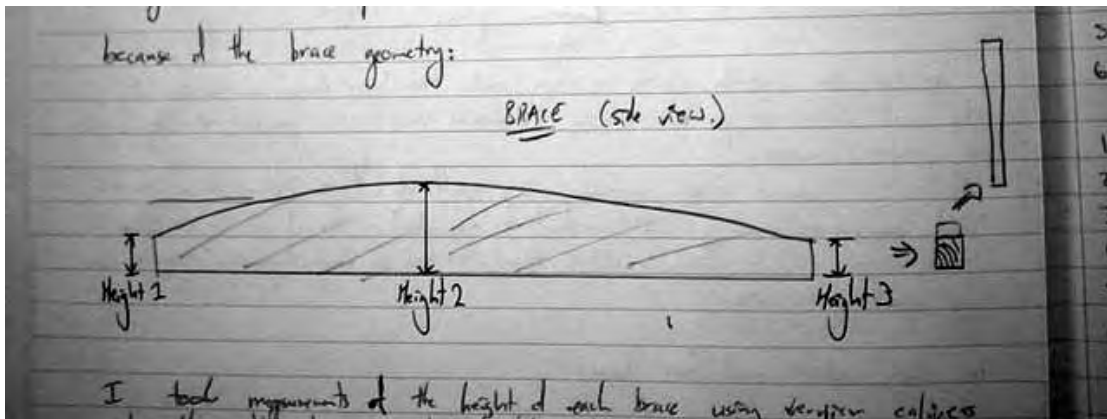
Figure 5.6: Measurement scheme for the dimensions of a brace. The effective height is the mean of the three heights.

consecutive groups (Figure 5.5).

Sitka spruce brace wood
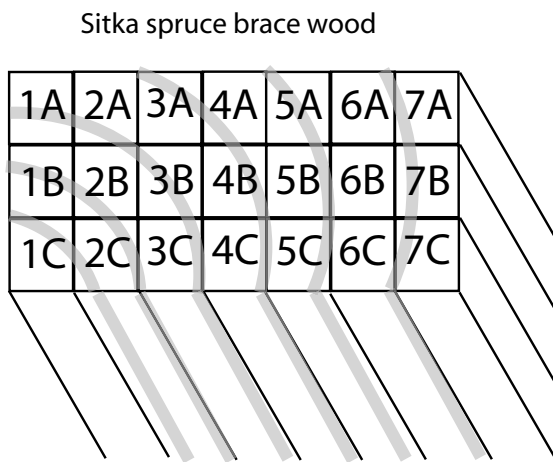
Figure 5.5: Labels of a block of Sitka spruce cut into brace material.

The dimensions and masses of these braces, as measured over an hour[4] are in Table 5.5.

The most important braces, for both structural and acoustic purposes, are the main cross-braces (§3.4) [Ross and Rossing, 1979]. Table 5.6 summarises the longitudinal Young's moduli, E_L (estimated from the first normal mode of a cantilever with the length dimensions of

---

[4]Effects due to possible changes in moisture content should not be noticeable over this short duration.

Table 5.5) of a selection of braces taken from the same block of Sitka spruce (*Picea sitchensis*).

Three pairs were selected to be as similar to each other as possible. If the entire set of Young's moduli is $Y = \{y_i\}_{i=1}^{N}$ where y_i represents, in increasing order of magnitude, the ith longitudinal Young's modulus in a sample of size N. The differences between the ith and jth Young's moduli are defined as $d_{ij} = -d_{ji} = (y_i - y_j)$. To simplify the notation, define $d_i \equiv d_{i,i+1}$. In order to find the most similar Young's moduli, d_i is minimised, by examining the differences *between these differences*. Defining the *second-order difference* as the difference between the y_ith, y_jth and y_kth Young's modulus in the longitudinal direction:

$$D_{ijk} \equiv d_{ij} - d_{jk} = y_i - 2y_j + y_k \tag{5.5.1}$$

and, for convenience, define:

$$D_i \equiv D_{i+2,i+1,i} = (d_{i+2} - d_{i+1}) - (d_{i+1} - d_i) = y_{i+2} - 2y_{i+1} + y_i \tag{5.5.2}$$

The lowest values of $|D_i|$ in the sample are retained for the cross-braces in the instruments. The most similar set is removed from the selection and then the calculation is repeated, without replacements. The lowest values of $|D_i|$ are then found in the modified set and this process is continued until all required specimens are obtained. Results from the cross-brace sample are summarised in Table 5.7.

From these results, the braces are arranged in sets of three with the most similar values of elasticity, as in Table 5.8, or pairs with the greatest similarity in Table 5.9.

Label	Mass	Length	Width	Height 1	Height 2	Height 3
	(g)			(mm)		
1A	24.133	460.00	8.00	11.24	12.20	11.42
2A	24.062	460.00	8.00	11.30	12.00	9.58
3A	24.277	460.00	8.00	11.71	13.70	13.24
4A	24.443	460.00	8.00	11.40	14.00	13.68
5A	24.968	460.00	8.00	11.58	13.84	13.40
6A	24.063	460.00	8.00	11.70	13.50	13.42
1B	23.644	460.00	8.00	13.60	14.08	11.48
2B	23.025	460.00	8.00	13.20	14.00	11.80
3B	22.494	460.00	8.00	11.64	13.98	11.52
4B	23.055	460.00	8.00	11.88	14.06	13.48
5B	22.304	460.00	8.00	13.00	13.54	11.70
6B	23.004	460.00	8.00	11.58	13.70	13.40
7B	23.306	460.00	8.00	13.30	13.68	11.30
1C	22.351	460.00	8.00	13.12	14.00	13.20
2C	24.661	460.00	8.00	13.22	14.18	10.72
3C	23.480	460.00	8.00	11.54	13.82	13.42
4C	23.403	460.00	8.00	11.68	13.90	13.10
5C	22.800	460.00	8.00	13.58	13.84	11.58
6C	22.588	460.00	8.00	11.72	14.00	13.28
7C	22.973	460.00	8.00	11.52	13.92	13.30
	±0.0005	±0.02	±0.01			

Table 5.5: Mass and length measurements of braces taken from a single block of Sitka spruce. (Sample moisture content $11.5 \pm 0.5\%$).

Strut	Mean volume	Density	f_1	E_L
	(mm^3)	$(\text{kg} \cdot \text{m}^{-3})$	(Hz)	(GPa)
1A	42762 ± 166	564.36 ± 2.20	133.24	16.19 ± 0.53
2A	40333 ± 163	596.58 ± 2.42	130.55	16.55 ± 0.56
3A	47435 ± 172	512.04 ± 2.40	131.89	14.49 ± 0.60
4A	47435 ± 172	509.89 ± 2.40	129.20	13.96 ± 0.60
5A	47619 ± 172	524.33 ± 1.90	135.93	15.72 ± 0.50
6A	47362 ± 172	508.07 ± 1.85	122.47	12.46 ± 0.43
1B	48024 ± 172	492.34 ± 1.78	138.62	15.34 ± 0.48
2B	47840 ± 172	481.29 ± 1.74	145.35	16.56 ± 0.50
3B	45558 ± 169	493.74 ± 1.85	145.35	16.92 ± 0.51
4B	48355 ± 173	476.79 ± 1.72	148.04	16.54 ± 0.49
5B	46920 ± 171	475.36 ± 1.74	145.35	16.28 ± 0.49
6B	47435 ± 172	484.96 ± 1.77	142.66	16.09 ± 0.49
7B	46957 ± 171	496.33 ± 1.82	141.31	16.23 ± 0.50
1C	49459 ± 174	451.91 ± 1.60	142.66	14.88 ± 0.45
2C	46773 ± 171	527.29 ± 1.94	139.97	16.62 ± 0.52
3C	45301 ± 164	518.31 ± 1.88	145.35	17.64 ± 0.53
4C	47435 ± 172	493.37 ± 1.80	138.62	15.46 ± 0.49
5C	47840 ± 172	476.59 ± 1.73	139.97	15.15 ± 0.47
6C	47840 ± 172	472.16 ± 1.71	149.39	16.95 ± 0.50
7C	47509 ± 172	483.55 ± 1.76	148.04	17.74 ± 0.53
			± 1.8 Hz	

Table 5.6: The longitudinal Young's moduli, E_L, of braces taken from a single block of Sitka spruce. Measurements were obtained of the fundamental vibratory mode (with frequency f_1) of each brace held in a cantilever beam apparatus. The sample moisture content was $11.5 \pm 0.5\%$.

E_L ranking	Label	E_L	Difference, d_i	Second order difference, D_i (GPa)
1	6A	12.46	1.5	-0.97
2	4A	13.96	0.53	-0.14
3	3A	14.49	0.39	-0.12
4	1C	14.88	0.27	-0.08
5	5C	15.15	0.19	-0.07
6	1B	15.34	0.12	0.14
7	4C	15.46	0.26	0.11
8	5A	15.72	0.37	-0.27
9	6B	16.09	0.1	-0.06
10	1A	16.19	0.04	0.01
11	7B	16.23	0.05	0.21
12	5B	16.28	0.26	-0.25
13	4B	16.54	0.01	0.00
14	2A	16.55	0.01	0.05
15	2B	16.56	0.06	0.24
16	2C	16.62	0.3	-0.27
17	3B	16.92	0.03	0.66
18	6C	16.95	0.69	-0.59
19	3C	17.64	0.1	-
20	7C	17.74	-	-

Table 5.7: Differences of first and second order in Young's moduli of a selection of braces. Data is obtained from Table 5.6.

Set	E_L ranking i, j, k	Label	Second order difference, D_{ijk} (GPa)
1	13,14,15	4B,2A,2B	0.00
2	10,11,12	1A,7B,5B	0.01
3	5,6,7	5C,1B,4C	-0.07
4	2,3,4	4A,3A,1C	-0.14
5	8,9,16	5A,6B,2C	0.16
6	18,19,20	6C,3C,7C	-0.59
7	1,17	6A,3B	-

Table 5.8: Braces from a single block of Sitka spruce arranged in triplets according to similarity of E_L magnitudes. This is achieved by calculating the minimum of the second order difference, $|D_{ijk}|$, without replacement. Data is from Table 5.6.

Set	E_L ranking i, j	Label	d_{ij} (GPa)
1	14,15	2A,2B	0.01
2	17,18	3B,6C	0.03
3	10,11	1A,7B	0.04
4	19,20	3C,7C	0.06
5	13,16	4B,2C	0.08
6	6,7	1B,4C	0.12
7	9,12	5B,6B	0.19
8	4,5	1C,5C	0.27
9	3,8	5A,3A	1.23
10	1,2	4A,6A	1.50

Table 5.9: Braces from a single block of Sitka spruce arranged in doublets according to similarity of E_L magnitudes. This is taken as the minimum of the differences $|d_{ij}|$ without replacement. Data is from Table 5.6.

Spatial Distribution of Young's Modulus
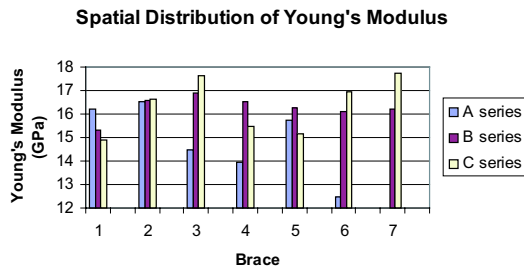
Figure 5.7: The spatial distribution of E_L for neighbouring braces made from a single block of Sitka spruce. There appears to be little correlation of E_L with near neighbours in either direction. The spruce block was of high quality seasoned timber. Data from Table 5.6.

Spatial distribution of mechanical properties of wood

The measured E_L of a brace might be expected to be similar to that of a proximate brace. This does not appear to be the case. Figure 5.7 shows the measured variation in E_L for wood to be used as cross-brace material (seasoned Sitka spruce of high quality). There appears to be little, if any, correlation between neighbours in the transverse (labels '1'-'7') or the radial (labels 'A'-'C') directions. Although the wood tested here is of high quality, these results are typical of a given wood sample [Forest Products Laboratory, 1999] and demonstrate the need to test each sample of wood individually to achieve acceptable quality control.

5.6   Soundboard material

Three soundboard materials most commonly used on steel-string guitars were compared and contrasted. Because the tests performed here are designed to control for the material similarity of as many important components as possible, *excepting the*

Sample	Length	Width	Thickness	Grain density	Comment
		mm		mm^{-1}	
WRC0	99.0	20.0	3.91	0.700	moisture control
WRC1	100.0	20.0	3.94	0.700	-
WRC2	99.5	20.0	3.84	0.450	-
WRC3	100.0	20.0	3.78	$0.429 \rightarrow 1.000$	cross-grain $(i = T)$
ES0	99.5	20.0	3.84	0.550	moisture control
ES1	100.0	20.0	3.96	0.425	-
ES2	100.0	20.0	3.78	0.650	-
ES3	90.0	20.0	3.82	$0.400 \rightarrow 0.923$	cross-grain $(i = T)$
SS1	99.0	20.0	4.44	0.850	-
	± 0.25 mm		± 0.01 mm	± 0.001 mm^{-1}	

Table 5.10: Dimensions of soundboard samples (at 9.0% moisture content).

soundboards, it was not necessary to control for variation between the soundboard materials; characterisation being sufficient.

Measurements of the dimensions, grain densities, and moisture conditions of samples of the wood from the soundboards of the guitars studied here are given in Table 5.10. The longitudinal Young's moduli and densities are given in Table 5.11. Note that only one sample was available from the Sitka spruce soundboard due to the loss of much of the surrounding wood. Because the soundboard is composed of two book-matched and quarter-sawn (§3.2) pieces of timber, identification of the distance of each sample from the centre of the soundboard is possible by examining the grain density. The higher the grain density, the closer the sample is to the central axis of the guitar.

Because the soundboard is constructed in an environment with a controlled relative humidity that is lower than the ambient ($43 \pm 2\%$), the soundboards are unable to be exposed to the ambient atmosphere for very long because of the tendency to

Sample	Direction i	Volume mm^3	Mass g	Density kg$\cdot$ m^{-3}	f_1 Hz	E_i GPa
WRC0	L	7700 ± 100	2.327	301 ± 5	1198.6	6.5 ± 0.2
WRC1	L	7900 ± 100	2.356	299 ± 5		
WRC2	L	7600 ± 100	2.417	316 ± 6		
WRC3	T	7600 ± 100	2.303	305 ± 6		
ES0	L	7600 ± 100	2.982	390 ± 7	1280.1	10.4 ± 0.4
ES1	L	7900 ± 100	3.003	379 ± 7		
ES2	L	7600 ± 100	2.963	392 ± 7		
ES3	T	6900 ± 100	2.715	395 ± 7		
SS1	L	8800 ± 200	3.797	432 ± 8		
			± 0.001		± 0.6	

Table 5.11: Some measured mechanical properties of soundboard samples at 9.0% moisture content. E_i is the Young's modulus of the sample, in the direction i (*viz.* L or T) obtained from f_1, the frequency of the first cantilever mode of the sample.

Sample	Direction i	Density kg$\cdot$ m^{-3}	f_1 Hz	E_i GPa	Moisture content (%)
WRC0	L	297 ± 5	1213	6.6 ± 0.2	7.8
WRC1	L	302 ± 5	1211	6.8 ± 0.2	10.0
WRC2	L	320 ± 6	-	-	10.2
WRC3	T	308 ± 6	-	-	10.2
ES0	L	390 ± 7	1284	10.2 ± 0.4	8.8
ES1	L	385 ± 7	1259	9.3 ± 0.3	10.7
ES2	L	398 ± 7	1289	11.1 ± 0.4	10.6
ES3	T	401 ± 7	414	0.70 ± 0.03	10.7
SS1	L	438 ± 8	1480	11.2 ± 0.4	10.6
			± 0.6		± 0.1

Table 5.12: Mechanical properties of soundboard samples, at various moisture contents. E_i is the Young's modulus of the sample, in the direction i (*viz.* L or T) obtained from f_1, the frequency of the first cantilever mode of the sample.

Sample	Axis	Moisture content	c_i	ρc_i	$\frac{c_i}{\rho}$
	i	(%)	(ms^{-1})	(kg $\cdot$ m$^{-2}s^{-1} \times 10^6$)	(m^{4}kg$^{-1}s^{-1} \times 10^{-3}$)
WRC0	L	7.8	4714 ± 82	1.40 ± 0.03	63 ± 2
WRC1	L	10	4745 ± 80	1.43 ± 0.03	64 ± 2
WRC2	L	10.2	-	-	-
WRC3	T	10.2	-	-	-
ES0	L	8.8	5114 ± 110	1.99 ± 0.06	76 ± 2
ES1	L	10.7	4915 ± 91	1.89 ± 0.05	78 ± 2
ES2	L	10.6	5281 ± 106	2.10 ± 0.06	75 ± 2
ES3	T	10.7	1321 ± 31	0.53 ± 0.02	304 ± 9
SS1	L	10.6	5057 ± 101	2.21 ± 0.06	87 ± 2

Table 5.13: Some properties of soundboard sample materials derived from Table 5.12.

Soundboard	Mass (g)
Sitka spruce	306.7
Engelmann spruce	276.3
Western Red cedar	249.3
	± 0.05

Table 5.14: Masses of the guitar soundboards before glueing to the sides and back. Measurements were made after storage in a humidity and temperature controlled environment, resulting in an equilibrium moisture content of approximately 8%.

curl or warp due to moisture absorption. Therefore measurements made outside of this controlled environment must be made as quickly as possible so that the soundboards do not reach the ambient equilibrium moisture content and suffer structural damage as a consequence. Measurements of the total masses of the soundboards (before glueing onto the sides and back) were made directly after removal from this controlled environment (Table 5.14).

Bridge sample	Mass (g)
1	57
2	57
3	57
4	56
5	57
6	57
7	57
8	57
	±1

Table 5.15: Masses of a selection of bridge stock material of similar dimensions.

5.7 Bridge material

The masses of a selection of eight potential pieces of bridge wood of approximately the same dimensions were measured (Table 5.15).

There was not a large variation in the mass of each sample. Three bridge sets were taken, each with a mass of 57 ± 1 g.

The bridges have been made to the same dimensions as each other to within ± 0.2 mm in any direction. Despite their seemingly complicated geometry (Figure 2.5) the shape is reproducible to this accuracy because there are specialised tools (*jigs*) to manufacture the bridges (§3.4) and the grain fibres in the species of wood used (Indian rosewood, *Dalbergia laterfolia*) are very short and packed closely together. This allows fine adjustments in thickness to be made. During construction, the sizes of all three bridges were compared to each other and adjusted.

In order to provide a convenient and reversible coupling between the excitation and measurement apparatus and the guitar, a single neodymium-iron-boron (NdFeB)

Sample	Mass	Density	f_1	E_L	Moisture content
	(g)	(kg · m^{-3})	(Hz)	(GPa)	(%)
1L	6.419	848 ± 2.6	557	13.4 ± 0.1	-
2L	6.883	847 ± 2.5	632	15.2 ± 0.1	-
3L	6.836	851 ± 2.6	608	14.6 ± 0.1	-
1M	0.331	994 ± 28	-	-	15.3 ± 0.1
2M	0.308	952 ± 27	-	-	17.6 ± 0.1
3M	0.285	998 ± 30	-	-	17.8 ± 0.2
	± 0.0005		$\pm 0.6\ Hz$		

Table 5.16: Properties of sample material from the bridges used here. The uncertainties for densities of the 'M' sample series are higher than that for the 'L' series because of their less regular geometry.

permanent rare-earth magnet was inserted into the bridge of each guitar. This modification to the bridge is discussed in Appendix E.

The three most similar magnets were selected from a sample of 16, following measurements of their magnetic flux densities (Table 5.17).

Each magnet was a cylinder, 6.0 mm in length, with a 6.0 mm diameter, and had a mass of 1.3 g. A hole was drilled into the centre of each bridge such that the magnets to be inserted would fit tightly and protrude 1.0 mm from the surface. A very small amount of cyanoacrylate adhesive ('Hot Stuff Superglue') was applied to the slight cone made by the drill bit.

5.8 Neck material

The wood used for the necks is the species *Amoora cucullata*. Because the appropriate material property to optimise here is not known, and obtaining a suitable sample from each set of neck stock material was difficult, the three neck woods most similar to each other in density were taken from a selection of 27. These measurements were

Magnet	Field Strength (mT)			
	Maximum	Minimum	$\frac{Maximum-Minimum}{2}$	$\frac{Maximum+Minimum}{2}$
1	384	-470	427.0	-86
2	394	-462	428.0	-68
3	399	-464	431.5	-65
4	369	-414	391.5	-45
5	399	-475	437.0	-76
6	372	-446	409.0	-74
7	337	-419	378.0	-82
8	388	-466	427.0	-78
9	386	-466	426.0	-80
10	409	-483	446.0	-74
11	394	-465	429.5	-71
12	376	-430	403.0	-54
13	389	-453	421.0	-64
14	392	-468	430.0	-76
15	363	-432	397.5	-69
16	371	-450	410.5	-79
	± 0.5			

Table 5.17: Selection of cylindrical rare earth (NdFeB) magnets to be incorporated into the bridges. Each is 6.0 mm high, with a 6.0 mm diameter, and has a mass of 1.3 g.

Bridge	Mass (g)	Density (kg $\cdot$ m^{-3})	E_L (GPa)	Moisture content (%)
1	34.094	478.6	13.4	15.3
2	34.212	509.9	15.2	17.6
3	34.805	500.1	14.6	17.8

Table 5.18: Some material properties of the bridges used on the guitars stupid here.

Length	(mm)	660 ± 2
Width	(mm)	85 ± 1
Height	(mm)	20 ± 0.5
Volume	(m^3)	1.12 ± 0.04

Table 5.19: Dimensions of neck wood timber (*Amoora cucullata*) in unprocessed form.

made in the workshop. The dimensions of the rough neck wood were identical within the uncertainty of each length (Table 5.19).

Each set was weighed on a balance (Maul digital balance. Limit of resolution: ± 5 g). The measured masses and densities are in Table 5.20. The wood sets with the same mass (670 g) were chosen, although inspection revealed that the uncertainty in the density, due largely to the volume uncertainty, was so high that only sets 4, 6, 8 and 20 were significantly different in magnitude from this choice of sets. The sets 12, 13 and 26 were chosen for the three guitars. Set 10 was found to have a visible defect. The density of the wood for the necks out of for all three guitars was 600 ± 30 kg · m^{-3}. Measurements of the moisture content and the E_i of the neck wood were not made.

5.9   Fingerboard material

Ebony or Rosewood are preferred woods for the fingerboard because of their resistance to mechanical wear. For the guitars in this thesis, the African rosewood species (*Dalbergia holideria*) was used. The masses of 25 similar fingerboard stock were measured and more detailed measurements were made of the dimensions of nine of the samples with very similar masses (Table 5.21). From this, samples 15, 22, 12

Neck sample	Mass (g)	Density (kg · m^{-3})
1	685	611 ± 26
2	700	624 ± 27
3	650	579 ± 25
4	735	655 ± 28
5	640	570 ± 25
6	740	660 ± 28
7	700	624 ± 27
8	810	722 ± 30
9	690	615 ± 26
10	670	597 ± 26
11	660	588 ± 25
12	670	597 ± 26
13	670	597 ± 26
14	700	624 ± 27
15	700	624 ± 27
16	680	606 ± 26
17	640	570 ± 25
18	685	611 ± 26
19	680	606 ± 26
20	810	722 ± 30
21	690	615 ± 26
22	665	593 ± 25
23	730	651 ± 28
24	625	557 ± 24
25	670	597 ± 26
26	670	597 ± 26
27	690	615 ± 26
	± 5	

Table 5.20: Masses and densities of neck wood before processing. Sets 12, 13 and 26 were chosen. Set 10 was found to have a visible defect and was discarded.

and 23 were the most similar by density, but sample 22 was visibly different to the other three and excluded. The densities of the fingerboards used on the three guitars are summarised in Table 5.22.

Sample	Mass (g)	Density (kg · m^{-3})
1	245	
2	305	
3	315	908 ± 68
4	325	
5	335	
6	385	
7	300	
8	320	
9	300	
10	315	940 ± 71
11	335	
12	310	899 ± 68
13	315	866 ± 61
14	315	1113 ± 85
15	310	894 ± 67
16	265	
17	305	
18	275	
19	295	
20	275	
21	340	
22	315	896 ± 67
23	310	899 ± 68
24	350	
25	310	804 ± 56
	± 2.5	

Table 5.21: Measured masses of fingerboard material (African rosewood, *Dalbergia holideria*) of similar dimensions. Approximate densities of fingerboard material were selected from similar masses of samples

Guitar	Sample	Density $(\text{kg} \cdot \text{m}^{-3})$
1	12	899 ± 68
2	15	894 ± 67
3	23	899 ± 68

Table 5.22: Densities of the fingerboards (African rosewood, *Dalbergia holideria*) used in the guitars studied in this thesis. The sample labels are from Table 5.21.

5.10   Back, sides, binding and other materials

The back and sides of all three guitars are of Sapele mahogany. It is desirable to have backs and sides possess a high incidence of *medullary rays*, a grain feature whereby there are clusters of cellulosic fibres running in a tangential direction to the main grain. These have high æsthetic value but may also contribute to an increase in strength in directions perpendicular to the grain. The three sets used on the guitars studied in this thesis were chosen by the master luthier, Gerard Gilet, as those possessing the highest density of medullary ray clustering from a selection of 20. Each set comprised a total of four plates: two for the sides and two for the back. Each set is from the same quarter-sawn, book-matched, block of mahogany. The binding, lining rosette and head-stock veneer materials were each consecutive specimens from identical sources. All of these materials were selected by eye and were based on the experience of the luthiers in the Gilet workshop.

5.11   Damping measurements

The damping factors of some braces were measured (Table 5.23). These results agree broadly with [Haines, 2000], although it is unknown what effect a variation in damping values of components have on the resulting instrument.

5.12   Results

Four experienced luthiers at the Gilet Guitars workshop tested the braces, using their own appraisal methods (static flexing and close visual examination). They broadly

Brace	f_1	Δf	Q	d	E_L	$E_L d$
	(Hz)			($\times 10^{-2}$)	(GPa)	
1A	241.1	6.1	39.7	2.51	16.19	0.55
1B	251.1	10.7	23.5	4.26	15.34	0.65
1C	257.1	11.1	23.2	4.31	14.88	0.61

Table 5.23: Damping measurements, d, of some braces used here. The damping is calculated from the quality factor of the dynamic mass of the first cantilever mode of the beam, Q, which is obtained from the bandwidth, Δf, and frequency f_1 of the fundamental cantilever mode.

Pair	E_L rank	Label	d_{ij}	Grain Density	Destination
	i, j		(GPa)	mm^{-1}	
1	17,18	3B,6C	0.03	$2.5, \lesssim 2.0$	XB1
2	10,11	1A,7B	0.04	$0.8, 1.0$	XB2
3	15,16	2B,2C	0.06	$1.6, 1.4$	XB3

Table 5.24: Final destination and description of wooden cross braces, selected according to similarity of E_L. The d_{ij} represent the difference in the magnitude of the E_L between the pair. Destination 'XB' represents a 'cross-brace'. See §3.4.

agreed upon the ranking of the brace stiffness as measured here. Also, the cause of the extremely low E_L value (12.5 GPa) for brace 6A was discovered: a knot and longitudinal grain discontinuity (a 'pitch pocket') was found to occur longitudinally through the brace material. This was not obvious from previous inspection but was discovered in the profiling process (§3.4), where wood was removed from the outside surface.

A summary of the braces used for the three soundboards is in Tables 5.24, 5.25 and 5.26.

Measurements for the important quantities of many of the components are listed in Table 5.27.

Triple	E_L ranking i, j, k	Label	D_{ij} (GPa)	Grain Density (mm^{-1})	Destination	Visible Differences
1	5,6,7	5C,1B,4C	-0.07	$1.0, 0.5, 0.9$	TB1,TB2,TB3	1B is much darker (almost grey). 5C and 4C many medullary rays
2	8,9,12	5A,6B,5B	-0.18	$1.1, 1.0, 1.0$	RB1,RB2,RB3	5A darker (greyish) and wavy grain. 6B many and 5B quite a lot of medullary rays

Table 5.25: Final destination and description of wooden tone and radial braces, selected according to similarity of E_L. The D_{ij} is the second-order difference of the magnitude of the E_L within the triplet. Destination 'TB' refers to a 'tone-brace' and 'RB' stands for 'radial brace'. See §3.4.

Guitar	Brace	Label	E_L (GPa)	Density (kg· m^{-3})
1	XBL	3B	16.9	493.7
(Western Red	XBR	6C	17.0	472.2
cedar)	TB	5C	15.2	476.6
	RB	5A	15.7	524.3
2	XBL	1A	16.2	564.4
Engelmann spruce	XBR	7B	16.2	496.2
	TB	1B	15.3	492.3
	RB	6B	16.1	485.0
3	XBL	2B	16.6	481.3
Sitka spruce	XBR	2C	16.6	527.3
	TB	4C	15.5	493.4
	RB	5B	16.3	475.4
			$\pm \leqslant 0.56$	$\pm \leqslant 2.42$

Table 5.26: Summary of soundboard brace properties incorporated into the three guitars. Exact uncertainties are in Table 5.6. The brace labels 'XBL' *etc.* follow the conventions given in §3.4

Guitar	Component(sample)	Density (kg · m^{-3})	Grain density (mm^{-1})	E_i (GPa)	Moisture content (%)
1	Soundboard(WRC1)	301.9	0.700	6.8	10.0
Western	Soundboard(WRC2)	320.0	0.450	-	10.2
Red	Soundboard(WRC3)	307.9	$0.429 - 1.000$	-	10.2
cedar	Brace, XBL(3B)	493.74 ± 1.85	2.5	16.92 ± 0.51	11.5 ± 0.5
	Brace, XBR(6C)	472.16 ± 1.71	2.0	16.95 ± 0.50	11.5 ± 0.5
	Brace, TB(5C)	476.59 ± 1.73	1.0	15.15 ± 0.47	11.5 ± 0.5
	Brace, RB(5A)	524.33 ± 1.90	1.1	15.72 ± 0.50	11.5 ± 0.5
	Brace		-		
	Brace		-		
	Brace		-		
	Brace		-		
	Bridge(1L)	847.6 ± 2.6	-	13.4 ± 0.01	15.33 ± 0.05
	Neck(12)	597 ± 26	-	-	-
	Fingerboard(12)	899 ± 68	-	-	-
2	Soundboard(ES2)	398.0	0.650	11.1	10.6
Engel-	Soundboard(ES1)	385.0	0.425	9.3	10.7
mann	Soundboard(ES3)	401.1	$0.400 - 0.923$	0.74	10.7
spruce	Brace, XBL(1A)	564.36 ± 2.20	0.8	16.2	11.5 ± 0.5
	Brace, XBR(7B)	496.33 ± 1.82	1.0	16.19 ± 0.53	11.5 ± 0.5
	Brace, TB(1B)	492.34 ± 1.78	0.5	15.34 ± 0.48	11.5 ± 0.5
	Brace, RB(6B)	484.96 ± 1.77	1.0	16.09 ± 0.49	11.5 ± 0.5
	Brace		-		
	Brace		-		
	Brace		-		
	Brace		-		
	Bridge(2L)	846.8 ± 2.5	-	15.2 ± 0.01	17.56 ± 0.06
	Neck(13)	597 ± 26	-	-	-
	Fingerboard(15)	894 ± 67	-	-	-
3	Soundboard(SS1)	483.3	0.850	11.2	10.6
Sitka	Brace, XBL(2B)	481.29 ± 1.74	1.6	16.56 ± 0.50	11.5 ± 0.5
spruce	Brace, XBR(2C)	527.29 ± 1.94	1.4	16.62 ± 0.52	11.5 ± 0.5
	Brace, TB(4C)	493.37 ± 1.80	0.9	15.46 ± 0.49	11.5 ± 0.5
	Brace, RB(5B)	475.36 ± 1.74	1.0	16.28 ± 0.49	11.5 ± 0.5
	Brace		-		
	Brace		-		
	Brace		-		
	Brace		-		
	Bridge(3L)	851.0 ± 2.6	-	14.6 ± 0.01	17.77 ± 0.07
	Neck(26)	597 ± 26	-	-	-
	Fingerboard(23)	899 ± 68	-	-	-

Table 5.27: Summary of measured properties of components used in the three guitars here.

5.13   Conclusion

Under direction of an experienced luthier the appropriate wood species to be incorporated into the guitars studied in this thesis have been determined. Techniques were then developed to measure important parameters relating to the vibratory behaviour of some of the more important components. These parameters and optimal values were inferred from the experience of luthiers. The three most similar sets of bridges, necks, backs, sides, fingerboards and soundboard braces were chosen from a selection of similar woods. In the case of the soundboards, which is the only designed difference between the three guitars, the longitudinal Young's moduli and densities were measured. The moisture contents of the brace-wood, soundboards and bridges were also determined.

It is now a matter to test the instruments as these components are added and modified in Chapters 6 and 7.

Chapter 6

Experimental: Plates, bodies and the guitar

"Sometimes a difference can be heard...[by] removing just 0.1 mm of wood from a few square centimetres of a plate of some 3 mm thickness [of a violin soundboard]" —M.E. McIntyre and J. Woodhouse, *The Acoustics of Stringed Musical Instruments*[McIntyre and Woodhouse, 1978]

Although the relationship between the vibratory modes of the free plate and those of the finished instrument is not determined (§2.9), important effects may be observed with the co-evolution of soundboards of the three different wood species used on the guitars studied in this chapter, as they progress from the free soundboard state to the finished instrument. Descriptions of each construction phase examined in this chapter are contained in chapter 3.

6.1 Experimental measurement techniques

Measurements of vibratory properties depend strongly on the support system. For example, resonances of the mounting and support structures may strongly interfere with those of the system being measured [Døssing, 1988a,b]. Because, in practice, only a finite range of frequencies may be measured, often the most effective method of minimising the effect of support resonances is to arrange the support resonances to be confined to frequencies outside the range of interest. If a high mass support of low stiffness is used, most of the energy of the supporting structural resonances will be at sufficiently low frequencies. Preliminary tests on a rectangular plywood plate and the free guitar soundboards used a suspension system comprising long rubber bands connected to massive retort stands. The rubber bands were attached to small squares of manila card and glued to the plates with polyvinyl acetate (PVA) adhesive and left to dry for approximately 14 hours. The total mass of these rubber/manila attachments are estimated to be 4 g. This system was chosen such that the energy of structural resonances of the support system occur at frequencies below that measured here. For the bodies and successive construction stages, a similar system was used, although with slight modifications to allow for a nondestructive means of attaching the supports to the guitar (Appendix E). The bodies were coupled to the supports initially by means of 'cup-hooks' (§E.2) but a simpler mechanical coupling method was adopted, using large rare-earth magnets (cylinders 10.0 mm high and 12.5 mm in diameter, a mass of 8.7 g and a surface magnetic flux density of 0.5 T at the surface) after the bindings (§3.4) were applied to the bodies. This coupling system is described in detail in Appendix E.3).

All of the vibratory measurements made in this chapter are of driving point dynamic masses, Chladni figures and pressure force ratios driven by a shaker (Brüel and Kjær 4809) attached to the *central bridge point*. On the soundboards this is the centre of the space occupied by the bridge (200 mm from the butt, along the central axis) and on the plywood pilot soundboard this is half the width and 200 mm from one end (Figure 6.1). This point is used because it is the centre of the line where the force from the excited ('played') string is transmitted to the soundboard, *via* the bridge. It is possible to measure at each of the string termination points on the bridge. However, this study compares three instruments at many stages of construction, and measurement at this many excitation points is not necessary. Investigations into transfer function measurements at these points on the bridge do not show a large variation, as long as they are made in the same direction [Richardson, 1982, Lai and Burgess, 1990].

The primary vibratory detector was an impedance head (Brüel and Kjær 8001) mounted to the shaft of the shaker. Coupling between the soundboard or guitar body and the excitation/detection apparatus was achieved by using a magnetic clamp system, as described in Appendix E. The end of the impedance head had a large NdFeB rare earth magnet (a cylinder 10 mm high and 12.5 mm in diameter, mass 8.7 g and magnetic flux density 0.5 T at the surface) attached via a locking shaft mechanism. The bridge point had a smaller magnet made of the same NdFeB material (a cylinder 6 mm high, diameter 6 mm, mass 1.2 g and magnetic flux density 0.2 T at the surface). For the rectangular plywood plate, the shaker and impedance head were supported by a rope, pulley and laboratory jack suspension system (Appendix E).

Material	Nonstructural plywood (3 ply pine, outside grains longitudinal)
Length	510.0 ± 0.5 mm
Width	254.0 ± 0.5 mm
Thickness	3.50 ± 0.25 mm
Total mass	289.4 ± 0.05 g
Bridge position	200 mm from one end, halfway along width
Magnet type	NdFeB permanent rare earth (250 mT at surface)
Magnet size	Cylinder 5.5 mm height, 5.5 mm diameter
Magnet mass	1.0 ± 0.05 g

Table 6.1: Properties of an anisotropic rectangular wooden plate used to develop a measurement system for the free guitar soundboards.

6.2 Simple plates

The vibrational properties of a simple plate are much more complicated than those of a homogeneous beam or string. In turn, the motion of an anisotropic plate is more complicated than that of an isotropic plate [Szilard, 1974, Lekhitskii, 1968, 1963]. In anticipation of measurements of the guitar soundboards (§6.3), which are not only anisotropic, but also have an additional bracing structure, it is useful to study a simpler system to investigate the essential characteristics and methodology to be applied in measurement of free guitar soundboards. This rectangular plate provides a rough approximation to the guitar soundboards. The overall dimensions, density (Table 6.1) as well as the nominal values of their elastic moduli, are similar enough to expect their low frequency behaviour to be qualitatively similar to that of the guitar soundboards studied in §6.3.

The rectangular plate is supported by three rubber bands on retort stands, adjusted so that the board is level with the coupling magnet and is facing down such that it is just above the magnetic clamp (Appendix E) connected to the shaker, as in Figure 6.3. The excitation and measurement position remains fixed, at the central
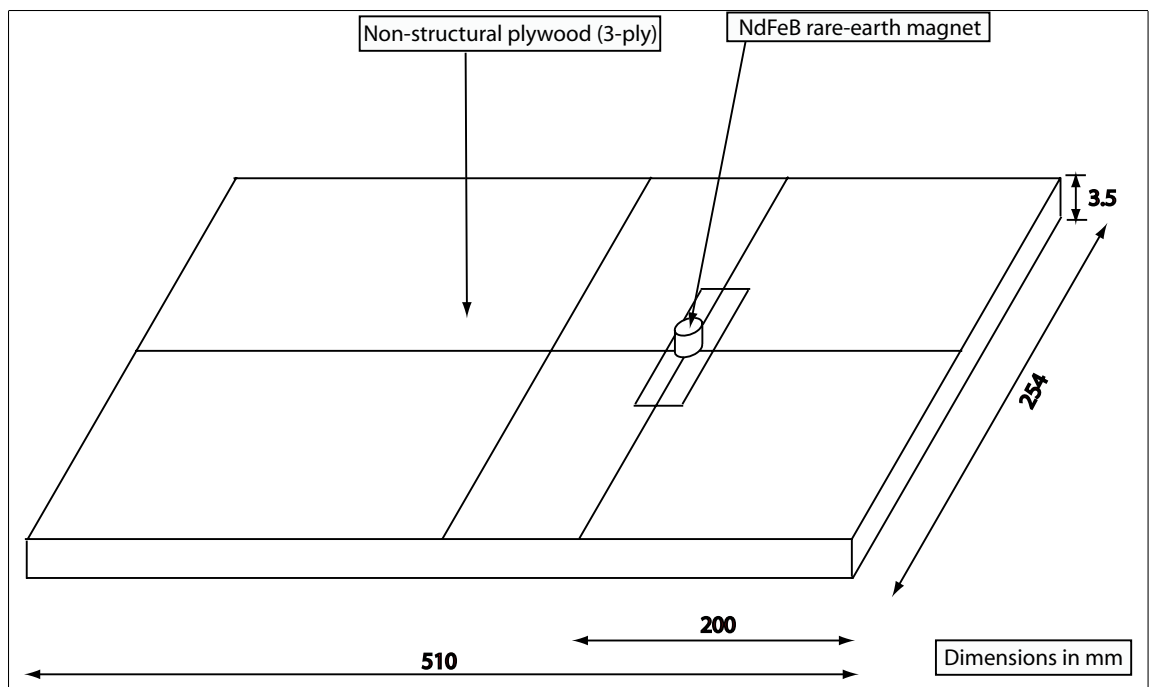
Figure 6.1: Dimensions of an anisotropic wooden plate, with approximately similar dimensions and mass to the guitar soundboards being studied.
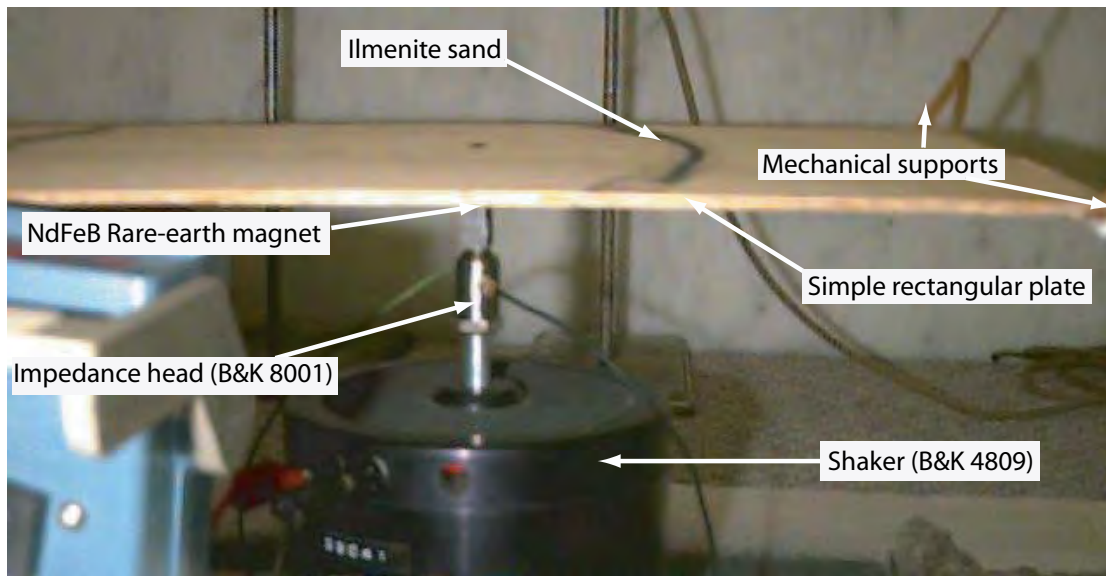
Figure 6.2: Side view of the set-up used to measure the dynamic mass spectrum and Chladni figures of a simple rectangular wooden plate. This is a developmental stage for the actual guitar soundboards studied in this thesis.
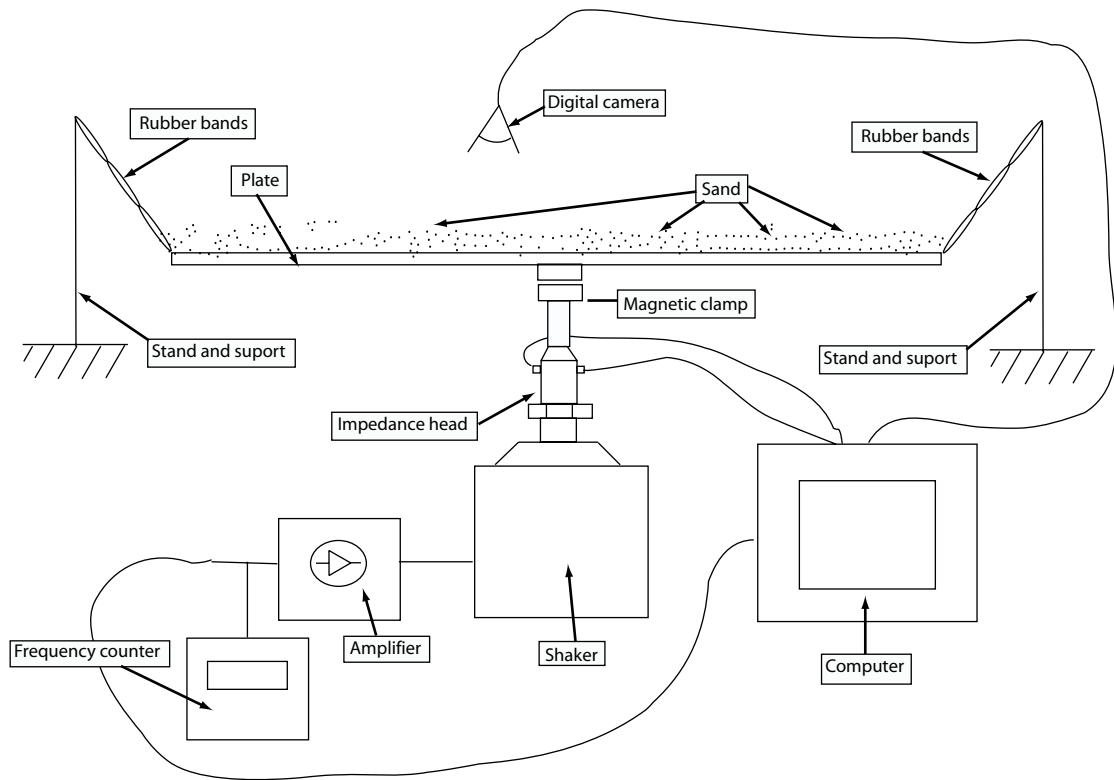
Figure 6.3: Diagram of the set-up used to measure the dynamic mass spectrum and Chladni figures of a simple rectangular wooden plate. The specifications of the apparatus used is supplied in the main text.

bridge point.

Dynamic mass of a rectangular wooden plate

The driving point dynamic mass spectrum at the bridge point is shown in Figure 6.4. Most of the peaks correspond to Chladni modes (§6.2), as illustrated in Figure 6.6. The peak at 349 Hz is an unidentified experimental artifact.
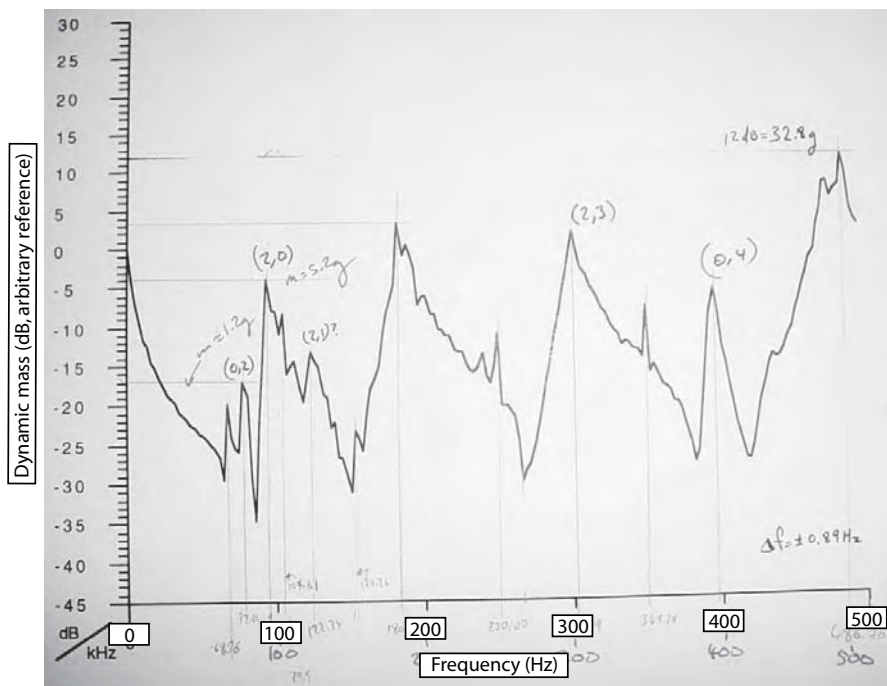
Figure 6.4: Measured dynamic mass spectrum of a thin rectangular plywood plate having dimensions roughly that of a guitar soundboard.

Chladni figures of an anisotropic rectangular wooden plate

The shaker(B&K 4809)/impedance head(B&K8001) combination is driven by a manual sweep function generator (TFG 8101, Topward Electronic Instruments Co.) and a power amplifier (ELWS 2-5007). Accurate frequency determination is made by connecting a frequency counter (Tektronix CDC250) to the function generator. The force and acceleration outputs from the impedance head are displayed through a digital oscilloscope (Tektronix TDS210). To take records of the Chladni figures, a digital camera (Apple Quicktake 100) is mounted directly above the board. The fine particulate used for imaging the Chladni figures is black ilmenite sand (Rainbow Beach, Fraser Island). From a sample of 11 Chladni figures, the average mass of sand used for each Chladni figure on each soundboard (§6.3) is 3.5 ± 0.2g, which gives a mean areal mass density of 20 gm^{-2} at the initial stage, when the sand is evenly distributed over the entire soundboard. This is approximately 1.4% of the total mass for the lowest mass (Western Red cedar) soundboard, although we would expect this mass load to have a minimal effect on the standing wave configuration and frequency once the sand is aligned along the nodal surfaces [Strutt, 1869].

The nomenclature convention is that described in §2.9. Frequencies of the modes are presented in Table 6.2 and photographs of these modes are given in Figure 6.5.

In practice, the identification of a standing wave configuration using the Chladni figure method occurs when the particles show the greatest motion. The uncertainty

of the frequency of each mode varies inversely with the Q-factor of the transfer function. Generally the largest frequency interval between that of a normal mode and the nearest frequency that is definitely not a normal mode is about 5 Hz, although this is approximate because many modes extend over a much broader frequency range. In many cases, most of the particles appear to move violently over this broad frequency range. The perceived loudness is also used as an additional tool to judge the frequency of the resonance peak, which can contribute to the uncertainty in the frequency of that mode. Some modes have a number of distinct phase relationships between the vibrating components. This results in the same mode being measured at more than one frequency. For example, the Western Red cedar soundboard exhibits a $(0,3)$ mode, at 171 Hz, 154 Hz and 166 Hz). However care must be taken with this interpretation, because it is sometimes unclear in the case where the vibratory modes have a high bandwidth and may not occur at distinct frequencies, but over a broad frequency range.

The results of a finite element simulation of this rectangular plate, using the ANSYS (Swanson Analysis Systems, Inc.) package, are compared to the measurements of the vibratory modes in Table 6.2. Values of the material properties of *Pinus radiata* were taken from [Forest Products Laboratory, 1999]. Because a single driving point is used, it is difficult to resolve modes that have nodal regions that intersect this point. All the calculated modes that are not detected with the Chladni method have modes with this property, with the exception of the (3,0) mode. Calculated at 194 Hz, this is close to the frequency measured for the (2,2) mode (180 Hz).

Mode	Frequency (Hz)	
	Measured	Calculated
(1,1)	-	36
(0,2)	69	70
(2,0)	95	92
(1,2)	-	101
(2,1)	122	117
(2,2)	180	188
(0,3)	-	194
(1,3)	-	221
(3,0)	-	253
(3,1)	-	275
(2,3)	307	308
(3,2)	-	342
(0,4)	398	379
(1,4)	-	405
(3,3)	-	495
(2,4)	-	484
(4,0)	-	495
(4,1)	-	514

Table 6.2: Comparison of measured and calculated frequency of vibratory modes of a suspended rectangular plywood soundboard. Calculations were performed using the ANSYS package with values of material properties of *Pinus radiata* taken from [Forest Products Laboratory, 1999]. The paired integer mode convention (m,n) is that of §2.9.
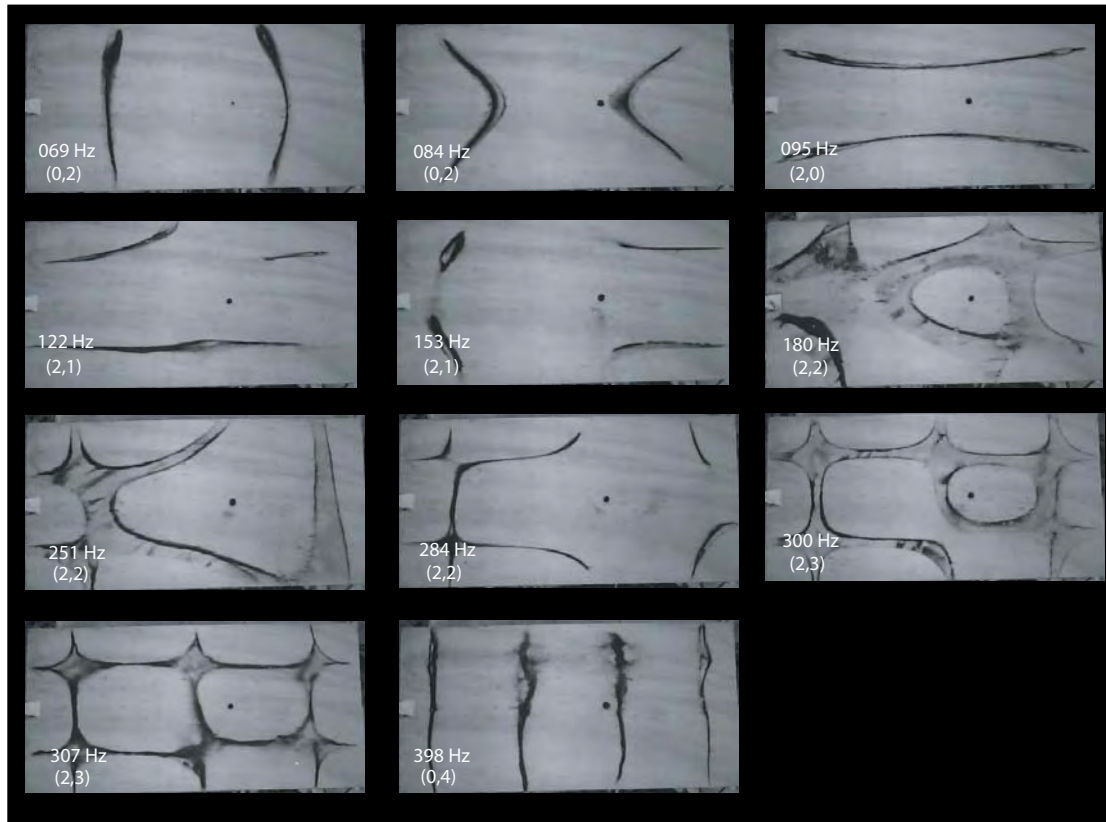
Figure 6.5: Modes shapes and frequencies of a thin rectangular plywood plate having dimensions roughly that of a guitar soundboard.

Conclusion: Simple rectangular plates

Structurally, the system here is simple enough to be able to interpret the Chladni modes of the plate without the complications introduced by the complex bracing structure of the free guitar soundboards. The modes in Figure 6.5 are able to be characterised completely by the simple (m, n) nomenclature described in §2.9. Most importantly, study of this plate is useful in the development of an excitation and measurement system for the guitar soundboards. An important result from this study is the relationship between the driving point function of the dynamic mass and the distribution of standing waves on the surface of the plate (*i.e.* Chladni figures, as in Figure 6.6): the Chladni figures occur at frequencies where the relative phase in the dynamic mass spectrum is a local extremum—usually where the magnitude has a highly negative gradient. It can be difficult to excite the plate with sufficient amplitude to identify all the vibratory modes. The detection of a particular mode, using Chladni figures, relies directly on human perception. This relationship might enable makers to identify Chladni modes from the dynamic mass spectrum, which would enable rapid, objective, and quantitative plate characterisation of the instrument.

6.3   Free guitar soundboards

How is the behaviour of the free plates related to that of the completed instrument? Work on this question is represented by a significant proportion of the studies on the behaviour of stringed instruments [Schleske, 2000, Ezcurra, 1996, Richardson, 1988, 1982, Jansson, 1988, Meyer, 1983a, Rodgers, 1990, 1991, Stetson, 1977, Krüger, 1982].

In §5.6, measurements were made on samples of the timber surrounding the
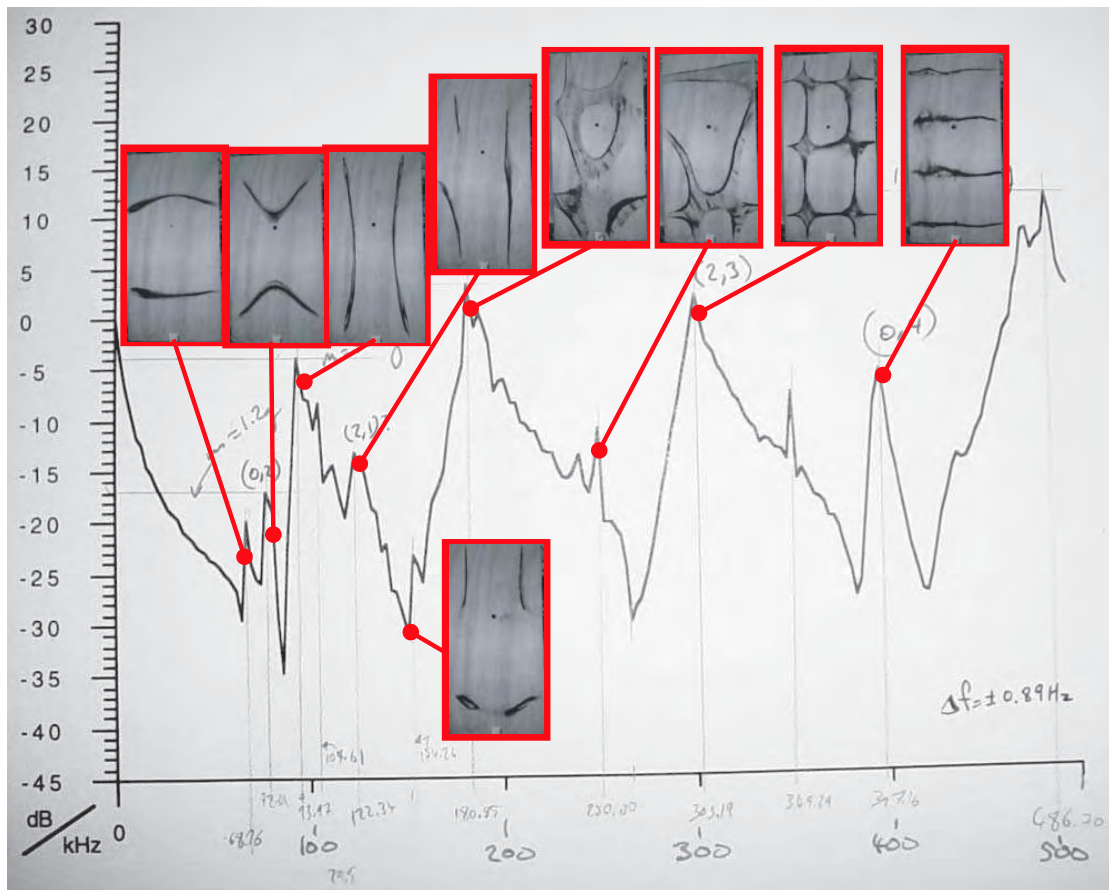
Figure 6.6: Illustration of the relationship between the dynamic mass spectrum and the Chladni modes of a simple rectangular plate.

soundboard. Each soundboard was weighed (Table 7.4) and the lengths of various parts were measured. The overall dimensions of each soundboard are described in Appendix A.4. Individual brace geometries of each were measured (such as in Figure 3.8).

The Western Red cedar soundboard has the lowest values of speed of sound in the longitudinal direction ($c_L \simeq 4700 \ ms^{-1}$) compared to the Engelmann spruce ($c_L \simeq 4900 \ ms^{-1}$) or the Sitka spruce ($c_L \simeq 5100 \ ms^{-1}$; Table 5.13). Therefore, because of the similar geometry and boundary conditions, most of the peaks in the dynamic mass spectrum of the Western Red cedar soundboard are of lower frequencies than for corresponding spectral features in the two spruce soundboards (Figure 6.8). Frequencies of the vibratory modes may be compared for all three soundboards as results of the Chladni figure method, Figure 6.7. The frequencies of the modes of the Sitka spruce soundboard, which has the highest value of c_L, are generally higher than that for the same given mode of the Engelmann spruce soundboard.

The system damping of measured dynamic mass spectra of the Western Red cedar soundboard is generally higher (a low quality factor for most peaks and a higher 'background level') than the other two, and most of the peaks are of a lower magnitude. The transfer function gives information on both the magnitude and the relative phase between the force and the acceleration at this point (the top and bottom graphs in Figure 6.8 respectively). A dramatic change in the value of phase with frequency indicates a change in vibratory mode. The frequencies of the Chladni figures of the plates (Figure 6.7) of the free soundboards correspond well to that of rapid phase variations in the dynamic mass measurements.
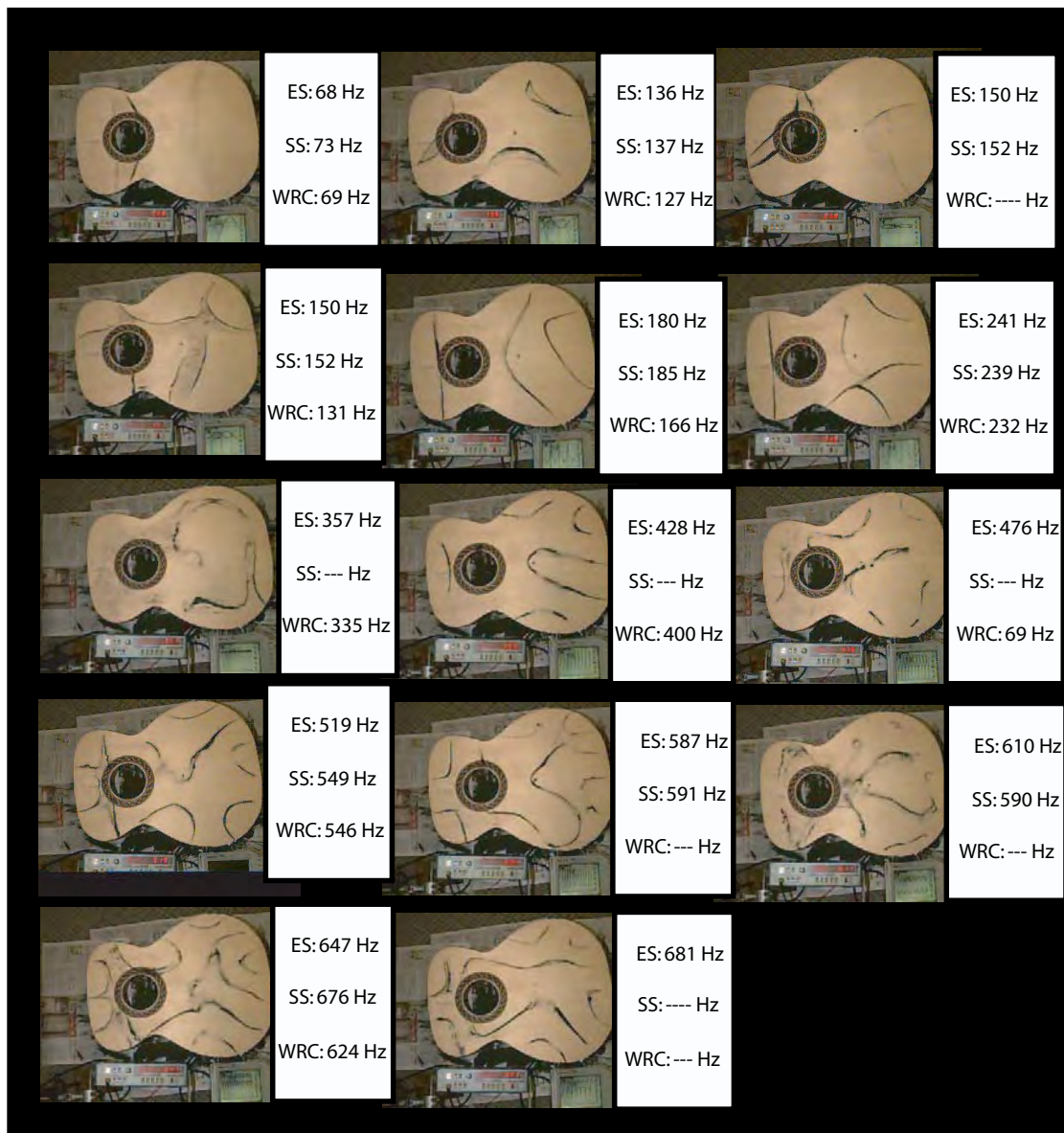
Figure 6.7: Chladni figures for free guitar soundboards. The figures presented are those for the Engelmann spruce soundboard and are representative of the topology of the other two soundboards.
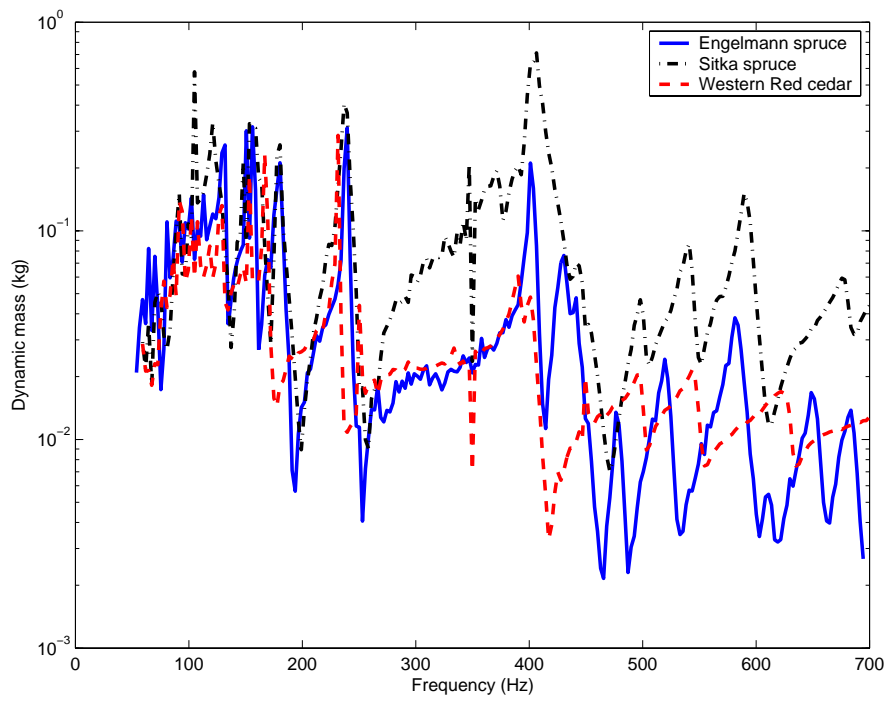
Figure 6.8: Magnitude of the dynamic mass spectra of the three soundboards, with free edges.

Because of the considerable local increase in stiffness and mass due to the bracing, most of the Chladni figures of guitar soundboards possess some nodal regions aligned with the braces, especially the transverse bar and that of the longest 'tone brace', which are located above the soundhole and in a central position on the soundboard respectively.

6.4 Guitar bodies

The soundboard of each guitar, including the bracing system, is glued onto the sides and back to form the body. The body is designed to exploit the coupling between the plates and the enclosed air cavity [Meyer, 1974, Firth, 1977, Caldersmith, 1978, Christensen and Vistisen, 1980]. This makes the vibratory properties more complicated (§2.5). The neck, added later, also couples with the body, producing low frequency modes (§2.5 and §7.1).

The mechanical support and coupling system for measurements of the vibratory behaviour of the guitar bodies studied here is described in Appendix E. The support system described in Appendix E.2 is used for this and all subsequent stages of construction until the bindings are installed (§6.6), after which the system described in Appendix E.3 is adopted.

Soundboard type	Sitka spruce	Engelmann spruce	Western Red cedar
Soundhole diameter d (mm)	96	96	96
Soundboard area (m^2)	0.1475	0.1475	0.1475
Mean depth (mm)	112	112.5	112.3
Volume V (l	16.52	16.60	16.57
Calculated f_H (Hz)	122.1	121.8	121.9
Measured f_H (Hz)	120.0	119.5	125.2

Table 6.3: Body and soundboard dimensions of the three guitars and their calculated Helmholtz frequencies and measured values. Measurements are derived from the response spectra in Table §7.7.

Measuring the Helmholtz resonance of the body

As shown in §2.4, some basic assumptions lead to the simple expression (Equation A.1.12) for the frequency of an ideal Helmholtz resonator. This concept may be applied to the low frequency air motion of the guitar body, and is important in sound production over a broad frequency range [Christensen, 1984].

The area of 0.1475 m^2 for the Sitka spruce soundboard is slightly greater than the area of two classical guitar soundboards calculated in [Christensen and Vistisen, 1980] of 0.1400 m^2.

The soundhole of each guitar was made circular with a relatively high precision: each has a diameter of 96.0 ± 0.1 mm.

The volume was measured by filling the air cavity with polystyrene spheres ('beans'), (Table 6.4).

Soundboard type	Internal volume	
	(direct) (l)	(mass difference) (l)
Sitka spruce	14.32	14.60 ± 0.07
Engelmann spruce	14.47	14.33 ± 0.06
Western Red cedar	14.32	13.99 ± 0.06

Table 6.4: The volume of the internal air cavities of the three guitars.

Dynamic mass spectra and Chladni figures of the bodies

The dynamic mass measurements of the bodies are given in Figure 6.9. These spectra are very different to those of the free soundboards, reflected also in the Chladni figures made at this construction stage (Figure 6.11). Because of the changes made to the boundary conditions of the edges of the plates, the vibratory modes have different characteristics. In addition to coupling between the internal air cavity and the soundboard, such as the low frequency coupling between the Helmholtz resonance and the plate fundamental gives rise to two prominent minima between 90 Hz and 200 Hz (Figure 6.10) the low frequency air-body coupling region, (§2.5, [Christensen and Vistisen, 1980]).

Because the measurement is only made at a single point, the dynamic mass spectrum alone does not illustrate the spatial distribution of a given vibratory mode of the soundboard. These measurements are supplemented with Chladni figures of the soundboard.

The transition between vibratory modes is indicated by a rapid variation in the dynamic mass spectrum. A demonstration of this relationship between the dynamic mass and the Chladni figures, for the Engelmann spruce guitar, is shown in Figure 6.12.
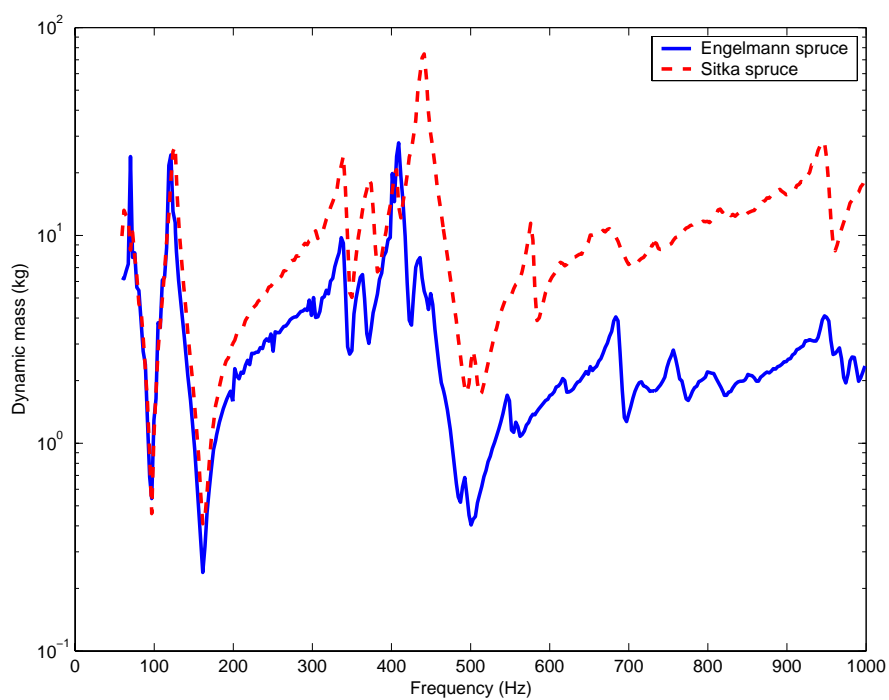
Figure 6.9: Dynamic mass of two of the three guitar bodies (Engelmann spruce and Sitka spruce) directly after glueing the soundboard to the back and sides.
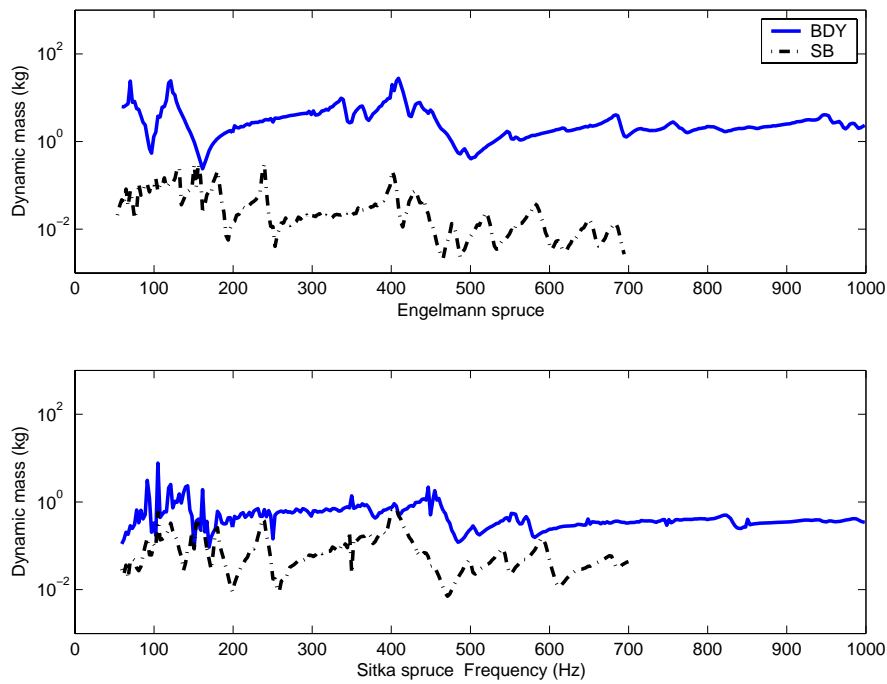
Figure 6.10: Dynamic mass of two of the three guitar bodies (Engelmann spruce and Sitka spruce) directly after glueing the soundboard to the back and sides, compared to that for the free soundboards. The free soundboard spectra have been raised in overall magnitude to be the same as for the bodies.
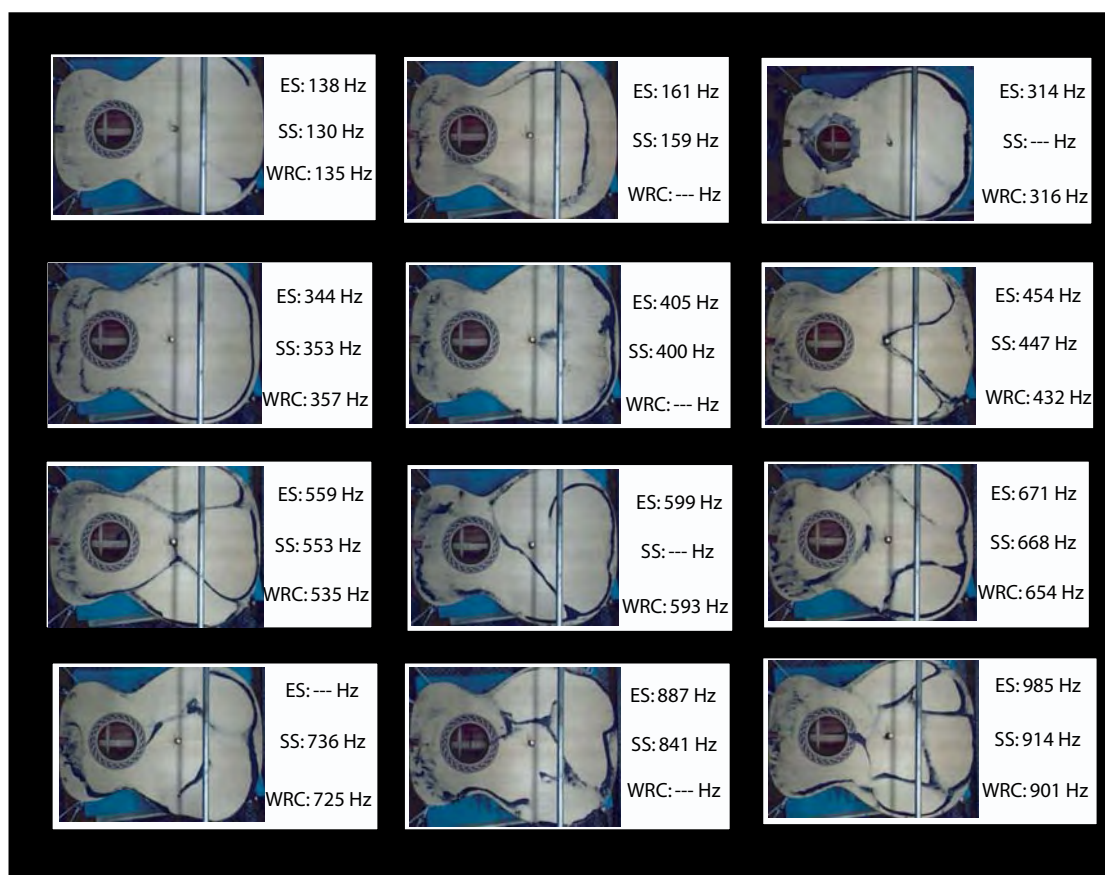
Figure 6.11: The set of Chladni figures for the guitar bodies after the soundboard is glued to the back and sides. The figures used are that of the body with a Sitka spruce soundboard. The T(2,1) mode at 314 Hz was not observed in Sitka spruce, hence the Engelmann spruce figure is used here.
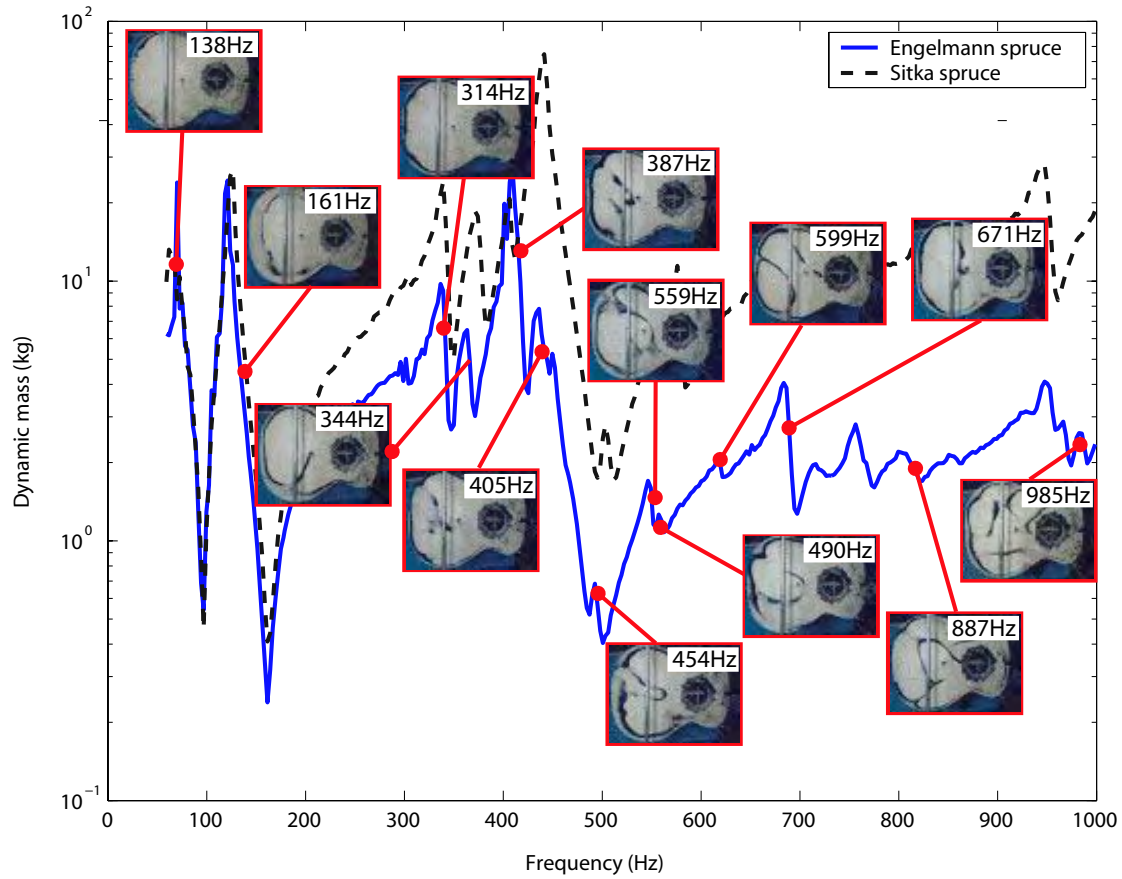
Figure 6.12: Illustration of the relationship between the dynamic mass and Chladni figures of guitar bodies directly after glueing the soundboard to the back and sides. The Chladni figures are those of the Sitka spruce soundboard.

6.5   The thinned soundboard

The soundboards of high quality guitars are not of uniform thickness (§3.4 and §D.1). It has been shown that the thickness distribution of the guitar soundboard is extremely important in determining the sound of the instrument [Richardson, 1998, Meyer, 1983a, Elejabarrieta et al., 2000]; there is evidence that radiation in middle frequencies (T(1,2) and T(3,1) [364 → 432 Hz for guitar BR2 in [Wright, 1996] and 400 → 550 Hz in the guitars studied here]) is strongly affected [Krüger, 1982]. It is common to thin the soundboards of high quality guitars *after* joining to the back and sides. In this case, the luthier often applies vibro-acoustic tests to determine the amount of thinning required. Describing the conventional testing procedure is difficult: the apprentice luthier is instructed to listen for an audible difference in the loudness of the tap response of the body [Gilet, 2000]. Measurement of the thickness of the soundboard at this stage is difficult because of the complicated geometry of the bracing system and the body itself. Consequently, luthiers performing this procedure have limited knowledge of the thickness distribution of the soundboard, which makes replication of a particular instrument difficult.

To solve this problem, John Smith and I developed a thickness measuring device based on a calibrated magnet-Hall probe system [Inta and Smith, 2003]. A permanent magnet in the shape of a cylinder is used as a source for which the resulting magnetic field strength is detected by a Hall probe. Because the magnetic flux density decreases monotonically with distance along the axis of the cylinder, and, because the relative magnetic permeability is very close to unity for all wood, the magnetic flux density can be calibrated to gauge the displacement from the surface
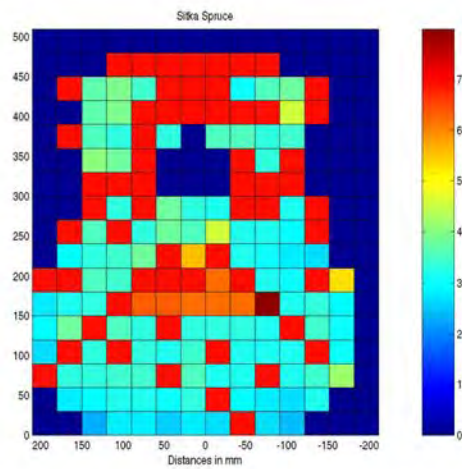
Figure 6.13: Thickness distribution of the Sitka spruce soundboard, as obtained from 'Giletometer' thickness measurements

of the magnet. The magnet can then be placed on the inner surface of the guitar soundboard and the thickness measured to the outer surface of the soundboard, at the point directly above, with the Hall probe (Appendix D).

It is thus possible to obtain the thickness distribution of the soundboards after they have been thinned but are attached to the back and sides. All three soundboards have been made so as to give the same thickness distribution, within ±0.2 mm, on measurements spaced at 40 mm, over the whole soundboard (Figure 6.13). Braces show clearly, of course (Figure 6.14). Because the thickness of the soundboard is not usually measured directly, it is difficult to compare the soundboard thickness distribution in Figure 6.13 to other guitars manufactured using this technique.

Dynamic mass spectra, measured at the bridge point on the guitars, after thinning the soundboards, are given in Figure 6.15. Because of the differences in the
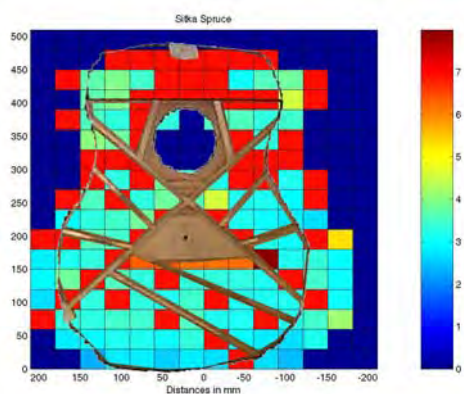
Figure 6.14: Superposition of the soundboard bracing geometry on the measured soundboard thickness distribution of the Sitka spruce soundboard.

soundboard timber, the removal of the same volume of material might be expected to result in different vibratory responses among the soundboards. The Western Red cedar soundboard underwent the larger changes than the two spruce soundboards, confirming the result in [Krüger, 1982] and showing much difference in the spectrum especially at the $T(1,2)$ mode, but also is affected at least to 1 kHz, the highest frequency measured here.

For this, and all subsequent construction stages, measurements of the pressure at the soundhole of the guitars, in response to a measured force (*pressure force ratio spectra*) are made at the central bridge point. This measurement for the guitars after the soundboard has been thinned is presented in Figure 6.16. The microphone used for these measurements is not calibrated and hence the overall air pressure magnitude is arbitrary. However, the response is linear over this small frequency range and so the pressure is subject only to a constant scaling factor.
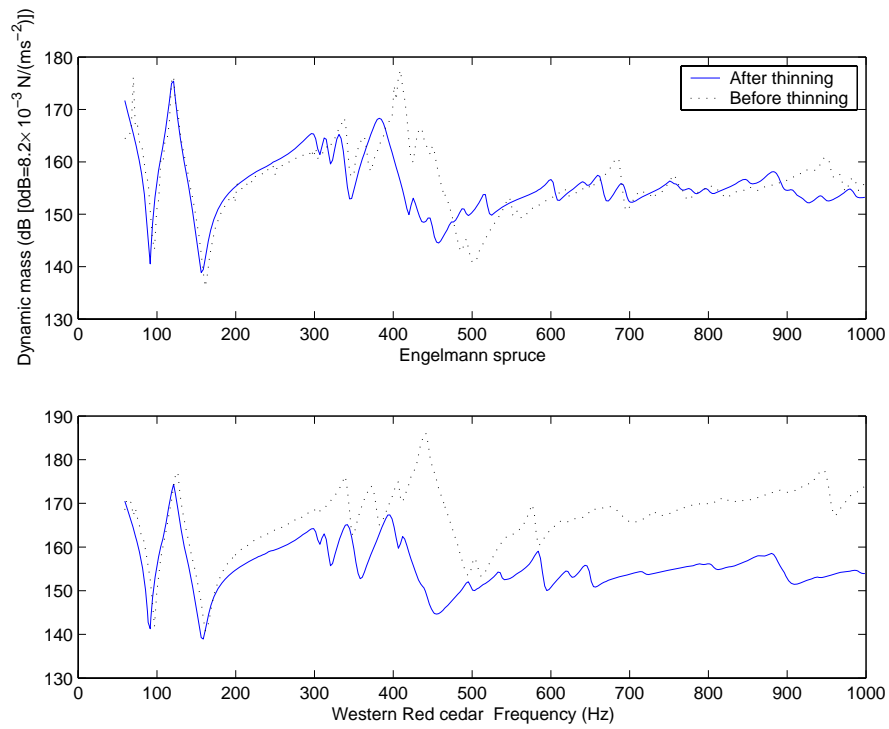
Figure 6.15: Dynamic mass of guitar bodies directly after 'thinning' the soundboard.
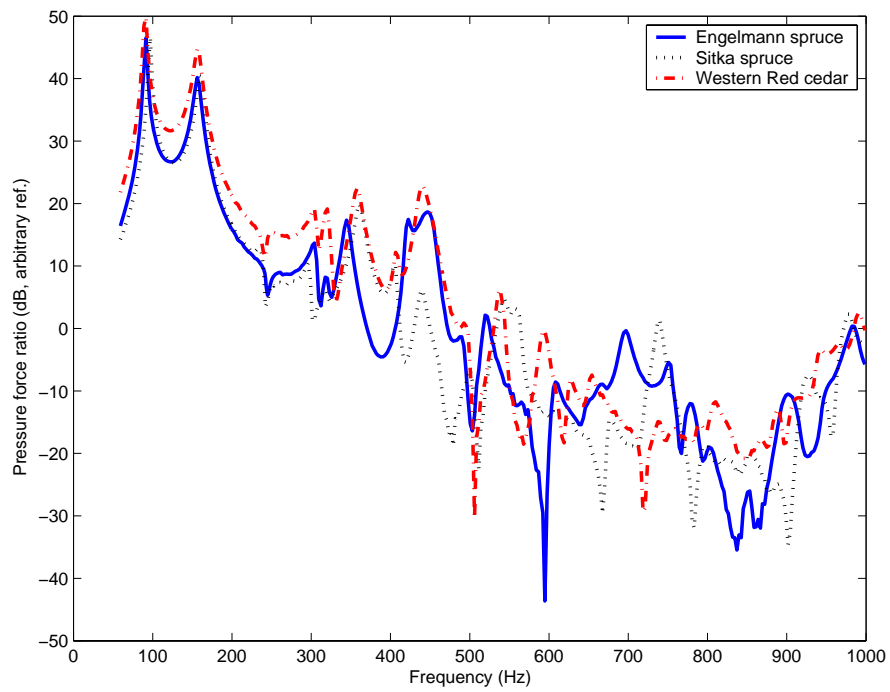
Figure 6.16: Pressure force ratio of guitar bodies directly after 'thinning' the soundboard.

Soundboard	f(T(1,2)) (Hz)	
	Top thinned	Bindings added
ES	382	409
SS	391	400
WRC	395	419

Table 6.5: The changes in the frequency of the T(1,2) soundboard mode of the guitar bodies with the binding process. The Western Red cedar soundboard is most affected.

6.6 Binding the soundboard

The joint between the sides and the soundboard constrains the edge of the soundboard so it is no longer free. The binding process, including the herring-bone (§3.4), reinforces this joint. The nature of this alteration has not been well investigated [Hutchins, 1962], although it should influence the vibratory behaviour of the bound soundboard. The dynamic mass spectra of the guitar soundboards after the binding process are presented in Figure 6.17. Like the thinning process, the T(1,2) mode is affected strongly by the binding process. However, the effect is to increase slightly the frequency of this mode (Table 6.5).

Perhaps the most dramatic differences are in the pressure force ratio spectra (Figure 6.18). The amplitude is generally lower for all three guitars, with the exception of the low frequency air-body coupled modes (f_- and f_+) which remain the same, although the Q-value of the associated peaks is noticeably increased. The Chladni figures are more pronounced with the addition of the bindings and there appears to be a new mode at approximately 800 Hz. This is presumably to do with a stiffening of the edges of the body, making the nodal regions more defined.
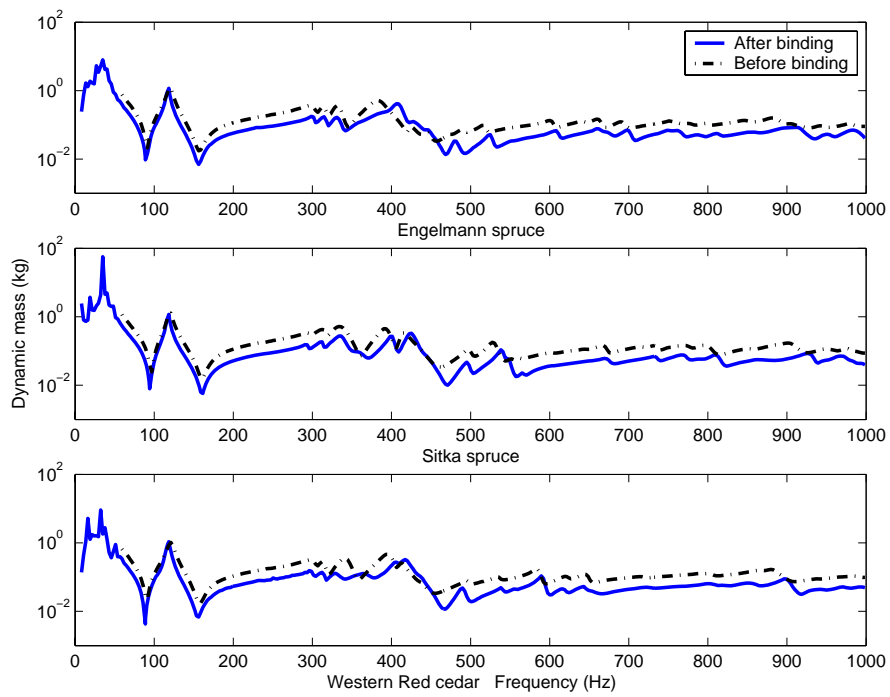
Figure 6.17: Dynamic mass spectra of guitar soundboards before and after binding.
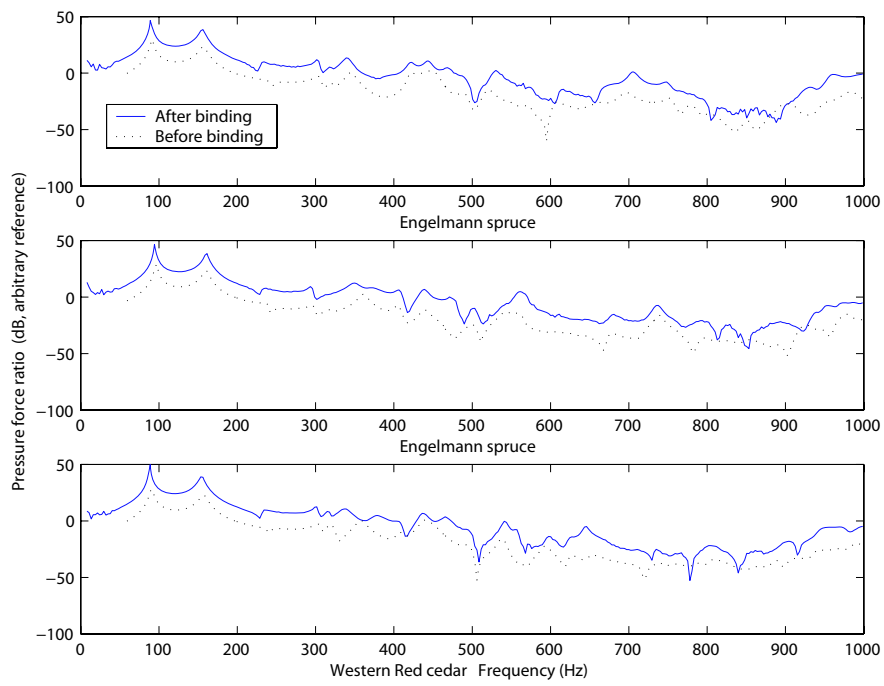
Figure 6.18: Pressure force ratios of the guitar bodies before and after binding.

6.7 Discussion

A simple relationship between the behaviour of the free soundboard and that of the soundboard attached to the body would be very useful. A relationship of this kind has not yet been found. Preliminary investigations on a rectangular plate have proven useful in quantifying the low frequency vibratory behaviour of a system similar enough to the free soundboards and agree well with finite element simulation of the system. These investigations illustrate the close relationship between the dynamic mass spectrum and the Chladni figures, which are more traditionally used by luthiers as a testing or diagnostic tool. However, unlike the Chladni figure method, the results of dynamic mass (and pressure force ratio) measurements give information on the relative amplitudes and Q-values of vibratory modes (Figure 7.42). In addition, measurements of this kind are able to be made in a fraction of the time it takes to characterise the instrument using Chladni figures over the same frequency range. These test methods are generally more sensitive to alterations made to the instrument and allow the luthier to compare measurements of particular instruments in their inventory as well as instruments made by another luthier.

Because of the differences in boundary and coupling conditions between the free soundboards and those of the soundboard attached to the back and sides, it is difficult to compare the vibratory behaviour directly. This is evident in the dynamic mass spectra (Figure 6.19). For instance, the nodal topology is 'open' for most of the low frequency modes of the free plates, whereas the nodal regions mostly form closed loops on the soundboard of the guitar bodies. However, the majority of mode

frequencies are higher for Sitka spruce in the free soundboard as well as the body state.

Aside from the poor control of the raw materials (in terms of quantitative measures, Chapter 5) there are other aspects of the manufacture of guitar soundboards that make it difficult to replicate accurately the acoustic output of any given instrument. There are other constraints imposed on instrument manufacture that potentially interfere with acoustic concerns, such as the æsthetic value of the instruments [Richardson, 1995b]. But probably the greatest impediment to the replication of good instruments is that the practising luthier generally has only a set of 'rules of thumb' when manufacturing their instruments. For example, the fact that there is still much active experimentation in soundboard bracing design [Ramirez, 1986, Rossing and Eban, 1999, Marty, 1987b] (and much debate on this subject [Brune, 1985b, Wyszkowski, 1985, Williams, 1986b]) means that an optimal soundboard bracing system is yet to be found.

How much soundboard material to remove? With the traditional method (§3.4), the final thickness distribution is not known. Using a magnet and a Hall probe, with the appropriate calibration, the thickness distributions of the three soundboards studied in this thesis were made equal to each other, after measurement and refinement of the thickness of each soundboard.

The process of thinning the soundboard has the effect of 'smoothing' and lowering the frequency of many of the peaks in the dynamic mass spectra (e.g. Engelmann spruce $409 \rightarrow 384, 338 \rightarrow 331$ Figure 6.20). Addition of the bindings reverses this to some extent: it raises the frequency of some of these modes (e.g. Engelmann spruce
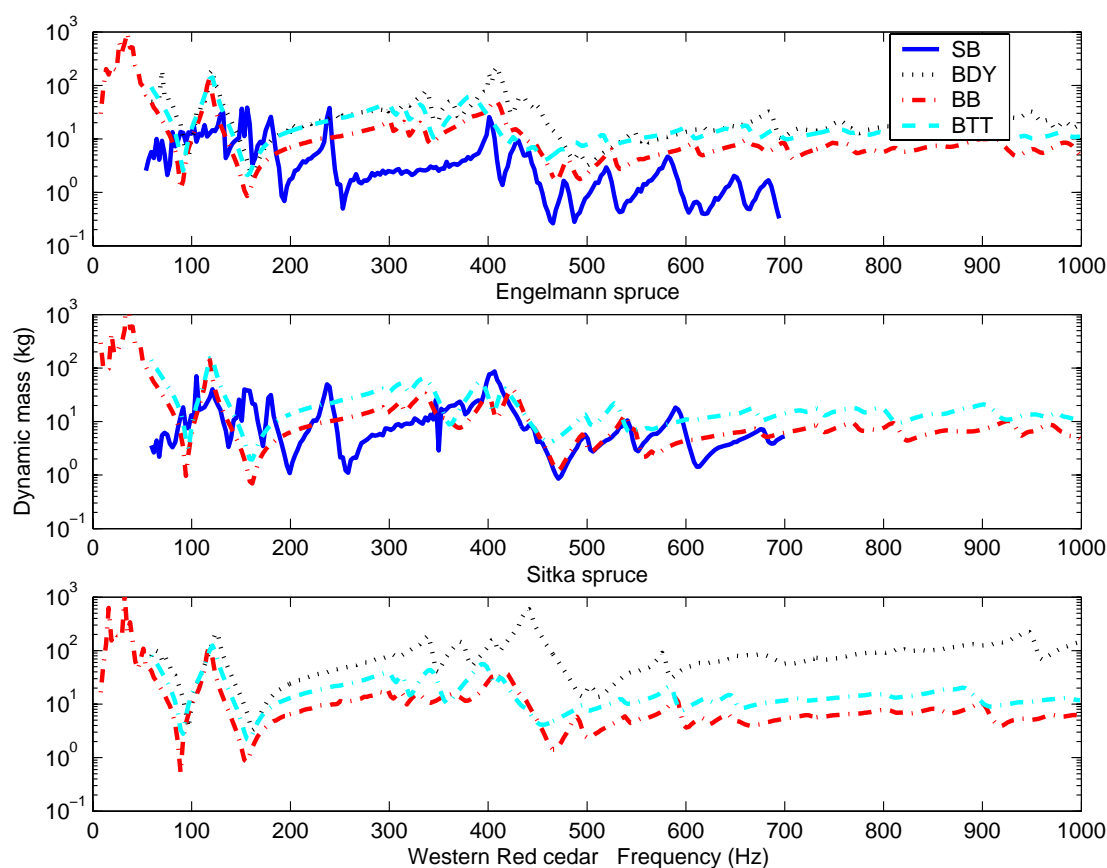
Figure 6.19: Dynamic mass spectra of each soundboard at successive stages of construction until the addition of the bindings. The construction stages are coded thus (Table 3.3): 'SB': free soundboards, 'BDY': Body (soundboard glued on to the back and sides), 'BTT': Body with the soundboard thinned, 'BB': The bodies after the bindings have been added.
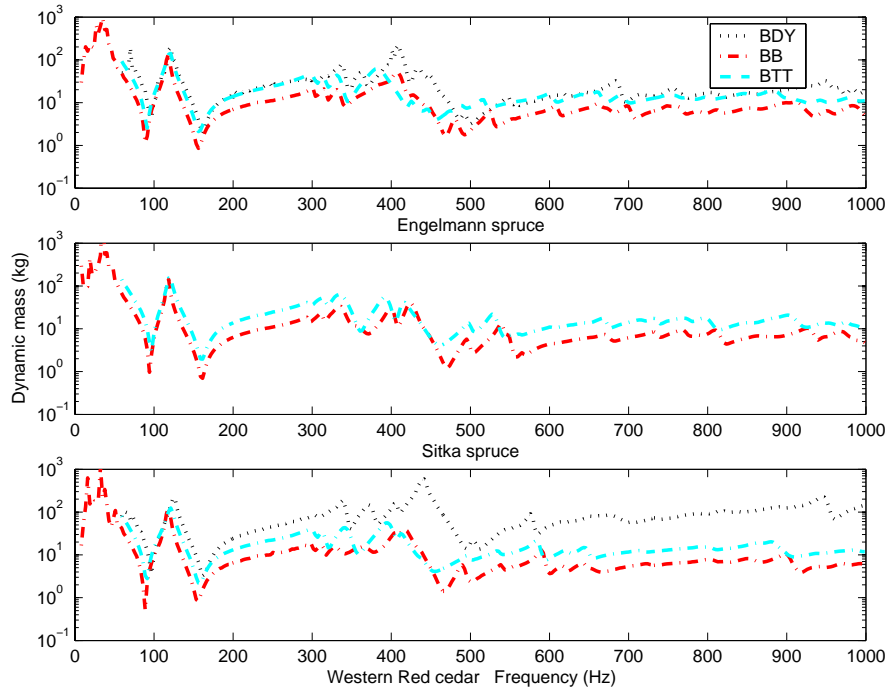
Figure 6.20: Dynamic mass spectra for the three guitar bodies at successive stages of construction.

$384 \rightarrow 409$) whilst altering others very little (e.g. Engelmann spruce $315 \rightarrow 315$, $333 \rightarrow 333$). In addition, the overall magnitudes of the dynamic masses are much lower for this stage, which, *cæteris paribus*, are an indication of better radiativity at these frequencies [Wright, 1996]. For both the soundboard thinning and the binding stage, the Western Red cedar soundboard was affected more than the Engelmann spruce or the Sitka spruce soundboards over the measured range. For example, the peak relating to the lowest frequency motion of the air in the soundhole, with frequency f_-, is very much lower in the case of Western Red cedar (Table 6.6).

Comparisons of the pressure force ratios for two stages (after the bodies were thinned and after addition of the bindings) are in Figure 6.21. The magnitude of the

	Coupled frequency (Hz)								
	ES			SS			WRC		
	f_-	f_H	f_+	f_-	f_H	f_+	f_-	f_H	f_+
BDY	97	121	162	100	121	162	97	125	164
BTT	91	121	157	97	120	160	90	121	158
BB	90	119	157	94	119	161	89	119	156
	± 1								

Table 6.6: Low frequency air soundboard coupling frequencies for the guitar bodies at successive construction stages.

pressure force ratio is generally much higher for that of the thinned soundboards. A notable equality is at the lowest air cavity-soundboard coupling mode, where the motion of the air in the soundhole is 180° out of phase with that of the soundboard, and is close to equal with the in-phase part of that mode.

Measurements made during subsequent construction phases are presented in Chapter 7, beginning with the addition of the neck.
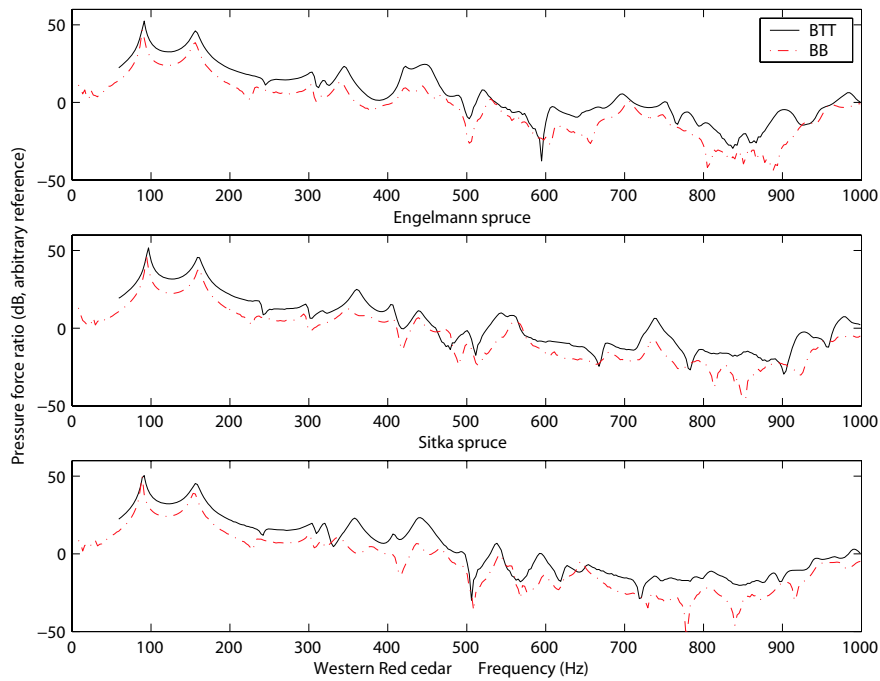
Figure 6.21: Pressure force ratio spectra for the three guitar bodies at consecutive stages of construction. The solid line is the measurement after the soundboards were thinned, while the dotted line is that of the soundboard before thinning.

Chapter 7

Experimental: Completed instruments and parameter evolution

"And when one sweetly sings, then straight I long,

To quaver on her lips ev'n in her song,

Or if one touch the lute with art and cunning,

Who would not love those hands for their swift running?" —P. Ovidius Naso, Amores

(English translation by Christopher Marlowe)

7.1 Effects from the addition of the neck

A description of the function of the neck and how it is attached to the guitar body is given in §3.4. The neck (including the head-stock, but not the fingerboard) is almost as long as the actual guitar body (476 mm and 493 mm respectively) and has a mass (including the fingerboard) of roughly 45% of the guitar bodies (Table 7.1). The neck is therefore a significant structural member of the instrument.

Soundboard	Mass of component (g)		
type	Neck	Bolts	Body
Sitka spruce	549.3	24.5	1269.7
Engelmann spruce	555.2	24.6	1225.5
Western Red cedar	561.7	24.6	1216.2

Table 7.1: Masses of components before assembling the neck and the body. Note that neck masses are measured without the tuning heads, and the body masses are measured after routing a small ($\sim 3 \times 10 \times 300$ mm) channel for the truss-rod (§2.2).

The extent of the influence of the neck on the vibratory behaviour of the guitar (*i.e.* the guitar body with a neck attached) may be reckoned by examining the vibratory properties of the body before and after neck assembly. Some results of this addition are quite obvious. Before the addition of the neck, Chladni figures show a nodal region along the perimeter of the head-block (the piece of solid wood that serves as an anchor-point on the body for the neck), at 700 Hz for the Engelmann spruce, 814 Hz for Sitka spruce (Figure 7.1—not detected in the Western Red cedar). With the addition of the neck, the nodal line in this area changes from a straight line, perpendicular to the axis of the body, to that of a concavity with a focus towards the head-block (Figure 7.2). This is probably a node of a flexural mode of the whole instrument, including the neck, although the motion of the neck is not directly measured here.

The phase relationships between the force and acceleration measured at the bridge point show there is a weak low frequency feature common to all three of the guitars with the necks attached which does not exist when the necks are not present (Figure 7.3). For the Engelmann spruce guitar, this occurs at 65 Hz, 57 Hz for the Sitka spruce and 62 Hz for the Western Red cedar guitar (Figure 7.7). This is in the frequency range observed in [French and Hosler, 2001]. Features are also seen in the
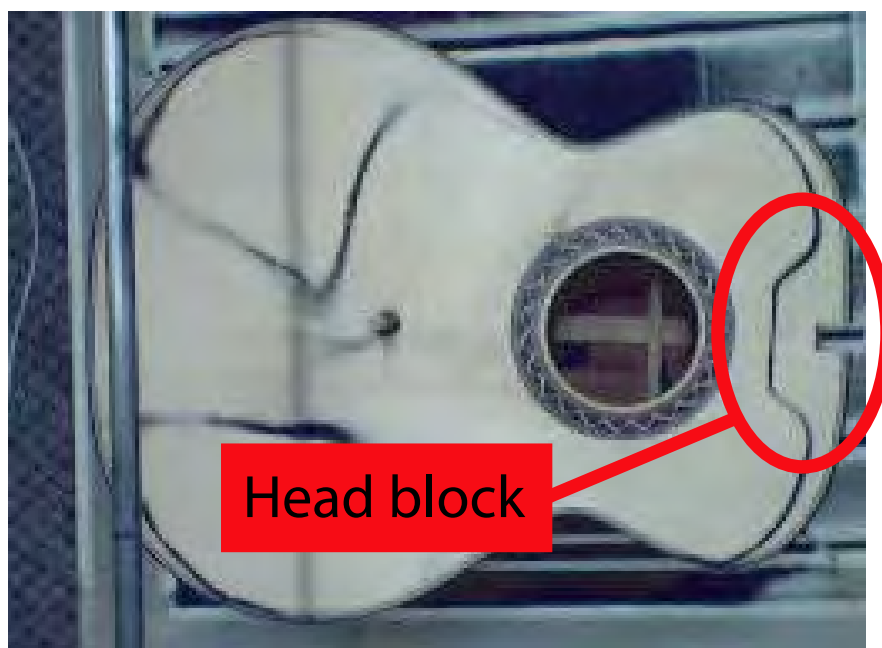
Figure 7.1: Chladni figure illustrating the detail of a nodal region taking the shape of the perimeter of the head-block. (From Engelmann spruce, after binding, at 700 Hz).
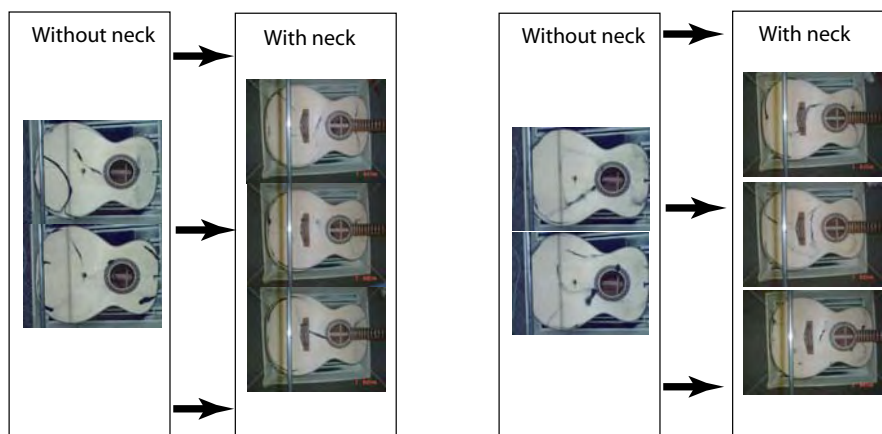
Figure 7.2: Changes in the shape of some Chladni figures with the addition of the neck, in the vicinity of the head-block. (Figures from Engelmann spruce with bindings compared to those with neck attached).

relative phases between the air pressure measured at the soundhole and the force measured at the bridge, at 59 Hz and 210 Hz for the Engelmann spruce soundboard, 57 Hz [95°](only) (49 Hz,[88°])for the Sitka spruce soundboard and 62 Hz and 205 Hz for the Western Red cedar soundboard (Figure 7.6.) *q.v.* In Figure 7.7 there are features at (65 Hz,[26°]) and (51 Hz,47°)] for the Engelmann spruce, (57 Hz,[22°]) and (38 Hz,49°) for the Sitka spruce and (62 Hz,[14°]) and (50 Hz,18°)] for the Western Red cedar soundboard.

There are also Chladni figures at the same frequencies for the Engelmann spruce and the Western Red cedar, with a node occurring near the bridge point, which again could be a node of the first flexural (free-free) mode of a beam equivalent to the entire instrument.

The low frequency features in the dynamic mass spectra are close to those calculated to be due to motion as a result of the addition of the neck (59 Hz and 188 Hz) in the FEM calculations performed by Laille and Maziere in §4.6.

Changes with the addition of the neck in Figure 7.8 show some differences around 600 Hz and 800 Hz. Examination of the Chladni figures shows the modification of modes at *e.g.* 609/675Hz $\rightarrow$ 581/616/638 Hz and 749/815Hz $\rightarrow$ 709/797/832Hz for the Engelmann spruce soundboard. The guitars studied here have a bolt-on neck system, and there are no vibratory losses detected, which might be expected if there were incomplete mechanical coupling between the body and the neck.
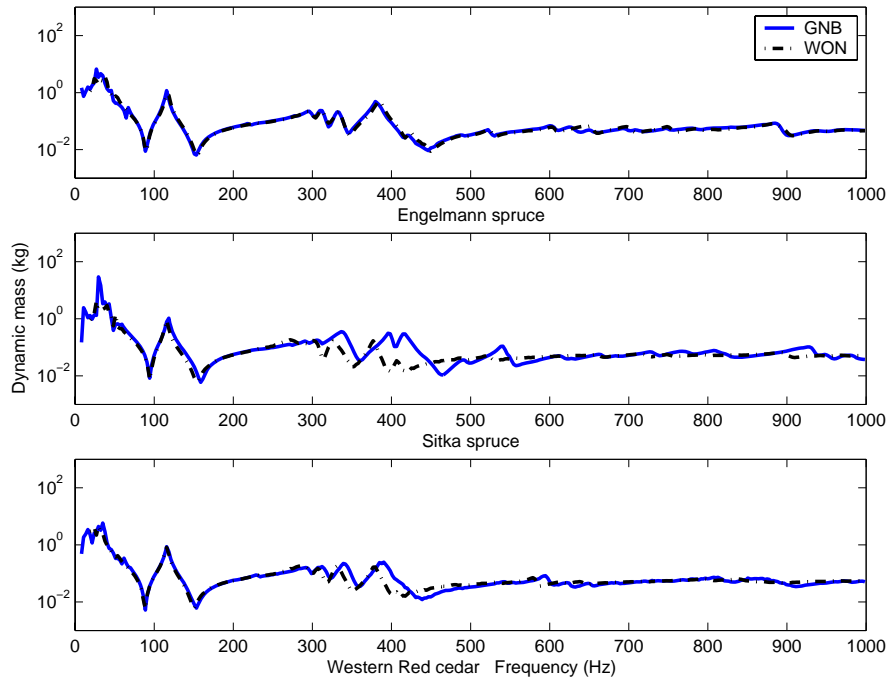
Figure 7.3: Dynamic mass spectra of the three guitars after the addition of the neck. The differences in the spectra Engelmann spruce and Western Red cedar observed about 400 Hz are the T(1,2) modes, where there is a node passing through the soundhole. This area might act as a pivot point for the vibration of the neck.
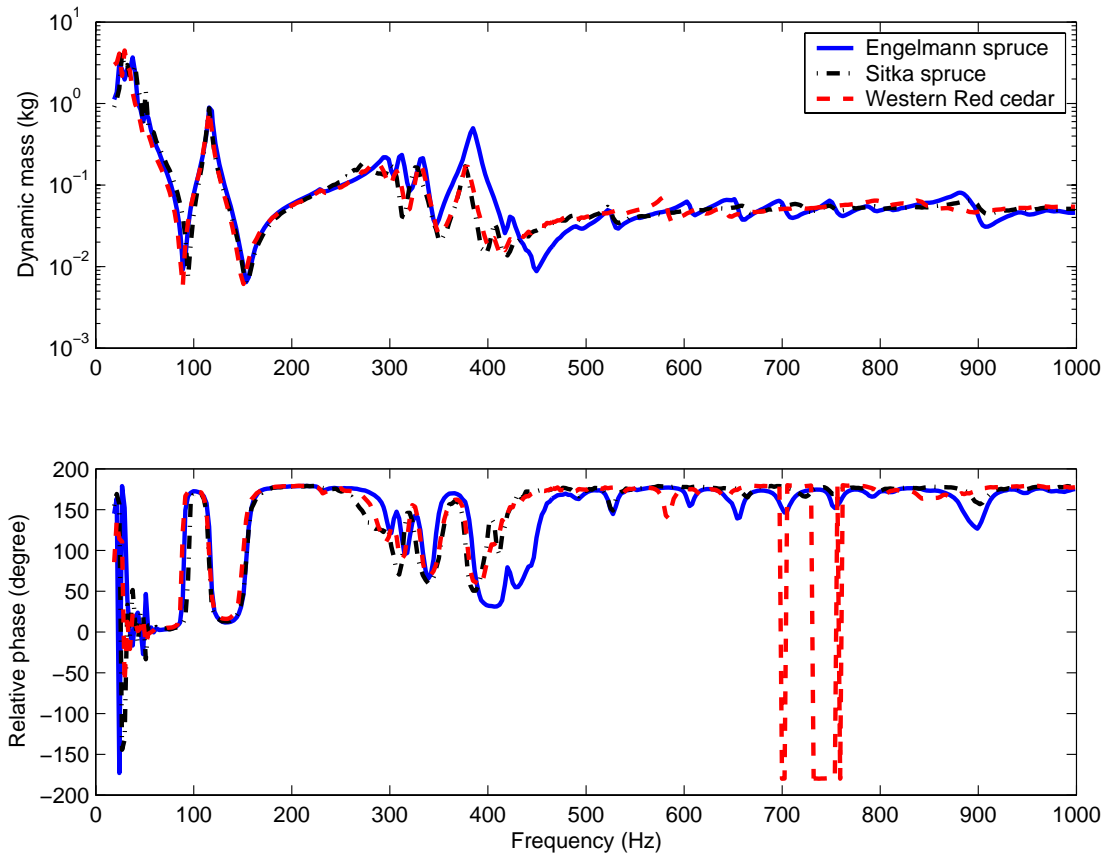
Figure 7.4: Magnitude and phase of the dynamic mass of the guitars before the addition of the neck, as a comparison of the three guitars.
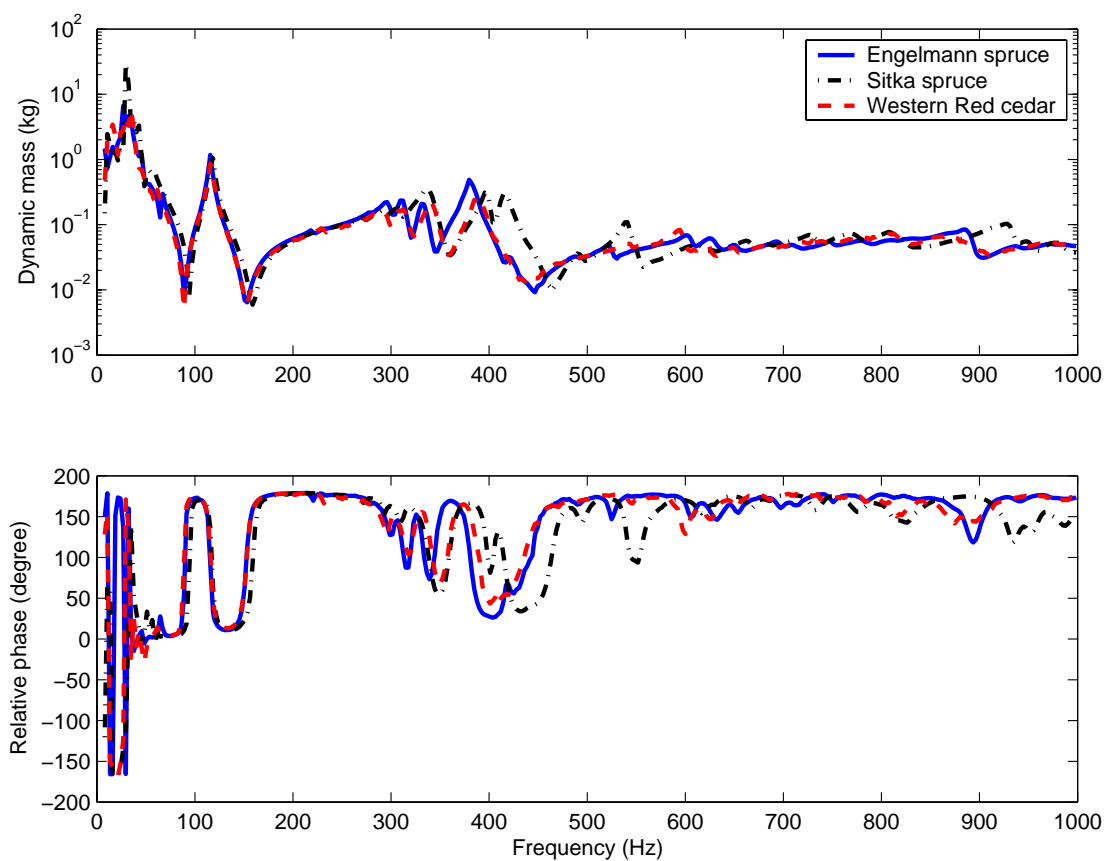
Figure 7.5: Magnitude and phase of the dynamic mass of the guitars after the addition of the neck, as a comparison of the three guitars.
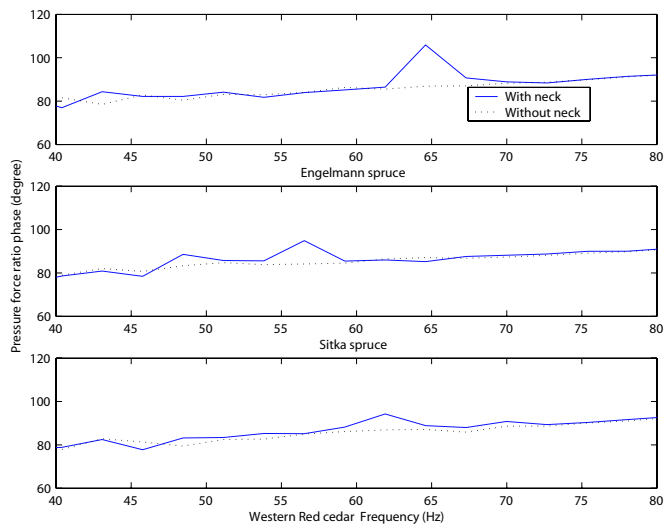
Figure 7.6: The low frequency effects of the neck on the phase of pressure force ratio.
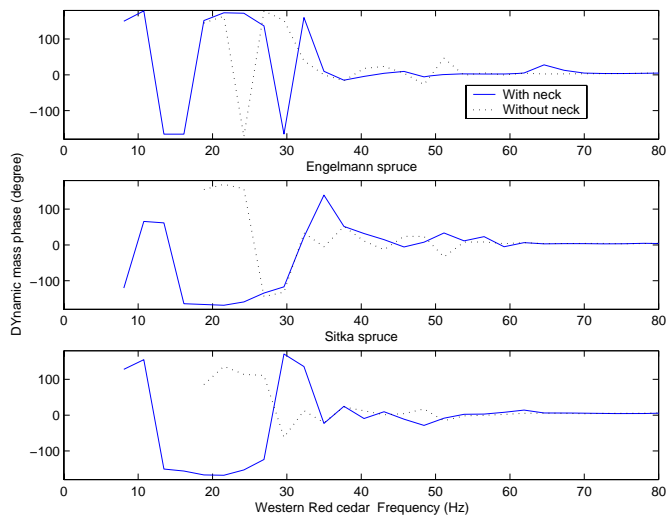
Figure 7.7: The effects of addition of the neck on the relative phase of low frequency dynamic mass.
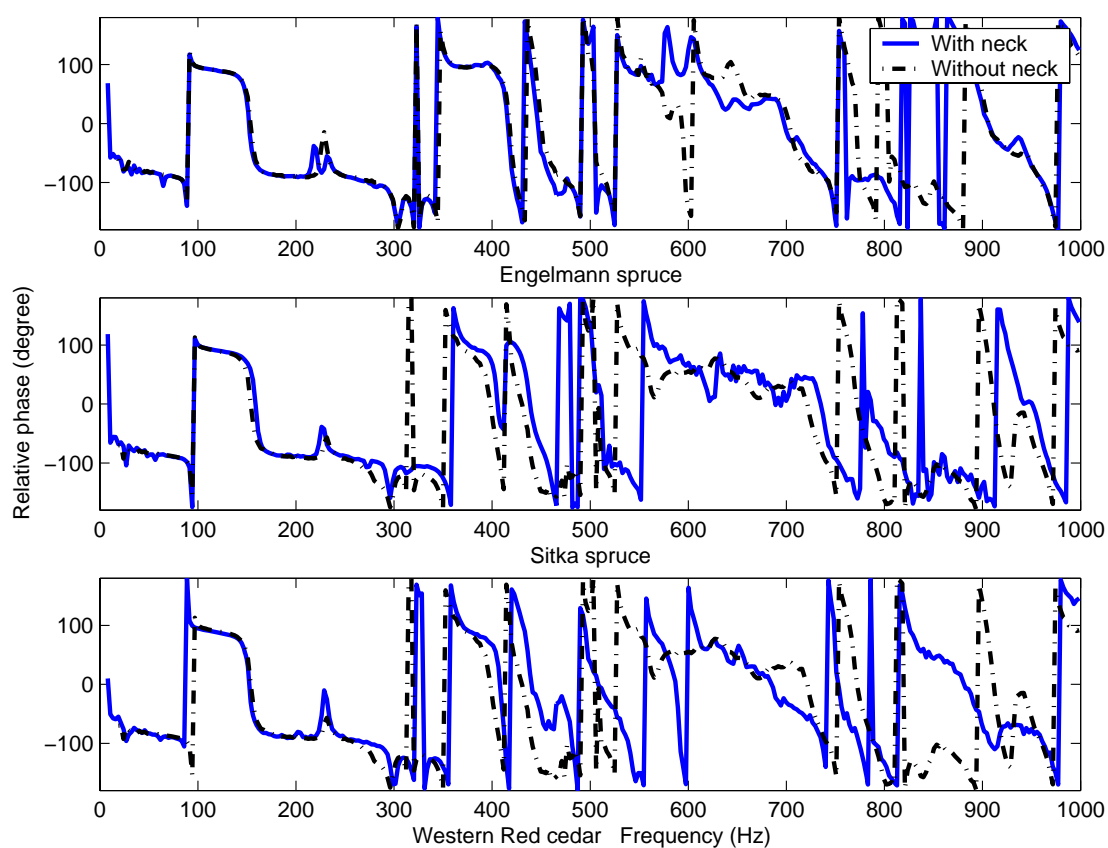
Figure 7.8: Phase of the pressure force ratio of the guitars before and after the addition of the neck.

7.2 Addition of the bridge

The mass of the bridge (34 g) is a significant fraction of the total mass of the soundboard (12% in the case of Engelmann spruce, 11% for Sitka spruce and 14% for the Western Red cedar soundboard). Because it occupies a central position of the soundboard, the bridge affects the vibratory behaviour of low frequency modes of the soundboard because of the mass load and the added stiffness also has an effect on higher frequency modes (Figure 7.9). In a study on the effect of various bridges on the behaviour of the guitar, Jürgen Meyer found that the most desirable bridge was that with the least mass [Meyer, 1983a].

After adding the bridge, the Western Red cedar has a lower magnitude of pressure force ratio in the frequency range $500 \rightarrow 650$ Hz, in comparison to the other two guitars; this includes the T(1,2) and T(2,2) modes (Figure 7.10). In both of these modes, nodal areas of the Chladni figures coincide with the position of the bridge for the Engelmann spruce and the Sitka spruce. For the Western Red cedar, the bridge is largely an antinodal area for most modes. One might expect that the efficiency in transmission of vibration from the bridge to the soundboard, at modes where the bridge occupies a node, should be greatly reduced [Jansson, 2002].

The phase difference between the force and the acceleration at the bridge point after addition of the bridge is shown in Figure 7.11. In all three guitars, the frequencies associated with the lowest coupled motion between the soundboard and the air in the soundhole (f_-, f_H and f_+) are increased slightly (Table 7.2). This includes the Helmholtz resonances, which might be expected because of the reduction of the
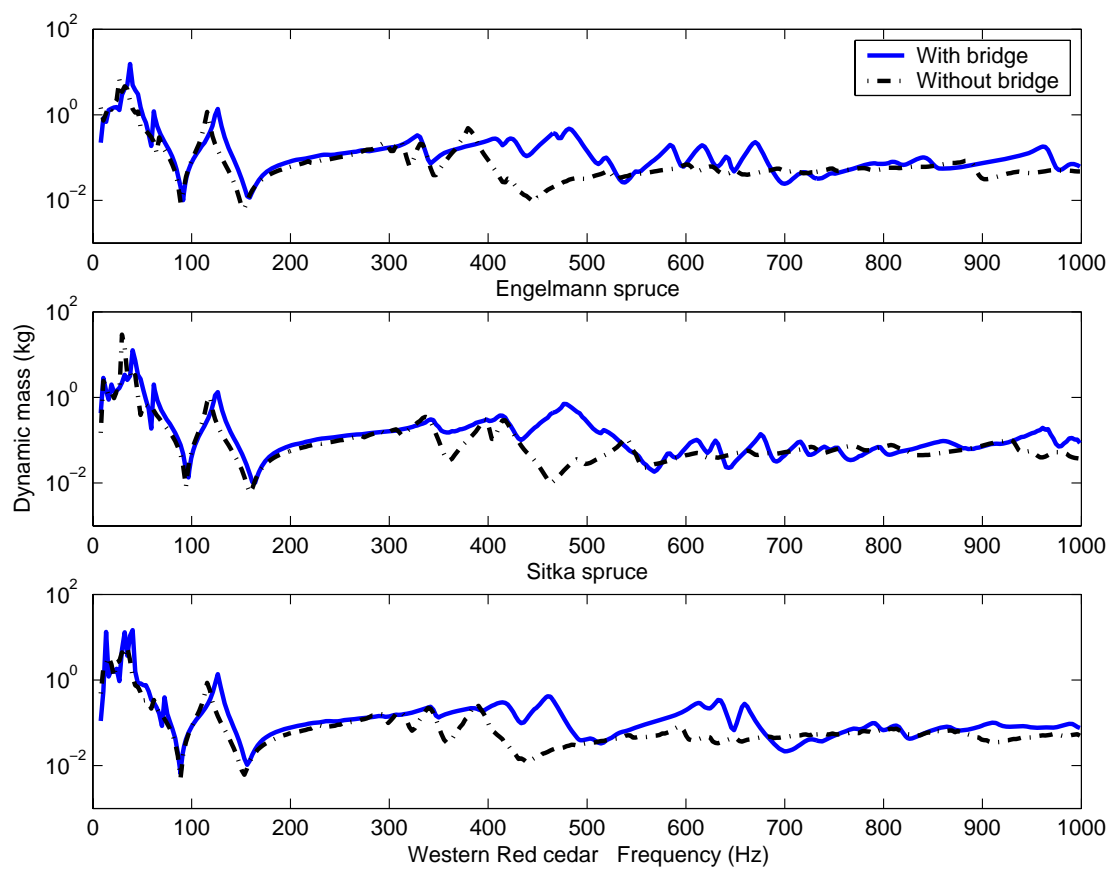
Figure 7.9: The changes in dynamic mass due to the addition of the bridge. Effects are great in the $T(1,2)_2$ frequency region $(300 \rightarrow 500$ Hz$)$
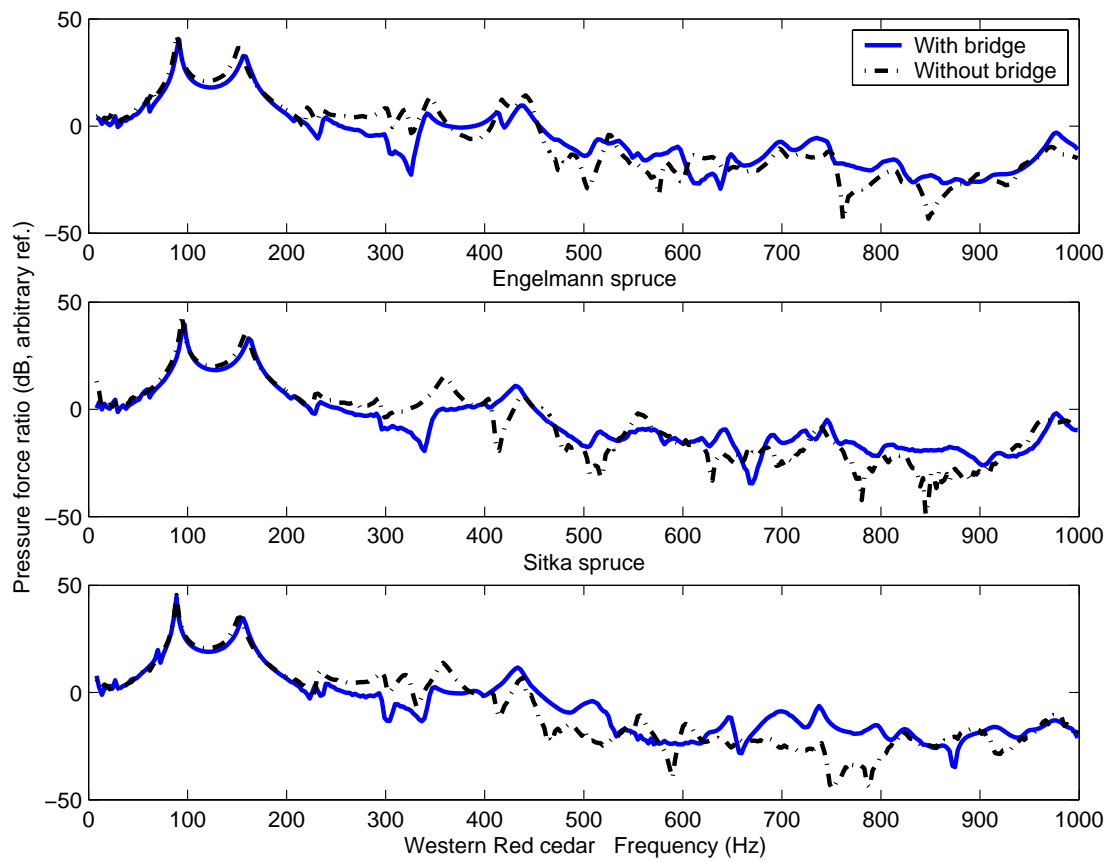
Figure 7.10: Changes in the pressure force ratio spectra due to the addition of the bridge.

Frequency	ES	SS	WRC
f_-	$89 \rightarrow 92$ Hz	$94 \rightarrow 97$ Hz	$89 \rightarrow 89$ Hz
f_H	$116 \rightarrow 127$ Hz	$119 \rightarrow 127$ Hz	$116 \rightarrow 127$ Hz
f_+	$153 \rightarrow 158$ Hz	$159 \rightarrow 164$ Hz	$153 \rightarrow 156$ Hz

Table 7.2: The change in low frequency air-body coupling due to the addition of the bridge. The effects on the shift in the coupled frequencies are much more pronounced than for any other construction stage considered here.

compliance of the body, especially in the lateral direction.

At higher frequency, there is little effect on the phase of the dynamic mass of the bridge point until the $T(1,2)_2$ mode, at about 300 Hz. Without the bridge, all three have a phase difference of nearly 180° which then decreases to about 60° (71°, 51° and 67° for Engelmann spruce, Sitka spruce and Western Red cedar respectively) at higher frequency, after five local turning points. The addition of the bridge reduces these turning points to a single minimum (with a phase difference in dynamic mass of 110°, 130° and 143° for Engelmann spruce, Sitka spruce and Western Red cedar), which is associated with the T(1,2) mode. Before the bridge is added, the modes between 350 Hz and 450 Hz comprise several different configurations of dividing the soundboard longitudinally into two vibrating areas. Two of these configurations are shown in the Chladni figures in Figure 7.12. These separate configurations occur at slightly different frequencies, which is evident in the dynamic mass spectra. With the addition of the bridge, there is only one configuration: a nodal line occurring along the axis of the bridge, perpendicular to the axis of the guitar. In the case of the T(2,2) mode, the effect of the increased local stiffness from the addition of the bridge (Figure 7.13) is evident: the nodal lines form along a direction perpendicular
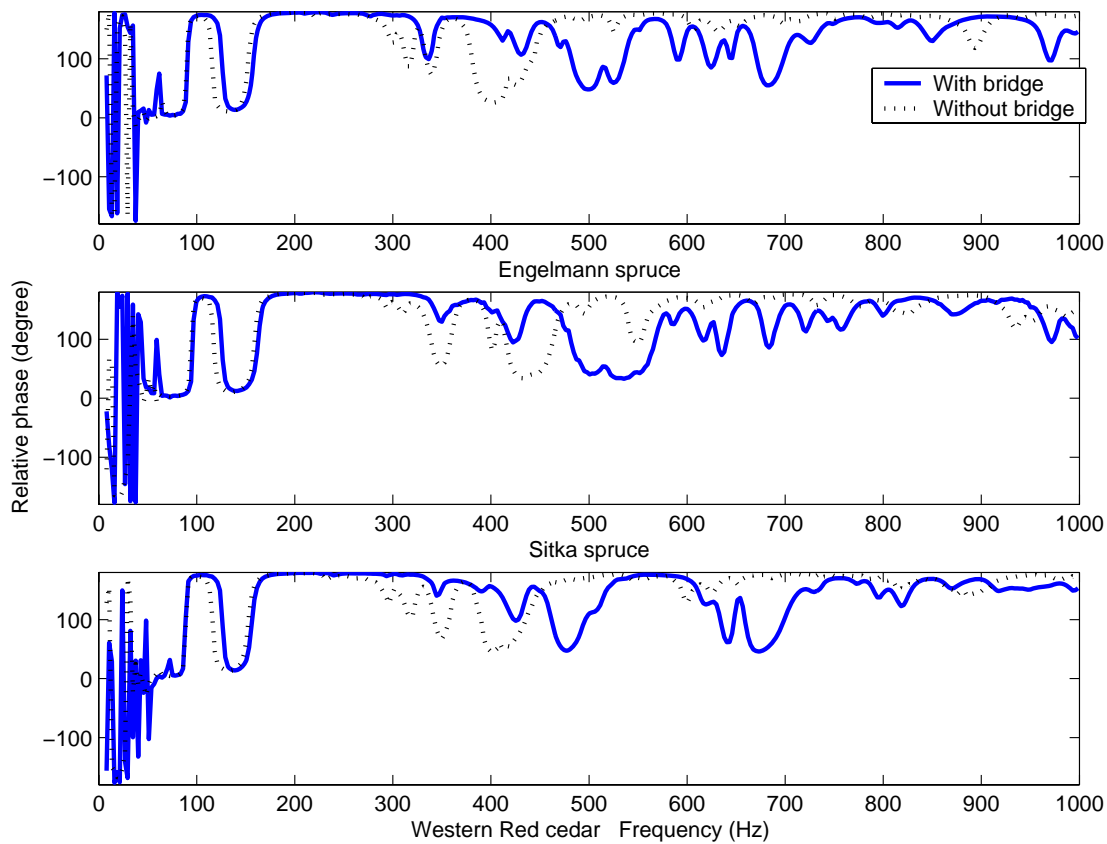
Figure 7.11: The change of relative phase between force and acceleration at the bridge point, upon adding the bridge.

to the axis of the guitar. The pressure force ratio in this region is greater when the guitars have no bridge. This situation is reversed at about 450 Hz, after which the phase difference is generally greater for the guitar with no bridge.

The bridge adds a highly anisotropic component of stiffness to the soundboard: it effectively another brace of the soundboard [Richardson, 1982]. Of all the construction phases following the manufacture of the soundboard and bracing, the addition of
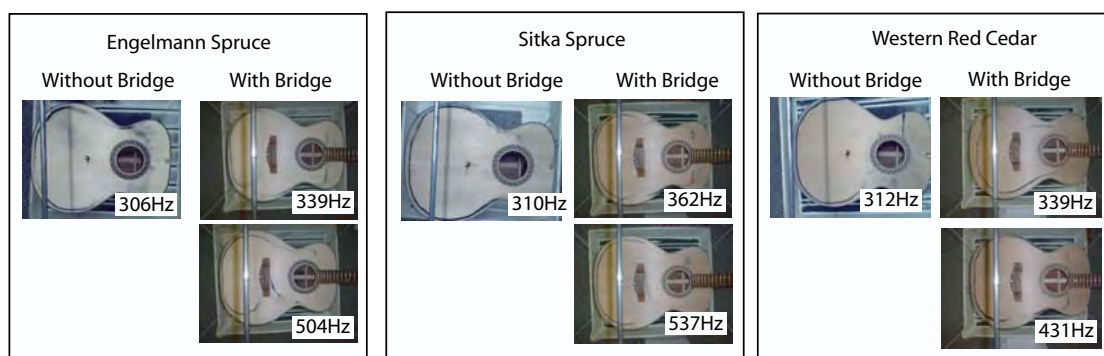
T(1,2) mode

Figure 7.12: Chladni figures of the T(1,2) mode before and after the addition of the bridge. Several distinct configurations of this mode are made degenerate with the addition of the bridge, simplifying the motion. This is most obvious in the case of the Sitka spruce soundboard. This is seen as a 'smoothing' effect in the dynamic mass spectra (Figure 7.9).
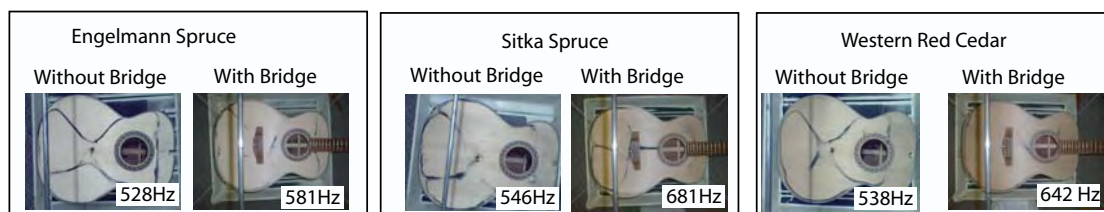
T(2,2) mode

Figure 7.13: Chladni figures of the T(2,2) mode before and after the addition of the bridge. Several distinct configurations of this mode are made degenerate with the addition of the bridge, simplifying the motion.

the bridge is the most influential on the sound output. Modes with nodal regions in the vicinity of the bridge position, such as the T(1,2) and T(2,2) modes, have a few possible configurations, which are reduced with the addition of the bridge. This is observed in the dynamic mass spectra as a reduction of the distinct maxima/minima around the frequency of these modes.

7.3   The polished instruments

The application of a protective coating to the external surfaces of the guitar (§3.4) may conceivably add some mass, damping and stiffness to the plates of the guitar. The significance of this on the resulting sound has been debated ([Haines, 2000, Schleske, 2000, Barlow and Woodhouse, 1989, Fryxell, 1984] §3.4).

The guitars studied here have a polish comprised of a thin coat ($\sim 150\mu$m) of nitrocellulose lacquer. The dynamic mass spectra of the guitars three days after application of the finish are presented in Figure 7.14 and the pressure force ratio spectra are in Figure 7.15.

The frequency of the modes occurring approximately between 810 and 840 Hz are lowered slightly (Engelmann spruce $832 \rightarrow 819$ Hz Sitka spruce $849 \rightarrow 842$ Hz and Western Red cedar $818 \rightarrow 814$ Hz) and the pressure force ratio is reduced in this region also.

The T(1,2) and T(2,2) modes are lowered by $5 - 6$ Hz, indicating that there is some effect of a mass load on these modes. The greatest differences in the dynamic mass spectra are at frequencies near 1 kHz (Figure 7.16). Is is expected that the effects on vibratory behaviour arising from the polish should be more significant at higher frequencies.
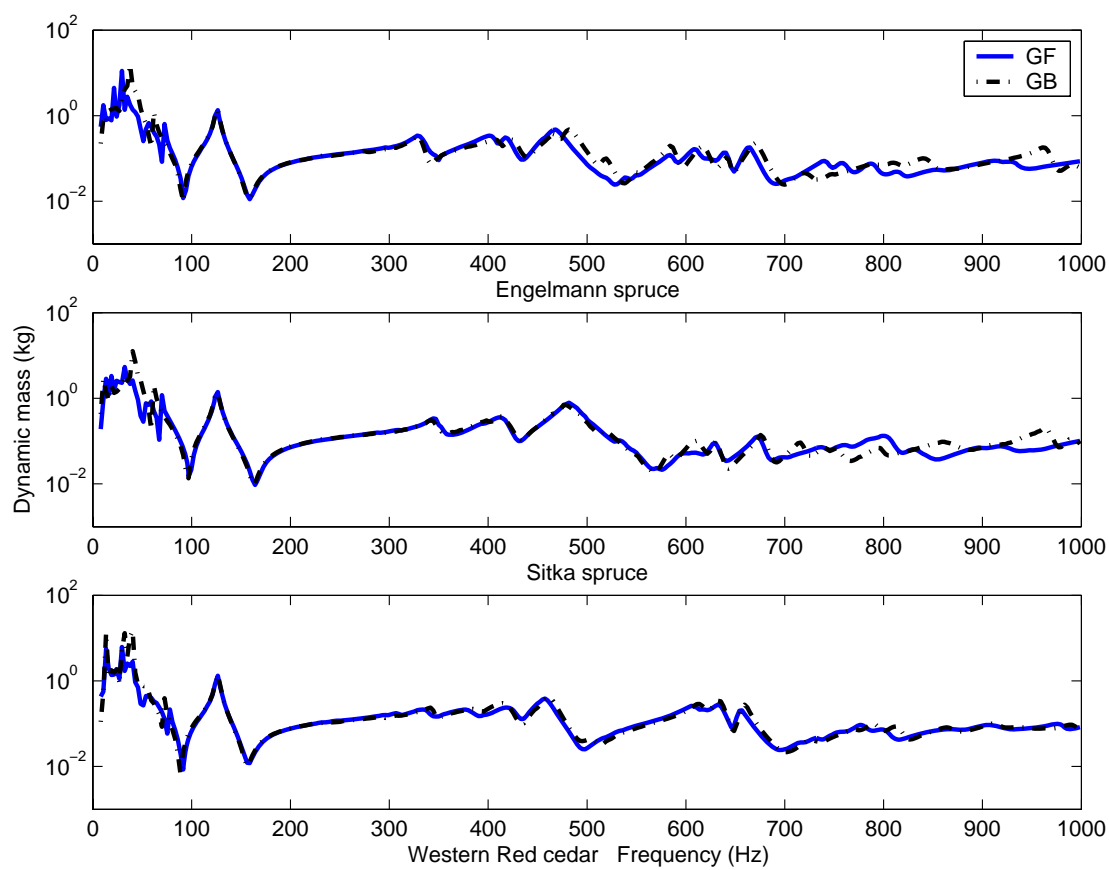
Figure 7.14: Dynamic mass of guitar bodies before and after application of a nitro-cellulose lacquer polish.
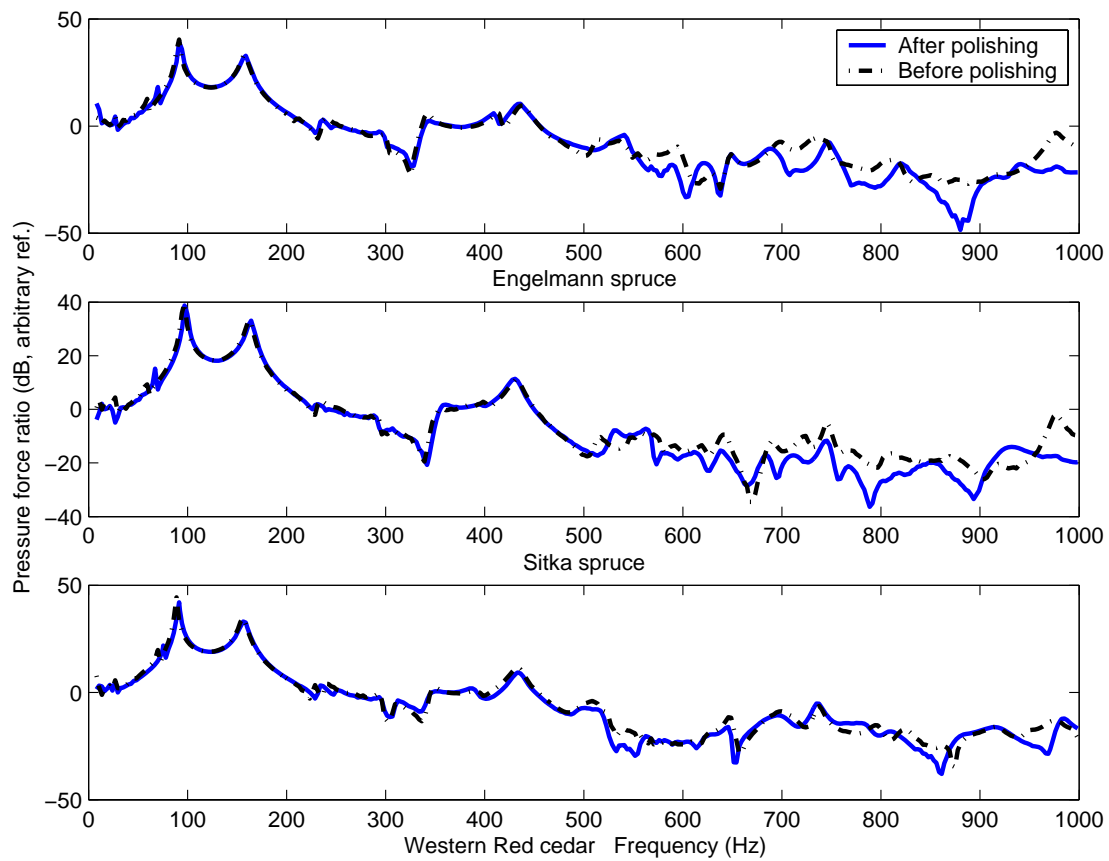
Figure 7.15: Pressure force ratios of guitar bodies after application of a nitrocellulose lacquer polish.
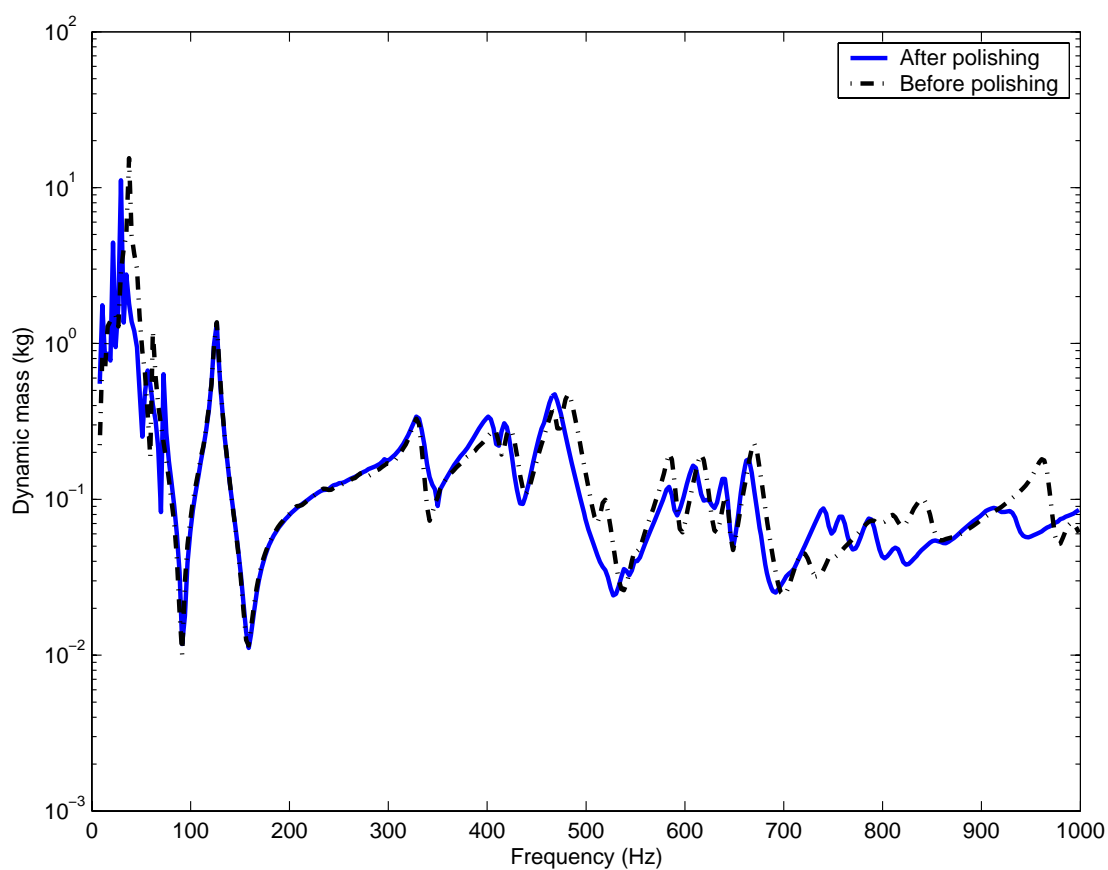
Figure 7.16: Dynamic mass spectrum of a guitar before and after applying a nitrocellulose lacquer polish. Shown are the measurements for the Engelmann spruce soundboard. There are measurable differences in the magnitudes at T(1,2), T(2,2) and what appears to be the T(5,3) soundboard mode.

7.4   Effects of lacquer curing

Because the polish is applied with the aid of a volatile solvent base, there is a period of time required to evaporate the solvent (*curing*). The dynamic mass spectra, after a curing period (53 days), are shown in Figure 7.17. The transfer function of the air pressure measured at the soundhole in response to a force at the bridge is given in Figure 7.18.
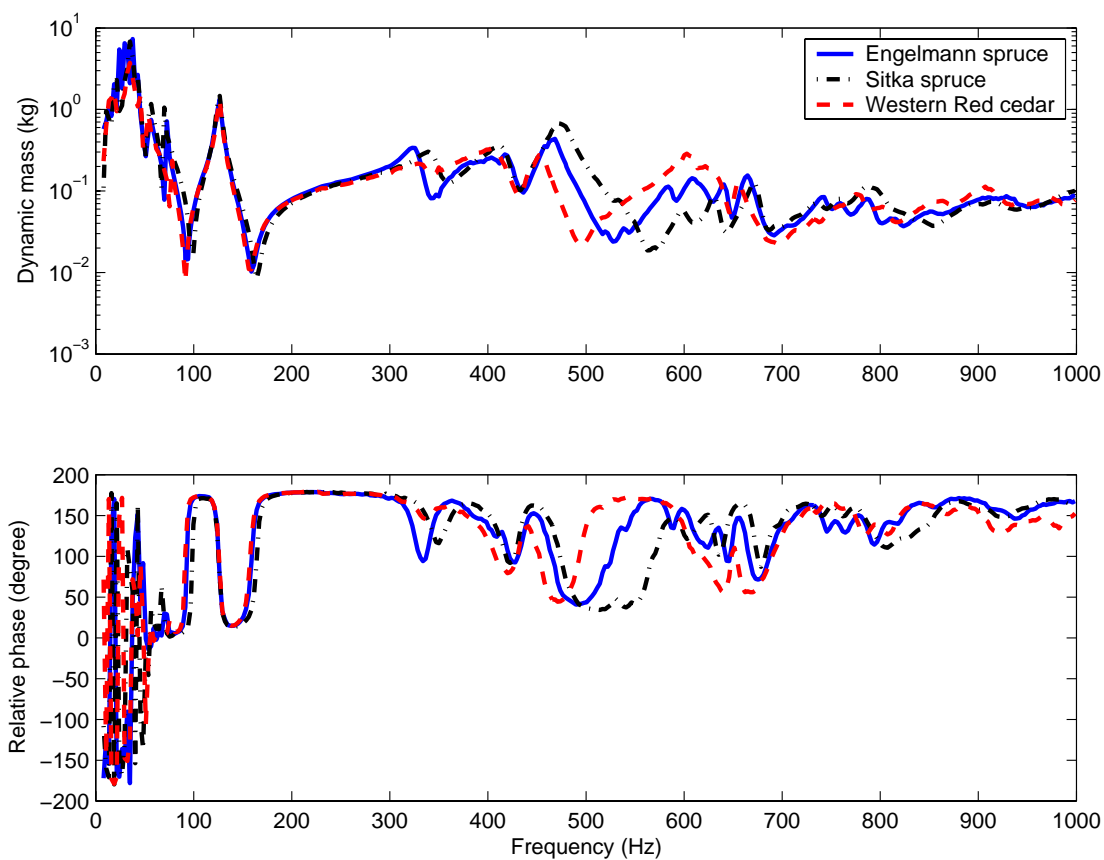
Figure 7.17: Dynamic mass of guitar bodies after hardening of the nitrocellulose lacquer polish.
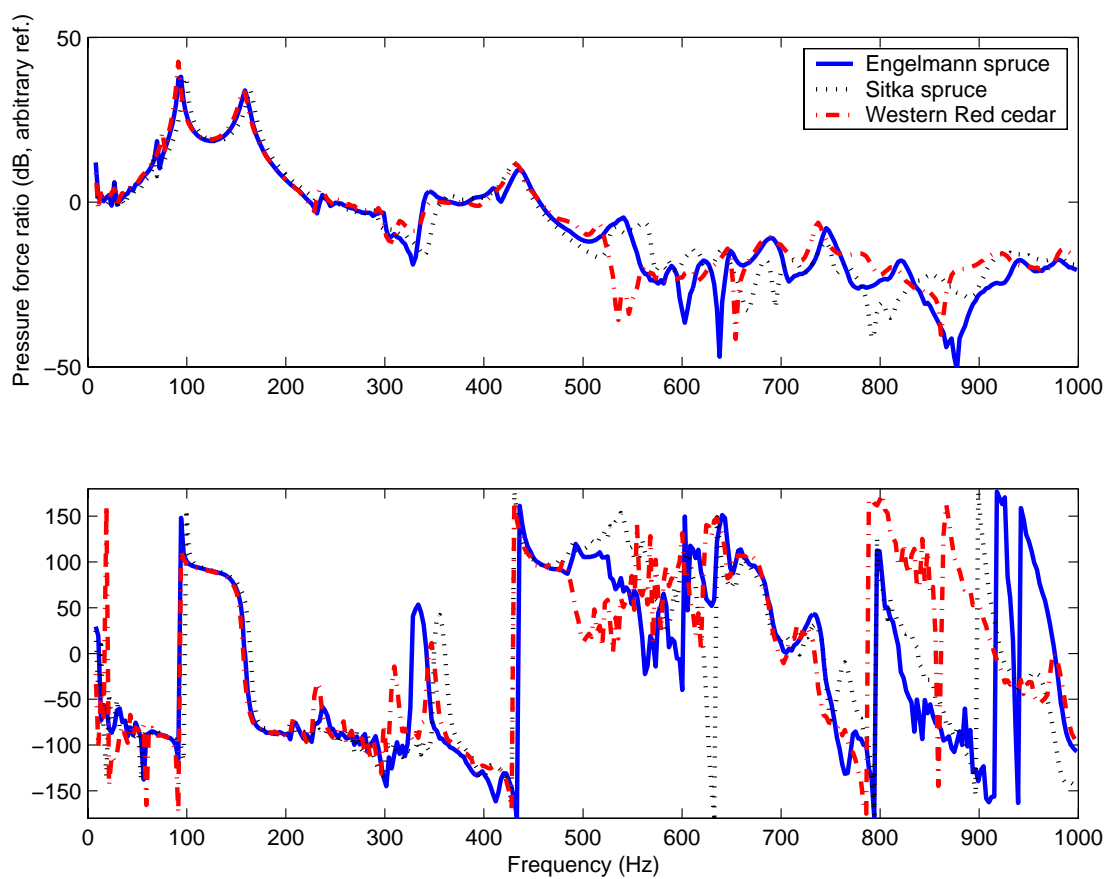
Figure 7.18: Pressure force ratio of guitar bodies after hardening of the nitrocellulose lacquer polish.
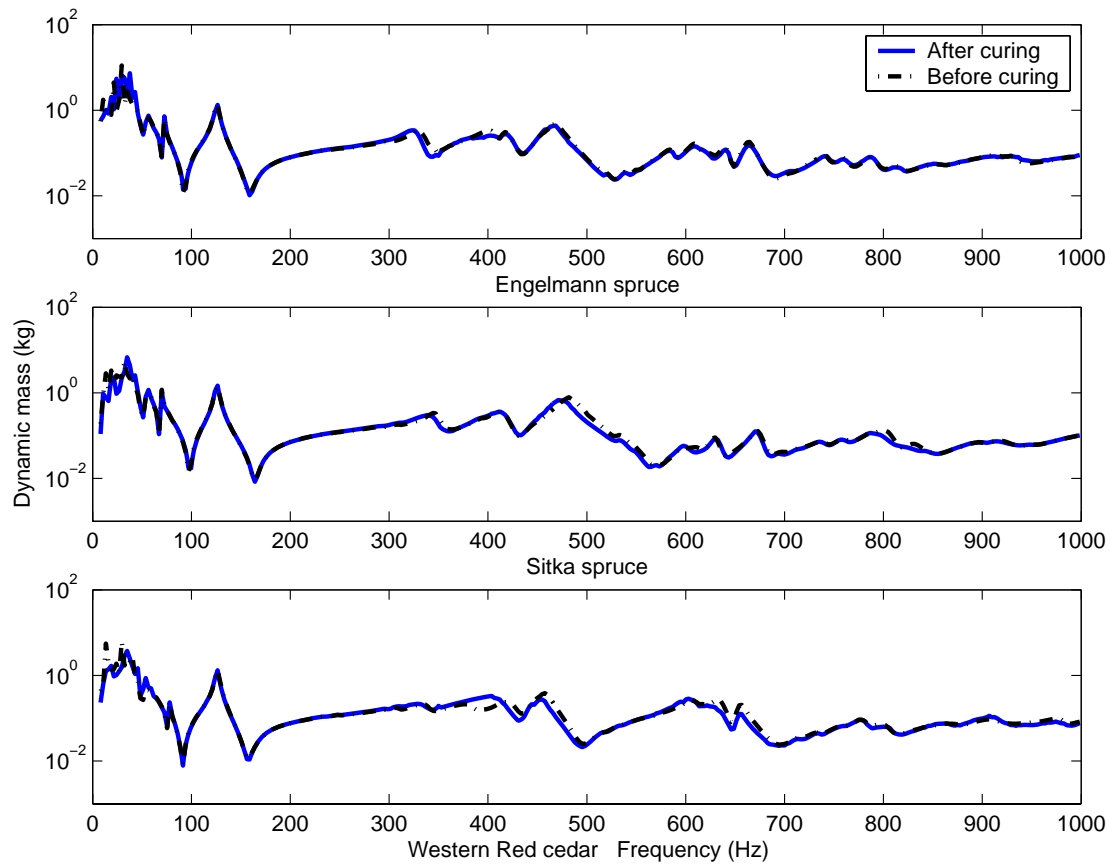
Figure 7.19: The changes in dynamic mass after the curing of the nitrocellulose polish on the guitars.

The effect of polish curing has little measurable effect on the dynamic mass spectra (Figure 7.19) or the pressure force ratio (Figure 7.20), except for some reduction in the magnitude of the dynamic mass around the $T(1,2)_2$ mode (about 504, 537 and 474 Hz for the Engelmann spruce, Sitka spruce and Western Red cedar guitars respectively.)
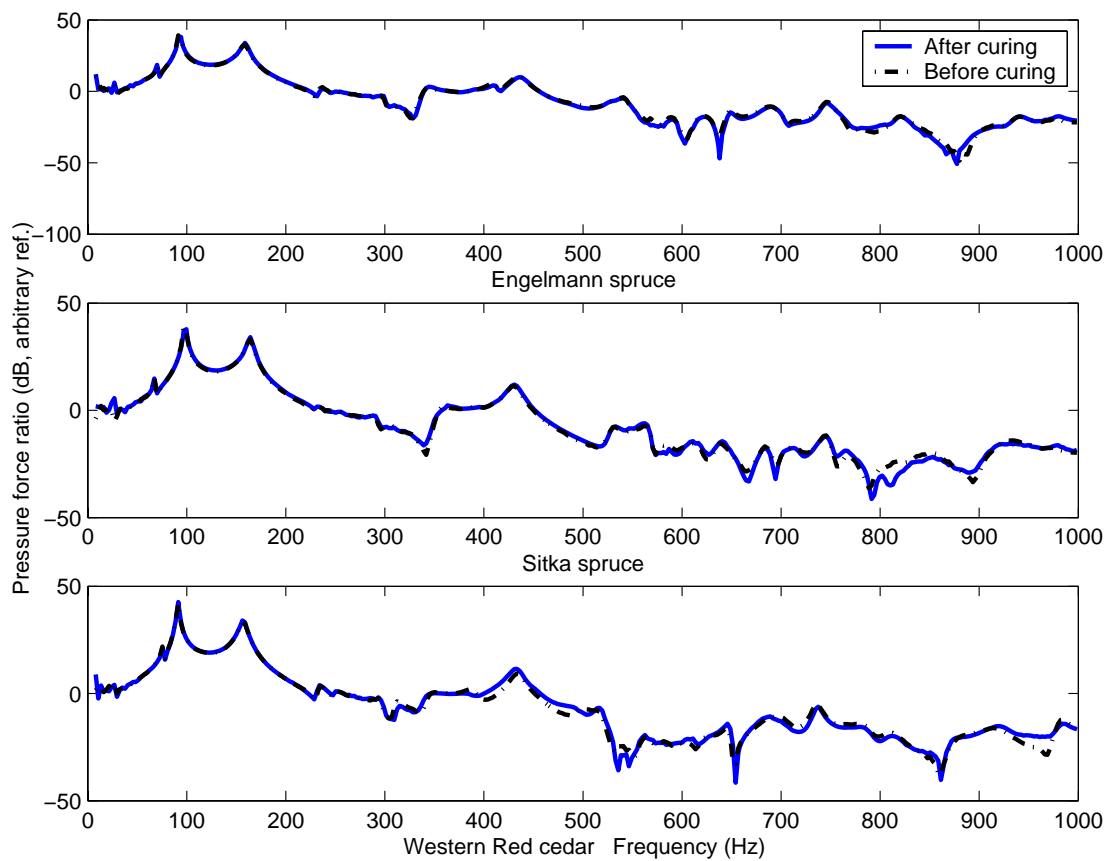
Figure 7.20: The changes in pressure force ratio after the polish is allowed 53 days to 'cure'.

7.5   Short term ageing and playing in

Some of the effects of 'playing in' have been studied in the violin [Hutchins, 1998, 1989]. It is very difficult to separate the effects of playing an instrument from that of ageing or environmental exposure [Inta et al., 2005]. It is also difficult to quantify the 'amount' any particular instrument has been played. The dynamic mass spectra of the three guitars after a period of two years of playing all three instruments, for roughly equal amounts, are given in Figure 7.21. The pressure force ratios at this stage are displayed in Figure 7.22. The total amount of playing time was not long, less than ten hours for each instrument. It is expected that any conceivable component of measured change in vibratory properties due to playing effects would be comparatively small. It is not known whether the small amount the guitars have been played have 'played in' the instruments to the extent that would alter the vibratory properties of the instrument commensurate with the anecdotal evidence of musicians [Hutchins, 1998, Turner, 1997].

There is very little difference in the dynamic mass after ageing (and a small amount of playing) the guitars for two years (Figure 7.23).

There is also little difference in the pressure force ratio spectra except between 800 and 1000 Hz, most obviously in the case of the Engelmann spruce guitar (Figure 7.24).
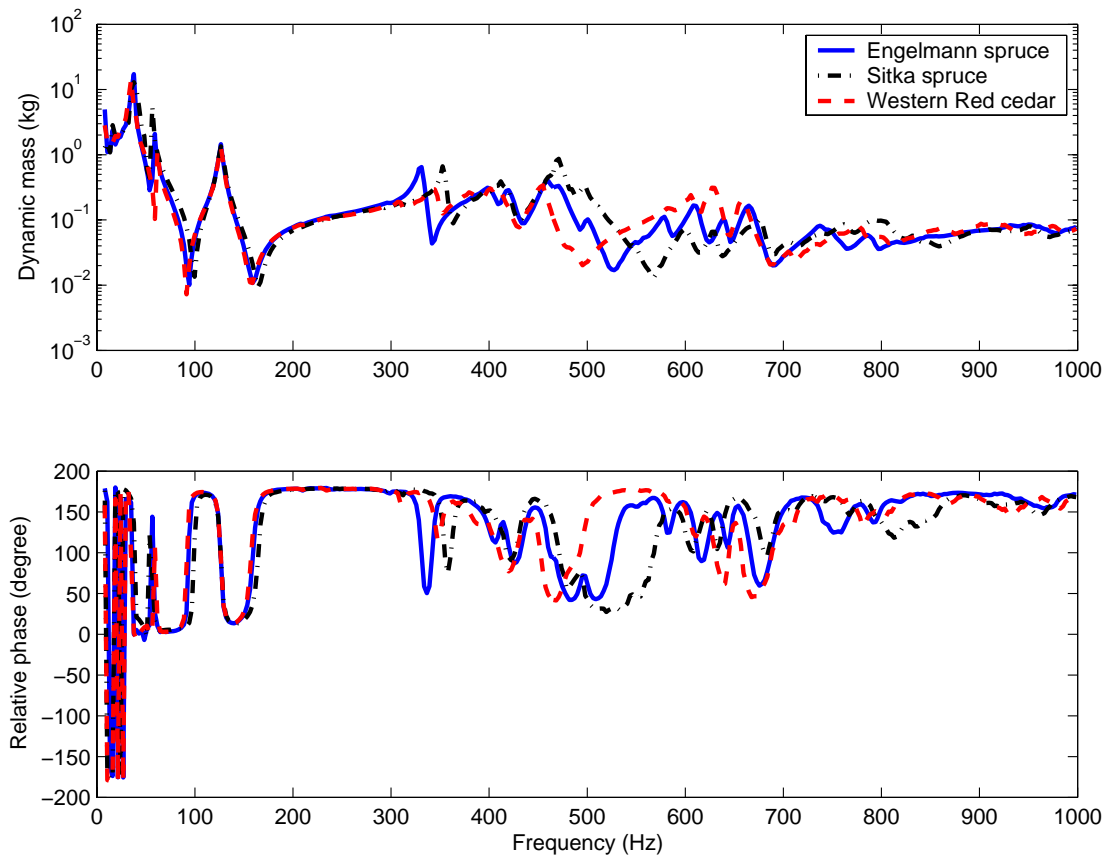
Figure 7.21: Dynamic mass of guitar bodies after ageing and some playing of all three guitars for two years.
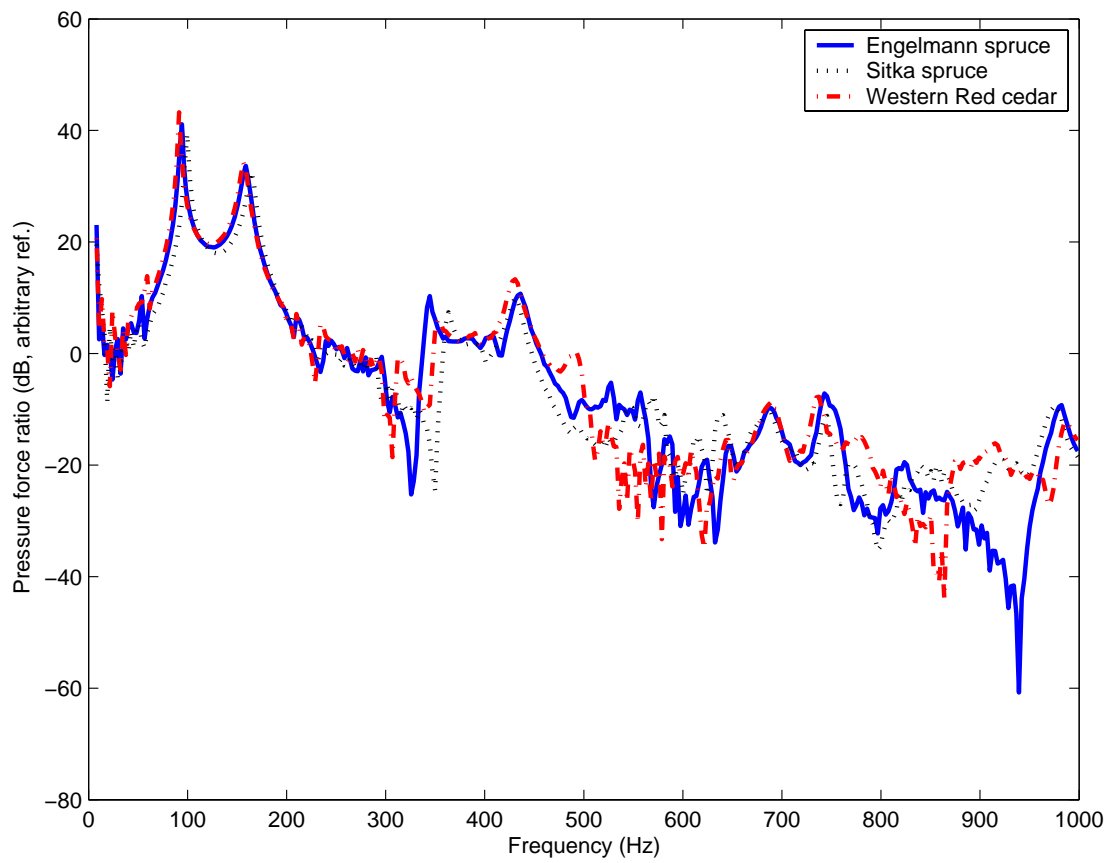
Figure 7.22: Pressure force ratio of the three guitars after ageing and some small amount of playing the instruments for two years.
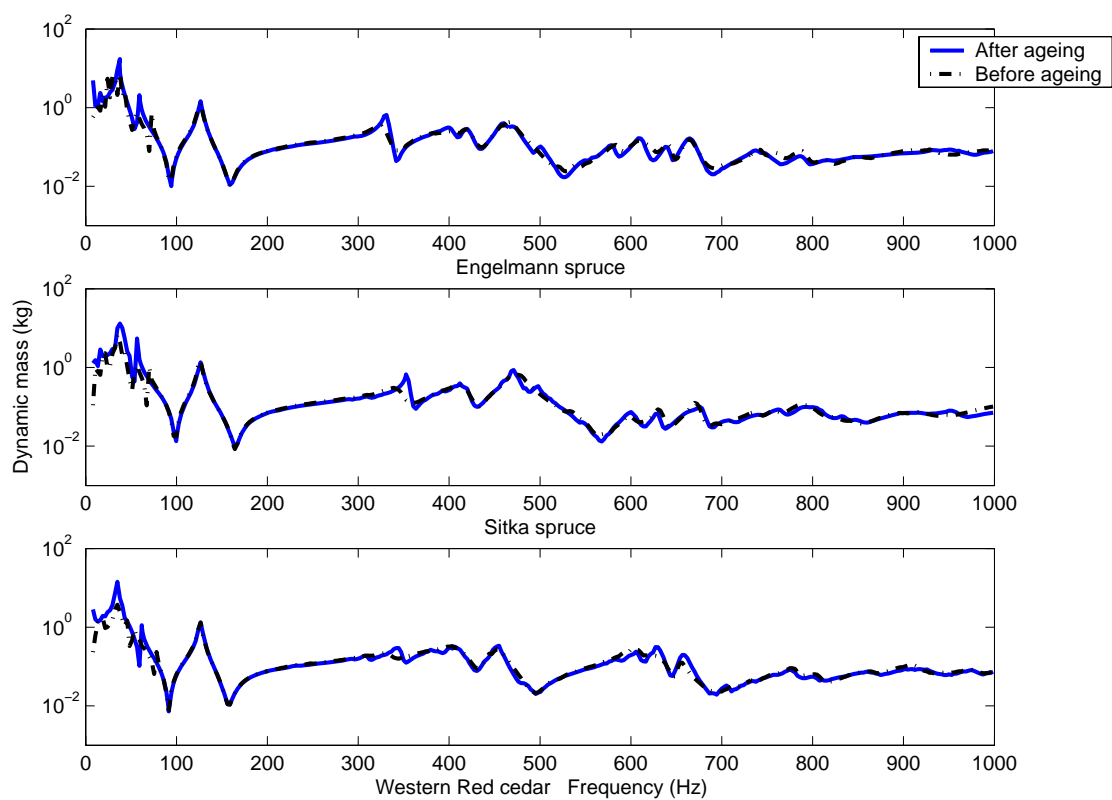
Figure 7.23: Changes to the three guitars due to an ageing (and some playing) period of two years.
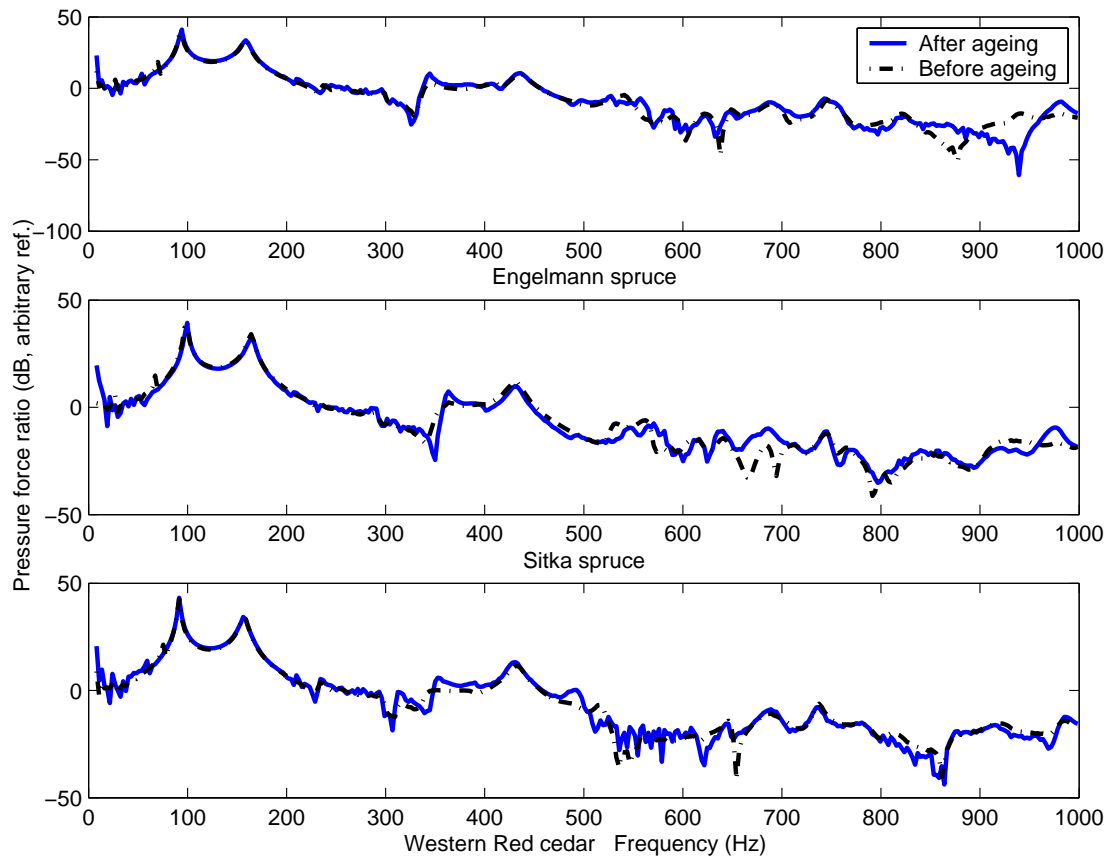
Figure 7.24: Pressure force ratio spectra due to an ageing (and some playing) period of two years. There is very little difference except small decreases about 900 Hz.

Effects due to an applied mass load

The effects of a mass load applied to the guitar soundboards were investigated. A load was applied by bonding a brass mass with a thin layer of plasticine to two different points on the soundboard: directly next to (but not touching) the driving point, and a central region of the soundboard about 10 mm below the base of the bridge. Both points were along the central axis of the guitar (Figure 7.29). The application of a mass load enables the characterisation of the soundboards in terms of a simple mass-spring system (§7.7) by measurement of the resulting vibratory properties. Some luthiers have been known to use plasticine as a diagnostic tool to indicate where mass should be removed to produce a desired alteration of the output sound of the instrument [Gilet, 2000].

The addition of a 100 gram mass to the driving point reduces the pressure force ratio in the low frequency soundboard/air cavity coupling region, at frequencies up to approximately 300 Hz (Figure 7.25). There is little difference in the frequency range $300 \rightarrow 800$ Hz. Most of the soundboard modes have antinodal areas in the region of the bridge, with the exception of the T(1,2) mode (occurring between $300 \rightarrow 800$ Hz) where a nodal line passes directly through the bridge region. A mass added to a nodal region has little effect on the motion, compared to that of an antinode [Strutt, 1869]. There is a reduction in the pressure force ratio of the guitars at about 900 Hz, where the bridge occupies an antinodal region of a soundboard mode around this frequency.

The induced phase differences due to mass loading are shown in Figure 7.26.

Figure 7.28 shows the same effect on the Engelmann spruce soundboard alone, with an intermediary 50 gram mass load at the driving point.
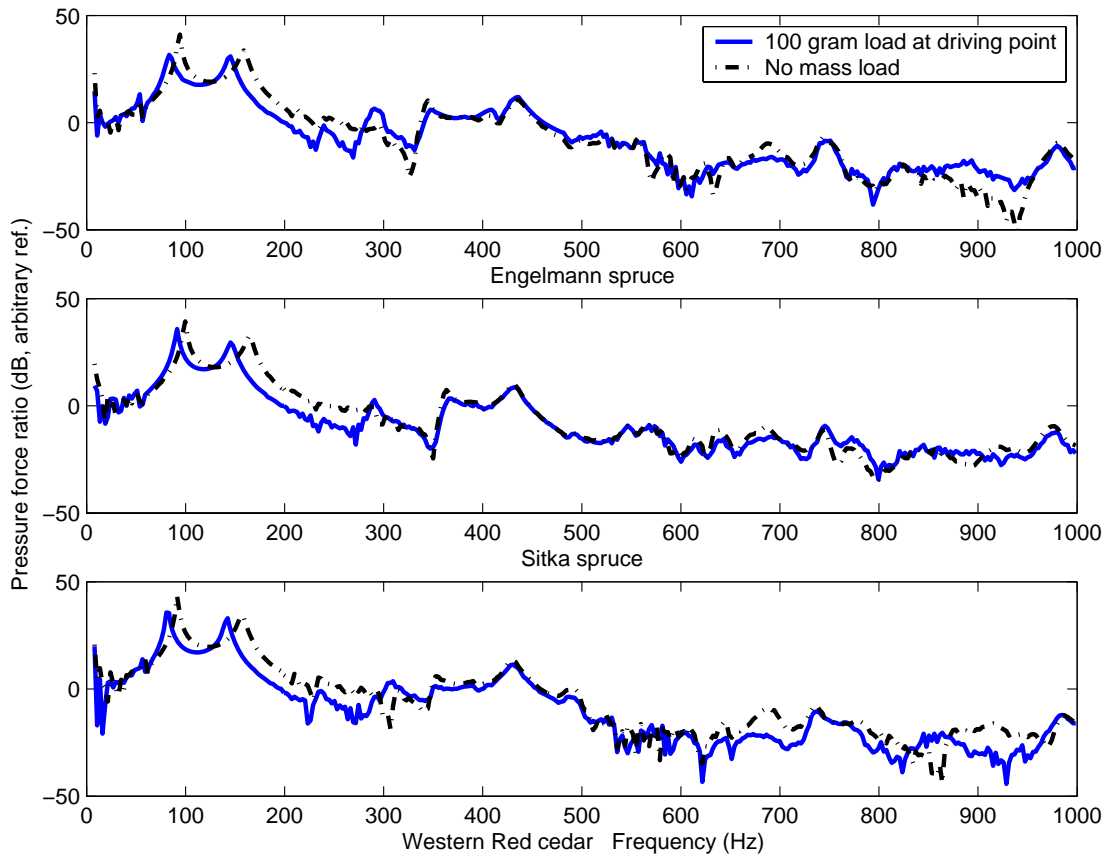
Figure 7.25: The effects on the pressure force ratio due to mass loading the three guitars, two years after finishing. Shown are the spectra for the unloaded soundboards and those for soundboards with 100 grams added to the driving point at the bridge.

Figure 7.27 shows the effect of adding the 100 gram mass to a point in the centre of the Sitka spruce soundboard on the pressure force ratio. In the low frequency soundboard/air cavity coupling region, the effect of the two positions of the 100
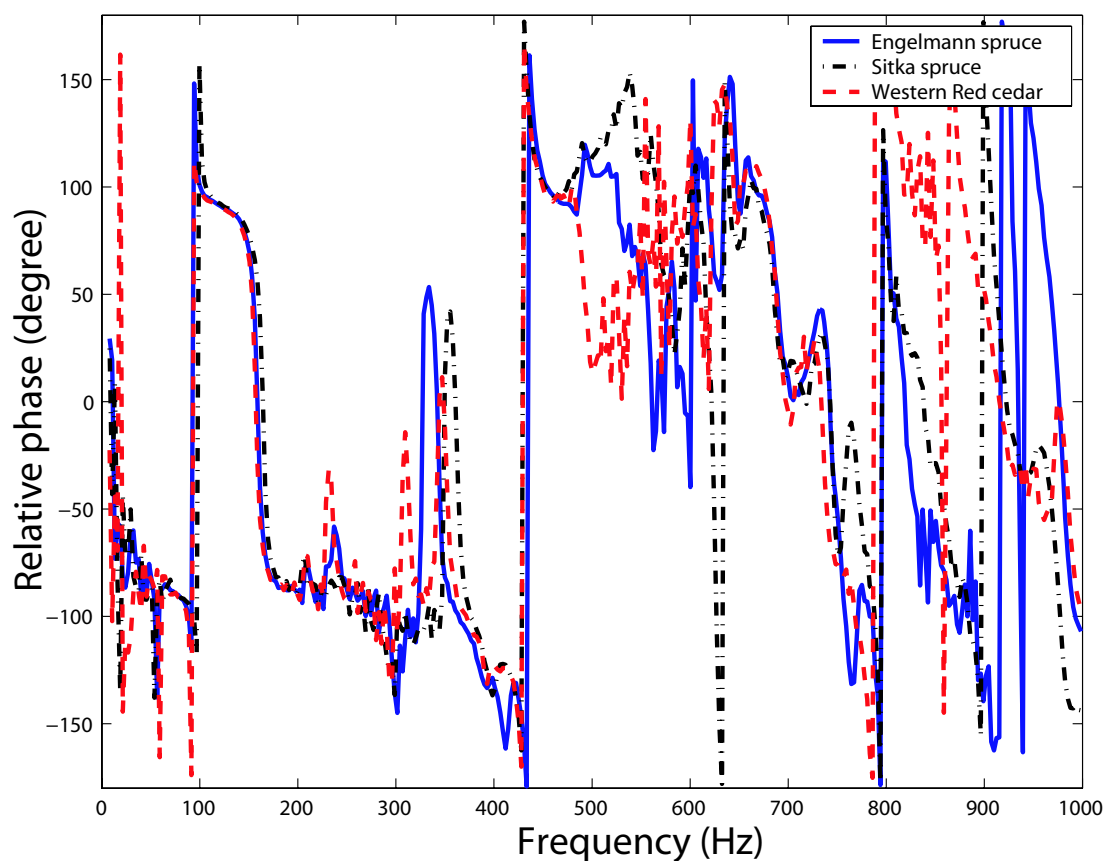
Figure 7.26: The effects on the phase between soundhole air pressure and the applied force at the bridge due to mass loading the three guitars, two years after finishing. Shown are the phases for the unloaded soundboards and those for soundboards with 100 grams added to the driving point at the bridge.
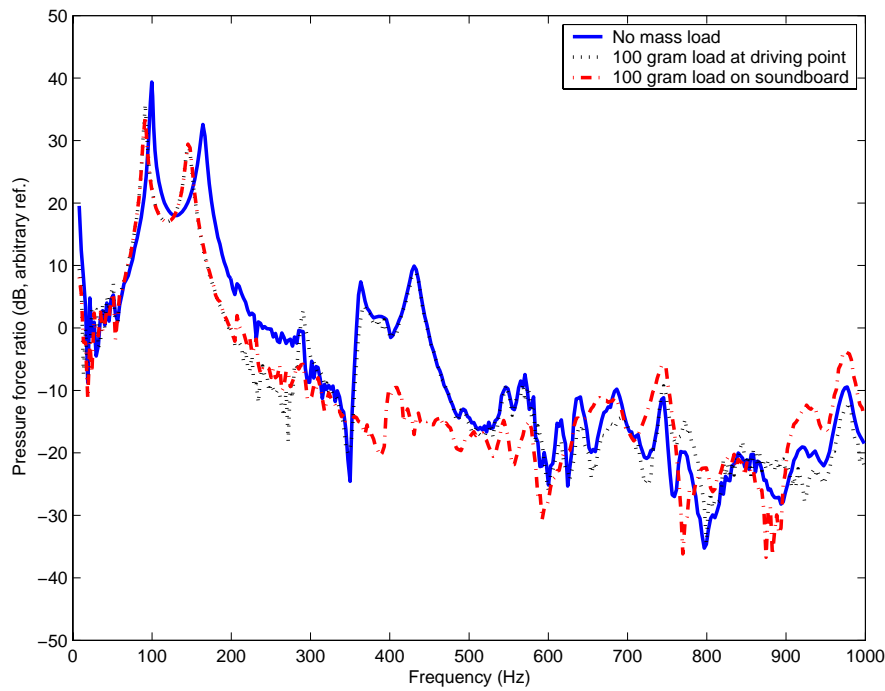
Figure 7.27: The effects of mass loading a guitar soundboard (Sitka spruce) on measured pressure force ratio spectra (two years after finishing) due to 100 grams added to the driving point and also to a central region of the soundboard, as in Figure 7.29.

gram mass is identical to the same mass load applied to the driving point. However, the pressure force ratio in the range $300 \rightarrow 800$ Hz, which was little altered by the same mass added to the driving point, is now greatly reduced. The T(1,2) mode (occurring about $300 \rightarrow 800$ Hz) has an antinode in the centre of the bridge and therefore is strongly affected by an added mass. Many modes above this have nodal lines along the axis of the guitar, especially in the lower bout below the bridge. It is interesting to note that there is some increase in the pressure force ratio above 700 Hz and it is likely the addition of mass to a nodal region of a particular vibratory mode could enhance this mode.

The addition of a mass load has a controllable perturbing effect on the vibratory behaviour of the guitar soundboard. This may be used as a means of characterising the guitar soundboard.
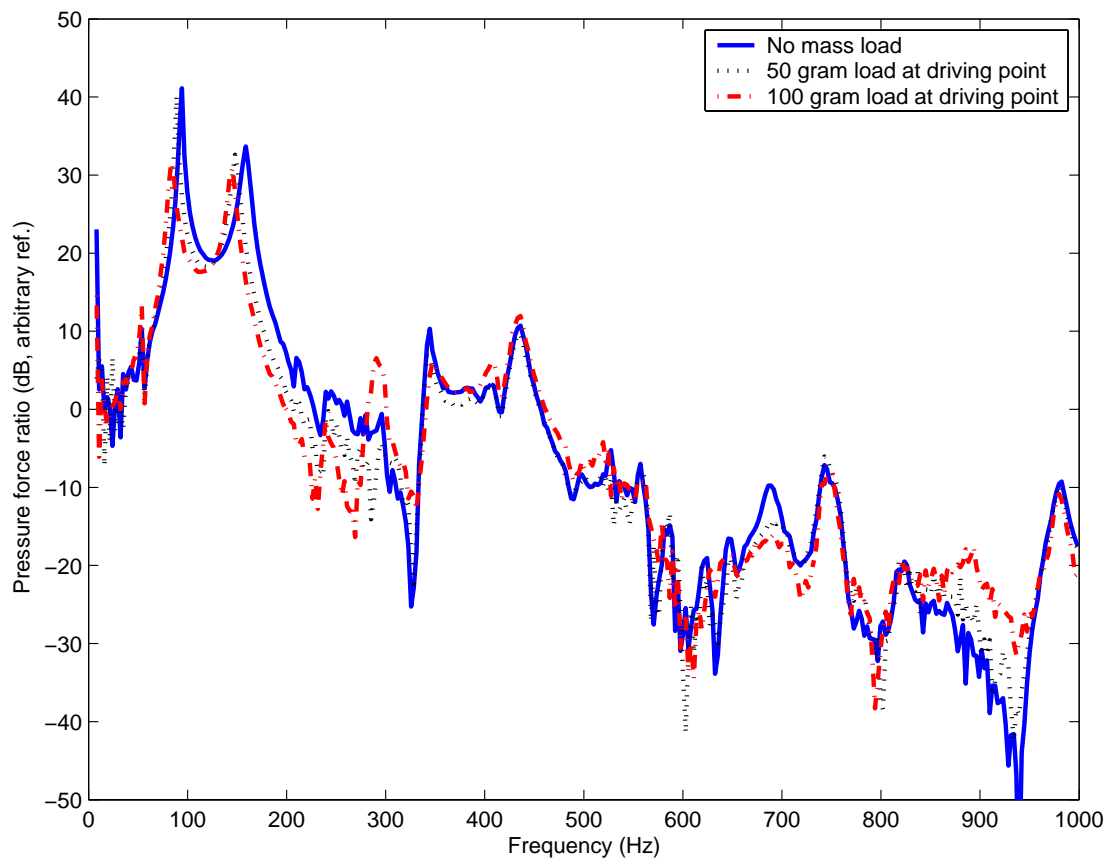
Figure 7.28: Effects on the pressure force ratio on the Englemann spruce soundboard due to mass loading at the driving point.
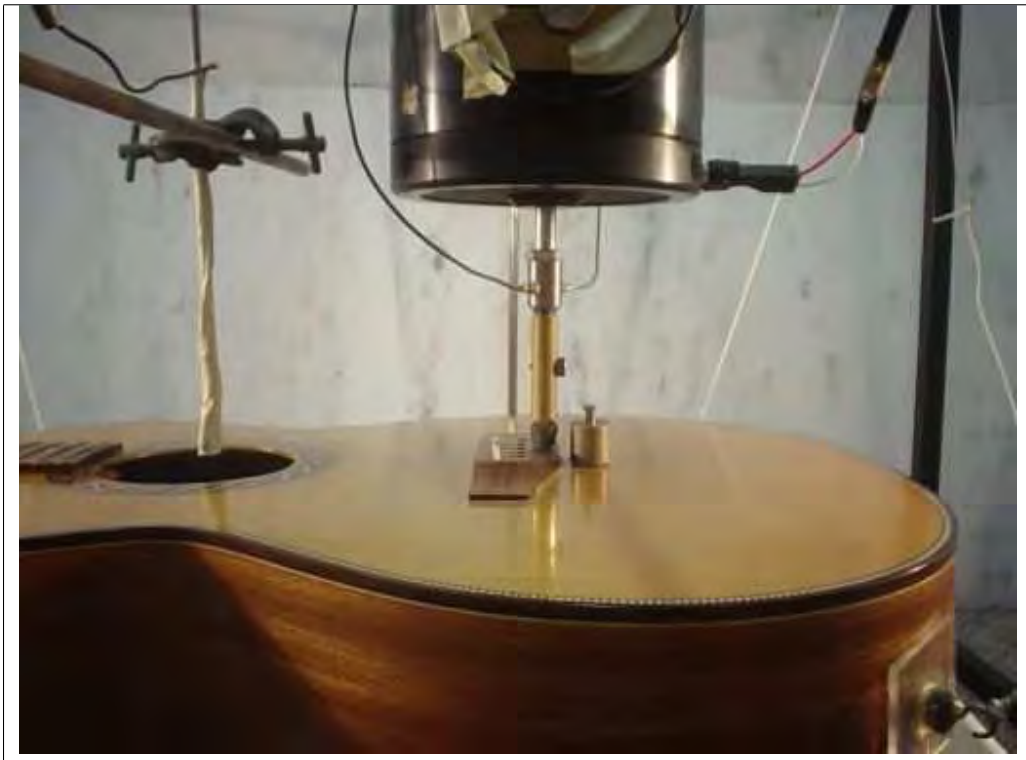
Figure 7.29: Photograph of the position of the 100 gram mass in a central position on the soundboard of the guitar. The masses are adhered using plasticine at this point or very close to the driving point at the bridge.

7.6 The effects of brace scalloping

Partly scalloped braces

Figure 7.30 shows the dynamic mass spectra and associated phases of the guitar soundboards after the tone-braces have been partly scalloped. Figure 7.31 shows the pressure force ratios and associated phases of the guitar soundboards after the tone-braces have been partly scalloped.
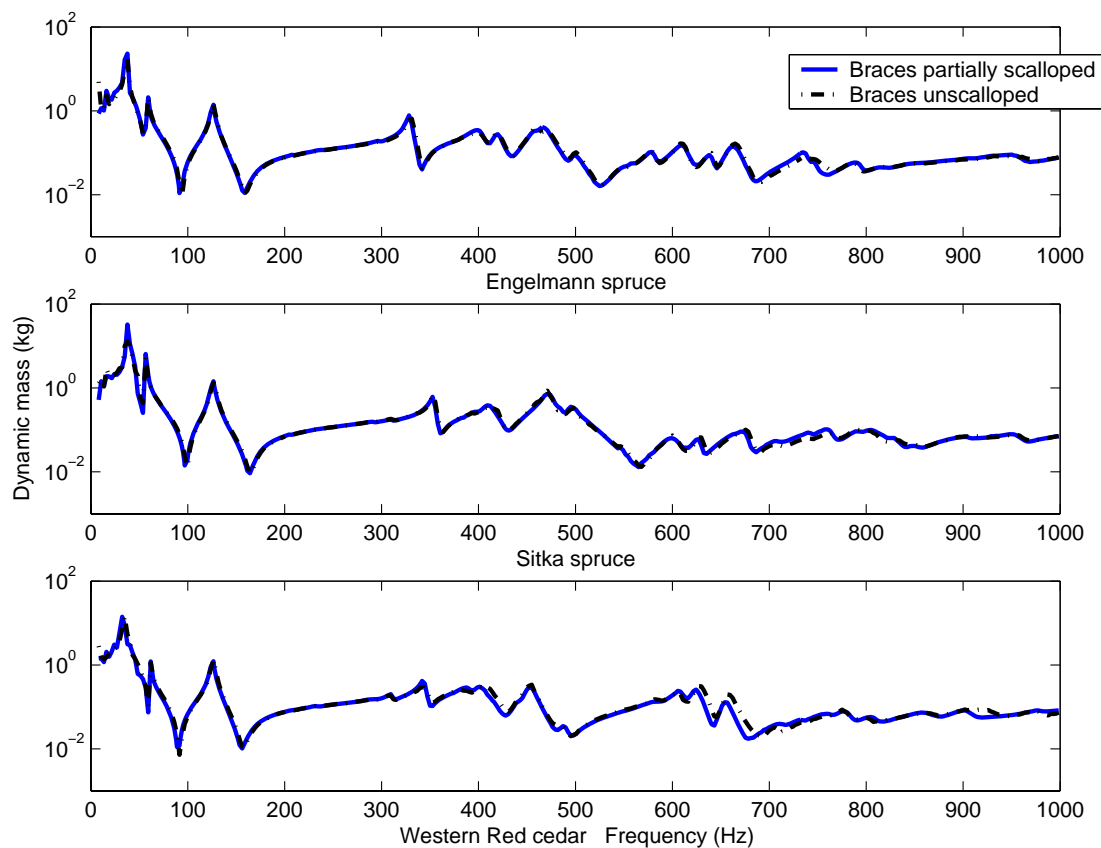
Figure 7.30: Dynamic mass spectra of the guitars before and after the tone-braces have been partly scalloped.
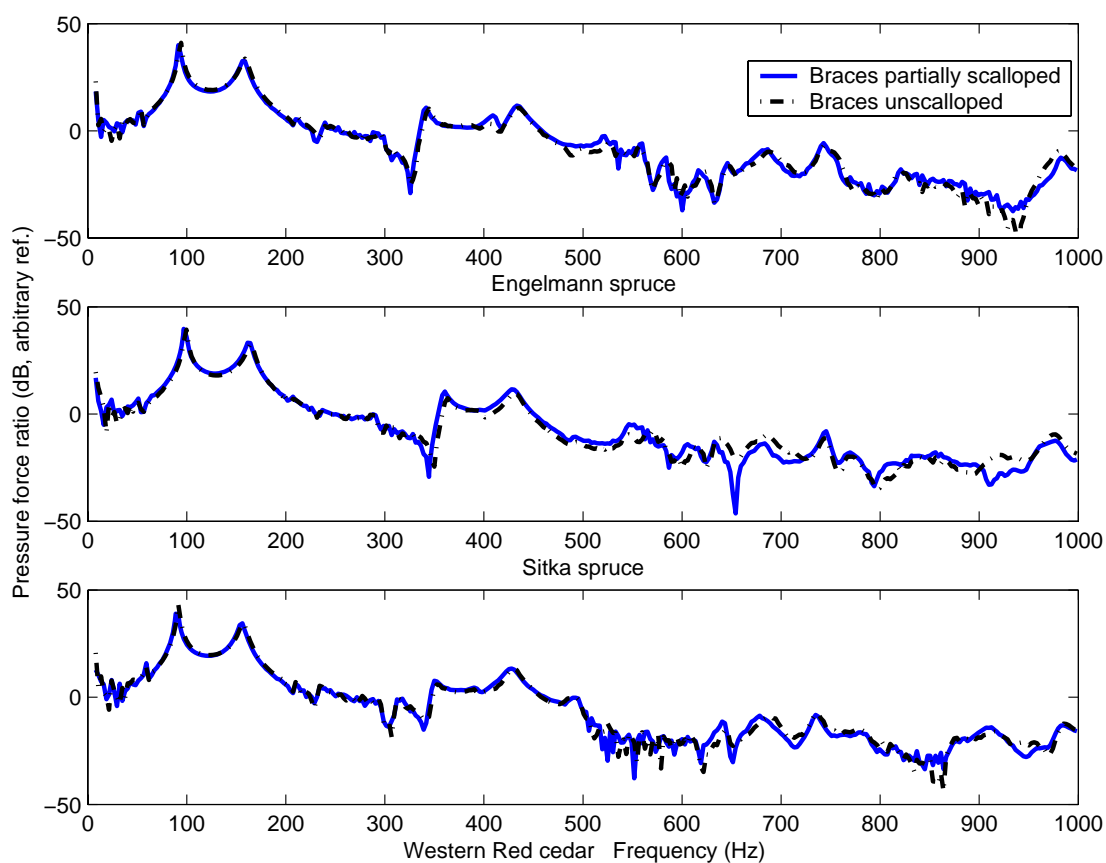
Figure 7.31: Pressure force ratio spectra of the guitars before and after the tone-braces have been partly scalloped.

Mass loading of partially scalloped braces

The soundboards were loaded with mass after the tone-braces had been partly scalloped. Figure 7.32 shows the effect on the pressure force ratio spectra, after mass was added to the driving point at the centre of the bridge. The effects of adding mass to different parts of the soundboard, in similar fashion to that illustrated by Figure 7.27, and in §7.5 are shown in Figure 7.33. Effects similar to that in §7.5 are observed for all three guitars.
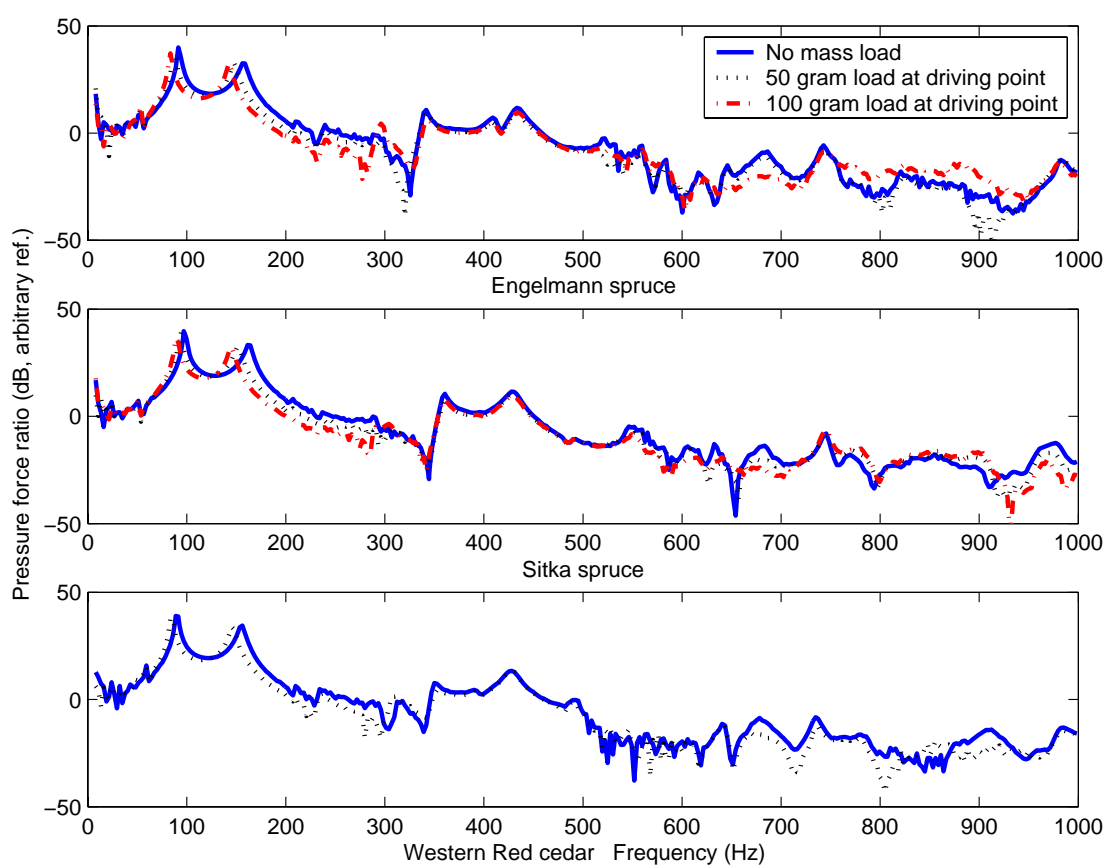
Figure 7.32: The effects of mass loading the driving point on the pressure force ratio of the guitars.
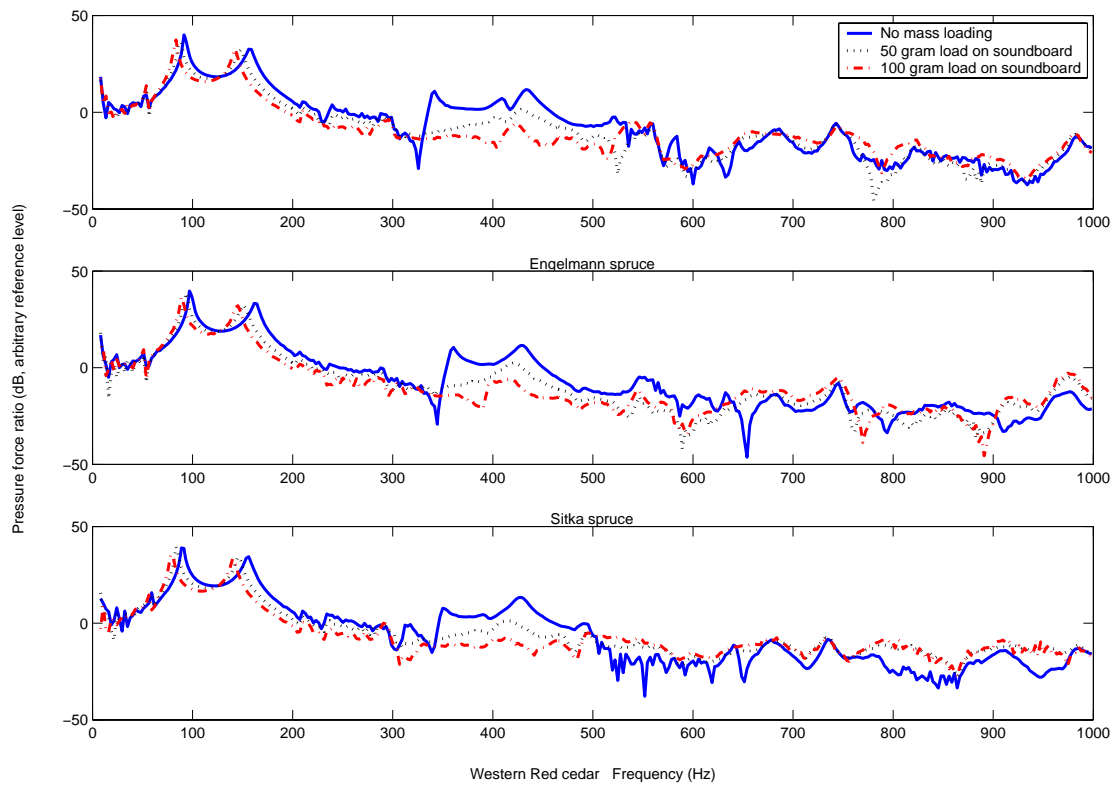
Figure 7.33: The effects of mass loading the soundboard on the pressure force ratio of the guitars.

Fully scalloped braces

The dynamic mass spectra after fully scalloping the tone-braces of the guitars and the associated phase between force and acceleration is given in Figure 7.34. The pressure force ratio spectra after fully scalloping the tone-braces of the guitars is given in Figure 7.35.
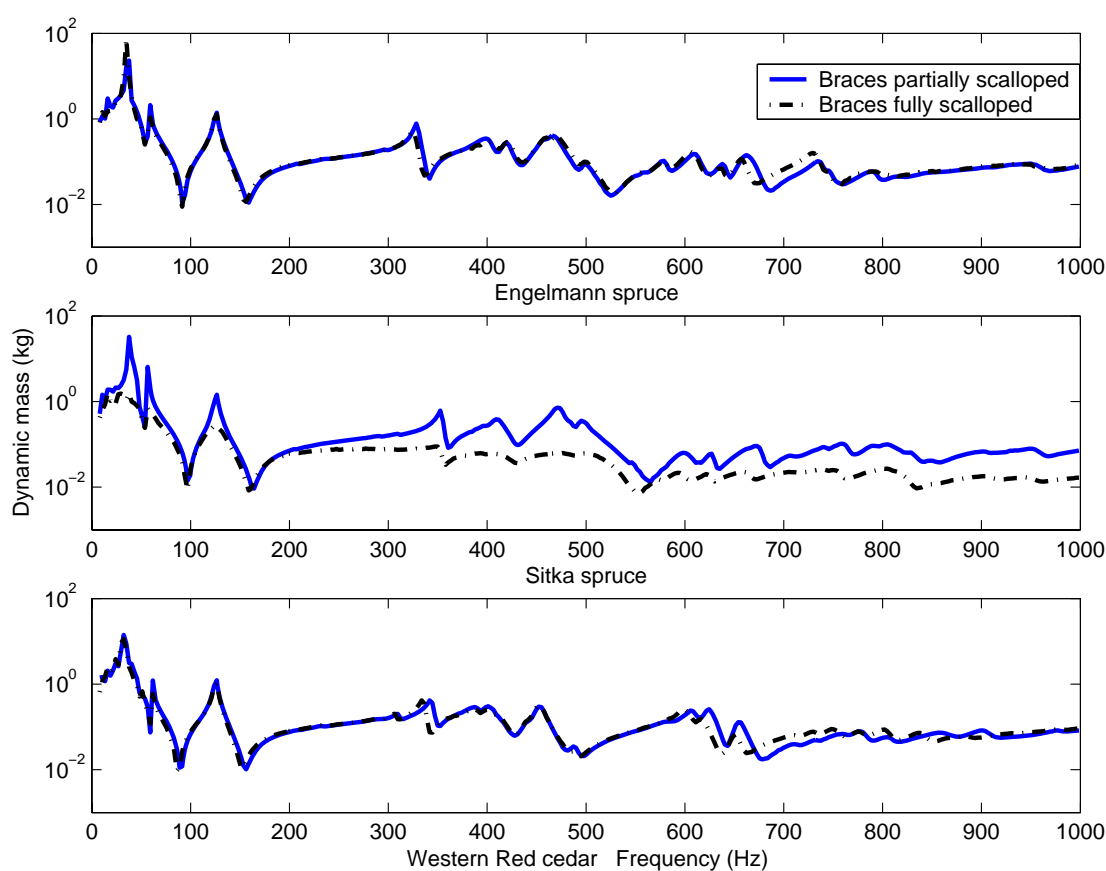
Figure 7.34: Dynamic mass spectra of the guitars with fully scalloped and partly scalloped tone-braces.
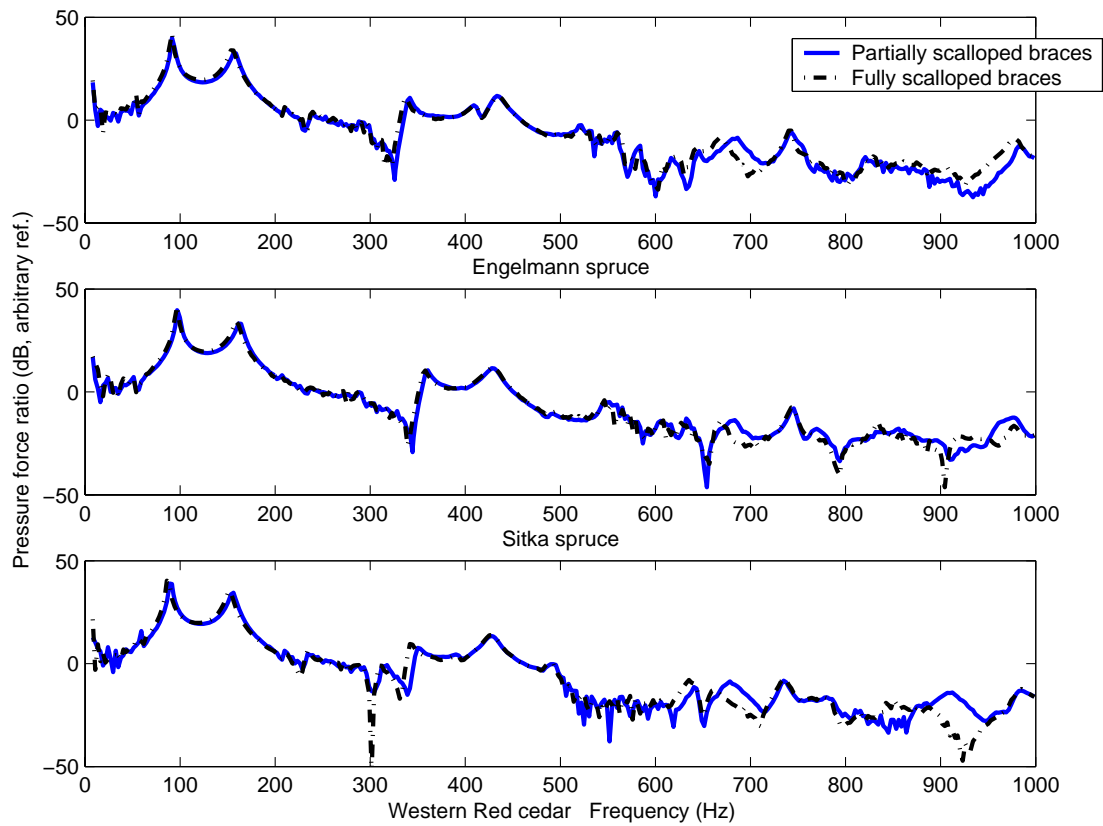
Figure 7.35: Pressure force ratios for guitars with fully scalloped and partly scalloped tone-braces.

$f(T(2,2)_2)$			$f(T(3,2))$		
	ES	SS	WRC	ES	SS	WRC
2yr	683	677	637	743	804	606
SCL50	679	680	638	744	762	666
SCL100	670	700	623	746	747	743

Table 7.3: The frequencies of Chladni figures, in response to brace scalloping.

Mass loading of fully scalloped braces

Pressure force ratios of Engelmann spruce soundboard after fully scalloping the tone-braces, with mass loading the driving point are given in Figure 7.36.

Mass loading at various points on the soundboard are shown for Engelmann spruce (Figure 7.37) and Sitka spruce (Figure 7.38.)

Summary of brace scalloping

The progression of the dynamic mass spectra during the three phases of brace scalloping studied here are given in Figure 7.39. The corresponding changes in pressure force ratio are given in Figure 7.40.

The dynamic mass spectra show that all three of the soundboards are affected in the frequency range $650 - 750$ Hz, which includes the $T(2,2)_2$ and the $T(3,2)$ modes (Table 7.3.)

These modes have nodal lines extending through the area reinforced by the 'tone-braces' responsible for the asymmetry of this particular bracing system (Figure 7.41.) This gives some evidence for the importance of these braces on the output sound of the instrument.
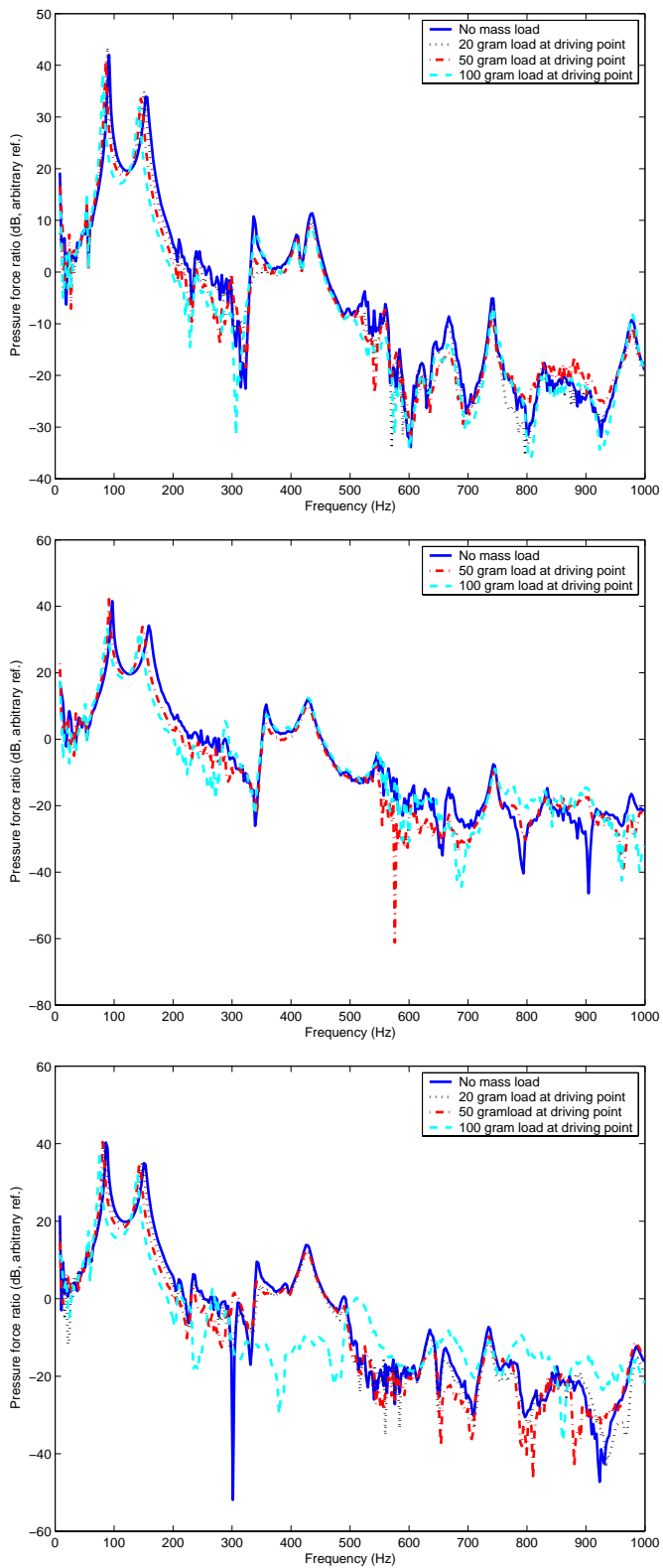
Figure 7.36: Pressure force ratios of the guitar soundboards after fully scalloping the tone-braces, and loading the driving point with additional mass.
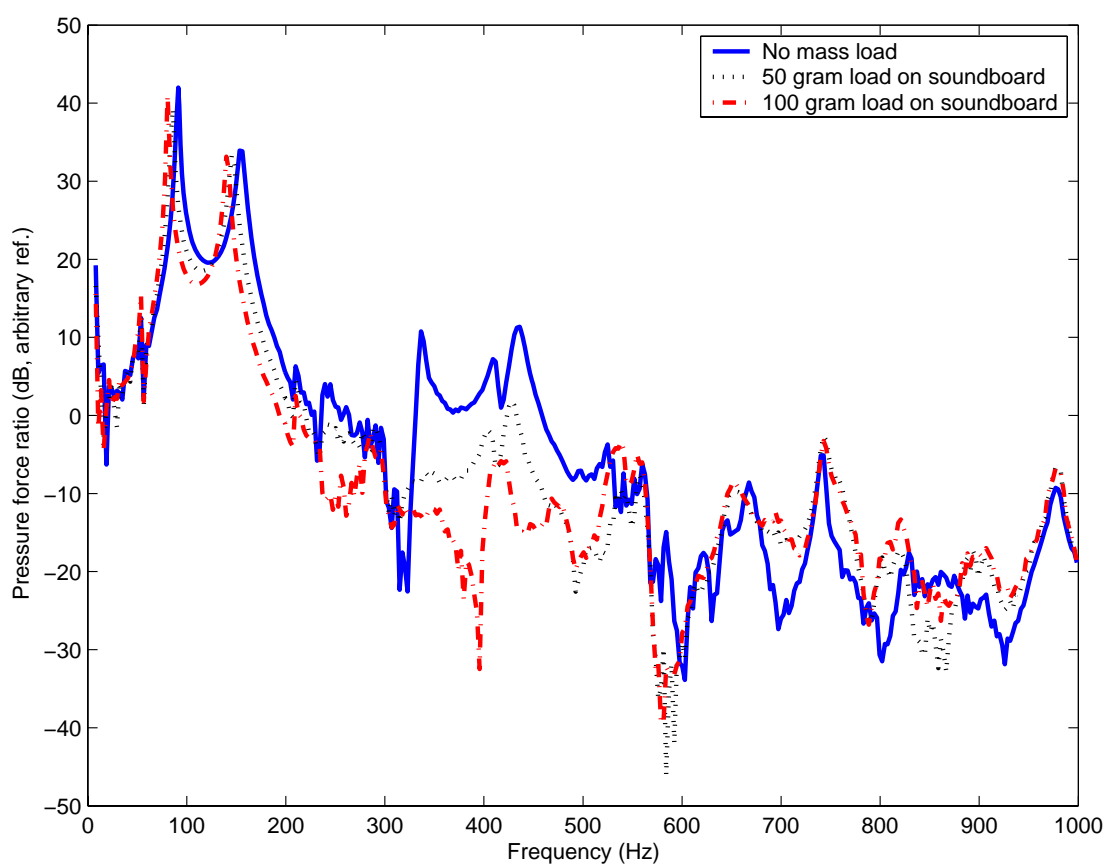
Figure 7.37: Pressure force ratios of the Engelmann spruce soundboard after fully scalloping the tone-braces, with mass loading at the bridge and a central position of the soundboard (Figure 7.29).
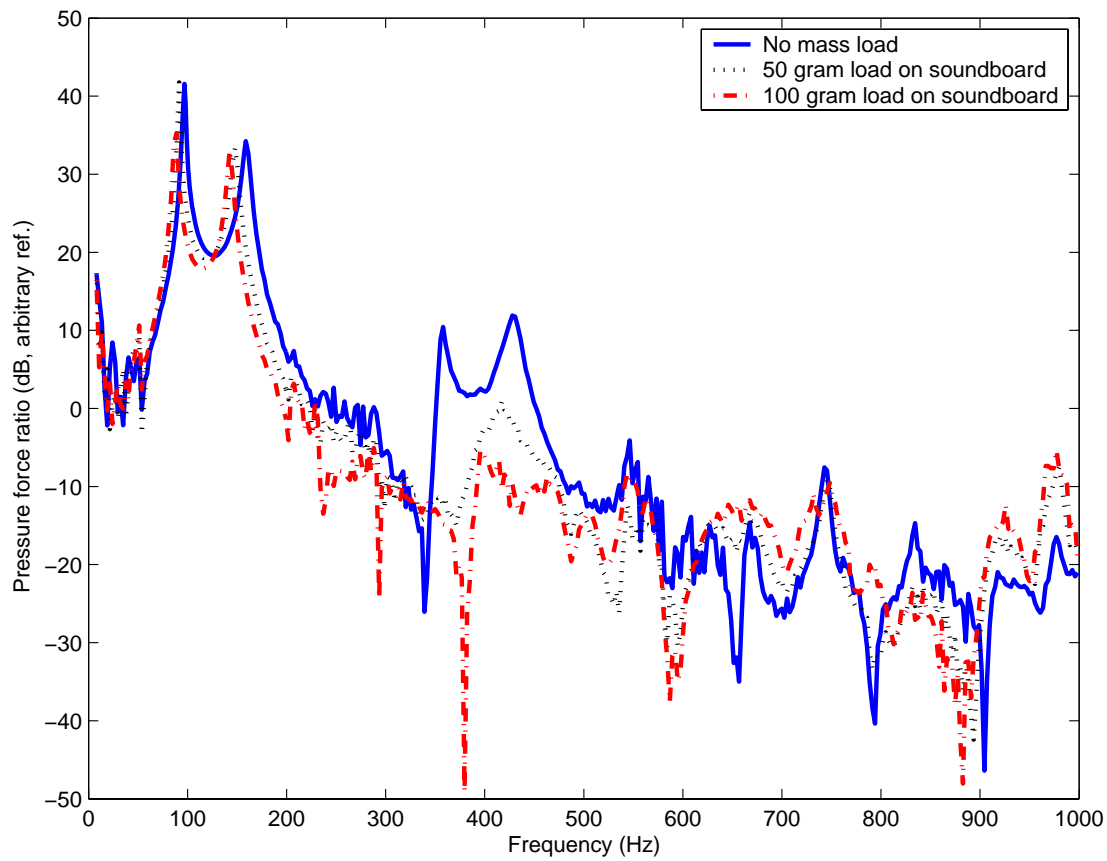
Figure 7.38: Pressure force ratios of the Sitka spruce soundboard after fully scalloping the tone-braces, with mass loading at the bridge and a central position of the soundboard (Figure 7.29).
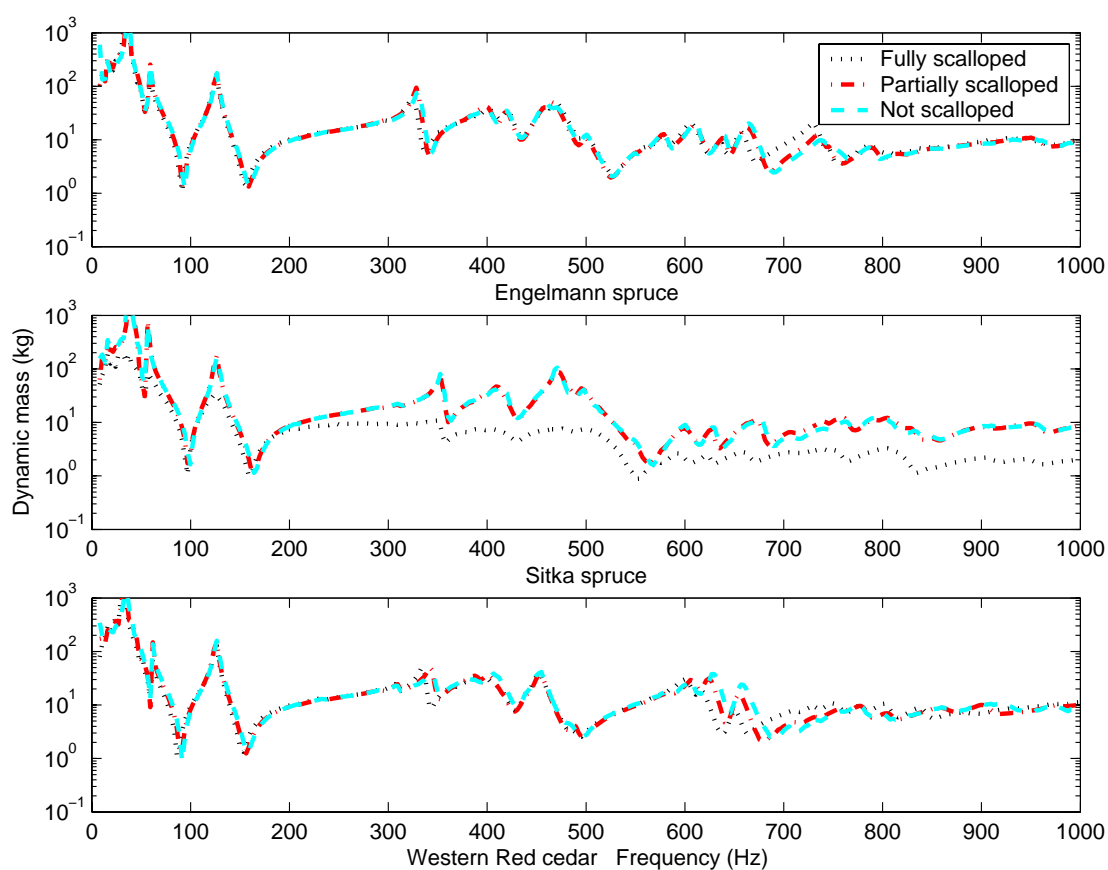
Figure 7.39: Dynamic mass spectra for all three guitars at three stages of tone-brace scalloping: no scalloping, partially scalloped and fully scalloped.
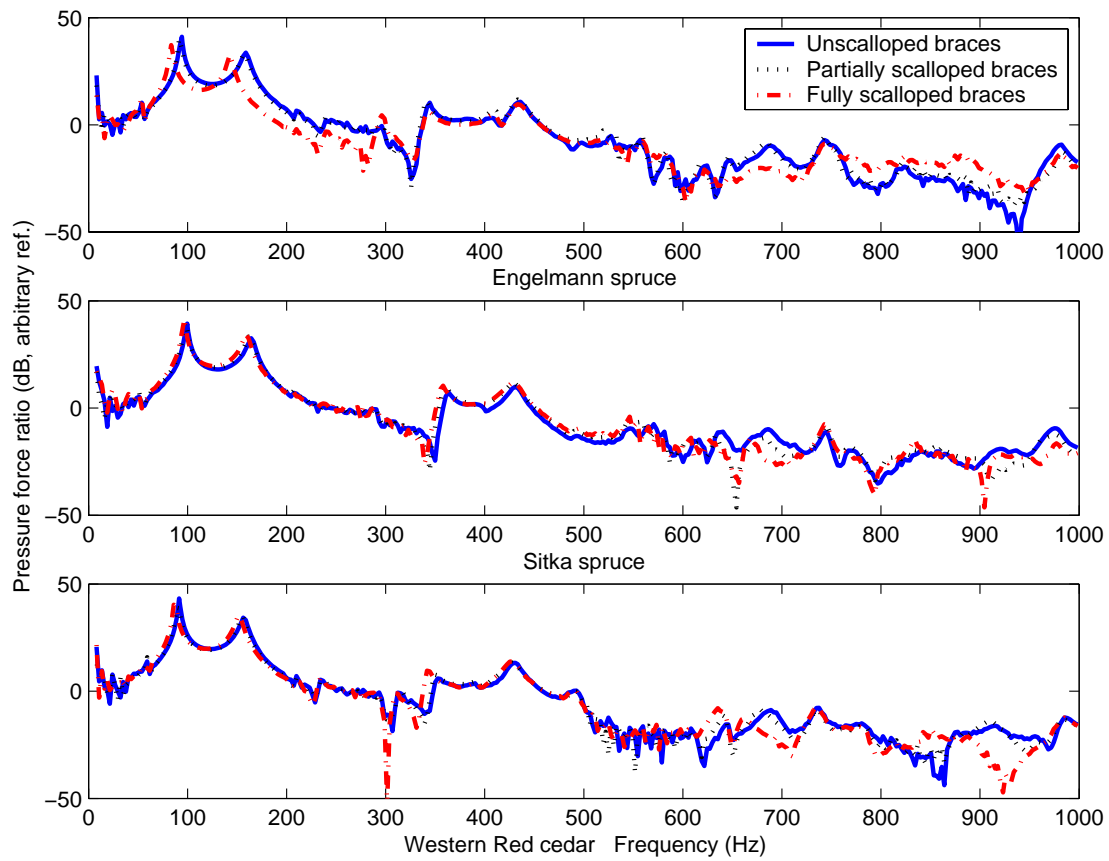
Figure 7.40: Pressure force ratios for all three guitars at three stages of tone-brace scalloping: no scalloping, partially scalloped and fully scalloped.
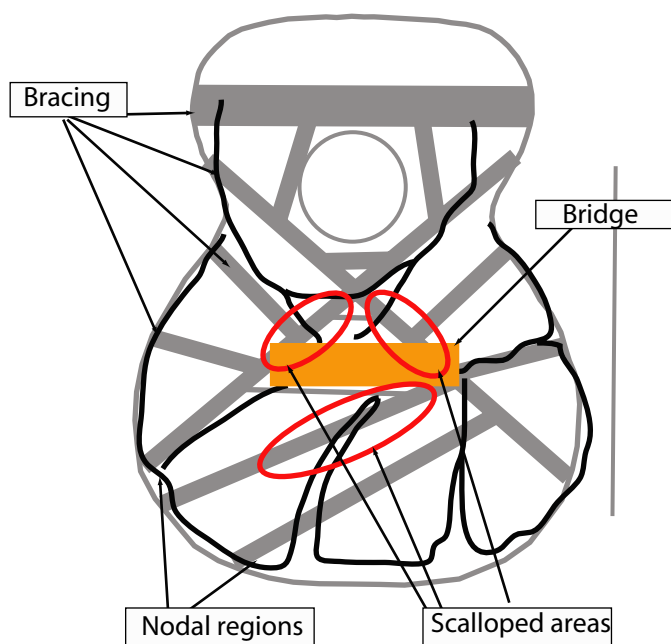
Figure 7.41: Schematic of the $T(3,2)$ soundboard mode, with the brace and bridge positions marked. Also marked are the areas of the braces that have been scalloped. This mode has many nodes aligning with the 'tone-braces', and therefore brace scalloping of these braces is influential on the measured vibratory spectra.
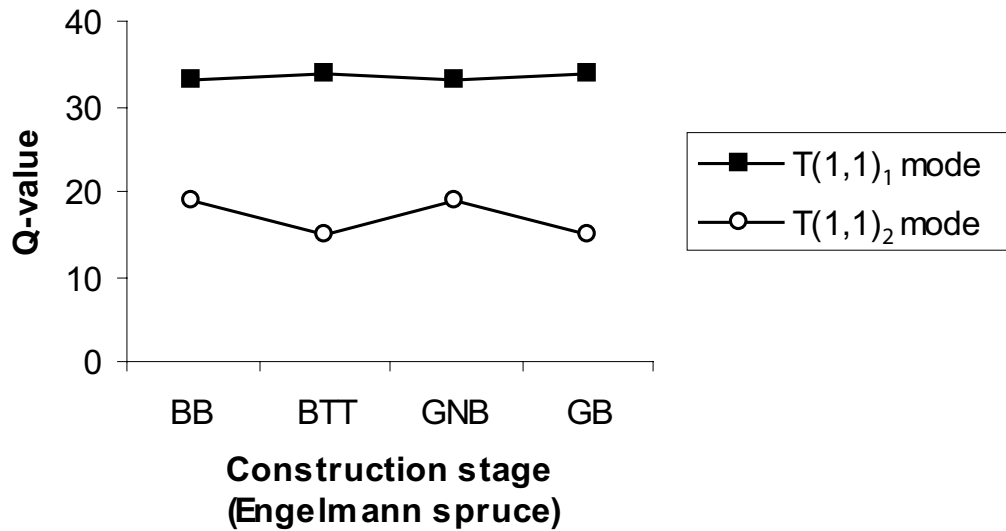
Figure 7.42: The evolution of the Q-values of the pressure force ratio of the $T(1,1)_1$ and $T(1,1)_2$ modes for the Engelmann spruce guitar. There is little measurable change for any construction stage.

7.7 Parameter evolution

The parameters derived in §2.5 change as a function of the stages of construction. Because measurements of vibratory spectra have been made at various construction stages (this chapter and Chapter 6) these parameters provide a simple means of characterising changes of the instruments during construction. For example, the Q-values of the soundboard modes of the guitars during construction (Figure 7.42) were able to be measured; little change overall was observed.

Soundboard	Mass (kg)	f_1 (Hz)	K_{p*} $(\text{kN} \cdot \text{m}^{-1})$
Engelmann spruce	0.2763	68	50.4
Sitka spruce	0.3067	73	64.5
Western Red cedar	0.2493	69	46.9

Table 7.4: Effective stiffness values for the free guitar soundboards. Frequencies are taken as the frequency where the phase in the dynamic mass spectrum (Figure 6.8) in the region of the free (2,0) mode (Figure 6.7) is a local minimum.

Effective free plate, Helmholtz, and membrane frequencies and low frequency coupling

This section is a summary of the low frequency parameters (§2.5) as measured for the three guitars at the various stages of construction examined in this chapter and Chapter 6.

Free soundboards: effective stiffnesses

By assuming the deflection of the soundboard obeys Hooke's law, the effective stiffness of a guitar soundboard may be defined (§2.5) as $K_{p*} = 4\pi^2 f_1^2 m$, where f_1 is the fundamental frequency (in this case the (0,2) mode) and m is the mass of the free plate. The effective free plate soundboard stiffnesses are given in Table 7.4. Values for f_1 are from Figure 6.8.

The effective stiffness values of the free guitar soundboards compare to $K_{p*} = 74\,\text{kN}\cdot\text{m}^{-1}$ given in [Caldersmith, 1978] for a classical guitar soundboard. This value results from a semi-empirical calculation of the soundboard and bracing, making simple assumptions about the structure. The effective stiffness for the soundboards attached to the back and sides are given in Table 7.5.

Soundboard	K_{p*} $(\mathrm{kN} \cdot \mathrm{m}^{-1})$
Engelmann spruce	232.5
Sitka spruce	279.7
Western Red cedar	201.3

Table 7.5: Calculation of the effective stiffness of guitar soundboards after glueing to the sides and back. Calculations are taken from the mass of the plate and the calculations of the free-plate frequencies (including fluid loading from the air) in the low frequency air coupled region (§7.7).

Guitar bodies: effective stiffness

The effective stiffness values for a steel-string guitar soundboard attached to the back and sides (Table 7.5) compare to the value of $K_{p*} = 128\ \mathrm{kN} \cdot \mathrm{m}^{-1}$ given in [Christensen and Vistisen, 1980], although, as the case with Table 7.4, the only available comparison is with a classical guitar soundboard.

The frequency at which the air pressure in the soundhole is closest to 180° out of phase with the force at the bridge, f_-, that of the in-phase motion, f_+ as well as that of the equivalent Helmholtz resonator, f_0, may be obtained from the low frequency turning points in the dynamic mass spectra of the guitars [Firth, 1977, Christensen and Vistisen, 1980]. These coupled frequencies are given in Table 7.6.

These data may then be used to calculate the frequency of the fundamental plate mode, f_p (Figure 7.44) as well as that uncoupled with the air, $f_{p,0}$ (Figure 7.45). The lowest frequency that the air and the soundboard couple at, f_{ph} (Figure 7.46), are given in Table 7.7.

Helmholtz Frequencies
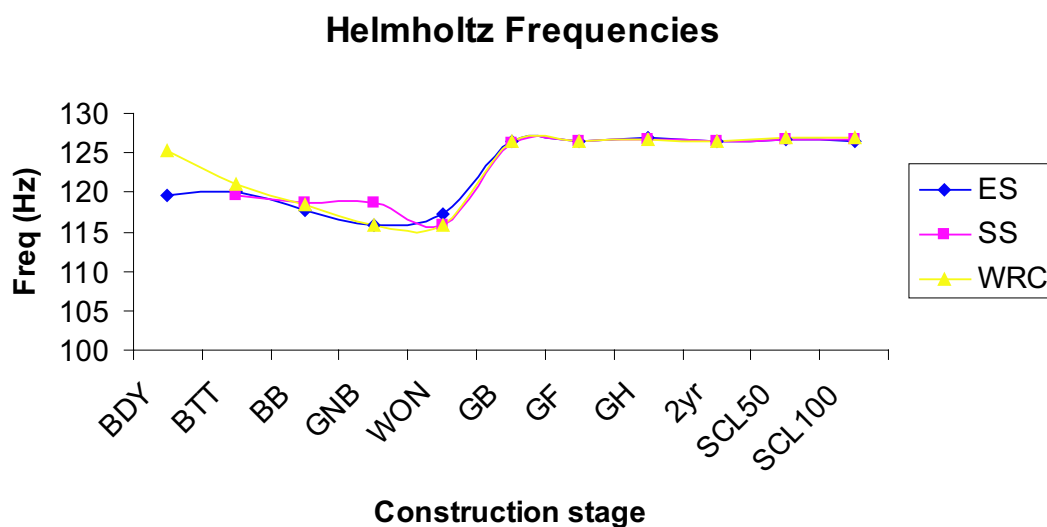
Figure 7.43: The progression of frequencies for an equivalent Helmholtz resonator.

Table 7.8 lists F_{pH} values calculated for the three guitars at various stages of construction. It is possible this parameter may be used to characterise a particular instrument, but it is not known how it relates to the measurable spectra or subjective quality of the instruments.

The equivalent Helmholtz resonance is altered as a result of successive construction stages (Figure 7.43.) The greatest change occurs when the bridge is added to the instruments, effectively reducing the body compliance, which raises the Helmholtz frequency by approximately 10%.

Soundboard	Construction stage	Frequency (Hz)		
		f_-	f_0	f_+
Engelmann spruce	Body	96.6	119.5	161.6
	Top-thinned	91.4	120.0	157.8
	Binding	90.2	117.8	156.0
	Guitar (no bridge)	88.8	115.8	152.5
	Without neck	89.0	117.2	154.5
	With bridge	91.6	126.5	157.6
	Finished	91.8	126.5	158.6
	Lacquer hardening	93.0	126.9	159.0
	Played 2 years	94.2	126.4	158.8
	Partially scalloped	91.5	126.6	158.6
	Fully scalloped	91.7	126.4	156.1
Sitka spruce	Body	98.0	120.0	160.0
	Top-thinned	97.0	119.7	160.1
	Binding	94.2	118.7	160.6
	Guitar (no bridge)	94.2	118.6	159.6
	Without neck	94.2	115.8	153.7
	With bridge	96.8	126.3	163.0
	Finished	97.0	126.5	164.2
	Lacquer hardening	98.1	126.6	164.4
	Played 2 years	99.5	126.4	164.1
	Partially scalloped	97.0	126.6	164.2
	Fully scalloped	97.0	126.7	159.0
Western Red cedar	Body	96.8	125.2	163.3
	Top-thinned	90.4	121.0	157.8
	Binding	88.9	118.5	154.9
	Guitar (no bridge)	88.8	115.8	153.5
	Without neck	89.0	115.8	150.7
	With bridge	89.0	126.5	156.3
	Finished	91.8	126.5	157.6
	Lacquer hardening	91.5	126.6	157.2
	Played 2 years	91.5	126.4	157.5
	Partially scalloped	88.9	127.0	156.2
	Fully scalloped	86.3	126.9	153.6

Table 7.6: A summary of the low frequency coupling frequencies, as derived from the measured dynamic mass spectra at each construction phase.

Soundboard	Construction stage	Frequency (Hz)		
		f_p	$f_{p,0}$	f_{ph}
Engelmann spruce	Body	145.5	130.6	87.5
	Top-thinned	137.3	120.2	89.2
	Binding	136.3	119.5	88.0
	Guitar (no bridge)	133.2	116.9	85.9
	Without neck	134.4	117.3	87.7
	With bridge	131.2	114.1	90.5
	Finished	132.5	115.1	91.2
	Lacquer hardening	133.5	116.5	90.9
	Played 2 years	134.6	118.3	90.0
	Partially scalloped	132.3	114.6	91.4
	Fully scalloped	129.6	113.2	89.3
Sitka spruce	Body	106.0	103.9	45.8
	Top-thinned	143.9	129.7	86.4
	Binding	143.5	127.5	88.4
	Guitar (no bridge)	142.4	126.7	87.7
	Without neck	138.2	125.1	82.5
	With bridge	141.4	125.0	91.4
	Finished	142.8	126.0	92.2
	Lacquer hardening	143.6	127.4	91.6
	Played 2 years	144.4	129.2	90.3
	Partially scalloped	142.6	125.8	92.2
	Fully scalloped	136.5	121.7	88.5
Western Red cedar	Body	142.7	126.3	91.2
	Top-thinned	135.7	117.8	90.3
	Binding	133.6	116.2	88.4
	Guitar (no bridge)	134.3	117.7	86.6
	Without neck	131.2	115.8	84.5
	With bridge	127.9	110.0	90.9
	Finished	131.3	114.3	90.4
	Lacquer hardening	130.6	113.6	90.3
	Played 2 years	131.2	114.0	90.5
	Partially scalloped	127.2	109.3	90.8
	Fully scalloped	122.2	104.5	89.7

Table 7.7: Derived low frequency parameters, as in §2.5 and §2.5 from data in Table 7.6.

Soundboard	Construction stage	F_{pH}
Engelmann spruce	Body	0.73
	Top-thinned	0.74
	Binding	0.75
	Guitar (no bridge)	0.74
	Without neck	0.75
	With bridge	0.72
	Finished	0.72
	Lacquer hardening	0.72
	Played 2 years	0.71
	Partially scalloped	0.72
	Fully scalloped	0.71
Sitka spruce	Body	-
	Top-thinned	0.72
	Binding	0.74
	Guitar (no bridge)	0.74
	Without neck	0.71
	With bridge	0.72
	Finished	0.73
	Lacquer hardening	0.72
	Played 2 years	0.71
	Partially scalloped	0.73
	Fully scalloped	0.70
Western Red cedar	Body	0.73
	Top-thinned	0.75
	Binding	0.75
	Guitar (no bridge)	0.75
	Without neck	0.73
	With bridge	0.72
	Finished	0.71
	Lacquer hardening	0.71
	Played 2 years	0.72
	Partially scalloped	0.72
	Fully scalloped	0.71

Table 7.8: Low frequency coupling parameter as a function of construction phase (low frequency coupling frequency normalised by the Helmholtz frequency, from [Christensen and Vistisen, 1980].)
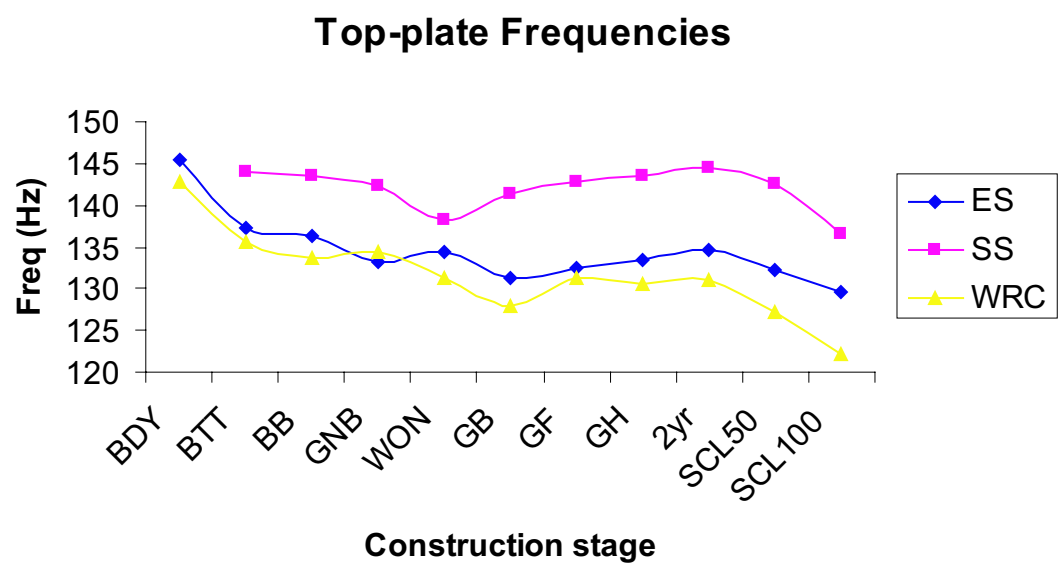
Figure 7.44: The progression of calculated frequencies of free soundboards, with an air load, from low frequency coupling features.
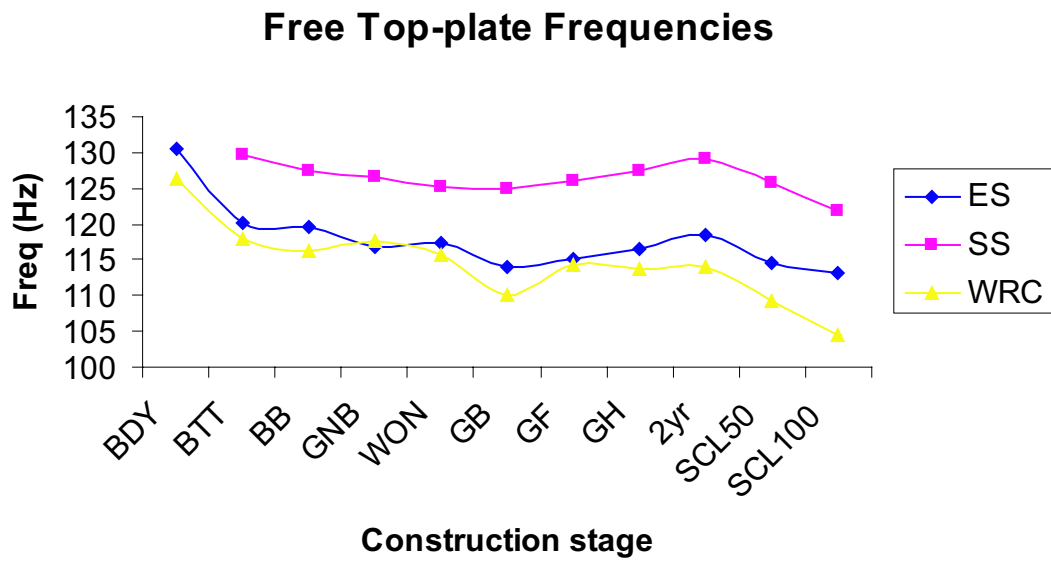
Figure 7.45: The evolution with construction of calculated uncoupled fundamental free-soundboard frequencies of the guitars.
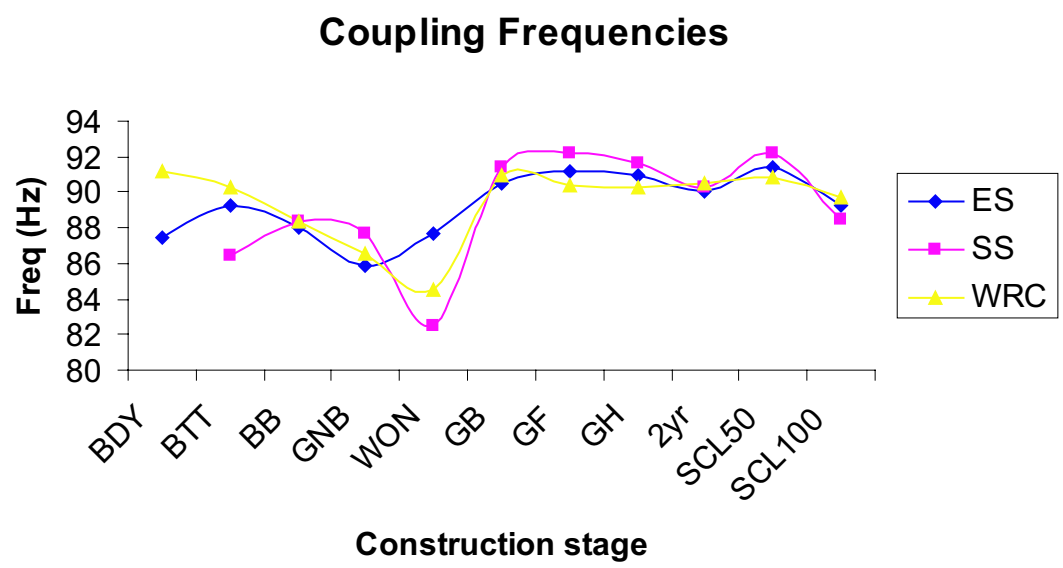
Figure 7.46: The evolution with construction of calculated low frequency air/soundboard coupling frequencies of the guitars.

Construction state	$\frac{df_{p,0}}{dm}$ (Hz $\cdot$ g^{-1})		
	ES	SS	WRC
No scalloping	-7.9	-8.5	-7.9
Partially scalloped	-6.1	-7.1	-5.7
Fully scalloped	-6.1	-6.6	-6.0

Table 7.9: The change in calculated free soundboard frequencies in response to added mass load. An indication of the linearity of the relationship is given by the least squares fit parameter: $R^2 > 98\%$. The added mass ranged from 0 to 200 grams. *cf.* Figure 7.49.

Effective mass, stiffness and area

The changes in frequency of the calculated free soundboard in response to mass loading at the driving point are given in Table 7.9.

The effect of brace scalloping was to lower the calculated free soundboard frequencies progressively (Figure 7.49.) Because little mass was removed in comparison to the total mass of the soundboard, this reduced the effective stiffness at low frequencies (Figures 7.48 and 7.49) being more important than the (modest) reduction in mass.

For the dimensionless low-frequency air-soundboard coupling parameter, F_{pH}, the scalloping process improves the (Hooke's) linear nature of the equivalent spring obtained from the response of low frequency coupling under an added mass load, but does not greatly affect the actual value (Table 7.10.) The construction stage that affects F_{pH} the most is the addition of the bridge.

7.8 Results/Comments

The construction stage that had the most profound effect on these measurements for all three guitars, was the addition of the bridge. The bridge, along with reducing
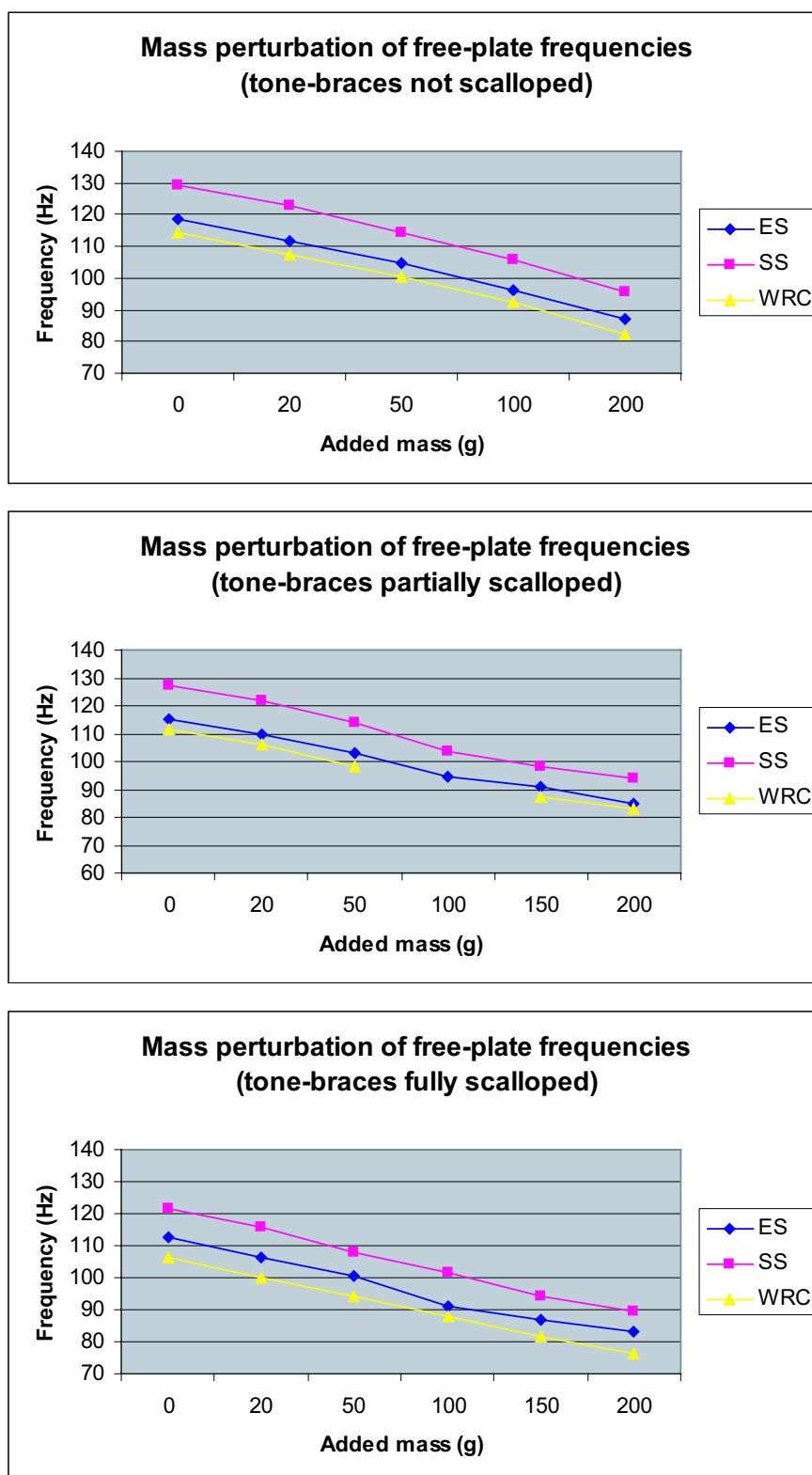
Figure 7.47: The effect on the calculated uncoupled free-plate fundamental frequency of guitar soundboards by mass loading at successive stages of tone-brace scalloping. The mass-loading gradient and linearity of the perturbation by mass loading progression, as calculated from least-squares linear fit are in Table 7.9.
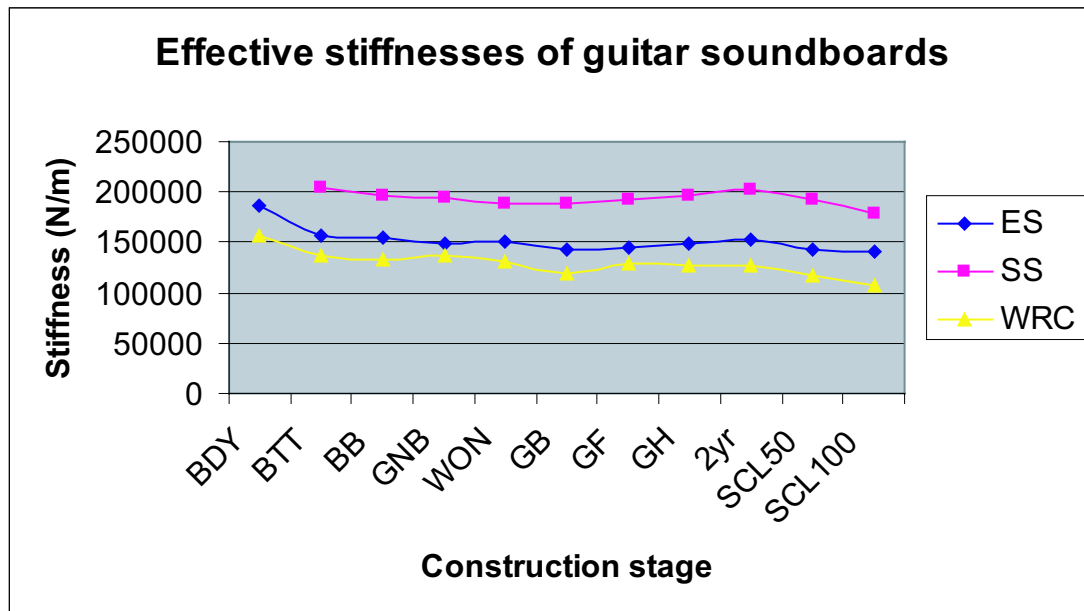
Figure 7.48: The effective stiffness of each guitar soundboard at successive construction phases, as calculated from the mass of plate and the uncoupled fundamental soundboard frequency.

Construction state	$\frac{dF_{pH}}{dm}$ (g^{-1})		
	ES	SS	WRC
No scalloping	-0.026	-0.027	-0.033
Partially scalloped	-0.027	-0.023	-0.020
Fully scalloped	-0.019	-0.02	-0.021

Table 7.10: The change in low frequency air soundboard coupling as an expression of the dimensionless low frequency coupling parameter F_{pH} (§2.5, §2.5). Here, the linear least-squares fit parameter, $R^2 > 96\%$
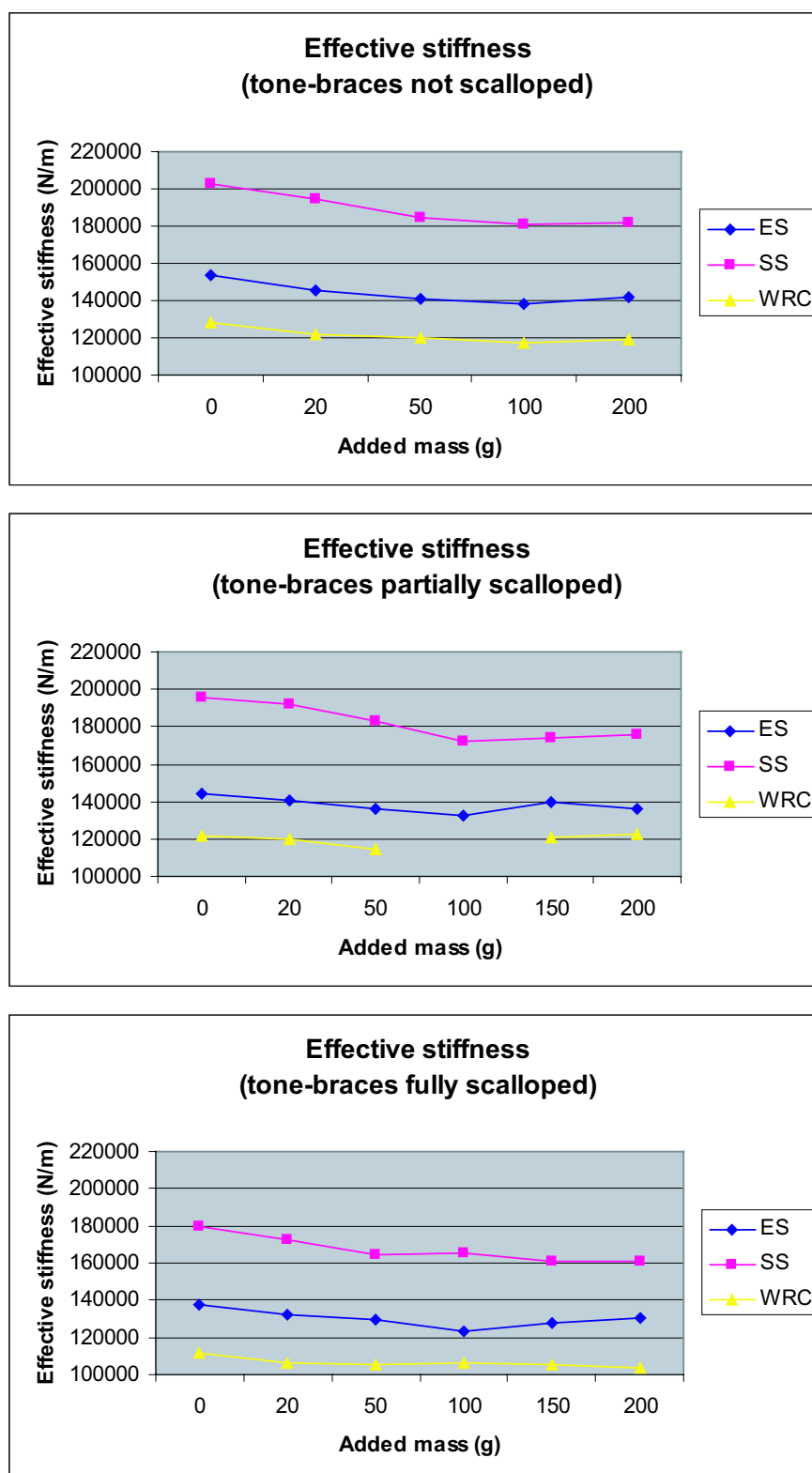
Figure 7.49: The effect of mass loading on effective stiffness of guitar soundboards, as calculated from the mass of each plate, plus load, and the calculated uncoupled fundamental soundboard frequency.

the number of distinct Chladni modes, increased the effective Helmholtz frequencies of the guitars. No other construction stage had a significant effect on the Helmholtz frequencies. Although the bridge adds some mass, it adds enough stiffness to alter the character of modes that have nodal regions nearby, notably the $T(1,2)_2$ and $T(2,2)$ modes. For this reason, the bridge should be considered as part of the brace system, and not just a termination point for the string.

The addition of the neck introduces low frequency modes, around 60 Hz, incorporating the entire length of the instrument and it is expected this would have implications for the tactile response of the instrument, but does not appear to greatly affect the radiated sound. In addition, there are no mechanical losses associated with an incomplete mechanical coupling between the neck and the body, suggesting that the bolt-on neck system used is equivalent to the more traditional glue-on neck system, in terms of vibratory response.

The effect of the polish used (nitrocellulose lacquer) has a small effect on the measured spectra, lowering and damping the $T(1,2)_2$, $T(2,2)$ and $T(5,3)$ modes. Allowing the volatile solvents in the polish to evaporate for a period of 53 days had the effect of slightly lowering the frequency of the $T(2,2)$ mode. There was little difference in the measured properties of the guitars after a period of ageing, with only a small amount of playing, for two years.

Apart from a small lowering in fundamental frequency, the effects of brace scalloping were not important at frequencies up until about 650 Hz, corresponding to the

T(3, 2) mode. The modes at these frequencies have nodal lines that are in areas that are close to the regions of the soundboard braces that are scalloped. The tone-braces especially appear important at these modes. Scalloping also appears to improve the fit of frequency change induced by an applied mass load at the driving point.

Chapter 8

A lexicon and a preliminary study of subjective responses to guitar sounds

"If ever there's an obscene noise to be made on an instrument, it's going to come out of a guitar. On a saxophone you can play sleaze. On a bass you can play balls. But on a guitar you can be truly obscene."—Frank Zappa (1940-1993)

8.1   Introduction

It would be desirable to determine how physical changes made to acoustic guitars affect how the sound is perceived by human beings. It is obviously important for a luthier to know how their manufacturing techniques influence the sensations experienced by a human listener. One approach is to perform measurements of the responses of human subjects exposed to sounds produced by the instrument with various physical configurations. This is a difficult task; previous studies on the results of changes to the instrument do not make it clear how traditional 'physical'

measurements of the response of an instrument relate to the resulting subjective impression [Meyer, 1983b, Hutchins, 1989, Richardson, 1994, Wright and Richardson, 1997, Boullosa et al., 1999].

Psychoacoustic studies of timbre [Grey, 1977, 1978, Kerrick et al., 1969, Lichte, 1941, McGee, 1964, Salomon, 1958, Terhardt, 1978, von Bismarck, 1974b, Wedin and Goude, 1972, Wessel, 1978, Wright, 1996, Meyer, 1983b, Gridnev and Porkenhov, 1976, Boullosa et al., 1999] typically examine the responses of a participant exposed to external stimuli. These responses are usually in the form of a difference between two stimuli, or with the ranking of certain parameters defined within the test.

However, the specific details of the type of stimulus and the mechanics of how the test is applied is often important, which imposes constraints on the range of the variables being studied. For example, the perceived timbre of notes of a guitar string plucked with the fingernail differs markedly from that when a plectrum is used [Schneider, 1977]. Because the purpose of Study I (§8.2) is to construct a vocabulary to describe the timbre of guitar sounds with *as large a range as possible*, no stimulus is given.

Once an agreed lexicon is established, it is then possible to determine the redundancy of particular terms, by analysing the responses of participants exposed to guitar sounds. From the results of other studies of the factor analysis of timbre (§1.3), it should be possible, in principle, to characterise guitar sounds using a limited number of dimensions. This is the purpose of Study II (§8.3).

8.2 Study I—establishing a guitar timbre lexicon

There is an extensive informal literature reporting descriptions of the timbre of acoustic guitar sounds. Within this literature there appears to be some consistency in the descriptive terms (*descriptors*) used. The aim of this study is to formalise these descriptors, producing an acceptable lexicon to describe the timbre of an acoustic guitar. The terms need to be meaningful (to a large proportion of the population requiring the use of these terms) and should be broad enough to cover the variation in timbre expressed by the instrument. This list could then be used to obtain information from the responses of participants in a test to determine the perceptual features of given guitar sounds, as in Study II (§8.3).

Method and procedure

This study consists of two parts: a controlled literature search to obtain a list of descriptors, and a survey to determine how these descriptors are rated, in terms of their usefulness in describing a guitar sound.

A selection of guitar magazines and websites were obtained from a collection of magazines and through a search of websites that sold or reviewed acoustic guitars. The terms used to describe the timbre of the instruments—usually adjectives—were taken from these reviews. The frequency that the terms occurred in this sample of the literature was recorded. In addition, some guitar repairers were consulted regarding the terms they used to describe guitar sounds.

The list of descriptors resulting from the literature search was presented to participants to rate in terms of how useful they found the descriptor in describing guitar music. The survey does not rely on stimuli. Instead, it relies on the participants' memory of *all* the acoustic guitar sounds they had heard before. There is precedence for this type of survey [Schubert, 2003]; this method does not constrain the participant to a narrow range of sounds (which may lack important components of interest) and is also convenient to administer. On the other hand this approach is strongly dependent on the participants' *memory of sounds* as well as their *experience with using the particular words* in this environment.

Because of the prevalence of the internet and World Wide Web networks, an 'online' format solved the logistical problems of distribution, advertising and supply. Because the test was conducted without external stimuli, data transfer consisted only of fairly small text files. The test was in the form of an interactive online 'web survey' spanning 9 pages and taking approximately 5-12 minutes to complete. Participants were asked to respond with their first impressions, to every term in the list, after the instructions:

"Take a few minutes to think of the sounds produced by any acoustic guitar being played. Which of the following terms (if any), in your opinion, would be useful for describing the tone quality ('timbre') of a guitar sound?"

The web-pages were written in PHP (Personal Home Page) and the interface were

forms generated by the users' web-browsers *via* HTML (Hyper-Text Mark-up Language.) The terms referred to are provided in Appendix F. The usefulness ('utility') of each term was rated on a seven-point scale, (1-7, 7 defining the most useful). The order that terms appeared in each examination was randomised to reduce ordering effects and biases. Participants were asked to state their general musical experience and how much they played or listened to acoustic guitar music. Opportunity was given to add additional comments and to suggest further expressions.

Validity checking of the survey

Because of the lack of control of the participants in a web-based test, it is necessary to ascertain whether the responses obtained were sufficiently consistent and valid. Participants were advised that some sort of validity check would be used during the test. Two types of checks were introduced for this purpose: *repeated measures* and *syntactic logic check*.

Repeated Measures There were exactly 3 repetitions of particular terms in each test. The difference in scores between the repeats and the original were taken for the three repeats. The terms that were repeated were selected at random, although the positions they occurred at were constant for each test:

1. Between term 27 and 28, a repeat of term 12 occurred

2. Between term 63 and 64, a repeat of term 47 occurred

3. Between term 102 and 103, a repeat of term 69 occurred

Syntactic logic check Exactly 3 terms were added that could not be used to make
a sensible sentence in the context of the survey. Generally, for a term to be a
useful timbre descriptor, it is required to be an adjective. The following terms,
not adjectival, were inserted:

1. Between term 15 and 16: 'please enter a 1 here'

2. Between term 58 and 59: 'albert einstein'

3. Between term 89 and 90: 'radium'

These terms also appeared at the same position for each participant.

It is not expected that a large portion of respondents would answer an identical
value for each of the repeated terms (Except for 'please enter a 1 here'). However
large enough discrepancies would render the entire data set from that participant
unusable because of their unreliability. The sum of the square of the differences in
the repeats was examined. If this was greater than eight, then the responses from
the participant was discarded. One participant was discarded for this reason.

The URL address for the web survey was distributed on the University of New
South Wales *all-physics* email list, posted on the newsgroups *rec.music.makers.guitar.acoustic*
and *rec.music.classical.guitar*, and various UNSW students, including those from the
music course MUSI2142 (Musicology 2B), participated.

Results of the literature search

The terms resulting from the literature search were almost all 'positive' in the evaluative sense. This is because it is usually guitars of relatively high quality that are reviewed in popular magazines and websites, and/or the reviewer is trying to sell the instrument. Because the largest possible range of acoustic guitar sounds was required, consultation was undertaken with some guitar repairers, who had seen a range of instruments requiring significant amelioration, in order to add terms with more negative emotive connotations to the list. The literature search ceased when 84 terms were found (Figure 8.1).
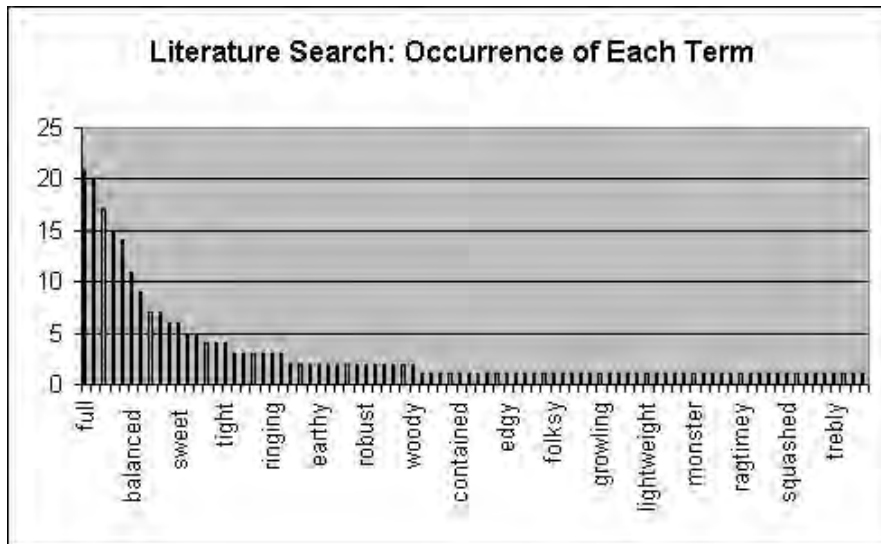
Figure 8.1: The frequency of all terms encountered in the literature study, illustrating the frequency distribution. Because of limitations on space, only a selection of terms are labelled.

A total of 112 words or short phrases were obtained. It was necessary to reduce this set to a more manageable number of terms. Judging from previous studies [Rasch and Plomp, 1982, Enomoto and Yoshida, 1968, Kerrick et al., 1969, Grey,

Rank	Descriptor	Frequency occurring in literature sample
1	full	21
2	rich	20
3	clear	17
4	bright	15
5	warm	14
6	balanced	11
7	mellow	9
8=	boomy	7
8=	clean	7
10=	powerful	6
10=	sweet	6

Table 8.1: The ten most frequently encountered descriptors in the selective literature search.

1977] the descriptions of the timbre of a variety of sound stimuli are able to be expressed using a small number of terms. Therefore data from listening tests should be expected to show a clustering in correlations between these terms and responses to stimulus in the form of guitar sounds with varying timbre.

Participant details and experience

The participants were asked for personal details, including name, age group, occupation, how often they heard live and recorded acoustic guitar music, years of experience playing a musical instrument, and years of experience playing the acoustic guitar. Comparing how certain demographic groups answered the survey may provide useful data. For example, one might expect those with many years of experience in guitar playing to be more familiar with the terms used than those who had never played at all. The distribution of participants' experience with playing a musical instrument, and those playing the acoustic guitar, are shown in Figures 8.2 and 8.3.
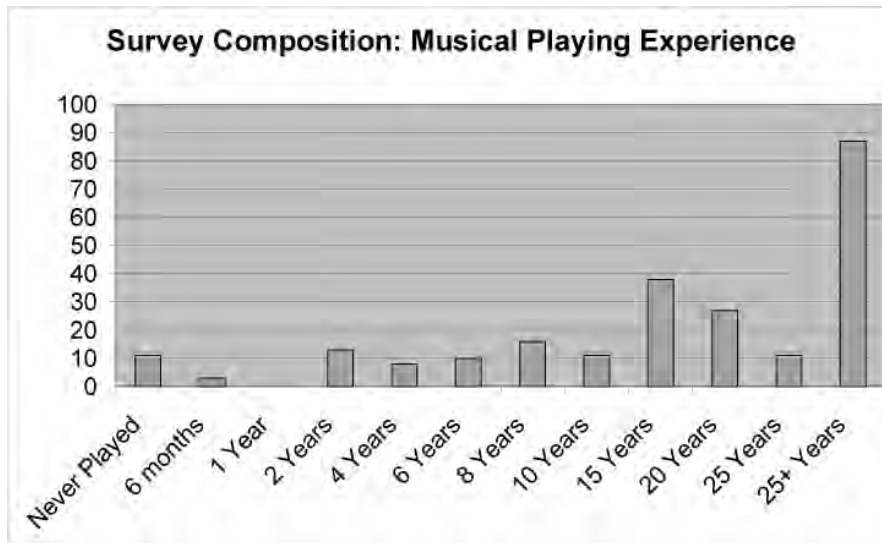
Figure 8.2: All participants, experience with a musical instrument.

Analysis

A total of 245 surveys were completed over a period of 30 days. The uncertainty of the mean of each term, ΔU, was taken as the standard error. With a possible range between one and seven, the mean score, from all terms and participants, was 3.74 ± 0.01 and ranged from 'bright' (5.67 ± 0.11) to 'boofy' (1.49 ± 0.07). The entire list, for all participants, is included in Table F.1 (Appendix F). There were no apparent effects due to the particular order the terms appeared in.

Lexicon responses		
Term	Mean response	Ranking
bright	5.7	1
warm	5.5	2
clear	5.5	3
crisp	5.4	4
rich	5.3	5
full	5.3	6
balanced	5.1	7
mellow	5.1	8
tinny	5.0	9
twangy	5.0	10
clean	5.0	11
bassy	5.0	12
thin	4.9	13
ringing	4.9	14
trebly	4.9	15
metallic	4.9	16.5 $(16_{=2})$
powerful	4.9	16.5 $(16_{=2})$
brilliant	4.8	18
boomy	4.7	19
deep	4.7	20
dead	4.7	21
vibrant	4.6	22

Table 8.2: The 22 terms of highest mean rating, from all 245 participants in the guitar timbre lexicon study. This is expressed as the mean response. Each term had a standard error of ±0.1.

Literature Study			
Term	Frequency	Ranking	
full	21	1	
rich	20	2	
clear	17	3	
bright	15	4	
warm	14	5	
balanced	11	6	
mellow	9	7	
boomy	7	8.5	$(8_{=2})$
clean	7	8.5	$(8_{=2})$
powerful	6	10.5	$(10_{=2})$
sweet	6	10.5	$(10_{=2})$
crisp	5	12.5	$(12_{=2})$
punchy	5	12.5	$(12_{=2})$
big	4	15	$(14_{=3})$
brilliant	4	15	$(14_{=3})$
tight	4	15	$(14_{=3})$
bassy	3	19.5	$(17_{=6})$
bluesy	3	19.5	$(17_{=6})$
natural	3	19.5	$(17_{=6})$
percussive	3	19.5	$(17_{=6})$
ringing	3	19.5	$(17_{=6})$
strong	3	19.5	$(17_{=6})$

Table 8.3: The 22 most frequent
terms from the literature search.

Comparison of guitar timbre lexicon to literature search

Of the 20 terms most frequently occurring in the literature and the 20 highest mean responses from the survey, 13 terms were the same (Table 8.2). To compare the ranking of both data sets, Spearman's rank correlation is an appropriate statistical measure.

Comparing the rankings of the frequency of the terms in the reviewed portion (*i.e.* omitting the descriptors obtained through consultation) of the literature study ($N = 84$), to the rankings of the terms from the responses of participants who had 25 years or more experience with the acoustic guitar, yielded a correlation coefficient of $r_s = 0.57$ ($p < 0.001$). Hence there is some positive correlation between the utility of a descriptor of guitar timbre and the frequency the term occurs in the literature.

Study I—conclusion

The descriptors of guitar sounds were obtained from a controlled literature search and were judged for usefulness in a web survey. A correlation of $r_S = 0.57$ was found between the utility rating of each descriptor and the frequency it occurred in the literature.

This list may be of use to the acoustic guitar community and will be used to help participants to describe their impression of a guitar sound recording in Study II. It is also possible this method of testing could be applied to other musical instruments.

8.3 Study II—evaluation of guitar sounds

In recordings of guitars being played, several variables could conceivably affect the timbre and other perceptual attributes of a guitar sound reproduced through an audio system. This study investigates the effect of some variables on the perceived distinctions among recordings of steel-string acoustic guitars.

Study II: method and materials

Three guitars of varying commercial value were recorded simultaneously at four different locations. Each instrument was played a total of eight times. Some of the variation in the recorded sound due to the type of guitar (GQ), the microphone positions (RM) and that due to the particular performance (RP) were quantified by varying these parameters.

Guitar quality

The three guitars ranged from a fairly expensive hand-made model, a medium-priced style guitar and an inexpensive model. There is no well-identified objective measure for the quality of an acoustic steel-string guitar. The commercial value generally attributed by musicians and dealers to similar instruments of each type is taken as a rough indicator of the quality of the instrument.
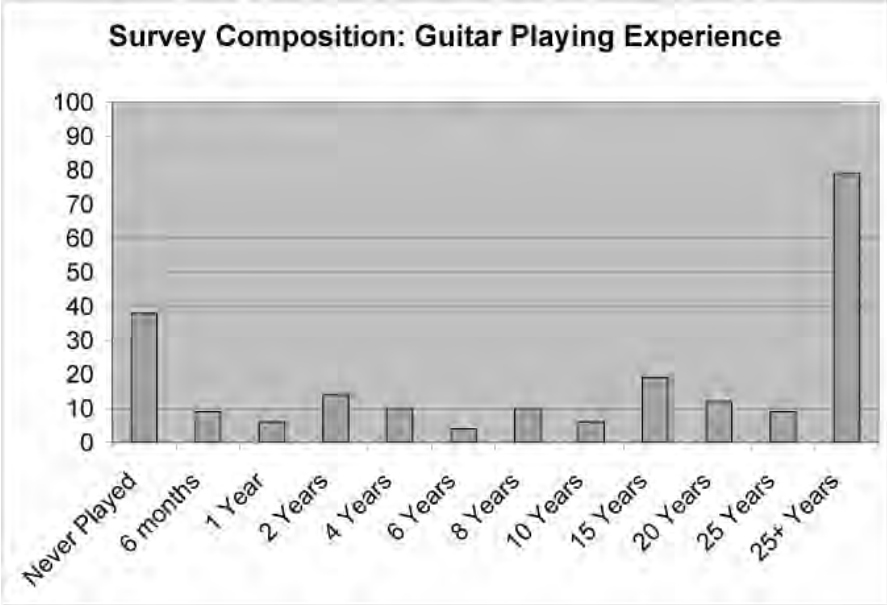
Figure 8.3: All participants, guitar playing experience

Parameter Value	Mass (kg)	Estimated price
GQ3	2.2300	Greatest
GQ2	2.0016	
GQ1	2.0212	Least

Table 8.4: The three guitars used in Study II to determine the effect of variation in the commercial value of the instrument.

Microphone position	Parameter value	Microphone type
Near guitar bridge	RM1	R0DE NT3
Near guitar neck	RM2	R0DE NT3
Overhead	RM3	R0DE NT3
Player's head (stereo)	RM4	2 Optimus tie clip microphones

Table 8.5: The four microphones systems, at separate positions around the guitar, to make recordings for the pilot test. The three R0DE microphones are of cardiod mono type, and the headphone system is a stereo combination of two small electret cardiod microhones.

Microphone position

The directivity of the radiation from stringed instruments is frequency dependent [Meyer, 1972], is influenced by the player's presence, and is complicated by reflections. The perceived timbre of sounds recorded at different positions may be different and it is not obvious where the most appropriate recording location is. The four microphone positions were (Figure 8.4, Table 8.5) near the bridge (RM=1), near the neck (RM=2), directly overhead (RM=3) (about one metre above the soundhole), and at the ears of the player (RM=4).

During the test, the participants were not explicitly aware of the recording position of any particular track they were exposed to.

Variation in performance

To further decrease variation in the performances, the same piece was played each time. The piece to be played is important: it is desirable to have the piece in a musical context, but it is not desirable to have a long excerpt. For the luthier, the most valuable piece is that which a potential buyer of a guitar might play, assuming they were to judge an instrument based solely upon the sound it made.

It was decided to play an ascending one octave G-major scale (from G2) followed by an arpeggiated open G,C,D chord progression. It would be ideal to have the sound produced by a particular instrument to be reproducible, while also sounding as realistic as possible. Usually the player has some degree of control over the timbre of the sound produced, in addition to the loudness and pitch. Using an automated device to excite the instrument is possible, but present models do not sound realistic [Cass, 2003]. Instead, a human player was chosen: Sydney guitar player and teacher John Morris.

The recordings were made in one session lasting three hours in a studio equipped with a professional digital recording system designed for the recording of acoustic guitar music. The performances were all made by the same performer, who was blindfolded and wore a headset with microphones attached near the position of the player's ears. Neither the performer nor the recording engineer knew the purpose of the test. The guitars were fitted with new strings (Martin 'Acoustic SP Phosphor Bronze', Light Gauge (0.30, 0.41, 0.64, 0.81, 1.07, 1.37 mm diameters))and tuned to standard tuning (E2, A2, D3, G3, B3 and E4) using an electrical guitar tuner. The tuning was checked periodically during the session. The player was handed each instrument in a prearranged pseudorandom order, with an associated three digit numerical performance code.

These recordings were recorded onto audio CD (sampling rate 44.1 kHz, with 16 bit depth audio). The factorial design of the study, gives a total of 96 separate tracks (eight performances of the three guitars, each recorded at four microphone positions).
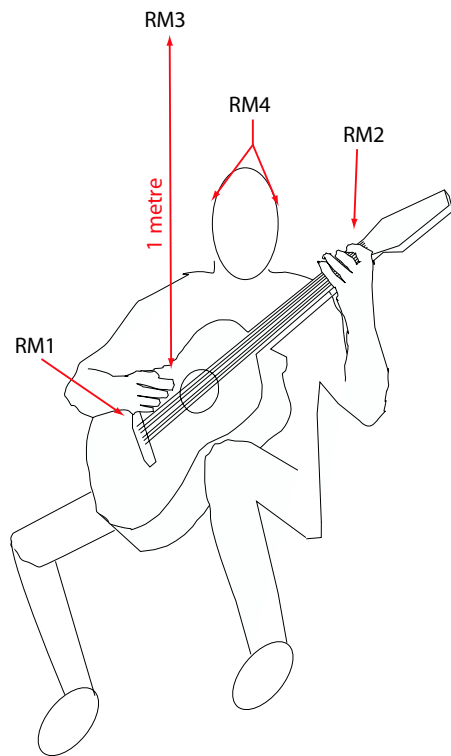
Figure 8.4: The four microphone positions used to record the guitar sounds used as stimuli in Study II.

Study II: procedure

The pilot study was installed on three computers in a survey format, using software developed by Emery Schubert. Three identical models of computer were used (Apple PowerMac 7200/120, running Mac OS 8.6 with a 120 MHz PPC 601 central processor and a 16 bit 44.1 kHz AWACS Sound IC[1] sound processor with Philips Stereo Headphones SBC HP100).

The participants were exposed to the stimuli in the form of the tracks from the audio CD. Each stimulus was associated with a survey page containing drop-down lists of the perceptual quantities obtained from §8.2, which the participant rated as an integer between zero and ten. The decision to use a unipolar (0 to 10), as opposed to a bipolar (-5 to +5) rating scale, was made after considering the semantic implications in some cases. It was thought many respondents would interpret a negative scale of *e.g.* 'brightness' as being the diametric opposite to 'brightness' ('anti-brightness'?), as opposed to a lack of the quality 'brightness'. Similarly, terms incorporating 'lacking X' were removed, if the quality 'X' were present. The participants underwent a small training session, comprising

---

[1] *Audio Waveform Amplifier and Converter.* Conforms to IT&T ASCO Audio-Stereo Codec Specifications.

How much did you like the sound? (preference))			
overall quality of this instrument (quality)			
dry	loudness	bright	balanced
bassy	boomy	trebly	warm
ringing	thin	tinny	full
bell-like	clear	dead	crisp
rich	muddy	powerful	brilliant
midrangey	clarity	deep	twangy
mellow	woody	punchy	bottomy
dull	metallic	shimmering harmonics	percussive

Table 8.6: The variables that participants rated in response to stimuli in the pilot test.

two stimuli deemed to span the range of guitar quality, both recorded from the headset microphones (*i.e.* taking GQ=1, 3 while holding RM=4). Thereafter, the stimuli were provided by playing tracks from the audio CD in pseudorandom order. Because this study required the participant to respond to many questions (34) on each sound stimulus (Table 8.6), there is a greater probability of operator fatigue. A test of 32 examples (*i.e.* 1/3 of the total stimuli on the audio CD) required a participant's undivided attention for at least 90 minutes. The test was designed with two rest breaks, as well as an option to end the test at any stage after the initial training period. As a result, the participants were not forced to respond to all stimuli and therefore the test is of an incomplete factorial design.

Results

Overall analysis of descriptors

There were a total of 95 observations, from five respondents. The training session was the same for all participants: tracks 78 and 92 (GQ=1,3, RM=4). The six terms with the highest variance from track 78 were (mean (variance), N=5): 'dry' 4.6 (18.8), 'bassy' 5.6 (16.3), 'punchy' 4.6 (13.3), 'dull' 4.8 (12.7), 'midrangey' 4.9 (11.3) and 'deep' 6.4 (11.3). The five terms with the highest variation from track 92 were: 'tinny' 3.2 (15.7), 'dull' 4.4 (13.8), 'twangy' 4.4 (11.3), 'brilliant' 4.6 (9.8) and 'ringing' 3.2 (9.7).

In addition to these two tracks, the randomised audio track sequence meant that there were five cases where two different participants were exposed to the same track. In these cases, there does not appear to be good agreement in the rating of the tracks with the term 'dry'. This may be an indication that the participants were unsure how to use this as a descriptor, because the magnitudes were very low in general (mean $\pm$ standard error(number observations) $4.0 \pm 0.5(62)$) second only to 'dull' ($3.9 \pm 0.5(62)$), compared to the overall mean for all descriptors ($4.95 \pm 0.04(3230)$). This is also a comparatively high standard error; the majority (26 of the 34 terms) had a standard error of 0.3 or less.

Effects of varying the guitar

The mean and standard errors of the preference and quality responses, as a function of guitar of varying commercial value, are given in Table 8.8. However, the differences in the preference and quality ratings with different guitars were not significant. A

Descriptor	Mean± standard deviation (observations)
dull	$3.88 \pm 3.14(93)$
dry	$3.98 \pm 2.90(89)$
thin	$3.57 \pm 2.87(94)$
dead	$2.52 \pm 2.59(93)$
muddy	$2.27 \pm 2.44(93)$
boomy	$4.18 \pm 2.41(95)$
punchy	$4.72 \pm 2.39(95)$
twangy	$4.36 \pm 2.36(95)$
tinny	$2.35 \pm 2.28(92)$
bassy	$4.76 \pm 2.27(94)$
percussive	$4.18 \pm 2.25(84)$
metallic	$4.35 \pm 2.19(93)$
powerful	$5.09 \pm 2.16(95)$
woody	$4.78 \pm 2.01(95)$
trebly	$5.33 \pm 2.00(95)$
brilliant	$5.65 \pm 1.96(95)$
ringing	$5.17 \pm 1.95(95)$
deep	$5.23 \pm 1.92(95)$
bell-like	$4.55 \pm 1.91(84)$
full	$6.27 \pm 1.86(95)$
warm	$5.59 \pm 1.85(95)$
mellow	$5.84 \pm 1.84(95)$
overall quality	$6.39 \pm 1.74(93)$
bright	$5.82 \pm 1.72(95)$
rich	$6.06 \pm 1.72(95)$
How much did you like the sound?	$6.47 \pm 1.71(94)$
midrangey	$4.71 \pm 1.68(90)$
clarity	$6.33 \pm 1.62(94)$
clear	$6.37 \pm 1.61(95)$
balanced	$5.49 \pm 1.56(91)$
bottomy	$5.54 \pm 1.54(95)$
loudness	$5.40 \pm 1.40(94)$
crisp	$5.34 \pm 1.36(95)$
shimmering harmonics	$5.07 \pm 1.31(88)$

Table 8.7: Overall mean of responses from Study II, in order of standard deviation, to show the range of the responses. The number of observations of each term are in parentheses.

Guitar	Mean±Standard error (count)	
	Preference	Quality
GQ1	$6.5 \pm 0.3(28)$	$6.6 \pm 0.3(28)$
GQ2	$6.8 \pm 0.2(42)$	$6.7 \pm 0.2(41)$
GQ3	$6.0 \pm 0.4(25)$	$5.8 \pm 0.4(25)$

Table 8.8: Overall mean response ratings of preference and quality, according to nominal quality of guitar. GQ1 is the instrument of lowest market value.

one-way ANOVA test for 'preference' gives $F_{2,92} = 2.01$ (p=0.14) and, for 'quality', $F_{2,92} = 2.24$ (p=0.11). It is therefore concluded that the listeners cannot distinguish between instruments of various market values, at least for such a small sample.

Effects of varying microphone position

There were apparently clear differences in the perceived timbre due to where the recording microphone was positioned (Table 8.9), although this was not significant for preference, $F_{3,91} = 2.16$ (p=0.10), quality $F_{3,91} = 1.55$ (p=0.21), loudness $F_{3,91} = 1.28$ (p=0.29) and dry $F_{3,91} = 0.13$ (p=0.95).

The headset microphone pair were rated higher (within the standard errors) than the other three positions in the case of 'preference', 'quality', 'balanced', 'warm', 'full', 'clear', 'mellow' and 'bottomy'. The microphone at the neck was rated higher than the others in 'bell-like', 'crisp', 'powerful', 'woody' and 'metallic'. For the overhead microphone, this was clearly higher in 'thin', 'dead' and 'dull'. Finally, the bridge microphone was seen as high in terms of the variables 'bassy' and 'midrangey'. Therefore the microphone position clearly has a great impact on the perception of timbre from the guitar, with a largely positive reaction to the stimulus from the

Descriptor	RM=1 (Bridge)	RM=2 (Neck)	RM=3 (Overhead)	RM=4 (Headset)
preference	$6.2 \pm 0.4(18)$	$6.6 \pm 0.3(29)$	$5.9 \pm 0.4(21)$	$7.1 \pm 0.3(27)$
loudness	$5.6 \pm 0.3(18)$	$5.6 \pm 0.3(29)$	$4.9 \pm 0.3(21)$	$5.7 \pm 0.3(27)$
bright	$5.7 \pm 0.4(18)$	$6.0 \pm 0.3(29)$	$5.8 \pm 0.4(21)$	$5.8 \pm 0.4(27)$
balanced	$5.2 \pm 0.3(18)$	$5.5 \pm 0.3(29)$	$5.4 \pm 0.3(21)$	$5.9 \pm 0.4(27)$
bassy	$5.4 \pm 0.4(18)$	$4.7 \pm 0.4(29)$	$4.1 \pm 0.4(21)$	$4.9 \pm 0.5(27)$
boomy	$4.3 \pm 0.5(18)$	$4.5 \pm 0.5(29)$	$3.5 \pm 0.5(21)$	$4.2 \pm 0.5(27)$
trebly	$5.2 \pm 0.4(18)$	$5.7 \pm 0.4(29)$	$5.4 \pm 0.4(21)$	$5.0 \pm 0.4(27)$
warm	$5.7 \pm 0.5(18)$	$5.4 \pm 0.4(29)$	$5.1 \pm 0.4(21)$	$6.1 \pm 0.3(27)$
ringing	$5.6 \pm 0.4(18)$	$5.5 \pm 0.4(29)$	$5.0 \pm 0.4(21)$	$4.7 \pm 0.4(27)$
thin	$3.0 \pm 0.7(18)$	$3.7 \pm 0.6(29)$	$4.3 \pm 0.6(21)$	$3.3 \pm 0.5(27)$
tinny	$2.3 \pm 0.6(18)$	$2.3 \pm 0.4(29)$	$2.6 \pm 0.5(21)$	$2.5 \pm 0.5(27)$
full	$6.2 \pm 0.4(18)$	$6.2 \pm 0.3(29)$	$5.6 \pm 0.4(21)$	$6.9 \pm 0.4(27)$
bell-like	$4.9 \pm 0.4(18)$	$5.2 \pm 0.3(29)$	$4.6 \pm 0.4(21)$	$3.7 \pm 0.3(27)$
clear	$6.1 \pm 0.4(18)$	$6.3 \pm 0.3(29)$	$6.0 \pm 0.3(21)$	$6.9 \pm 0.3(27)$
dead	$2.7 \pm 0.7(18)$	$1.8 \pm 0.4(29)$	$3.7 \pm 0.6(21)$	$2.5 \pm 0.4(27)$
crisp	$5.3 \pm 0.3(18)$	$5.7 \pm 0.3(29)$	$5.0 \pm 0.4(21)$	$5.3 \pm 0.2(27)$
rich	$5.9 \pm 0.4(18)$	$6.2 \pm 0.3(29)$	$5.5 \pm 0.3(21)$	$6.5 \pm 0.4(27)$
muddy	$3.0 \pm 0.7(18)$	$1.8 \pm 0.4(29)$	$2.7 \pm 0.6(21)$	$2.2 \pm 0.4(27)$
powerful	$5.4 \pm 0.5(18)$	$5.7 \pm 0.4(29)$	$4.0 \pm 0.4(21)$	$5.2 \pm 0.4(27)$
brilliant	$5.9 \pm 0.4(18)$	$5.6 \pm 0.4(29)$	$5.3 \pm 0.4(21)$	$5.8 \pm 0.4(27)$
midrangey	$5.1 \pm 0.3(18)$	$4.7 \pm 0.4(29)$	$4.4 \pm 0.3(21)$	$4.7 \pm 0.3(27)$
clarity	$5.9 \pm 0.5(18)$	$6.6 \pm 0.3(29)$	$5.8 \pm 0.4(21)$	$6.9 \pm 0.2(27)$
deep	$5.4 \pm 0.3(18)$	$5.2 \pm 0.3(29)$	$4.9 \pm 0.4(21)$	$5.4 \pm 0.5(27)$
twangy	$4.8 \pm 0.5(18)$	$4.6 \pm 0.4(29)$	$4.1 \pm 0.5(21)$	$4.0 \pm 0.5(27)$
mellow	$5.5 \pm 0.4(18)$	$5.4 \pm 0.4(29)$	$5.9 \pm 0.4(21)$	$6.4 \pm 0.4(27)$
woody	$4.8 \pm 0.4(18)$	$5.1 \pm 0.4(29)$	$4.7 \pm 0.4(21)$	$4.4 \pm 0.5(27)$
punchy	$5.0 \pm 0.4(18)$	$5.2 \pm 0.5(29)$	$4.3 \pm 0.5(21)$	$4.3 \pm 0.5(27)$
bottomy	$5.7 \pm 0.4(18)$	$5.4 \pm 0.3(29)$	$5.0 \pm 0.3(21)$	$6.0 \pm 0.3(27)$
dull	$3.6 \pm 0.8(18)$	$3.0 \pm 0.5(29)$	$5.1 \pm 0.8(21)$	$4.1 \pm 0.6(27)$
metallic	$4.4 \pm 0.4(18)$	$5.0 \pm 0.4(29)$	$3.9 \pm 0.5(21)$	$4.1 \pm 0.4(27)$
shimmering harmonics	$5.1 \pm 0.4(18)$	$5.2 \pm 0.1(29)$	$5.0 \pm 0.4(21)$	$4.8 \pm 0.2(27)$
percussive	$4.6 \pm 0.4(18)$	$4.8 \pm 0.4(29)$	$4.2 \pm 0.5(21)$	$3.6 \pm 0.4(27)$
dry	$4.2 \pm 0.7(18)$	$4.1 \pm 0.5(29)$	$4.2 \pm 0.7(21)$	$3.8 \pm 0.6(27)$
quality	$6.2 \pm 0.5(18)$	$6.3 \pm 0.3(29)$	$6.0 \pm 0.4(21)$	$7.0 \pm 0.3(27)$

Table 8.9: Responses to stimuli in the pilot study, as a function of microphone position. Responses expressed as (mean $\pm$ standard error (number of observations)).
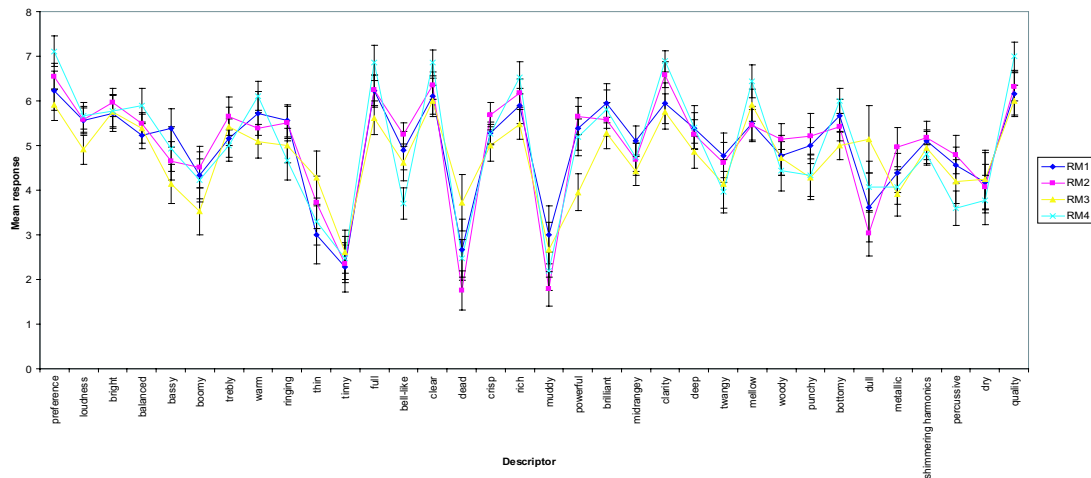
Figure 8.5: Mean responses to stimuli in the pilot study, as a function of microphone position. The errors are taken as standard errors.

headset microphone pair and a mildly negative reaction from the overhead microphone. However, these differences are not significant, as rated through ANOVA of key descriptors.

Effects of variation in performance

Within this experimental design, this is the least controllable—and least reliable—parameter that is varied. Each performance is at least subtly different, even when performed on the same instrument and recorded by the same microphone. In this study, there were a total of 24 separate performances, but, because the instrument was varied, the performance was also a function of changing guitar quality. These were recorded at the four different microphone positions, described in the previous section. In listening tests, Jürgen Meyer showed that the performance slightly affects

the perceived quality of a guitar sound [Meyer, 1983b]. It is concluded that there is only a minor effect on the perception of timbre from the performances used in this pilot study.

Reduction of response data

Because of the factorial design of this study, an efficient method of reducing the data is with a factor analysis. The analysis is exploratory because we have no *a priori* expectation of the effect each descriptor contributes to any potential factor.

I performed a maximum likelihood common factor analysis, conducted using Matlab, to construct orthogonal axes based on the extent of correlation between the descriptors. These axes were rotated using the varimax method so that they were aligned with the principal components (*i.e.* the 'main effects').

The optimal number of dimensions to describe guitar sounds

The number of dimensions describing a semantic space is generally a compromise between simplicity of interpretation (fewer dimensions) and an adequate span of the semantic space.

Overall, for the data analysed here, a single linear factor would be inadequate to describe the space: there are 28 descriptors (from a total of 34) that have a very large estimated specific variance (Table 8.11). On the other hand, while a ten factor model would account for more of the variance of the space (77.3% compared to 23.7%), it would would be unwieldy as a descriptive tool.

Descriptor	Standard error
dull	0.4
boomy	0.3
dry	0.3
thin	0.3
bassy	0.3
dead	0.3
powerful	0.3
muddy	0.3
full	0.3
percussive	0.3
tinny	0.3
preference	0.3
brilliant	0.2
punchy	0.2
clarity	0.2
bottomy	0.2
woody	0.2
deep	0.2
metallic	0.2
quality	0.2
ringing	0.2
bell-like	0.2
rich	0.2
twangy	0.2
trebly	0.2
clear	0.2
warm	0.2
bright	0.2
shimmering harmonics	0.2
loudness	0.2
mellow	0.2
midrangey	0.1
balanced	0.1
crisp	0.1

Table 8.10: The variation (expressed as a standard error for all 24 performances) in the response of each descriptor as a function of the performance.

Number of factors	Proportion of total variance (%)	Range of specific variance of descriptors		
		$\psi \gtrsim 0.50$	$\psi \gtrsim 0.85$	$\psi \lesssim 0.25$
1	23.7	28	18	0
2	39.4	21	9	4
3	56.4	11	0	6
4	63.1	5	0	8
5	66.8	3 (midrangey, balanced, bassy)	0	10
6	69.5	2 (midrangey, balanced)	0	11
7	71.7	2 ” ” ”	0	13
8	73.5	2 ” ” ”	0	14
9	74.9	2 ” ” ”	0	17
10	77.3	1 (midrangey)	0	19

Table 8.11: The optimal number of dimensions of the semantic space used to describe guitar sounds, in terms of the number of descriptors (out of the total 34) not adequately spanned by the number of independent linear factors (showing high relative variance) and those well represented by the dimensions of the space (showing low relative variance).

The high degree of variance observed in some variables (*viz.* 'midrangey', 'balanced' and 'bassy') in the models with more than four factors is probably due to the uncertainty in the meaning of the descriptor. This is not surprising, because participants were forced to respond to each sound stimulus by rating all 34 descriptors. These terms can therefore be interpreted as statistically very noisy, and are *ipso facto* not useful in a description of guitar sounds.

A common 'rule of thumb' for choosing the number of dimensions resulting from a factor analysis is the Kaiser-Guttman rule: there are a sufficient number of factors if they have eigenvalues greater than one. However, this strictly applies only to principal component analysis [DeCoster, 1998] and often overestimates the true number of factors [Lance et al., 2006]. Another criterion for suitability is the 'scree

Factors	1	2	3	4	5	6	7	8
eigenvalues	8.07	7.85	7.89	6.35	7.01	6.47	6.52	6.19
		5.54	5.79	5.63	5.27	4.57	4.60	4.57
			5.50	4.98	4.47	4.49	4.22	4.23
				4.51	3.80	2.91	2.84	3.00
					2.16	2.87	2.81	2.95
						2.33	2.36	2.40
							1.02	0.91
								0.73

Table 8.12: The eigenvalues of each dimension for multiple factor models of the entire data set. The model having an eigenvalue less than one is the eight factor model. Therefore, according to the Kaiser-Guttman rule, no more than seven dimensions are required to span the semantic space here.

test' whereby the eigenvalues (or total variance spanned by the model) are plotted against the number of factors in the model. An optimal number of dimensions may be found near a sharp change in slope of the graph (an 'elbow'). Finally, another common factor optimisation method is examining the proportion of the total variance spanned by the factors, although this is an arbitrary cut-off. For the present study it is most important that the results may be interpreted in a context suitable for describing guitar sounds.

According to the Kaiser-Guttman rule, a seven factor model adequately spans the semantic space (Table 8.12). However, this method tends to overestimate the optimal number of dimensions [Lance et al., 2006].

A scree-plot of the data (Figure 8.6) has an elbow between the three and four factor models suggesting that this many dimensions are optimal.

The descriptors with a high positive correlation, assuming a single linear factor,
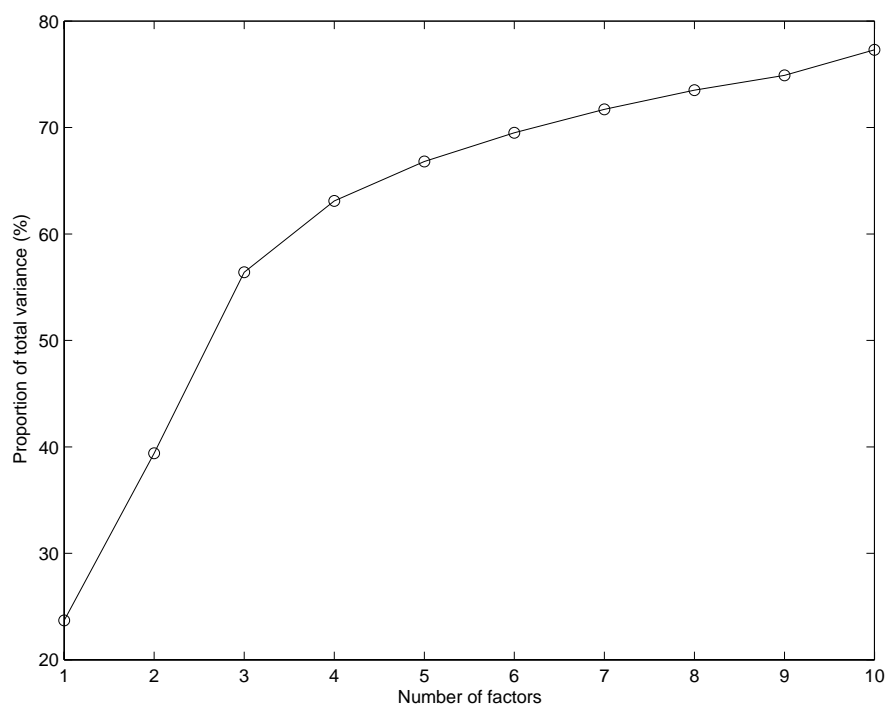
Figure 8.6: A scree plot of the total amount of variance spanned against the number of linear factors in a model for the overall responses to the pilot study. The optimal number of factors is obtained at the 'elbow' of the graph.

Sign	Factor			
	F_1 'Preference'	F_2 'Power'	F_3 'Brightness'	F_4 'Percussion'
+	preference (0.74) quality (0.73) rich (0.72) brilliant (0.61) clear (0.60)	mellow (0.76) bottomy (0.75) full (0.69) deep (0.69) loud (0.64)	bright (0.76) trebly (0.75) metallic (0.69) clear (0.59) clarity (0.59)	percussive (0.90) punchy (0.82) woody (0.78) bell-like (0.78) boomy (0.61)
-	dull (-0.87) dry (-0.81) dead (-0.71) muddy (-0.59) tinny (-0.54)	thin (-0.41) tinny (-0.30) shimmering (-0.26) harmonics bell-like (-0.17) trebly (-0.15)	midrangey (-0.28) deep (-0.2457) muddy (-0.23) warm (-0.22) bassy (-0.16)	warm (-0.28) dull (-0.22) preference (-0.21) dead (-0.19) quality (-0.18)

Table 8.13: The principal factors associated with a four factor model of the overall responses. The factors are listed in order of influence on the variation in the data. The titles of each factor are merely a label to represent the group of descriptors. The five terms with the largest factor loadings (positive and negative) are included, along with their factor loadings.

are: 'preference', 'quality', 'clear', 'rich' and 'brilliant'. Those having a highly negative weighting for this factor are 'dry', 'dull', 'dead', 'muddy' and 'tinny'. This single factor could be roughly associated with the preference each participant has for the sound and accounts for 23.7% of the variance overall. A two factor model retains this original factor for preference, with a second factor associated positively with 'punchy', 'woody', 'boomy', 'percussive' and 'ringing', and negatively with 'dead', 'warm', 'preference', 'dull' and 'bright'.

The best compromise according to the criteria mentioned, and considering the advantages of parsimony, is a model assuming four linear factors, in Table 8.13.

Not surprisingly, all models have a very strong positive correlation between the responses for 'preference' and 'quality' of a given stimulus. This factor is important

Sign	Factor			
	F_1 'Power'	F_2 'Brightness'	F_3 'Percussion'	F_4 'Dullness'
+	full (0.76) bottomy (0.75) mellow (0.74) deep (0.68) warm (0.66)	bright (0.83) trebly (0.74) clear (0.69) metallic (0.69) clarity (0.67)	percussive (0.91) punchy (0.85) woody (0.80) bell-like (0.76) boomy (0.64)	dull (0.91) dry (0.80) dead (0.73) muddy (0.56) tinny (0.55)
-	thin (-0.48) tinny (-0.39) shimmering (-0.28) harmonics trebly (-0.19) bell-like (-0.18)	muddy (-0.31) midrangey (-0.24) deep (-0.24) dead (-0.21) warm (-0.14)	warm (-0.27) full (-0.16) bright (-0.16) dull (-0.15) clarity (-0.14)	rich (-0.59) brilliant (-0.51) clear (-0.47) clarity (-0.39) full (-0.35)

Table 8.14: The principal factors associated with a four factor model of the overall responses, with the descriptors 'preference' and 'quality' removed from the data pool. The factors are listed in order of influence on the variation in the data. The titles of each factor are merely a label to represent the group of descriptors. The five terms with the largest factor loadings (positive and negative) are included, along with their factor loadings. Notice that, after the factor associated with 'preference', the structure has residual factors occurring in a very similar order.

for the study here, but has not, in general, been addressed by the above studies. Results of a four factor model of the same data set, with the responses to 'preference' and 'quality' removed, is similarly displayed in Table 8.14.

Notice that, after the initial factor of 'preference', similar factors arise and in the same order as the four factors in Table 8.13. This suggests that these factors are robust, despite the fact that this new model accounts for only 59% of the total variance of the responses (compared to 63% including 'preference' and 'quality'). A three factor model (Table 8.15), accounting for 52% of the variance, retains similar factors, although the order of the factors associated with 'Brightness' and 'Power' are reversed.

Sign	Factor		
	F_1 'Brightness'	F_2 'Power'	F_3 'Percussion'
+	clear (0.86) brilliant (0.84) bright (0.81) clarity (0.79) rich (0.70)	full (0.75) bottomy (0.73) mellow (0.72) deep (0.69) warm (0.66)	punchy (0.87) percussive (0.83) woody (0.80) bell-like (0.72) ringing (0.72)
-	dull (-0.61) dry (-0.60) muddy (-0.60) dead (-0.59) deep (-0.27)	thin (-0.53) tinny (-0.44) shimmering (-0.31) harmonics trebly (-0.27) twangy (-0.20)	warm (-0.31) full (-0.11) dead (-0.07) rich (-0.06) dull (-0.04)

Table 8.15: A three factor model of the overall responses, with the descriptors 'preference' and 'quality' removed from the data pool. The factors are listed in order of influence on the variation in the data. The titles of each factor are merely a label to represent the group of descriptors. The five terms with the largest factor loadings (positive and negative) are included, along with their factor loadings. Again, the structure is similar to the model including the 'preference' and 'quality' descriptors, although in this case factor F_1 ('Brightness') is a more significant factor than factor F_2 ('Power'). Factor F_3 remains associated with 'Percussion'.

It is interesting to speculate on the role of these factors in describing the timbre of sounds. The importance of the factor associated with 'brightness' has been emphasised by many studies (*e.g.* [Grey, 1977, von Bismarck, 1974b, Wessel, 1978]), and might be related to the position of the spectral centroid [Wessel, 1978, Wold et al., 1996, Schubert et al., 2004]. The existence of the factor of 'percussion' might reflect the important effect of transients on the sound of the guitar [Jansson, 2002].

Study II—Conclusion

For the stimulus considered, it was found that there was more agreement with some timbral descriptors than others (*i.e.* some were more 'useful' than others), based on the degree of variation of the ratings of these terms on the stimuli. For instance, the descriptors 'dry', 'dull', 'thin', 'dead' and 'muddy' had a high degree of variation, while there was comparatively little for 'crisp', 'shimmering harmonics' and 'loudness'. This extends some of the results from Study I, but is constrained by the particular stimulus used in this test.

Surprisingly the instrument with the highest commercial value was generally rated with a slightly lower quality and preference than the other two instruments. It was also shown that listeners could consistently rate different instruments according to 'quality', which is not, *a priori*, obvious. However, the differences were not significant, which is not surprising for the small sample size.

It was shown that the position of the recording microphone might have some effect on the timbre of the resulting sound, although again, ANOVA did not show

a significant difference. The stereo pair at the ears of the player were rated slightly higher on many attributes, including 'preference' and 'quality'.

In timbre ratings, the variation in responses was small between separate performances, agreeing with [Meyer, 1983b].

The dimensionality of the semantic space associated with the timbre of the recorded guitar sounds appears to be four, *viz.* 'preference', 'power', 'brightness' and 'percussion'. However, the four factor model accounts for only 63.1% of the variance of the data examined here.

8.4   Discussion

An important element of the sound of the guitar is the timbre, and would form an indispensable element in a study to determine the perceptual differences in the three guitars studied in this thesis. However, the phenomenon of timbre is poorly understood. Considering the difficulty of finding an explicit relationship between parameters associated with physical acoustics and the resulting timbre, the creation of an agreed list of terms to describe the range of timbre of acoustic guitar sounds is a good initial step towards a programme to quantify the musical concept of timbre. The on-line survey of the usefulness of terms obtained from guitar literature and language used by guitar makers has given a list of terms useful in describing the timbre of guitar sounds (Appendix F). A positive link was also found between the frequency of terms or expressions found in a selective literature review with a

large enough sample ($r_S = 0.57$, $p < 0.01$). This naturally suggests similar studies be made on the lexicon of the timbre of other instruments. This would reduce the labour required in a more general search for relationships between physical acoustics and musical timbre.

This list was then used in a pilot study to determine the dimensionality of these descriptions, finding it to be at least four dimensional ('Power', 'Brightness', 'Percussion' and 'Dullness'). Important to the perception of the sound of the guitar are the microphone position and the quality of the instrument. The particular performance was found to be important also, but not as much as the other variables considered.

Chapter 9

Conclusion and Further Work

"Unfortunately what is little recognized is that the most worthwhile scientific books are those in which the author clearly indicates what he does not know; for an author most hurts his readers by concealing difficulties"—Evariste Galois (1811-1832)

Many of the problems associated with the construction and design of the guitar result from the generally *ad hoc* or trial-and-error approach to manufacturing principles. This thesis has illustrated that a possible solution to these problems is to isolate key measurable parameters, and to optimise these parameters. However, it is recognised that the isolation and measurement of many of these parameters are confounded by the complexity involved in engineering the instrument, and the variability of the materials and components used therein.

To this end, it was found here that characterisation of important material properties relating to the vibratory behaviour of components, such as the Young's moduli and mass densities of the soundboard braces and the soundboard and bridge materials (§5.5, §5.6 and §5.7), was necessary in order to control the resulting instruments

330

(Chapter 5). The general techniques developed therein might help luthiers to isolate optimisation criteria for the guitar as part of a routine testing programme in the workshop.

It has also been shown that measurement of the dynamic mass and pressure force ratio transfer functions of the soundboard complement analysis using Chladni figures (§6.2), the more traditional diagnosis tool used by luthiers. However, measurement of these transfer functions enable much more rapid and accurate assessment of the properties of a guitar during and after construction than the traditional method and has the added advantage of being able to be compared to other instruments measured in the same way.

The effect of different soundboard timbers. The construction and measurement of very similar guitars would enable the luthier to better understand the effect and importance of timber selection for the soundboard. In this thesis, such a study was conducted on three similarly made guitars, using three commonly used wood species but with very different properties. Not surprisingly, out of the three timbers used for the soundboards here, Sitka spruce, Engelmann spruce and Western Red cedar, the Sitka spruce and Engelmann spruce were the most similar throughout all construction phases measured here (Chapters 6 and 7). Comparing the same modes, the Western Red cedar soundboard had lower frequencies than the corresponding modes for the other two soundboards for the free soundboards, except in the case of the mode at *ca.* 546 Hz (§6.3). The differences in mode frequencies between the soundboard materials is not as definite at low frequency, but at frequencies above 400 Hz, corresponding modal frequencies are also lower for the Western Red cedar

than for the other two soundboards. The effect of thinning (§6.5), binding (§6.6) adding the bridge (§7.2) have a much greater effect on the Western Red cedar soundboard than the other two. The effect of tone- and cross-brace scalloping was much more marked on the effective soundboard stiffness on the Western Red cedar than the Sitka spruce and Engelmann spruce, which were again very similar (§7.7).

The relative importance of major construction phases. The vibratory properties of ten major construction phases were measured in this thesis (§3.6). The motion of the free soundboard (§6.3) is very different to that of the soundboard attached to the back and sides (§6.4) because of the different boundary conditions and coupling with the internal air cavity.

After gluing the soundboard to the back and sides, the construction stage with the most impact on the vibratory behaviour of the guitar is the addition of the bridge to the soundboard (§7.2). This suggests that proper characterisation or design of the guitar soundboard ought to include the bridge as a component; several possible configurations of some modes (because of the phase relations between the oscillating elements) are reduced in number by the addition of the bridge (§7.2). In addition, the measured (effective) Helmholtz resonance of each of the three guitars was affected the most by the addition of the bridge (§7.2).

The polish used on the guitars studied in this thesis (nitrocellulose lacquer) had little effect on the measured vibratory behaviour of the guitars (§7.3), except a damping and slight lowering of the frequency of some modes (*viz.* $T(1,2)_2$, $T(2,2)$ and $T(5,3)$).

The effect of scalloping the cross- and tone-braces did not have a great effect on the dynamic mass or pressure force ratio at low frequency, except for soundboard

modes that had nodes near the areas of the braces that were scalloped, such as the T$(3,2)$ mode, *ca.* 650 Hz (§7.6). However, the calculated effective stiffness of each soundboard was greatly reduced with the brace scalloping process, especially between the partly and fully scalloped states (§7.7).

The effect of thinning the soundboard. Many, if not most, high quality guitars do not have a uniform thickness distribution (§3.4). Often the thinning of the soundboard occurs after it is glued to the back and sides, which makes it surprisingly difficult to measure the thickness except at points close to the soundhole. John Smith and I constructed a device employing magnetic field strength measurement to measure the thickness distribution of a non-uniform guitar soundboard [Inta and Smith, 2003], which could be employed routinely in a workshop (§6.5).

The use of Finite Element Modelling for guitar makers. The free soundboard was modelled by David Vernet, Davy Laille and Matheiu Maziere in §4.5, comparing well with Chladni figures made on the soundboard having the same measured properties. A FEM model of the complete guitar was also made (§4.6). However, in this case, comparison to experiment was only able to be made on a qualitative basis because the FEM models were not constructed to enable model coupling with the air, which has a great effect on the vibratory motion of the instrument (§2.5). The effects of brace scalloping were modelled (§4.3), agreeing with experiments showing that scalloping decreases the Q-value of resonances of the brace and slightly lowers the resonant frequencies. The data collected on these three instruments might be used in a more advanced simulation of the guitar.

The problem of describing the timbre of guitar sounds. Finally, a lexicon of terms for the timbre of guitar sounds was constructed by sampling a number of terms from the literature and surveying a group of people to get the most useful descriptors arising (§8.2). A positive correlation was found between the frequency of descriptors found in the literature and the mean responses from the survey. The timbre of these guitar sounds appeared to be able to be determined by using three to four parameters (§8.4). An obvious extension of this work is to apply this method to other instruments to generate a more general description of musical timbre. This would provide a basis for investigating the effect that changes to the design of the guitar have on the timbre of the instrument, and thus provide measurable parameters to optimise, thereby improving the instrument. Considering the extent of the characterisation of the the properties of the guitars studied in this project, it would be advantageous to perform psychoacoustic listening tests on the instruments. The work performed in Chapter 8 provides necessary background in order to make such tests more meaningful.

Appendix A

Some derivations and measurements

A.1 The Helmholtz resonator

Consider a container with rigid walls, enclosing a relatively large volume of air, V, and a cylindrical throat with length l, of small ($S \ll \pi l^2$) constant cross-sectional area S. Assuming the wavelength is much longer than the largest single dimension of the container so that the pressure distribution is effectively uniform. Knowing the density, ρ, and speed of sound, c, in air, the mass-acceleration for the air in the throat may be expressed as:

$$lS\rho\ddot{\xi} \qquad\qquad (\text{A.1.1})$$

where ξ is the time dependent displacement of the air in the throat of the container and the Newtonian dot notation, $\dot{\xi}$ and $\ddot{\xi}$, represent the time derivative and the second time derivative of the displacement of the air from the equilibrium position.

The air inside forms a 'spring', with a restoring force of:

$$\frac{c^2 \rho \xi S^2}{V} \tag{A.1.2}$$

where the angular frequency, ω is related to the frequency, f, by $\omega = 2\pi f$

Approximating the damping as viscous, the frictional force may be expressed as:

$$\frac{\rho \omega k}{2\pi} S^2 \dot{\xi} \tag{A.1.3}$$

where the wavenumber, k, is related to the wavelength, λ, by $k = \frac{2\pi}{\lambda}$ and the speed of sound in air may be expressed as $c = f\lambda = \frac{\omega}{k}$.

Adding equations A.1.1, A.1.2 and A.1.3, the time dependent force equation due to an external force is:

$$lS\rho\ddot{\xi} + \frac{\rho \omega k}{2\pi} S^2 \dot{\xi} + \frac{c^2 \rho \xi S^2}{V} = SPe^{\hat{j}\omega t} \tag{A.1.4}$$

The forcing function on the right hand side of Equation A.1.4 is composed of the pressure amplitude, P, and a time-varying complex exponential ($e = 2.718...$ and $\hat{j}^2 = -1$) with angular frequency, ω and time, t.

Substitution of the volume displacement, $X = S\xi$, makes algebraic manipulation more convenient [Wood, 1940]. Then $\dot{X} = S\dot{\xi}$ and $\ddot{X} = S\ddot{\xi}$ and Equation A.1.4 may be re-expressed:

$$lS\rho\ddot{X} + \frac{\rho \omega k}{2\pi} S^2 \dot{X} + \rho S = \frac{c^2 \rho X S^2}{V} = SPe^{\hat{j}\omega t} \tag{A.1.5}$$

which is analogous to an oscillatory electrical circuit.

$$\dot{X} = \frac{Pe^{\hat{\jmath}\omega t}}{\frac{\rho\omega k}{2\pi} + \hat{\jmath}(\frac{\rho\omega l}{S} - \frac{\rho c^2}{V\omega})} \tag{A.1.6}$$

Using this analogy an acoustic impedance, Z_A, may be defined as the ratio of the sound pressure at the source to the rate of change of volume displacement of the surface of the source:

$$Z_A = \frac{Pe^{\hat{\jmath}\omega t}}{\dot{X}} = \frac{Pe^{\hat{\jmath}\omega t}}{S\dot{\xi}} = \frac{\rho\omega k}{2\pi} + \hat{\jmath}(\frac{\rho\omega l}{S} - \frac{\rho c^2}{V\omega}) \tag{A.1.7}$$

The *acoustic resistance* is the real component:

$$R_A \equiv \mathbb{R}(Z_A) = \frac{\rho\omega k}{2\pi} \tag{A.1.8}$$

and the *acoustic reactance* is the imaginary component:

$$\mathbb{I}(Z_A) = \frac{\rho\omega l}{S} - \frac{\rho c^2}{V\omega} \tag{A.1.9}$$

Where the term $\frac{\rho\omega l}{S}$ is the *mass reactance* and the term $\frac{\rho c^2}{V\omega}$ is known as the *stiffness reactance*. The frequency of resonance of the system is where the reactance becomes zero. Defining the frequency where this occurs as $\omega = \omega_H$:

$$\frac{\rho\omega_H l}{S} = \frac{\rho c^2}{V\omega_H} \tag{A.1.10}$$

So:

$$\omega_H = c\sqrt{\frac{S}{Vl}} \tag{A.1.11}$$

Or:

$$\frac{\omega_H}{2\pi} = f_H = \frac{c}{2\pi}\sqrt{\frac{S}{Vl}} \tag{A.1.12}$$

Volume	$2.920 \pm 0.005 \times 10^{-3}$ m^3
Throat length	80 ± 1 mm
Throat diameter:	32.5 ± 0.1 mm
Throat cross-section	$8.30 \pm 0.05 \times 10^{-4}$ m^2
Calculated f_0 (no length correction)	102.9 ± 0.1 Hz
Calculated f_0 (length correction at both ends)	92.1 ± 0.1Hz

Table A.1: Data from a simple Helmholtz resonator. Excitation is a simple pressure impulse. Calculation of f_0 assumes $c = 343$ ms^{-1}. End corrections are made assuming circular unflanged pipe at both ends.

Thus the Helmholtz frequency is determined by the speed of sound in air and basic geometric properties of the resonator.

Simple experiment validating effective length due to an end correction

Data from an experiment conducted on a simple Helmholtz resonator are given in Table A.1. The frequencies calculated differ strongly between corrected and uncorrected values. The length correction was obtained from the assumption of a circular unflanged pipe at each ends, so $l_* = 2 \times 0.6133R$ [Levine and Schwinger, 1948]. The Fourier transform of the pressure response in the experiment is shown in Figure A.1, where the frequency of the main peak, associated with the Helmholtz resonance, was found to be 92.2 ± 0.7 Hz.
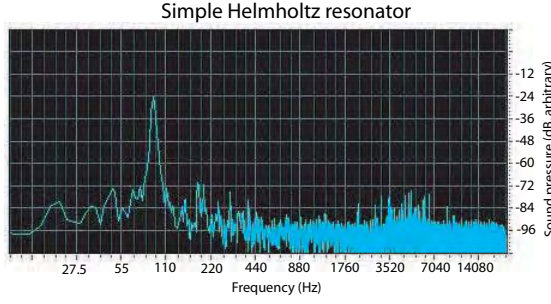
Figure A.1: Fourier transform of sound pressure response of an experiment on a simple Helmholtz resonator. Note the peak at 92 Hz.

A.2 Soundboard-air cavity coupling parameters

This treatment is largely a summary of [Christensen and Vistisen, 1980] and [Caldersmith, 1978]. Consider the uncoupled elements. Assuming no air loading or coupling, a simple vibrating plate of mass m_p, and effective stiffness K_{p*}, has a resonance frequency:

$$f_{p,0} = \frac{1}{2\pi}\sqrt{\frac{K_{p*}}{m_p}} \tag{A.2.1}$$

Now consider the soundboard as if it had negligible stiffness and an effective area A_{p*} enclosing the internal air cavity. The resonant frequency of this air may be expressed:

$$f_a = \frac{1}{2\pi}\sqrt{\frac{\mu A_{p*}^2}{m_p}} \tag{A.2.2}$$

Where $\mu \equiv \frac{\rho c^2}{V}$. The natural frequency of the soundboard loaded by the air in the cavity volume is then given by:

$$f_p = \frac{1}{2\pi} \sqrt{\frac{K_{p*} + \mu A_{p*}^2}{m_p}} \qquad\qquad (A.2.3)$$

or, alternatively:

$$f_p^2 = f_{p,0}^2 + f_a^2 \qquad\qquad (A.2.4)$$

The finite stiffness of the soundboard causes the total volume and losses of the cavity to deviate from the uncoupled state as a function of time. Assuming the associated fluctuations in each vibratory cycle to be adiabatic, the cavity is subject to a pressure change of $\Delta p = -\mu \Delta V$. The resulting force exerted on the two oscillators is then $A_{p*}\Delta p$ on the soundboard and $S\Delta p$ on the air in the soundhole. Assuming viscous damping associated with the motions of each oscillator (R_p and R_V) and, defining the driving force on the soundboard as F, the coupled equations of motion for the two oscillators are:

$$
\begin{aligned}
m_p \ddot{x}_p &= F - K_p x_p - R_p \dot{x}_p + A_{p*}\Delta p \qquad\qquad (A.2.5)\\
m_h \ddot{X}_h &= S\Delta p - R_h \dot{X}_h
\end{aligned}
$$

Where x_p is the net displacement of the soundboard from the equilibrium position, X_h is the net volume displacement of the air in the soundhole from equilibrium, and $m_h = \rho S l_*$ is the mass of air in the soundhole. If the soundboard is constrained from moving ($x_p = 0$) the frequency of the air in the soundhole is

$$f_h = \frac{1}{2\pi} \sqrt{\frac{\mu S^2}{m_h}} \qquad\qquad (A.2.6)$$

whereby the familiar expression for the Helmholtz frequency (Equation A.1.12) may be obtained.

For a sinusoidally time-varying force, $F :\to F_0 e^{\hat{\jmath}\omega t}$ and taking the loss parameters $\gamma_p \equiv \frac{R_p}{m_p}$ and $\gamma_a \equiv \frac{R_a}{m_a}$, the velocity of the soundboard is:

$$v_p = \hat{\jmath}\omega \frac{F_0}{m_p}[\frac{\omega_h^2 - \omega^2 + \hat{\jmath}\omega\gamma_p}{D}] \tag{A.2.7}$$

Similarly, the velocity function of the air in the soundhole is:

$$v_h = \frac{-\hat{\jmath}\omega F_0}{m_p} \frac{A_{p*}}{S}[\frac{\omega_h^2}{D}] \tag{A.2.8}$$

Where the denominator, D, is:

$$D = (\omega_p^2 - \omega^2 + \hat{\jmath}\omega\gamma_p)(\omega_h^2 - \omega^2 + \hat{\jmath}\omega\gamma_h) - \omega_{pH}^2 \tag{A.2.9}$$

The coupling frequency f_{pH}, is then given by:

$$f_{pH}^4 = \frac{1}{(2\pi)^4} \frac{\alpha^2}{m_p m_a} = f_H^2 f_a^2 \tag{A.2.10}$$

Resonances in the velocity functions occur when $D = 0$. Solving the quadratic in Equation A.2.9 yields the solution:

$$f_{\pm}^2 = \frac{1}{2}(f_p^2 + f_h^2) \pm \frac{1}{2}\sqrt{(f_p^2 - f_h^2)^2 + 4f_{pH}^4} \tag{A.2.11}$$

And hence [Christensen and Vistisen, 1980]:

$$f_p^2 + f_H^2 = f_+^2 + f_-^2 \tag{A.2.12}$$

This is a special case of the more general result of coupled oscillatory systems, where the quadrature sum of the uncoupled oscillator frequencies is the same as that for the coupled oscillators [Christensen and Vistisen, 1980].

A.3 Two mass model for a cantilever beam driven at the base

Consider the motion of a cantilever beam held by a clamp that is applying a sinusoidally varying force to the base, in a direction perpendicular to the longitudinal axis of the beam. The model of two coupled oscillators may be applied thus [Harjono, 1998]: take the mass of the beam to be M, the displacement of the free end (from equilibrium) as x_2, the mass of the clamp system as m and its displacement (also from equilibrium) as x_1, the effective stiffness of the entire system, k, and the viscous damping (of the system) to be R. The equation of motion for the beam is then:

$$-M\omega^2 x_2 + (k + \hat{\jmath}\omega R)(x_2 - x_1) = 0 \tag{A.3.1}$$

and that for the clamp:

$$-m\omega^2 x_1 + (k + \hat{\jmath}\omega R)(x_1 - x_2) = F(\omega) \tag{A.3.2}$$

and by noting that, because, $\ddot{x}_1 = -\omega^2 x_1$,

$$x_2 = x_1 \frac{\hat{\jmath}\omega R + k}{-M\omega^2 + k + \hat{\jmath}\omega R} \tag{A.3.3}$$

The force resulting from the clamp acceleration is then:

$$F(\omega) = x_1[-m\omega^2 + (k + \hat{\jmath}\omega R)(1 - \frac{k + \hat{\jmath}\omega R}{-M\omega^2 + k + \hat{\jmath}\omega R})] \qquad \text{(A.3.4)}$$

$$= x_1[-m\omega^2 + (k + \hat{\jmath}\omega R)(\frac{-M\omega^2}{-M\omega^2 + k + \hat{\jmath}\omega R})] \qquad \text{(A.3.5)}$$

$$\qquad \text{(A.3.6)}$$

And therefore the dynamic mass of the beam is then:

$$\frac{F(\omega)}{\ddot{x}_1(\omega)} = \frac{-1}{\omega^2}[-m\omega^2 + (k + \hat{\jmath}\omega R)(\frac{-M\omega^2}{-M\omega^2 + k + \hat{\jmath}\omega R})] \qquad \text{(A.3.7)}$$

$$= m + \frac{M(k + \hat{\jmath}\omega R)}{-M\omega^2 + k + \hat{\jmath}\omega R} \qquad \text{(A.3.8)}$$

A.3.1 Change in frequency of bending mode of a profiled beam

Rectangular cross-section

To find the second moment of area (*i.e.*moment of inertia) about a neutral bending axis, it is necessary to find the centre of mass about the given axis. Considering only the y component, the centre of mass for a rectangular cross-section of width b and height a (Figure A.2) is:

$$y_{CM} = \frac{1}{M} \int_{y=0}^{a} y dm \qquad \text{(A.3.9)}$$

Now

$$m(y) = M\frac{y}{a}$$
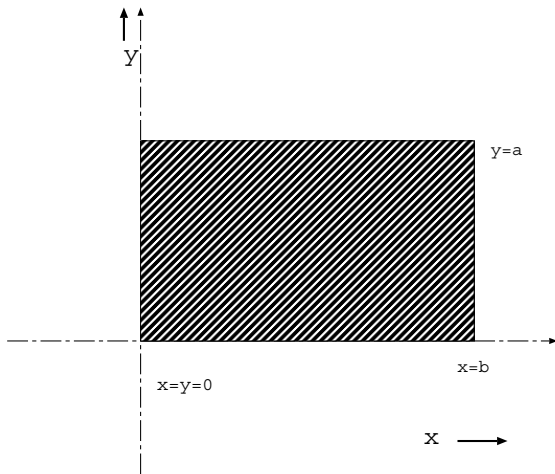
Figure A.2: Beam with rectangular cross-section

so:

$$\frac{dm}{dy} = \frac{M}{a} \tag{A.3.10}$$

therefore:

$$y_{CM} = \frac{1}{M} \int_{y=0}^{a} y\frac{M}{a}dy$$

$\Rightarrow$

$$y_{CM} = \frac{1}{a}\Big[\frac{y^2}{2}\Big]_0^a = \frac{a}{2}$$

similarly,

$$x_{CM} = \frac{b}{2}$$

The moment of inertia, defined as

$$I = \int_{r=0}^{R} r^2 dm \tag{A.3.11}$$

and using Equation A.3.10 gives:

$$
\begin{aligned}
I_T &= \frac{M}{a} \int_{y=0}^{a} y^2 dy \\
&= \frac{M}{a} \int_{y=0}^{a} y^2 dy \\
&= \frac{M}{a} [\frac{y^3}{3}]_{y=0}^{a}
\end{aligned}
$$

So:

$$
I_T = \frac{Ma^2}{3}
$$

The parallel axis theorem (Equation A.3.12)

$$
I_T = I_{CM} + Md^2 \tag{A.3.12}
$$

gives the total moment of inertia I_T, at some point a distance d from the axial point passing through some point with a parallel axis of bending. Yet

$$
d^2 = y_{CM}^2 = \frac{a^2}{4}
$$

so:

$$
I_{CM} = I_T - Md^2 = \frac{Ma^2}{3} - \frac{Ma^2}{4} = Ma^2 \left(\frac{4-3}{12} \right)
$$

Where I_{CM} is the moment of inertia at the centre of mass, and M the total mass of the beam.

Hence:

$$
I_{CM} = \frac{Ma^2}{12} \tag{A.3.13}
$$

Triangular cross-section

For an isosceles triangle, height h and width b (Figure A.3)

$$m(y) = M \frac{\text{area from } y = 0 \text{ to } y}{\text{total area}}$$

$$= M \frac{y(\frac{b}{2} + \frac{b(h-y)}{2h})}{\frac{bh}{2}}$$

$$= M \frac{y(2 - \frac{y}{h})}{h}$$

ie: $m(y) = M \frac{y(2h-y)}{h^2}$

$$\Rightarrow \frac{dm}{dy} = M \frac{2(h-y)}{h^2} \tag{A.3.14}$$

And thus:

$$I_T = \int_{y=0}^{h} y^2 \frac{2m}{h^2}(h-y)dy = \frac{2M}{h^2} \int_{y=0}^{h} (hy^2 - y^3)dy$$

$$= \frac{2M}{h^2} \left[\frac{hy^3}{3} - \frac{y^4}{4} \right]_{y=0}^{h} = \frac{Mh^2}{6}.$$

From Equation A.3.9, $y_{CM} = \frac{1}{M} \int_{y=0}^{h} y \, dm$

And, using Equation A.3.14,

$$y_{CM} = \frac{1}{M} \int_{y=0}^{h} \frac{2M}{h^2}(h-y)dy$$

$$= \frac{2}{h^2} \left[\frac{hy^2}{2} - \frac{y^3}{3} \right]_{y=0}^{h}$$

$$= \frac{2Mh^4}{h^2} \left[\frac{1}{3} - \frac{1}{4} \right] = \frac{h}{3}$$

The square of the distance from $y = 0$ to $y = \frac{h}{3}$ is $d^2 = \frac{h^2}{9}$

Hence, from Equation A.3.12:

$$I_{CM} = \frac{Mh^2}{6} - Md^2 = Mh^2(\frac{1}{6} - \frac{1}{9}) = Mh^2(\frac{3-2}{18})$$
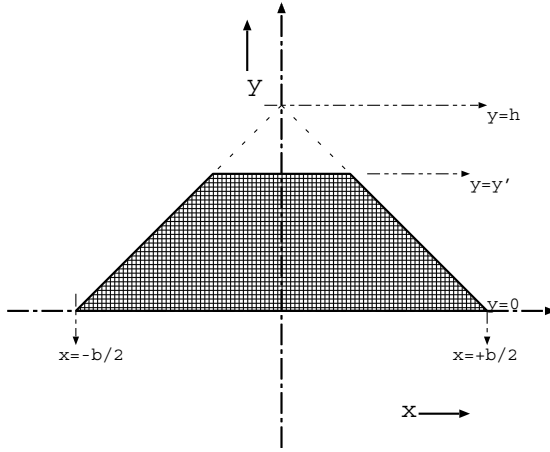
Figure A.3: Isosceles triangle, height h, base length b

Therefore:

$$I_{CM} = \frac{Mh^2}{18} \qquad (A.3.15)$$

Pentagonal cross-section, symmetric about x_{CM}

Often the cross-section of the key braces on the soundboard of the guitar are modified from a rectangular shape to that of an isoceles triangle atop a rectangle with the same width as the base of the triangle, as in Figure A.4.

For the triangular section,

$$y = \frac{h_2 - 2(h_2 - h_1)}{b} x \qquad (A.3.16)$$

so

$$m(y) = M \left(1 - \frac{\frac{b}{2} \frac{(h_2 - y)^2}{h_2 - h_1}}{\frac{b}{2}(h_2 + h_1)} \right) = M \left(1 - \frac{(h_2 - y)^2}{h_2^2 - h_1^2} \right) \qquad (A.3.17)$$
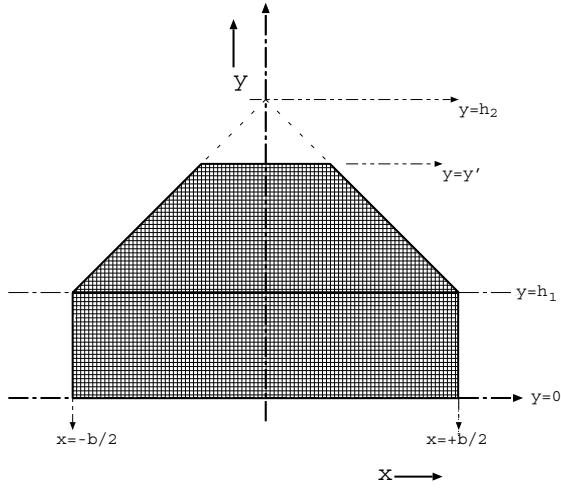
Figure A.4: Schematic of a beam with pentagonal cross-section, symmetric upon reflection about the centre of mass in the x-direction.

and thus

$$\frac{dm}{dy} = M\left(\frac{2(h_2 - y)}{h_2^2 - h_1^2}\right) \tag{A.3.18}$$

So

$$
\begin{aligned}
y_{CM} &= \frac{1}{M}\left(\int_{y=0}^{h_1} y\frac{2M}{h_1 + h_2}\cdot dy + \int_{y=h_1}^{h_2} y\frac{2M(h_2 - y)}{h_2^2 + h_1^2}\cdot dy\right) \tag{A.3.19}\\
&= \frac{h_1^2}{h_1 + h_2} + \frac{2h_1^3 + h_2^3 - 3h_1^2 h_2}{3(h_1^2 + h_2^2)}
\end{aligned}
$$

And, using Equation A.3.18,

$$
\begin{aligned}
\frac{I_y}{M} &= \int_{y=0}^{h_1} y^2\frac{2}{h_1 + h_2}\cdot dy + \int_{y=h_1}^{h_2} y^2\frac{2(h_2 - y)}{h_2^2 + h_1^2}\cdot dy \tag{A.3.20}\\
&= \left(\frac{2h_1^3}{3(h_1 + h_2)} + \frac{h_2^4 + 3h_1^4 - 4h_1^3 h_2}{6(h_1^2 + h_2^2)}\right)
\end{aligned}
$$

Using Equation A.3.12, the radius of gyration about the centre of mass is κ_{CM}:

$$\kappa_{CM}^2 \quad = \quad \frac{I_y}{M} - y_{CM}^2 \tag{A.3.21}$$

$$= \quad \frac{2h_1^3}{3(h_1 + h_2)} + \frac{3h_1^4 + h_2^4 - 4h_1^3 h_2}{6(h_1^2 + h_2^2)} - \left(\frac{h_1^2}{h_1 + h_2} + \frac{2h_1^3 + h_2^3 - 3h_1^2 h_2}{3(h_1^2 + h_2^2)} \right)^2$$

This unwieldy expression may be simplified by substitution of values for a brace with a profiled cross-section.

For slender homogeneous beams of constant cross-section with common boundary conditions, $f_i \propto \kappa$ (Equation 2.7.5). So the change in frequency of the normal bending modes of a beam, as a result of the profiling process from a brace (§3.4) with an original height of h_2 may be found thus:

$$\left(\frac{f_{\text{new}}}{f_{\text{old}}} \right)^2 = \frac{12}{h_2^2} \left(\frac{2h_1^3}{3(h_1 + h_2)} + \frac{h_2^4 + 3h_1^4 - 4h_1^3 h_2}{12(h_1^2 + h_2^2)} - \left(\frac{h_1^2}{h_1 + h_2} + \frac{2h_1^3 + h_2^3 - 3h_1^2 h_2}{3(h_1^2 + h_2^2)} \right)^2 \right)$$

$$\tag{A.3.22}$$

A.4 Measurements of dimensions of the guitar sound-boards

Overall widths of the guitar soundboards were measured at 35 mm intervals (Figure A.5).
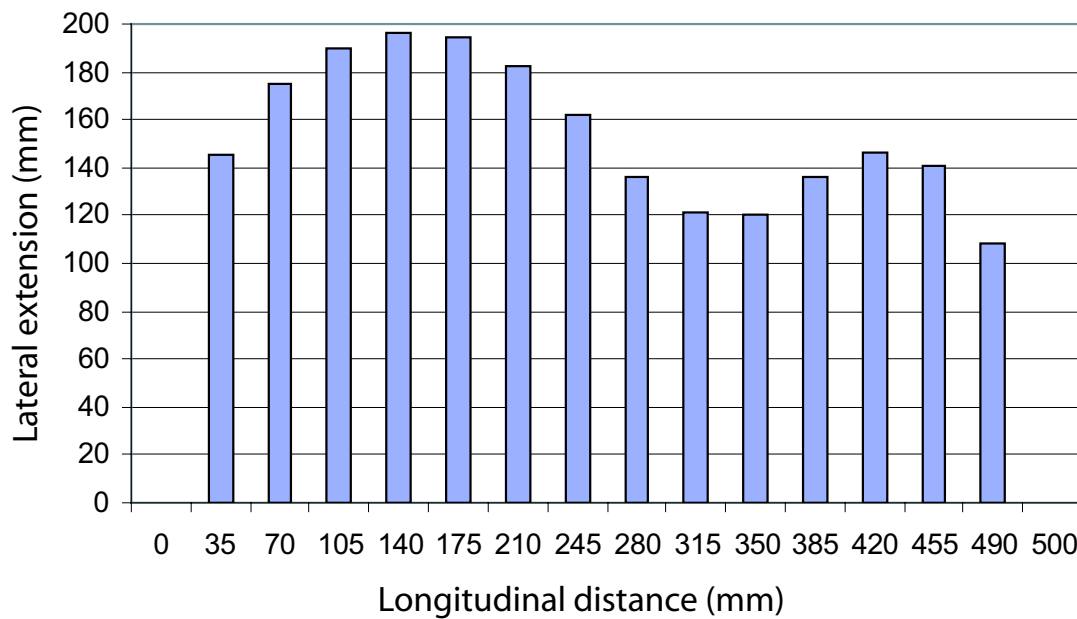
Figure A.5: Measurements of the lateral dimensions of the Sitka spruce guitar sound-board as a function of distance along the main axis of the guitar.

Appendix B

Vibratory data acquisition system (ACUZ)

"Fourier's Theorem is not only one of the most beautiful results of modern analysis, but it may be said to furnish an indispensable instrument in the treatment of nearly every recondite question in modern physics"—Lord W. T. Kelvin and P. G. Tait [Thomson and Tait, 1867]

B.1   Background

The measurements reported in this thesis are made using variants of 'ACUZ'[1], a system developed within the Music Acoustics Laboratory of The University of New South Wales for the rapid measurement of the frequency dependence of transfer functions. [Wolfe et al., 1995]. Although the system is most commonly used for the acoustic impedance spectroscopy of musical wind instruments, it is used here to measure the transfer functions of a range of linear vibro-acoustic systems.

---

[1]'ACoUstic Z', where Z represents the impedance to be measured
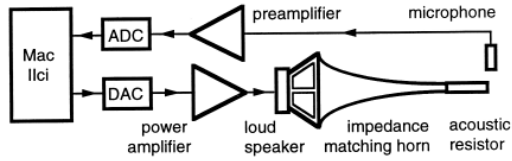
Figure B.1: The ACUZ system, as applied to wind instruments. From [Wolfe et al., 1995].

B.2   Design and operation

The version of ACUZ used is based on an Apple Mac IIci computer with a 16 bit analogue interface card (National Instruments NB-A2100).

The electrical stimulus is synthesised from a series of equally spaced frequency components covering the frequency range of interest - in most of these experiments they are spaced $\simeq 0.69$ Hz apart, covering the range $10 \rightarrow 1000$ Hz. (There is always a compromise between frequency resolution and signal to noise ratio: more frequency components produces improved frequency resolution, but the signal to noise ratio of each component is reduced).

The relative phase between the frequency components is adjusted to minimise the resultant maximum amplitude of the synthesised waveform. This improves the overall signal to noise ratio as the overall amplitude of all components can then be increased [Smith, 1995]. This is achieved by introducing random phase relationships between the Fourier components such that the maximum amplitude of the sum of the Fourier components is minimised with respect to that of any other attempted configuration (minimisation of the 'crest-factor'.) This process may be repeated and the best solution accepted by the user. The approach is similar to the Monte Carlo

method, except that the choice of the number of configuration attempts is left to the user. Consequently there are usually only a small number of configurations tried before a solution is accepted. It is possible to apply a numerical algorithm for this purpose [Guillaume et al., 1991, Shroeder, 1970] although this has not been implemented at this time.

If the system is linear (this is the case for vibratory modes of the guitar soundboard [Richardson, 1982]) the choice of signal averaging is possible, by repeating the output signal a number of times.

This electrical stimulus is then amplified and passed to an electromagnetic shaker (B& K 4809). The driving point dynamic masses are detected by a B& K 8001 impedance head with a stereo input line back to the computer. The pressure force ratio measurements are driven in the same way, and the force portion is also measured with the B& K 8001 impedance head, but the pressure response is measured using an Optimus tie-clip microphone.

Although presently a laboratory measurement tool, ACUZ was designed to be capable of industrial application in the workshop or factory.

Dynamic mass measurements

The dynamic mass is a measure of the frequency dependent effective mass ($\frac{\text{force}(\omega)}{\text{acceleration}(\omega)}$) of a system in response to vibratory excitation. In general the force and acceleration

may be measured at distinct points in space (the transfer function) but here the force and acceleration are made at identical positions and is known as the *driving point dynamic mass*.

Pressure force ratio measurements

Because the ultimate product of the acoustic guitar is the sound it produces, it would seem logical to measure some kind of pressure response of the instrument. Direct pressure measurements in response to some time-varying excitation at the bridge are sometimes difficult to apply in comparative tests, because the applied force at the bridge is variable and we would expect this to have a large effect on the output pressure. This issue is resolved if we examine the transfer function of a measured pressure response to the time-varying force applied to the bridge ($\frac{\text{pressure}(\omega)}{\text{force}(\omega)}$). Because of the complex geometry of acoustic radiation, the spatial position that pressure measurements are made is also important. I have chosen the centre of the soundhole, in the plane of the top of the soundboard, as a fixed point to measure the pressure response of the instrument.

The transfer functions of the pressure measured at the soundhole to the force applied to the bridge gives some indication of the magnitude of pressure arising from a particular force applied and may be more useful in the sense that we can measure the resulting sound pressure output due to a known applied force at the bridge. This quantity may also be used to calculate an effective area, $A_{\text{eff.}}(\omega) = \frac{\text{force}(\omega)}{\text{pressure}(\omega)}$. This effective area must not be interpreted directly as a geometric area of the soundboard, but as relating to the effective area of a simple piston source of radiation. The ratio

of this effective area to the effective mass, $\frac{A_{\text{eff.}}}{M_{\text{eff.}}}$ is proportional to the total output pressure of the guitar, assuming it is a simple, uncoupled, source of radiation as in Equation B.2.1 from [Christensen and Vistisen, 1980] and developed in [Wright, 1996].

$$p(\omega) = F(\omega)\frac{A_{\text{eff.}}}{M_{\text{eff.}}}\frac{\omega^2}{(\omega_0^2 - \omega^2) - \hat{\jmath}\gamma\omega} \tag{B.2.1}$$

Where γ represents the losses of the simple radiator.

B.3 Impedance spectroscopy

Interpretation of impedance spectra (or transfer functions) can be difficult because of the great volume of data usually received. As with any other branch of experimental physics, it is important to minimise the information recieved while retaining the important features. In the case of vibratory measurements, often the means of mechanically support has an influence on the measured spectra, and interpretation must be made with this in mind.

Appendix C

Alternative methods of measuring mechanical properties of wood

"Every piece of wood will have a unique set of vibrational properties because it has a unique set of elastic moduli and damping rates, even if cut from the same log"
—Graham Caldersmith [Caldersmith and Freeman, 1990]

There are viable alternatives to the technique used to measure the Young's modulus of a wooden beam, in §5.2. For example, by exciting a wooden beam, simply supported at the nodes of the mode of interest, through the attachment of a small permanent magnet to the beam, in close proximity to a mechanically fixed solenoid, driven by a signal generator, it is possible to measure the free-free vibrations of the beam. Impulse excitation may also be used, and this is in fact applied widely by luthiers as the primary selection method for musical instrument woods (as the 'tap-tone' method, §3.4). The methods that I developed in the following are not only useful as a comparison to the clamping method, but also may be of use to a luthier in accurate material selection.

A: Optoelectronic detection

Similar tests on the normal modes of vibration of a wooden beam may be achieved, using a different excitation, support, and detection system to that used in §5.2. Figure C.1 shows the set-up for measuring the normal modes of a beam, simply supported by two foam-rubber triangular prisms. The beam is simply supported at 22.4% of the total length from each end, giving a good approximation to free-free boundary conditions at the lowest normal mode. This is where the two nodes of the fundamental of the free-free beam would occur, thereby minimising mechanical interference effects due to the support system. A small permanent rare-earth magnet (A NdFeB cylinder 3 mm high and 6 mm in diameter, with mass 1.3 g and a surface field strength of $\simeq 200$ mT) was attached to the underside of the centre of the brace, using double-sided tape, and a small square (5 mm $\times$ 5 mm) of silvered mica was affixed to the top. The apparatus used to excite the beam was an air-core solenoid (inductance: 170 mH, resistance: 0.53 Ω) driven by an amplified signal generator, placed about 5 mm directly below the rare-earth magnet. The optoelectronic detection system comprised a 10 mW HeNe laser ($\lambda = 633$ nm) incident on the mica sheet and a position sensing device (UDT Sensors, Inc. SLS5-1 duo-lateral super-linear PSD (one-dimensional series)) was placed in the path of the reflected light, aligned so that when the beam flexed, the reflected light would move along the sensing axis of the detector. The output voltage of the detector is analysed using an oscilloscope (Kenwood 20 MHz CS-1021).

This detection system is essentially a crude laser vibrometer.
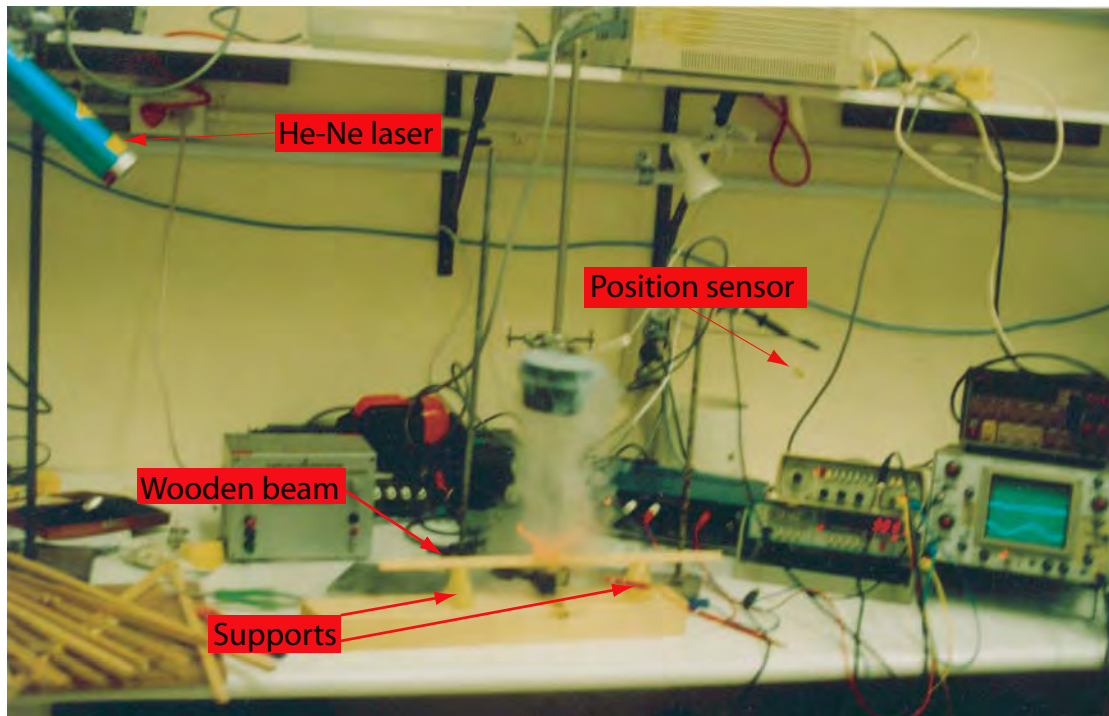
Figure C.1: Set up for measuring the normal modes of a simply supported wooden beam. Excitation is electromechanical and detection is optoelectronic. Water vapour (from evaporating liquid nitrogen) is used in to illustrate the path of the laser beam for illustrative purposes and is not used in actual measurement.

Mass loading of the braces, by adding another magnet of the same mass to the original, did little to alter the frequency or amplitude of the normal modes, although this method is extremely sensitive to manner of beam support, and it is likely that better results may be obtained by using more rigid supports than those used here.

B: 'Tap-tone' method

The 'tap-tone' method is able to be carried out with a minimum of equipment, and it is likely this has been used in wood selection by luthiers for hundreds of years [Hutchins, 1999, Bissinger, 2001]. A wooden beam is held vertically at a nodal position for the fundamental free-free mode (for a beam of constant cross-section this is about 22.4% of the total length from each end) between finger and thumb and impulse excitation is achieved through impact. This is essentially the traditional method presented in §3.4 although objective measurement of the pressure response of the impact is recorded through a microphone fixed on a stand, approximately 15 mm from the centre of the beam, onto Digital Audio Tape. This is then transferred to a computer and a fast Fourier transform is taken to obtain the frequency and damping of the fundamental mode. The impact is achieved by striking the beam lightly in the centre with a small hand-held brass rod. This rod was used, as opposed to a luthier's traditional striking tool (a bare knuckle), to improve reproducibility of the applied force and striking point. The microphone was also positioned at the end of the beam to compare height and width modes.

Although the human hearing system is well known for its sophisticated sensing capabilities, sensitive to small relative variations in frequency and amplitude [Helmholtz, 1885], much additional information can be provided by tactile feedback though the fingers, especially with regards to mechanical damping. This provides vital information on bulk defects such as grain irregularities (§3.2), which tend to produce undesirable vibratory, acoustic and æsthetic properties.

Table C.1 shows the results of listening tests using a reference tone through the

Strut	Profiled	Fundamental frequency (Hz)	
		Height	Width
1A	yes, complicated	245	171.0
2A	yes (cracked grain)	304.5	182.75
3A	yes	-	-
4A	yes	301	182.25
5A	no	179.5	109.0
6A	yes, fully	265.3	161.5
1B	no	189	110.0
2B	yes	318	202.5
3B	yes	173	108.0
4B	yes	278	198.0
5B	no	190	116.0
6B	no	188	116.0
7B	yes, asymm	-	-
1C	yes	322.75	197.25
2C	yes	195	308.5
3C	yes	323.75	198.75
4C	no	189	110.5
5C	no	191	111.0
6C	yes	169.5	103.0
7C	yes	323.5	204.25
		± 0.25Hz	

Table C.1: Fundamental frequencies of wooden beams using a variant of the 'tap-tone' method

right channel in a set of stereo headphones and playing the recorded tap tone in the left channel.

Appendix D

Soundboard thickness measurement device

"What soundboard thickness does he work to? He gestured with his thumb meeting his index finger raised to eye level, squinting slightly and rubbing them as if feeling an imaginary soundboard. 'I prefer to use these rather than a caliper. It does not really interest me what the measurement is.'...clearly, he finds that he can dimension his guitar plates better without a micrometer, because he believes only the fingers can ask all the necessary questions of a piece of wood"—William Cumpiano, interviewing Manuel Velázquez [Cumpiano, 1982]

D.1   Outline of soundboard thickness problem

The practice of thinning the soundboard of high quality guitars has been discussed in §3.4. The shape of the guitar body makes it extremely difficult to introduce a traditional mechanical gaging device such as a rule, callipers, or a spring-loaded thickness gage. The soundhole is generally less than 100 mm in diameter, reducing
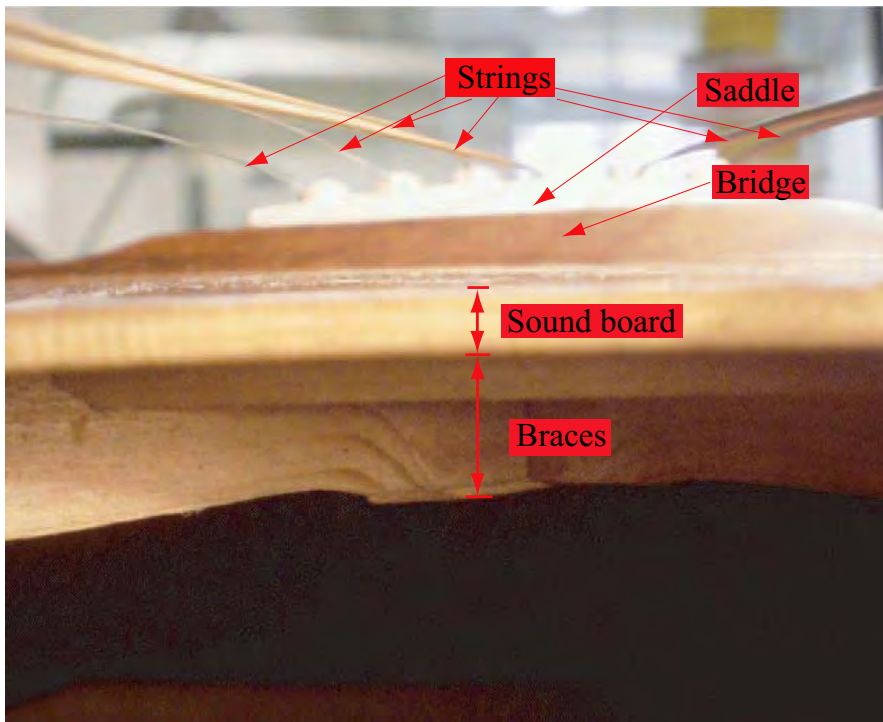
Figure D.1: The soundboard as viewed from within the soundhole, looking toward the bridge. Observe that the intervening braces are much thicker than the soundboard itself.

access or mobility of such devices. Even if this were overcome, the device in question would have to navigate the complicated geometry of the wooden braces on the soundboard (Figure D.1) which can be more than four times the thickness of the actual soundboard.

Possible mechanisms to measure thicknesses in woods

Vibro-acoustic

Ultrasonic methods are commonly used for nondestructive thickness measurements [McMaster, 1959]. This can include pulse return time (time-of-flight) or standing wave methods. The disadvantages of using ultrasonic pulses to determine the elastic properties of wood are discussed in §3.2. These disadvantages, such as grain layer scattering, dependence on moisture content, and frequency dependence also make accurate thickness determination difficult.

Nuclear radiation

For most matter, we are able to apply Equation D.1.1 and calibrate the reduction in transmitted intensity I of some specific type of nuclear radiation through a thickness, x, of material with a characteristic linear absorption coefficient μ.

$$I = I_o e^{-\mu x} \tag{D.1.1}$$

Generally, μ is dependent on the kinetic energy as well as the type of radiation used (*viz.* α, β, γ or $^1_0 n$)

Because α-particles are strongly ionising, they interact very strongly with normal matter and as a consequence do not tend to penetrate more than a few millimetres at any energy. For γ and β radiation, the linear absorption coefficient varies directly with both moisture content and density and inversely with energy, although the difference in the magnitude of μ for the two types of radiation mean that wood is virtually opaque for even very thin specimens of wood (For 0.047 MeV

γ, $\mu_\gamma = 0.65 \rightarrow 1.1$ mm^{-1} [density range $330 \rightarrow 620$ kg $\cdot$ m^{-3}], compared to β energies of 0.5 MeV, giving $\mu_\beta \simeq 30$ mm^{-1}). Because neutrons interact very strongly with hydrogen, the transmission of lower energy particles are dependent on moisture content. Higher energy neutrons enable nondestructive analysis of trace elements in the wood by analysing radioisotope production [Forest Products Laboratory, 1999].

Therefore, although useful for other purposes, the use of radioactive sources to determine wood thickness is problematic at best. Aside from the issues of safety and social stigma, this method suffers considerably from the fact that obtaining radioactive sources is probably difficult for most luthiers.

Magnetic fields

Because most non-ferromagnetic materials, including wood, have a relative permeability close to one (*i.e.* $\mu_R \simeq 1$) [American Institute of Physics, 1972], it is possible to insert wood into a magnetic field without noticeably altering the flux geometry. If a source provides a magnetic field with suitable geometry, such as one with monotonically decreasing flux density with distance, it is possible to determine the distance from the source by measuring the flux density. Wood that is entered into this field will not affect the intensity or geometry of the measured magnetic field.

D.2 The Hall effect

The effect of an external magnetic field, with flux density $\mathbf{B}$, applied to a charge of magnitude q, moving with velocity $\mathbf{v}$, is to exert a force $\mathbf{F}$ according to Equation

D.2.1.

$$\mathbf{F} = q\mathbf{v} \times \mathbf{B} \tag{D.2.1}$$

This applies to free charges as well as those moving in the environment of an electrical conductor. If we arrange a steady rate of charge flow at right angles to the external magnetic field then the force on the charges will be in a direction orthogonal to both the direction of charge flow and the direction of the applied magnetic field. Thus, for a flow of electrons in a conductor of a finite size, charges will tend to accumulate on one side of the conductor. The separation of charges produces an electric field $\mathbf{E} = \frac{\mathbf{F}}{q}$ in the direction of the electron accumulation. The resulting potential difference across the conductor is known as a *Hall voltage*, V_H in Equation D.2.2.

$$V_H = |\mathbf{v}| \cdot |\mathbf{B}| \tag{D.2.2}$$

This phenomenon is known as the *Hall effect*, after investigation into this in 1879 by the then 24 year old graduate student, Edwin H. Hall.

A useful application of this effect involves measurement of the Hall voltage in response to an unknown magnetic field. By knowing the carrier density and the dimensions of the element used as a *Hall probe*, calibration of the probe provides a sensitive and accurate means of measuring a magnetic field. The prevalence of modern electronic integrated circuit technology has enabled Hall probes to be made compact and cheap. Consequently there have been many useful applications, from

automobile velocimeters to liquid level sensors [Micronas Semiconductor Holding AG, 2004].

Choice of magnetic field source

For a permanent cylindrical magnet, the flux density decreases monotonically with distance from the source along the cylindrical axis, so we may calibrate the magnetic field strength to determine the distance from the source in this direction. Ferromagnetic materials are able to hold a bulk net magnetisation due to the formation of *magnetic domains* on the crystal scale in response to an externally applied magnetic field. This magnetisation is stable if the members of the crystal lattice are free to align with the external field and this freedom is then restricted. This is usually performed thermodynamically. The crystal is heated above a critical temperature where the magnetic phase transition occurs (known as the *Curie temperature*) and then cooled quickly (*quenched*) so that the magnetic field configuration is 'frozen'. This may also be performed mechanically, as is found when a wood chisel is able to align with the Earth's magnetic field upon continual impact. The long-lived stability of this magnetic field leads to the term 'permanent' magnet, although the magnetic field is hardly permanent if the magnet is raised above the Curie temperature without an externally applied magnetic field.

Modern research into material properties and manufacturing techniques have led to the availability of cheap and very strong permanent magnets. These so-called

'rare-earth' magnets also rely on the properties of crystalline ferromagnetic materials, but supplement the iron lattice with the addition of elements from the lanthanide series. The strong net magnetic moment of individual lanthanide atoms greatly increases the coercivity of the material and thus is able to maintain a permanent magnetic field strength many orders of magnitude above that achievable by ferromagnetic materials alone.

Magnetic field distribution around a finite solid

The spatial distribution of the magnetic field strength surrounding permanent magnets in the shape of finite solids, even for relatively simple geometries, is more complicated to calculate than many elementary treatments might imply. A permanent magnet in the shape of a cylinder is not a pure magnetic dipole. Especially in the case where the diameter is of a similar size to the height of the cylinder, **end effects are not negligible**.

If we take a permanent magnet with the geometry as in Figure D.2 we may get the magnetic field strength along the axis of the magnet (*ie* parallel to the polarisation of the magnetic field) as a function of the distance from the surface as in Equation D.2.3.

$$B = \frac{B_r}{2}\left[\frac{(x + h)}{\sqrt{R^2 + (x + h)^2}} - \frac{x}{\sqrt{R^2 + x^2}}\right] \tag{D.2.3}$$

(For $R = 3.0$ mm and $h = 3.0$ mm)
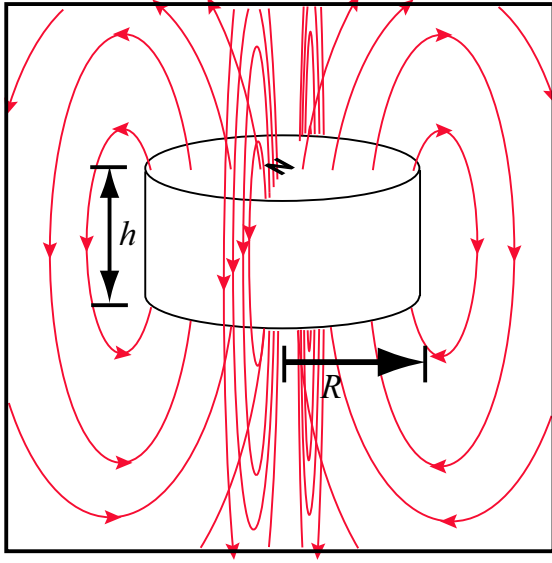
Figure D.2: Magnetic field around a finite cylindrical permanent magnet, of height h and radius R.

Also:

$$F \simeq 0.577B^2A \qquad (D.2.4)$$

D.3 Measurements of soundboard thinning

[Rodgers, 1990][Krüger, 1982][Stetson, 1977][Burkhardt and Fisher, 2002][Schleske, 2002] The soundboard thinning process occurs after the soundboard is attached to the back and sides. Because glueing of the soundboard to the sides is a difficult and risky procedure to reverse, measurements of the mass reduction effects of thinning each soundboard, such as in Table D.1, are taken of the guitar body *in toto* even though it is only from the soundboard that material is removed.

Soundboard	Sitka spruce	Engelmann spruce	Western Red cedar
Initial thickness (mm)	3.2	3.2	3.2
Body mass, before (kg)	1.3035	1.2312	1.2530
Body mass, after (kg)	1.2836	1.2241	1.2448
Mass loss (g)	19.9	7.1	8.2
Mass loss (%)	1.52	0.58	0.65
Initial soundboard mass (kg)	0.3067	0.2763	0.2493

Table D.1: Soundboard mass reduction due to thicknessing. Note that the mass change measurements are made on the guitar bodies, not the soundboards.
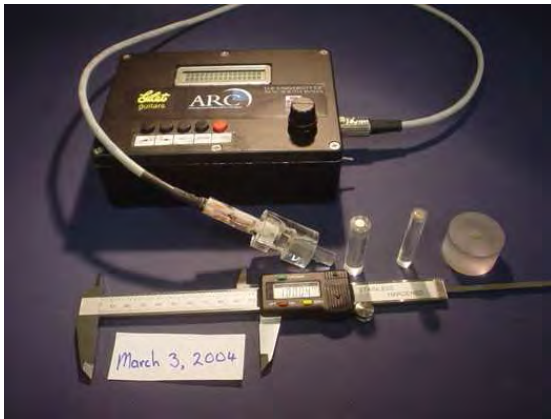
Figure D.3: A version of the Hall Effect thickness measurement device designed to measure thickness changes in guitar soundboards

D.4   The device

A diagram giving the conceptual layout of the device is given in Figure D.4. A version of the thickness device using the principles exemplified above is illustrated in Figure D.3.
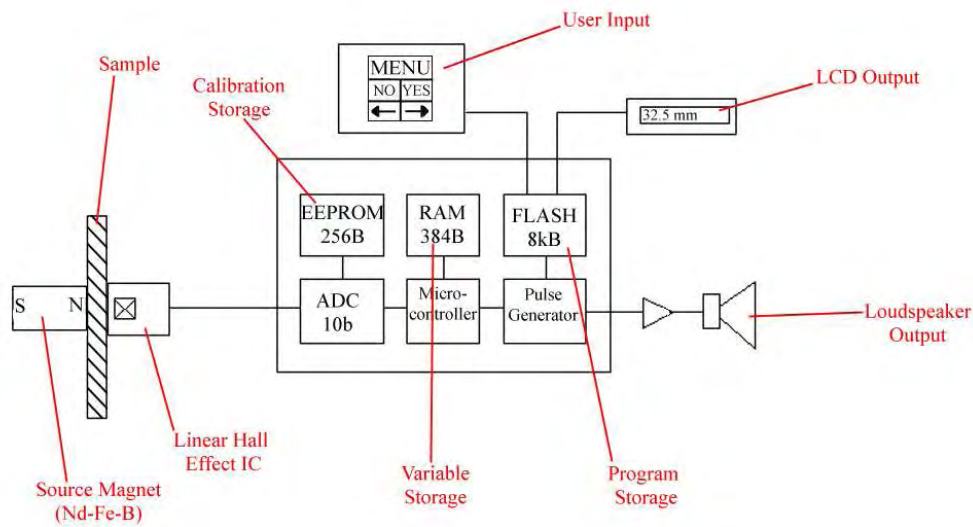
Figure D.4: Schematic of Hall effect thickness device

D.5   Methodology and usage

Initial tests

An acrylic (Polymethyl-methacrylate (PMMA)/Perspex™) plate has holes drilled in a grid formation such that the rare-earth source magnet may be inserted into each grid-point. The plate is placed flat on the guitar soundboard and the source magnet is inserted into a grid-point. The 'Giletometer' is positioned on the other side of the soundboard, approximately opposite the source magnet. The output is examined for a local distance minimum and recorded. This enables a matrix of soundboard thicknesses to be made. This method was initially trialled on three pieces of flat spruce with arbitrary thickness. A comparison is made between this

probe and conventional vernier measurements in Table D.2. This initial trial is with eight separate magnets of similar length dimensions and field strengths to the single source.

Preliminary tests on the guitar

A new measurement device requires new measurement techniques. The complicated geometry of the guitar makes it hard to determine an internal point directly opposite any given point on the external surface of the soundboard. This problem of 'point location' is able to be solved magnetically if we use another magnet (the 'locating magnet') on one side of the soundboard to align the source magnet on the other surface. If the diameter of the locating magnet is similar to the source, and the mutual attraction is strong enough, the source magnet is forced into a position directly opposite the locating magnet. If the source magnet is then held in this position while the locating magnet is carefully replaced by the 'Giletometer', measurements of the thickness at this point may be made. In practice small perturbations are required to find the local minimum, but this method is quick, convenient, and accurate with a small amount of training. In making a thickness matrix of a guitar soundboard it is convenient to embed a locating magnet into an acrylic cylinder, having the same diameter as the 'Giletometer' probe, and to use a plate with holes of this diameter arranged in a grid. The grid used here is illustrated in Figure D.5.

The spacing of each grid-point is 30 mm, small enough to detect some possible thickness variation yet large enough to cover the entire soundboard in less than one hour. Measurements of wood dimensions made with uncontrolled humidity should ideally be made over the shortest timescale possible. Because of the methods used

Position	Magnet	Distance (mm)		
		Probe	Callipers	Probe-Callipers
0	1	0.35	0.00	0.35
	2	0.20	0.00	0.20
	3	0.05	0.00	0.05
	4	0.05	0.00	0.05
	5	0.20	0.00	0.20
	6	0.20	0.00	0.20
	7	0.35	0.00	0.35
	8	0.35	0.00	0.35
1	1	2.1	2.06	0.04
	2	2.1	2.16	-0.06
	3	1.9	2.00	-0.10
	4	1.8	1.90	-0.10
	5	2.2	2.38	-0.18
	6	2.1	2.10	0.00
	7	2.0	2.20	-0.20
	8	1.9	2.26	-0.36
2	1	2.2	2.00	0.20
	2	2.1	2.10	0.00
	3	2.2	2.20	0.00
	4	2.2	2.16	0.04
	5	2.1	2.04	0.06
	6	2.0	2.00	0.00
	7	2.2	2.10	0.10
	8	2.1	2.10	0.00
3	1	1.80	1.88	-0.08
	2	2.00	1.96	0.04
	3	2.10	2.10	0.00
	4	2.10	2.16	-0.06
	5	2.10	2.06	0.04
	6	2.05	2.00	0.05
	7	2.10	2.06	0.04
	8	1.70	1.68	0.02

Table D.2: Comparison between 'Giletometer' output and vernier calliper measurement for pieces of flat spruce
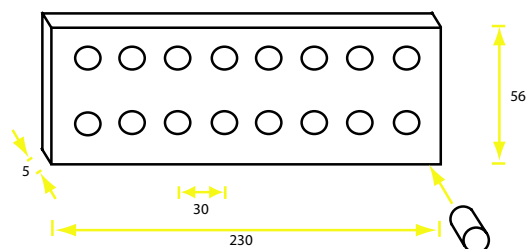
Figure D.5: Plan of grid template used for determination of thickness matrices of guitar soundboards

to thin the soundboard (§3.4)we would not expect any local variation of thickness

on scales of less than about 20 mm in the longitudinal or lateral dimensions.

Appendix E

Excitation and coupling apparatus

The acquisition and excitation system is a variant of the ACUZ system described in Appendix B.

Adopted temporarily, the cup-hook support mechanism was improved by using powerful permanent NdFeB rare earth magnets (each with a surface magnetic field density of 0.5 T at the surface).

E.1   Magnetic coupling apparatus

Because the primary method of excitation and detection is distributed over a small area of the instrument to be studied (the *driving point*), great care must be taken in mechanically bonding the two systems. A reversible and nondestructive bond is required, ruling out the use of strong adhesives or physically intrusive bonds such as nails or tacks. Also the support method described here makes it impracticable to employ a bolt or screw coupling method because of restricted rotational freedom of both systems. Figure E.1 illustrates the mechanical coupling apparatus used here, based on the attractive forces between two strong permanent rare-earth (NdFeB)

magnets. Using a strong epoxy adhesive, the cylindrical magnet (height: 12.5 mm, diameter: 12.5 mm, surface field strength at one pole: 0.5 T) is fixed to the end of a brass shaft, which is able to slide into an encasing brass tube. The tube has a threaded end, able to screw into the impedance head at the end of the shaker. A locking pin with a threaded end secures the two together when the shaft is completely inside the tube. This *magnetic clamp* is able to bond to another magnet, arranged with a north magnetic pole facing the clamp. This then enables the magnetic clamp to bond to a mechanical system, having a magnet attached, in a reversible and nondestructive manner. It is important that the bonding forces are larger than the forces exerted by the excitation system on the driving point of the instrument, including torque along axes perpendicular to the shaft axis, which may easily lead to inadequate coupling if the support system is not properly implemented. Incomplete coupling leads to mechanical damping effects and of course, in the case of complete decoupling, no measurements are possible at all.

It is a simple matter to place a permanent rare-earth magnet on the other side of a thin, flat plate of wood and in most cases arranged here, the coupling forces are adequate. In the case of the finished guitar, it is possible to place a magnet on the other side of the soundboard and use this as our driving point, but because we have chosen the central bridge point for this purpose, and the wood thickness here makes the magnetic coupling forces rather weak, we have instead chosen to modify the actual bridge of the instrument, so there is a magnet embedded into the bridge dedicated for this application. This enables ready identification of the central bridge point and reduces the time taken in positioning magnets for coupling at each measurement stage. Addition of a magnet in the bridge also enables magnetic
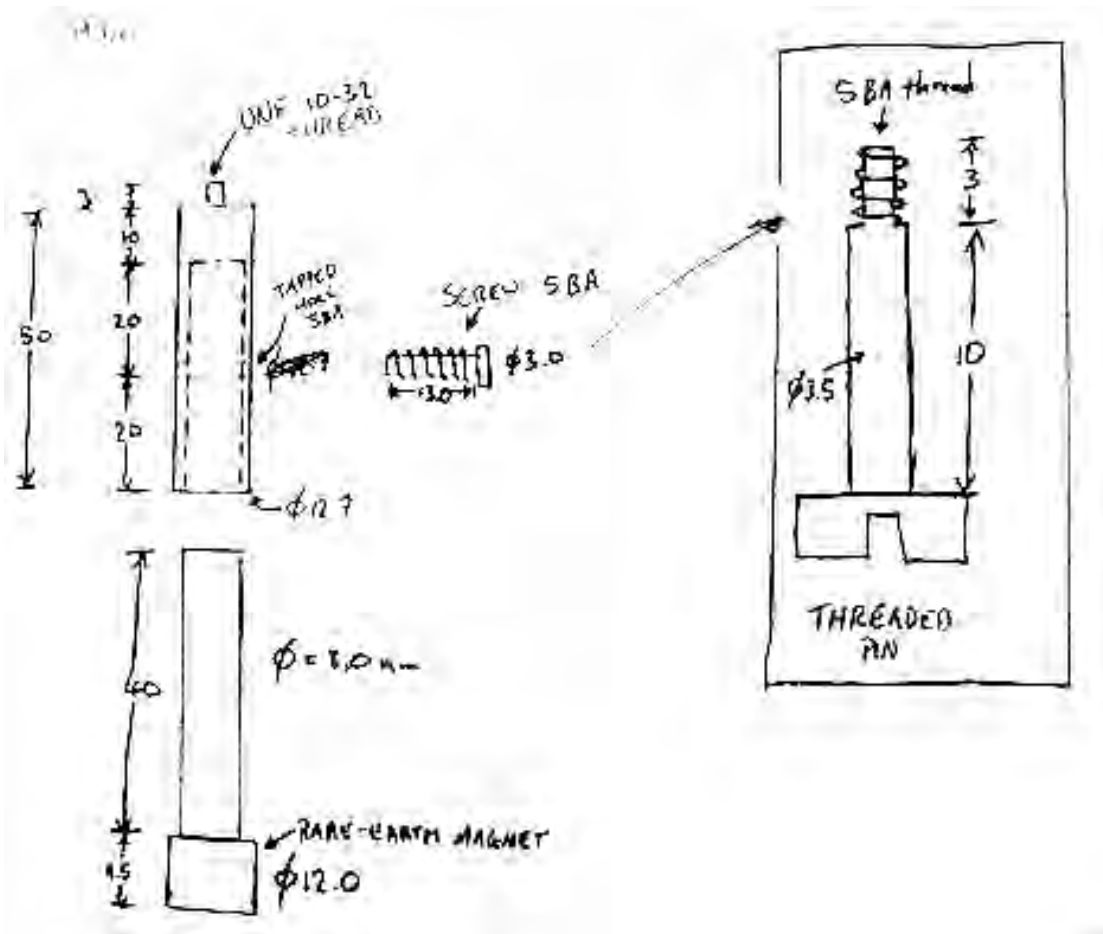
Figure E.1: Magnetic clamp apparatus, coupling the excitation and detection system to the element to be measured.

velocimetry measurements to be made at this point and excitation of the instrument to be performed through a solenoid.

Figure E.3 illustrates this method of modifying an existing bridge design by embedding a rare earth magnet into the central region. Although this was performed here before attaching to the guitar body, it would also be convenient to do this as a modification to an existing instrument. The added mass is relatively very small,
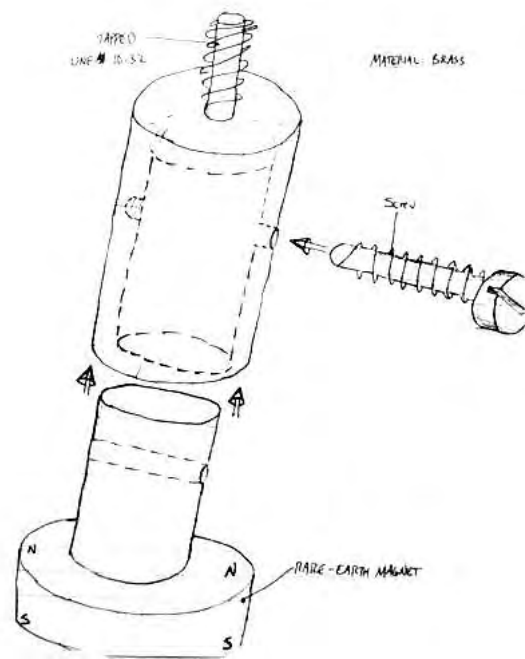
Figure E.2: Magnetic clamp (isometric sketch.)

Figure E.3: One of the guitar bridges with an embedded rare-earth magnet to couple the instrument to the excitation/detection apparatus. The visual effect is not unæsthetic

roughly 0.6% of the total mass of the bridge[1] and the small reduction in stiffness of the top surface of the bridge would only become noticeable at relatively high frequencies. If this point is coupled to the shaker, it is forced to be a point of maximum amplitude and the added mass of the magnet will not affect the vibratory response to excitation.

E.2   Cup-hook support mechanism

Mass of body: 1.3 kg, giving a weight of 12.73 N. Breaking strain of each hook: 4.9 N (500g). Spring constant, k, of long bands ($8 \times$ size 62 bands):

Long bands ($8 \times$ size 62)		
Force applied (N)	extension (mm)	k (Nm^{-1})
0.2	0	—
3.2	170	18.82
4.7	295	15.93
6.2	435	14.25

So $\overline{k} = 16.33$ Nm^{-1}

---

[1]($V = \frac{\pi}{4}d^2h$, $d = h = 6.0$ mm, $\rho = 700$ kg $\cdot$ m^{-3}. Percentage of total mass: $\frac{M_{\text{magnet}} - \rho V}{M_{\text{total}}} = \frac{1.3 - 1.70 \times 10^{-7} \cdot 700}{200}$)

Short bands (5 × size 62)		
Force applied (N)	extension (mm)	k (Nm^{-1})
1.4	0	—
3.2	70	25.71
4.6	175	18.29
6.1	280	16.79

And $\overline{k} = 20.26\ Nm^{-1}$ (graphs in notebook 5)

We are required to suspend a 1.3 kg object with two rubber bands having $k_1 = k_2 = 16$ Nm^{-1} and two with $k_3 = k_4 = 20$ ms^{-1}.

E.3 Magnetic support mechanism

Small rubber bands are useful for low mass objects, such as a violin or guitar soundboards, but the higher masses of guitar bodies and the finished instruments means we could not use the same bands in the same manner. In this case, I have found 'shock-cord' (an elastic cord made from nylon and elastic rubber fibres commonly used on modern sailing vessels) with an uncompressed diameter of 2.5 mm, to serve this purpose well. The advantages of this support are that it is geometrically simpler (*viz.* no knots are required) and is more convenient to attach to the pulley suspension system. The higher spring constant per unit length means that a small number are able to be used to support an entire instrument, but it also has a much higher ultimate strain than the rubber bands—so much so that there is practically no problem with mechanical failure, which is not the case with small rubber bands. This is an important consideration because mechanical failure of the support system may have disastrous consequences for the instrument involved. I have experienced

mechanical failure of the rubber band supports and it has only been circumstantial that no instrument was injured. No problems of this kind occurred with the shock-cord.

For an unstretched length of 0.488 m, the shock-cord was measured to have a spring constant of 13.07 ± 0.15 Nm^{-1}. For the guitars used here, the unstretched lengths of each cord was 1.37 metres.

E.4   Materials used in excitation stand

The NdFeB rare earth magnets used have the following properties:

Mass density	7.07×10^3 kg $\cdot$ m^{-3}
Diameter of large magnets	12.0 mm
Height of large magnets	10 mm
Field strength at surface	0.494 ± 0.001 T

E.5   Design of excitation stand

The mechanical support system for the guitar and the excitation and detection apparatus is a rectangular prism made of steel 'Speed-E-Frame'$^{\text{TM}}$ material that is able to be disassembled for storage (Figure E.4.)
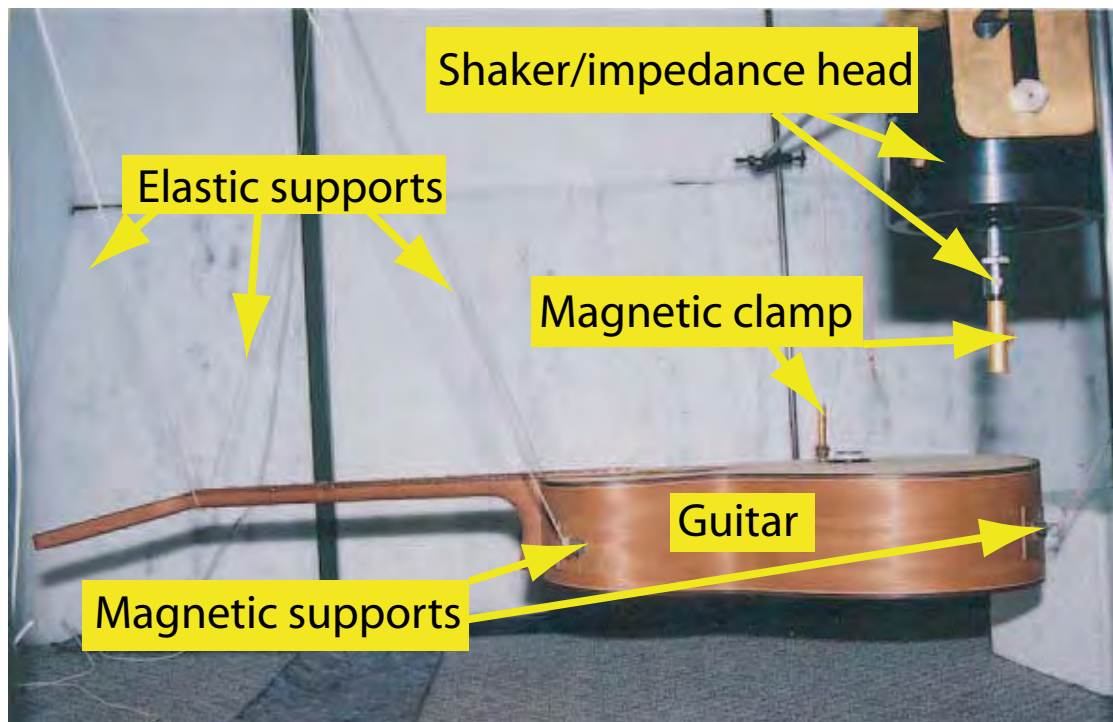
Figure E.4: System used to support the guitars during all measurements of transfer functions after the soundboards were glued to the back and sides.

E.6 Specific operating techniques

Docking

Coupling the excitation/detection apparatus to the element being tested is an important process for accurate measurement. The length of the magnetic clamp unit, from the end of the impedance head to the tip, is 28 mm. Because the magnet at the central bridge point of the element to be measured is usually fixed, it is easier to align the two systems without the internal shaft of the magnetic coupling apparatus (Figure E.1), introducing it when the system is properly aligned. Once this is performed, and the shaft is locked into place, it is necessary to check the contact at the bridge point is good; this may be done by inspection.

Appendix F

Lists of terms in describing the timbre of guitar sounds

F.1

Table F.1 gives the entire list of terms used in the on-line survey to determine a lexicon of agreed terms to describe the timbre of acoustic guitar sounds, described in §8.2, arranged in alphabetical order. Also provided are the results of the utility rating of each term from all 245 respondents. This differed slightly from the responses of those who had more experience in describing the timbre of guitar sounds, as in Table F.2.

Term	Utility (1-7)	Term	Utility (1-7)	Term	Utility (1-7)
balanced	5.1 ± 0.1	focussed	3.6 ± 0.1	ragtimey	2.7 ± 0.1
bassy	5.0 ± 0.1	folksy	3.3 ± 0.1	recessed	1.9 ± 0.1
beautiful	3.9 ± 0.1	formal	2.2 ± 0.1	rich	5.3 ± 0.1
beefy	3.3 ± 0.1	fresh	3.1 ± 0.1	ringing	4.9 ± 0.1
bell-like	4.5 ± 0.1	full	5.3 ± 0.1	robust	3.9 ± 0.1
big	4.0 ± 0.1	gently swinging	2.2 ± 0.1	round	3.7 ± 0.1
bland	3.6 ± 0.1	glassy	3.4 ± 0.1	scalloped	1.6 ± 0.1
bluesy	4.1 ± 0.1	growling	3.7 ± 0.1	scooped	1.8 ± 0.1
bold	3.8 ± 0.1	Hawaiian flair	2.2 ± 0.1	sharp	4.2 ± 0.1
boofy	1.5 ± 0.1	jazzy	3.7 ± 0.1	shimmering	4.2 ± 0.1
boomy	4.7 ± 0.1	killer sound	2.4 ± 0.1	harmonics	
bottomy	3.7 ± 0.1	lacking body	3.8 ± 0.1	shiny	2.5 ± 0.1
boxy	3.1 ± 0.1	lacking character	3.6 ± 0.1	silky	3.7 ± 0.1
bright	5.7 ± 0.1	lacking clarity	4.4 ± 0.1	smooth	4.4 ± 0.1
brilliant	4.8 ± 0.1	lacking midrange	4.5 ± 0.1	spatial	2.7 ± 0.1
character	3.2 ± 0.1	lacking spatiality	2.4 ± 0.1	spikey	2.7 ± 0.1
classic Martin	3.0 ± 0.1	lacklustre	3.3 ± 0.1	squashed	2.2 ± 0.1
Dreadnaught		lifeless	4.0 ± 0.1	steely	4.2 ± 0.1
in spades		lightweight	3.1 ± 0.1	stiff	3.3 ± 0.1
clean	5.0 ± 0.1	liquid	2.6 ± 0.1	strong presence	4.1 ± 0.1
clear	5.5 ± 0.1	loose	2.9 ± 0.1	sweet	4.4 ± 0.1
clinical	2.5 ± 0.1	mellow	5.1 ± 0.1	thick	4.0 ± 0.1
closed	2.8 ± 0.1	metallic	4.9 ± 0.1	thin	4.9 ± 0.1
compressed	3.5 ± 0.1	midrangey	4.1 ± 0.1	tight	4.1 ± 0.1
contained	2.9 ± 0.1	modest	3.8 ± 0.1	tinny	5.0 ± 0.1
crisp	5.4 ± 0.1	monster tone	2.5 ± 0.1	toppy	2.6 ± 0.1
dead	4.7 ± 0.1	muddy	4.5 ± 0.1	transparent	3.3 ± 0.1
deep	4.7 ± 0.1	mushy	3.2 ± 0.1	trebly	4.9 ± 0.1
defined	4.3 ± 0.1	natural	4.0 ± 0.1	tremendous	2.5 ± 0.1
detailed	3.3 ± 0.1	open	4.1 ± 0.1	twangy	5.0 ± 0.1
dull	4.4 ± 0.1	out of control	2.0 ± 0.1	unbalanced	4.1 ± 0.1
earthy	3.4 ± 0.1	overbearing	2.8 ± 0.1	undisciplined	2.0 ± 0.1
edgy	3.5 ± 0.1	peaky	2.6 ± 0.1	vibrant	4.6 ± 0.1
electric	3.4 ± 0.1	penetrating	4.3 ± 0.1	vivacious	2.6 ± 0.1
fat	4.1 ± 0.1	percussive	4.5 ± 0.1	warm	5.5 ± 0.1
fine	3.1 ± 0.1	pleasant	3.8 ± 0.1	woody	4.5 ± 0.1
fizzy	1.9 ± 0.1	powerful	4.9 ± 0.1	woofy	2.6 ± 0.1
flat	4.2 ± 0.1	punchy	4.5 ± 0.1		
floppy	2.0 ± 0.1	pure	4.5 ± 0.1		

Table F.1: The entire list of terms, in alphabetical order, used in the prepilot study to obtain an agreed lexicon on descriptions of the timbre of acoustic guitar sounds, described in §8.2. Included is the means of the utility rating for each term, for all 245 valid respondents. The uncertainty is taken as the standard error.

Term	Utility (1-7)	Term	Utility (1-7)	Term	Utility (1-7)
bright	6.1 ± 0.1	tight	4.4 ± 0.2	earthy	3.0 ± 0.2
balanced	5.9 ± 0.2	sweet	4.4 ± 0.2	closed	3.0 ± 0.2
bassy	5.8 ± 0.2	defined	4.3 ± 0.2	beefy	3.0 ± 0.2
boomy	5.7 ± 0.2	penetrating	4.3 ± 0.2	monster tone	2.9 ± 0.2
trebly	5.7 ± 0.1	lifeless	4.3 ± 0.2	woofy	2.9 ± 0.2
warm	5.5 ± 0.2	big	4.2 ± 0.2	folksy	2.8 ± 0.2
ringing	5.5 ± 0.1	fat	4.2 ± 0.2	fine	2.8 ± 0.2
thin	5.4 ± 0.2	lacking	4.2 ± 0.2	overbearing	2.7 ± 0.2
lacking	5.4 ± 0.2	character		lightweight	2.7 ± 0.2
midrange		vibrant	4.2 ± 0.2	loose	2.7 ± 0.2
tinny	5.4 ± 0.2	pure	4.1 ± 0.2	contained	2.7 ± 0.2
full	5.3 ± 0.2	smooth	4.1 ± 0.2	liquid	2.7 ± 0.2
bell-like	5.3 ± 0.2	flat	4.0 ± 0.2	ragtimey	2.7 ± 0.2
clear	5.2 ± 0.2	robust	4.0 ± 0.2	toppy	2.6 ± 0.2
dead	5.2 ± 0.2	bluesy	3.9 ± 0.2	lacking spatiality	2.5 ± 0.2
crisp	5.2 ± 0.2	growling	3.9 ± 0.2	killer sound	2.5 ± 0.2
rich	5.1 ± 0.2	lacking body	3.9 ± 0.2	peaky	2.5 ± 0.2
muddy	5.1 ± 0.2	focussed	3.9 ± 0.2	spatial	2.4 ± 0.2
powerful	5.1 ± 0.2	compressed	3.8 ± 0.2	spikey	2.4 ± 0.2
brilliant	5.1 ± 0.2	round	3.7 ± 0.2	tremendous	2.3 ± 0.2
midrangey	5.0 ± 0.2	transparent	3.6 ± 0.2	shiny	2.3 ± 0.2
lacking clarity	4.9 ± 0.2	mushy	3.6 ± 0.2	fresh	2.2 ± 0.2
deep	4.9 ± 0.2	steely	3.6 ± 0.2	Hawaiian flair	2.2 ± 0.2
twangy	4.9 ± 0.2	silky	3.6 ± 0.2	clinical	2.1 ± 0.2
mellow	4.9 ± 0.2	boxy	3.6 ± 0.2	squashed	2.0 ± 0.2
woody	4.9 ± 0.2	natural	3.6 ± 0.2	modest	2.0 ± 0.2
punchy	4.8 ± 0.2	stiff	3.5 ± 0.2	vivacious	2.0 ± 0.2
bottomy	4.7 ± 0.2	beautiful	3.5 ± 0.2	formal	2.0 ± 0.1
dull	4.7 ± 0.2	glassy	3.5 ± 0.2	gently swinging	1.8 ± 0.2
metallic	4.6 ± 0.2	bold	3.5 ± 0.2	scooped	1.7 ± 0.1
shimmering	4.6 ± 0.2	lacklustre	3.5 ± 0.2	scalloped	1.7 ± 0.1
harmonics		thick	3.4 ± 0.2	floppy	1.7 ± 0.1
percussive	4.6 ± 0.2	bland	3.4 ± 0.2	fizzy	1.6 ± 0.1
unbalanced	4.6 ± 0.2	sharp	3.4 ± 0.2	recessed	1.6 ± 0.1
clean	4.5 ± 0.2	jazzy	3.3 ± 0.2	out of control	1.5 ± 0.1
open	4.5 ± 0.2	edgy	3.1 ± 0.2	undisciplined	1.5 ± 0.1
strong presence	4.5 ± 0.2	pleasant	3.1 ± 0.2	boofy	1.4 ± 0.1
classic Martin	4.4 ± 0.2	electric	3.1 ± 0.2		
Dreadnaught		character	3.0 ± 0.2		
in spades		detailed	3.0 ± 0.2		

Table F.2: The entire list of terms used in the prepilot study, as rated by the respondents with more experience in describing the timbre of acoustic guitar sounds.

Bibliography

Ali Abdul-Aziz. Structural evaluation of a space shuttle main engine (SSME) high pressure fuel turbopump turbine blade. Final Contractor Report E-10018, Lewis Research Center, NASA, Cleveland, Ohio, June 1996.

Acoustical Society of America. *American Standards Association-Acoustical Terminology*. Number ANSI S1.1. Acoustical Society of America, New York, 1960.

Alaska specialty woods. Alaska—specialty woods. 2005. URL `http://www.alaskaspecialtywoods.com/asn.html`. (Accessed June 26, 2005).

J. Alonso Moral and Erik V. Jansson. Eigenmodes, input admittance and the function of the violin. *Acustica*, 50:329–337, 1982.

American Institute of Physics. *American Institute of Physics Handbook*. McGraw-Hill Book Company, 3rd edition, 1972.

A. Askenfelt and Erik V. Jansson. On vibration sensation and finger touch in stringed instrument playing. *Music Perception*, 9(3):311–350, 1992.

Michael Atherton. *Australian Made, Australian Played*. New South Wales University Press, Sydney, 1990.

Claire Barlow and Jim Woodhouse. Of old wood and varnish: peering into the can of worms. *Journal of the Catgut Acoustical Society*, 1(4):2–9, 1989.

Elaine Bécache, Antoine Chaigne, Gregoire Derveaux, and Patrick Joly. Numerical simulation of a guitar. *Computers and structures*, 83:107–126, 2005.

Belair guitars. Belair guitars. October 2002. URL http://www.belairguitars.com/wood_picture.htm. (Accessed June 26, 2005).

Arthur Benade. *Horns, Strings and Harmony*. Study Science Series. Anchor Books, New York, 1960.

Arthur Benade. *Fundamentals of Musical Acoustics*. Dover, New York, 2nd edition, 1990.

Charles Besnainou. From wood mechanical measurements to composite materials for musical instruments: New technology for instrument makers. *MRS Bulletin*, 20(3):34–36, 1995.

W. J. Bethancourt. The guitar, pre-1650. URL http://www.whitetreeaz.com/guitar1650/guitar.htm. (Accessed: December 17, 2005), November 1999.

George Bissinger. Testing of acoustic stringed musical instruments: part 4. *Experimental Techniques*, pages 43–46, July/August 2001.

George Bissinger and Carleen M. Hutchins. Air-plate→neck fingerboard coupling and the 'feel' of the violin. *Journal of the Catgut Acoustical Society*, 4(3), May 2001. Reproduced from Catgut Acoustical Society Newsletter #44, November 1985.

388

Mary L. Boas. *Mathematical Methods in the Physical Sciences*. John Wiley and Sons, Inc., 2nd edition, 1983.

J. Bodig and B. A. Jayne. *Mechanics of wood and wood composites*. Van Nostrand Reinhold, New York, 1982.

Emmanuel Bossy and Renaud Carpentier. Simple methods for studying violin plates. Technical report, The University of New South Wales and the École Normale Supérieure, 1998.

R. R. Boullosa, F. Orduna-Bustamante, and A. P. Lopez. Tuning characteristics, radiation efficiency and subjective quality of a set of classical guitars. *Applied Acoustics*, 3(56):183–197, March 1999.

Dana Bourgeois. Tapping tonewoods. how the selection of species helps define the sound of your guitar. *Acoustic Guitar*, (23), March/April 1994.

A. J. Brisben, S. S. Hsiao, and K. O. Johnson. Detection of vibration transmitted through an object grasped in the hand. *The Journal of Neurophysiology*, 81(4): 1548–1558, April 1999.

R. E. Brune. Comments on the Kasha question. *Guild of American Luthiers*, 4:42, 1985a.

R. E. Brune. Lutherie: Art or science? *Guild of American Luthiers*, 1:38, 1985b.

R. E. Brune. Letter to the editor. *Guild of American Luthiers*, 8:3, 1986.

Voichita Bucur. *Acoustics of wood*. CRC Press, 1995.

G. L. Burkhardt and J. L. Fisher. Clad thickness measurement system. *Non-destructive Detection Journal*, 7(8), 2002.

Graham Caldersmith. Low range guitar function and design. *CAS Newsletter*, 27: 19–25, May 1977.

Graham Caldersmith. Guitar as a reflex enclosure. *Journal of the Acoustical Society of America*, 63(5):1566–1575, May 1978.

Graham Caldersmith. Radiation from lower guitar modes. *American Lutherie*, 2: 20–24, 1985.

Graham Caldersmith. Vibration geometry and radiation fields in acoustic guitars. *Acoustics Australia*, 14(2):47–51, August 1986.

Graham Caldersmith and Elizabeth Freeman. Wood properties from sample plate measurements I. *Journal of the Catgut Acoustical Society*, 1(5):8–12, May 1990.

Sheryl E. Campbell. Random vibration analysis of the TOPAZ-II nuclear reactor power system. Master's thesis, Naval Postgraduate School, Monterey, California, June 1995.

Stephen Cass. A guitar so good it plays itself. *IEEE Spectrum*, page 15, September 2003.

Antoine Chaigne. Numerical simulations of stringed instruments-today's situation and trends for the future. *Journal of the Catgut Acoustical Society*, 4(5):12–20, May 2002.

Antoine Chaigne, Anders Askenfelt, and Erik Jansson. Time domain simulation of string instruments. a link between physical modeling and musical perception. *Journal de Physique*, III(2):51–54, 1992.

Antoine Chaigne and Michel Rosen. Analysis of guitar tones for various structural configurations of the instrument. *Journal of the Catgut Acoustical Society*, 3(8): 24–32, November 1999.

Ernst Chladni. *Entdeckungen ber die Theorie des Klanges ('Discovery of the Theory of Pitch')*. Weidmanns Erben und Reich, Leipzig, Germany, 1787.

A. Chomcharm and C. Skaar. Moisture and transverse dimensional changes during air-drying of small green hardwood wafers. *Wood Science and Technology*, 17(3): 227–240, September 1983.

Ove Christensen. The response of played guitars at middle frequencies. *Acustica*, 53:45–48, 1983.

Ove Christensen. An oscillator model for analysis of guitar sound pressure response. *Acustica*, 54:289–295, 1984.

Ove Christensen and Bo B. Vistisen. Simple model for low-frequency guitar function. *Journal of the Acoustical Society of America*, 68(3):758–766, September 1980.

Kathy S. Cruz. Trading notes: a Honolulu store owner mixes money with music. *Hawaii Business (Online)*, October 2003. URL: `http://goliath.ecnext.com/coms2/gi_0199-3268753/ Trading-notes-a-Honolulu-store.html` Accessed November 4, 2004.

A. Cummings. Ducts with axial temperature gradients: an approximate solution for sound transmission and generation. *Journal of Sound and Vibration*, 51:55–67, 1977.

William R. Cumpiano. Manuel Velázquez: grandmaster of guitarmaking. *Journal of Guitar Acoustics*, 5:13, 1982.

Jamie DeCoster. Overview of factor analysis. 1998. URL `http://www.stat-help.com/notes.html`. (Accessed December 13, 2005).

P. Derogis, R. Causse, and O. Warusfel. On the reproduction of directivity patterns using multi-loudpeaker sources. pages 387–392, 1995.

Gregoire Derveaux, Antoine Chaigne, Patrick Joly, and Elaine Bécache. Time-domain simulation of a guitar: Model and method (part 1). *Journal of the Acoustical Society of America*, 6(114):3368–3383, December 2003.

F. T. Dickens. Inertance of the guitar soundhole. *Catgut Acoustical Society Newsletter*, (29):27–28, 1978.

Ole Døssing. Structural testing part 1. Technical report, Brüel and Kjær, April 1988a.

Ole Døssing. Structural testing part 2. Technical report, Brüel and Kjær, March 1988b.

John I. Dunlop and M. Shaw. Acoustical properties of some australian woods. *Journal of the Catgut Acoustical Society*, 1(7):17–20, May 1991.

Gila Eban. Comments on the Kasha question. *Guild of American Luthiers*, 4:42, 1985.

M. J. Elejabarrieta, A. Ezcurra, and C. Santamaría. Evolution of the vibrational behaviour of a guitar soundboard along successive construction phases by means of the modal analysis technique. *Journal of the Acoustical Society of America*, 108(1):369–378, July 2000.

M. J. Elejabarrieta, A. Ezcurra, and C. Santamaría. Vibrational behaviour of the guitar soundboard analysed by the finite element method. *Acustica*, 87:128–136, 2001.

Y. Enomoto and T. Yoshida. Descriptive adjectives on the listening of reproduced sounds. pages A–5–10, Tokyo, 1968.

Thomas Erndl. Measurement of modes of vibration and transfer functions of the guitar. Technical report, The University of New South Wales, Sydney, Australia,

January 1999. A selection of Chladni patterns from this have been put onto the World Wide Web: http://www.phys.unsw.edu.au/~jw/guitar/patterns_engl.html.

A. Ezcurra. Influence of the material constants on the low frequency modes of a free guitar plate. *Journal of Sound and Vibration*, 194(4):640–644, 1996.

Ian M. Firth. Mechanical admittance measurements on the sound post of the violin and its action. *Acustica*, 36:332–339, 1976/77.

Ian M. Firth. Physics of the guitar at the Helmholtz and first top-plate resonances. *Journal of the Acoustical Society of America*, 61(2):588–593, February 1977.

Fishman Transducers. Fishman acoustic matrix professional system preamp installation. 2004.

Neville H. Fletcher and Thomas D. Rossing. *The Physics of Musical Instruments*. Springer-Verlag, 1998.

Richard A. Flinn and Paul K. Trojan. *Engineering materials and their applications*. Houghton Mifflin Company, Boston, 2nd edition, 1975.

Barbara J. Forbes and E. Roy Pike. Acoustical Klein-Gordon equation: A time-independent perturbation analysis. *Physical Review Letters*, 93(5):1–4, July 2004.

Frank Ford. Frets.com. June 2005. URL `http://www.frets.com/`. (Accessed June 26, 2005).

Forest Products Laboratory. Wood handbook: Wood as an engineering material. Technical report, Forest Products Laboratory, U.S. Dept. of Agriculture, Forest Service, 1999.

M. French and George Bissinger. Testing of acoustic stringed musical instruments—an introduction. *Experimental Techniques*, pages 40–43, January 2001.

M. French and D. Hosler. Testing of acoustic stringed musical instruments: part 3. *Experimental Techniques*, pages 45–46, May 2001.

Robert Fryxell. Did early makers use mineral additives in varnish? *Journal of the Catgut Acoustical Society*, (41):18–19, May 1984.

Robert Fryxell. Further studies of 'moisture breathing' by wood. *Journal of the Catgut Acoustical Society*, 1(5):37–38, May 1990.

Teja Gerken. To infinity and beyond. *Acoustic Guitar Magazine*, 103, July 2001.

Sophie Germaine. *Recherches sur la Theorie des Surfaces Elastiques*. Courcier, Paris, 1821.

L. J. Gibson. Modelling the mechanical behaviour of cellular materials. *Materials Science and Engineering A*, 110:1–36, March 1989.

L. J. Gibson and M. F. Ashby. *Cellular solids: Structure and properties*. Cambridge University Press, 2nd edition, 1997.

Andrew Gilbert. The steel string guitar. URL `http://sres.anu.edu.au/associated/fpt/nwfp/guitarsteel/guitar.html`. (Accessed December 17, 2005), 1999.

Gerard Gilet. private communication. 2000.

Colin E. Gough. Theory of string resonances on musical instruments. *Acustica*, 49 (2):124–140, 1981.

John M. Grey. Multidimensional perceptual scaling of musical timbres. *Journal of the Acoustical Society of America*, (61):1270–1277, 1977.

John M. Grey. Timbre discrimination in musical patterns. *Journal of the Acoustical Society of America*, 2(64):467–472, 1978.

M. Gridnev and V. Porkenhov. On quality estimation of violins and guitars. *Akusticheskil Zhurnal*, 22(5):691–698, 1976.

S. Griffen, H. Luo, and S. Hanagud. Acoustic guitar function model including symmetric and asymmetric plate modes. *Acustica*, 84:563–569, 1998.

Patrick Guillaume, Johan Schoukens, Rik Pintelon, and Kollár, István. Crest-factor minimization using nonlinear Chebyshev approximation methods. *IEEE Transactions on Instrumentation and Measurement*, 40(6):982–989, December 1991.

Daniel W. Haines. The essential mechanical properties of wood prepared for musical instruments. *Journal of the Catgut Acoustical Society*, 4(2), November 2000.

Donald E. Hall. *Musical Acoustics-An Introduction*. Wadsworth Inc., 1980.

Jesse Hamlin. In lake superior's frigid waters, a berkeley man found the key to hand-making excellent violins, July 2004. URL `http://www.sfgate.com/cgi-bin/article.cgi?file=/chronicle/archive/2004/07/31/DDGS97VA8M1.DTL`. (Accessed November 24, 2005).

Jamey Hampton. Letter to the editor. *Guild of American Luthiers*, 3:5, 1985.

Roger J. Hanson. Analysis of 'live' and 'dead' guitar strings. *Journal of the Catgut Acoustical Society*, (48):10–16, November 1987.

Redes D. Harjono. Acoustical properties of some Australian and Indonesian woods. Master's thesis, University of New South Wales, March 1998.

Redes D. Harjono and John I. Dunlop. Acoustic properties of some Australian and Indonesian woods. *Journal of the Catgut Acoustical Society*, 3(5):10–15, May 1998.

Hermann L. F. Helmholtz. *On the Sensations of Tone as a Physiological Basis for the Theory of Music*. Longmans and Co., 2nd edition, 1885.

John Huber. *The development of the modern guitar*. Bold Strummer Ltd., revised edition, 1991.

Carleen M. Hutchins. The science of the violin. *Scientific American*, 207(5):77–89, November 1962.

Carleen M. Hutchins. Effects of an air-body coupling on the tone and playing qualities of violins. *Journal of the Catgut Acoustical Society*, (44):12–15, November 1985.

Carleen M. Hutchins. A measurable controlling factor in the tone and playing qualities of violins. *Journal of the Catgut Acoustical Society*, 1(4):10–15, November 1989.

Carleen M. Hutchins. Mode tuning for the violin maker. *Journal of the Catgut Acoustical Society*, 2(4):5–9, November 1993.

Carleen M. Hutchins. A measurable effect of long-term playing on violin family instruments. *Journal of the Catgut Acoustical Society*, 3(5):38–40, May 1998.

Carleen M. Hutchins. Acoustics and the violin-past, present, and future. URL: `http://shemesh.larc.nasa.gov/Lectures/OldColloq/c-990302.htm` Accessed November 4, 2004, March 1999.

Ra Inta and John Smith. Determining top plate profiles in assembled guitars via measurements of magnetic field. In C. Don, editor, *Proceedings of the Eighth Western Pacific Acoustics Conference*, Castlemaine, Australia, April 2003. Australian Acoustical Society.

Ra Inta, John Smith, and Joe Wolfe. Measurement of the effect on violins of ageing and playing. *Acoustics Australia*, 33(1):25–29, April 2005.

Erik V. Jansson. A study of acoustical and hologram interferometric measurements of the top-plate vibrations of a guitar. *Acustica*, 25:96, 1971.

Erik V. Jansson. Acoustical properties of complex cavities: Prediction and measurement of resonance properties of violin-shaped and guitar shaped cavities. *Acustica*, 37(4):211–221, 1977.

Erik V. Jansson. Experiments with free violin plates. *Journal of the Catgut Acoustical Society*, 1(2):2–6, November 1988.

Erik V. Jansson. Admittance measurements of 25 high quality violins. *Acustica*, 83 (2):337–341, 1997.

Erik V. Jansson. *Acoustics for violin and guitar makers*. Kungl Tekniska Hogskolan (Swedish Department of Speech, Music and Hearing), Stockholm, 4th edition, 2002.

K. Jensen and J. Arnspang. Binary decision tree classification of musical sounds. Proceedings of the 1999 International Computer Music Conference, San Francisco, CA, 1999. International Computer Music Association.

Michael Kasha. Designing and testing of new guitars by criteria of applied physics and psychoacoustics. *Journal of the Acoustical Society of America*, 97(5):3355, May 1995.

G. W. C. Kaye and T. H. Laby. *Tables of Physical and Chemical Constants*. Longman Group, 14th edition, 1973.

Jozef Keckes, Ingo Burgert, Klaus Frühmann, Martin Müller, Klaas Kölln, Myles Hamilton, Manfred Burghammer, Stephan V. Roth, Stefanie Stanzl-Tschegg, and Fratzl Peter. Cell-wall recovery after irreversible deformation of wood. *Nature Materials*, 2:810–814, December 2003.

J. S. Kerrick, D. C. Nagel, and R. L. Bennet. Multiple ratings of sound stimuli. *Journal of the Acoustical Society of America*, 45:1014, 1969.

W. Krüger. Findings in manipulation of guitar top-plates. *Journal of the Catgut Acoustical Society*, 38:19, 1982.

Joseph C. S. Lai and Marion A. Burgess. Radiation efficiency of acoustic guitars. *Journal of the Acoustical Society of America*, 88(3):1222–1227, September 1990.

D. Laille and M. Maziere. The virtual guitar. 2002. URL `http://www.phys.unsw.edu.au/music/virtualguitar.html`. (Accessed December, 2002).

Davy Laille. Report on a finite element model of the guitar. Technical report, The University of New South Wales and the École Normale Supérieure, July 2002.

Charles E. Lance, Marcus M. Butts, and Lawrence C. Michels. The sources of four commonly reported cutoff criteria: what did they really say? *Organizational Research Methods*, 9(2):202–220, 2006.

L. D. Landau and E. M. Lifshitz. *Theory of Elasticity*. Number 7 in Course of Theoretical Physics. Pergamon Press, 2nd (English) edition, 1970. English translation by J. B. Sykes and W. H. Reid.

J. Laplane, E. Minsen, and S. Charron. Different configurations of the same concert guitar characterised by means of modal analysis and noise transfer. pages 552–557, 1995. (English version).

Alexis Le Pichon, Svein Berge, and Antoine Chaigne. Comparison between experimental and predicted radiation of a guitar. *Acustica*, 84:136–145, 1998.

398

S. G. Lekhitskii. *Theory of elasticity of an anisotropic elastic body.* Holden-Day Series in Mathematical Physics. Holden-Day, Inc., San Francisco, 1963. English translation by P. Fern.

S. G. Lekhitskii. *Anisotropic Plates.* Gordon and Breach Science Publishers, New York, English edition, 1968.

Harold Levine and Julian Schwinger. On the radiation from an unflanged circular pipe. *Physical Review*, 73(4):383–406, February 1948.

Mark Lewney. *The acoustics of the guitar.* PhD thesis, University of Wales, Cardiff, Wales, 2000.

W. H. Lichte. Attributes of complex tones. *Journal of Experimental Psychology*, 28: 455, 1941.

Jeremy Locke. Timber selection and its acoustic properties. February 2005. URL `http://www.classicalandflamencoguitars.com/Acoustic.htm`. (Accessed March 21, 2006).

Anthanas Lolov. Bent plates in violin construction. *Galpin Society Journal*, 37: 10–15, March 1984.

Mike Longworth. *Martin guitars: A history.* Omnibus Press, London, 1975.

George Manno. Is your wood ready to use? *American Luthierie*, (13):44, 1988.

Carl Margolis. Comment on the Kasha question. *Guild of American Luthiers*, 6:45, 1986.

K. D. Marshall. Modal analysis of a violin. *Journal of the Acoustical Society of America*, 2(77):695–709, 1985.

Simon M. Marty. Assessment of innovations in the construction of the classical guitar. part I: Analysis of top-plate resonances using FFT techniques and holographic interferometry. *Journal of the Catgut Acoustical Society*, 47:26–33, May 1987a.

Simon M. Marty. Assessment of innovations in the construction of the classical guitar: Part II. New developments in guitar construction. *Journal of the Catgut Acoustical Society*, (47):30–33, May 1987b.

Matthieu Maziere. Modelling a guitar using the finite elements method. Technical report, The University of New South Wales and the École Normale Supérieure, July 2002.

V. E. McGee. Semantic components of the quality of processed speech. *Journal of Speech and Hearing Research*, 7:310, 1964.

M. E. McIntyre and J. Woodhouse. The acoustics of stringed musical instruments. *Interdisciplinary Science Reviews*, 3:157–173, 1978.

M. E. McIntyre and J. Woodhouse. On measuring wood properties, part 3. *Journal of the Catgut Acoustical Society*, (45):14–23, May 1986.

N. W. McLachlan. *Theory of Vibrations*. Dover Publications, 1951.

John E. McLennan. The profile of violin no. 2. 1993. URL http://www.phys.unsw.edu.au/music/publications/mclennan/profile2.pdf. (Accessed June, 2004).

John E. McLennan. A new bowing machine. *Journal of the Catgut Acoustical Society*, 4(2):55, November 2000.

D. McLeod and R. Welford. *The classical guitar: Design and construction*. The Dryad Press, Leicester, 1971.

400

Robert C. McMaster, editor. *Nondestructive Testing Handbook*, volume 2, chapter 50. The Ronald Press Co., New York, 1959.

Jürgen Meyer. Directivity of the bowed stringed instruments and its effect on orchestral sound in concert halls. *Journal of the Acoustical Society of America*, 51: 1994–2009, 1972.

Jürgen Meyer. Die abstimmung der grundresonanzen von guitarren. *Das Musikinstrument*, 23:179–186, 1974. (English translation in Journal of Guitar Acoustics **5**, 19 (1982)).

Jürgen Meyer. The function of the guitar body and its dependence upon constructional details. *Publications of the Royal Swedish Academy of Music*, 38:77–100, 1983a.

Jürgen Meyer. Quality aspects of the guitar tone. *Pub. Royal Swedish Academy of Music*, 38:51–75, 1983b.

Micronas Semiconductor Holding AG. Sensors overview and system solutions. URL `http://www.micronas.com/products/overview/sensors/index.php#apps`. (Accessed November 2, 2004), 2004.

John Morrish, editor. *The classical guitar: a complete history*. Outline Press Ltd., London, September 1997.

D. Ouis. On the frequency dependence of the modulus of elasticity of wood. *Wood Science and Technology*, 36:335–346, 2002.

Maria Pavlidou. *A Physical Model of the String-Finger Interaction on the Classical Guitar*. PhD thesis, University of Wales, Cardiff, Wales, 1997.

H. F. Pollard and R. W. Harris. *An Introduction to Physical Acoustics*. First Year Teaching Unit, School of Physics, University of New South Wales, 1979.

Jose (III) Ramirez. Bars and struts. *American Luthierie*, 8:38, 1986. Reprinted in The Big Red Book of American Lutherie, Volume One (p.292).

R. A. Rasch and R. Plomp. *The Psychology of Music*, chapter 1: The Perception of Musical Tones, pages 1–24. Academic Press, New York, 1982.

Bernard E. Richardson. *A physical investigation into some factors affecting the musical performance of the guitar*. PhD thesis, Department of Physics and Astronomy, University of Wales, Cardiff, Wales, 1982.

Bernard E. Richardson. The influence of strutting on the top-plate modes of the guitar. *Catgut Acoustical Society Newsletter*, (40):13–17, 1983.

Bernard E. Richardson. Vibrations of stringed musical instruments. *University of Wales Review*, 4, 1988.

Bernard E. Richardson. The acoustical development of the guitar. *Journal of the Catgut Acoustical Society*, 2(5):1–10, May 1994.

Bernard E. Richardson. Acoustical design criteria for the guitar. *Journal of the Acoustical Society of America*, 97:3354, 1995a.

Bernard E. Richardson. The art and science of guitar construction. July 1995b.

Bernard E. Richardson. *The Encylopedia of Acoustics*, chapter 132 (Stringed instruments: plucked), pages 1627–1634. John Wiley and Sons, Inc., 1997.

Bernard E. Richardson. The classical guitar: Tone by design. pages 115–120, 1998.

Bernard E. Richardson and G.W. Roberts. The adjustment of mode frequencies in guitars: a study by means of holographic interferometry and finite element analysis. volume 2 of *SMAC*, pages 285–302, Stockholm, 1985. Publication of

402

the Royal Swedish Academy of Music. looked at changes during construction, w/interferometry.

Oliver E. Rodgers. Influence of local thickness changes on violin plate frequencies. *Journal of the Catgut Acoustical Society*, 1(5):13–16, May 1990.

Oliver E. Rodgers. Effect on plate frequencies of local wood removal from violin plates supported at the edges. *Journal of the Catgut Acoustical Society*, 1(8):7–11, November 1991.

J. L. Romanillos. *Antonio de Torres, guitar maker—his life and work*. Element Books Ltd, Dorset, 1987.

Michel Rosen. Guitar sounds analysis for various structural configurations of the instrument. page 572, 1995.

R. E. Ross and Thomas D. Rossing. Plate vibrations and resonances of classical and folk guitars. *Journal of the Acoustical Society of America*, 65:S72A, 1979.

Thomas D. Rossing. Modes of vibration of guitar plates with and without bracing. *The Journal of the Acoustical Society of America*, 71(S1):S27, April 1982.

Thomas D. Rossing. *The Science of Sound*. Addison-Wesley, 1990.

Thomas D. Rossing. *Science of percussion instruments*, volume 3 of *Series in popular science*. World Scientific Publishing Co. Pty. Ltd., 2000.

Thomas D. Rossing and Gila Eban. Normal modes of a radially braced guitar determined by electronic TV holography. *Journal of the Acoustical Society of America*, 106(5):2991–2996, November 1999.

Vincent Roussarie, Stephen McAdams, and Antoine Chaigne. Perceptual analysis of synthesized struck bars. In *Journal of the Acoustical Society of America*, volume 103, page 3007. Journal of the Acoustical Society of America, May 1998.

Dan Russell and Paul Pedersen. Modal analysis of an electric guitar. URL `http://www.kettering.edu/~drussell/guitars/electric.html`. (Accessed December 3, 2004), January 1999.

Richard Sacksteder. How well do we understand Helmholtz resonance? *Journal of the Catgut Acoustical Society*, 48:27–28, Novemember 1987.

L. N. Salomon. Semantic approach to the perception of complex sounds. *Journal of the Acoustical Society of America*, 30:421, 1958.

John C. Schelleng. The violin as a circuit. *Journal of the Acoustical Society of America*, 35(3):326–338, March 1963.

John C. Schelleng. Acoustical effects of violin varnish. *Journal of the Acoustical Society of America*, 44(5):1175–1183, 1968.

A. Schlägel. *Measurements of Elasticity and Loss Factor for Solid Materials*, volume 4 of *Brüel and Kjær Technical Review*. October 1957.

Martin Schleske. Speed of sound and damping of spruce in relation to the direction of grains and rays. *Journal of the Catgut Acoustical Society*, 1(6):16–20, 1990.

Martin Schleske. Eigenmodes of vibration in the working process of a violin. *Journal of the Catgut Acoustical Society*, 4(1):90–95, May 2000.

Martin Schleske. Empirical tools in contemporary violin making, part I: Analysis of design, materials, varnish, and normal modes. *Catgut Acoustical Society Journal*, 4(5):50–64, May 2002.

John O. Schneider. *The contemporary guitar: The search for new sounds since 1945*. PhD thesis, Department of Physics, University of Wales, Cardiff, August 1977.

404

John O. Schneider. *The contemporary guitar*, volume 5 of *The new instrumentation*. University of California Press, Berkeley and Los Angeles, 1985.

Emery Schubert. Update of the hevner adjective checklist. *Perceptual and Motor Skills*, 96:1117–1122, 2003.

Emery Schubert, Joe Wolfe, and Alex Tarnopolsky. Spectral centroid and timbre in complex, multiple instrumental textures. In S.D. Lipsomb, R. Ashley, R.O. Gjerdingen, and P. Webster, editors, *Proceedings of the 8th International Conference on Music Perception and Cognition*, pages 654–657, Adelaide, Australia, August 2004. Causal Productions.

W. T. Sedgwick and H. W. Tyler. *A short history of science.* The Macmillan Company, New York, 1917.

Gerald Sheppard. *Acoustic fingerstyle guitar*, chapter The question of handcrafted versus mass-produced instruments. 1997. URL http://www.acousticfingerstyle.com/HMvsMP.htm. (Accessed November 24, 2005).

M. R. Shroeder. Synthesis of low-peak-factor signals and binary sequences with low autocorrelation. *IEEE Transactions on Information Theory*, 16:85–89, January 1970.

William T. Simpson. Equilibrium moisture content of wood in outdoor locations in the United States and worldwide. Technical Report FPL-RN-0268, Forest Products Laboratory, US Dept. Agriculture, Madison, Wisconsin, August 1998.

Eugen Skudrzyk. *Simple and Complex Vibratory Systems.* Pennsylvania State University Press, 1968.

John R. Smith. Phasing of harmonic components to optimize measured signal-to-noise ratios of transfer functions. *Measurement Science and Technology*, 6:1343–1348, 1995.

I. S. Sokolnikoff. *The Mathematical Theory of Elasticity.* McGraw-Hill Book Co., Inc., 1946.

Karl A. Stetson. The effect of thickness perturbations on the vibration modes of plates. *Catgut Acoustical Society Newsletter*, 28:32–34, 1977.

John William (3rd Baron Rayleigh) Strutt. *The Theory of Sound*, volume 1 & 2. The Macmillan Company, 2nd edition, 1869.

Rudolph Szilard. *Theory and Analysis of Plates—Clasical and Numerical Methods.* Prentice-Hall, Inc., Englewood Cliffs, New Jersey, 1974.

K. P. Szlichcinski. The art of describing sounds. *Applied Ergonomics*, 10(3):131–138, September 1979.

E. Terhardt. Psychoacoustic evaluation of musical sounds. *Perception and Psychophyics*, 23:483–492, 1978.

Greg 'the Doc'. How to build an acoustic guitar vol. 5. URL `http://www.musicianshotline.com/archive/monthly/guitar_er/04_05.htm`. (Accessed November 24, 2005), May 2005.

William (Lord Kelvin) Thomson and Peter G. Tait. *Treatise on natural philosophy (2 vols).* Cambridge University Press, Cambridge, England, 1867.

S. P. Timoshenko. *Theory of elasticity.* McGraw-Hill, Inc., New York, 1934.

Rick Turner. Instant vintage. *Acoustic Guitar Magazine*, pages 36–41, February 1997.

S. Šali and J. Kopač. Measuring the quality of guitar tone. *Experimental mechanics*, 40(3):242–247, September 2000.

Igor Štubňa and Marek Liška. Formula for correction coefficients for calculating Young's modulus from resonant frequencies. *Acustica*, 87(1):149–150, 2001.

Scott van Linge. Parabolic guitar braces. *American Luthierie*, (47):15–17, September 1996.

David Vernet. Influence of the guitar bracing using the finite element method. Technical report, The University of New South Wales and the École Normale Supérieure, August 2001.

G. von Bismarck. Sharpness as an attribute of the timbre of steady sounds. *Acustica*, 30:159–172, 1974a.

G. von Bismarck. Timbre of steady sounds: A factorial investigation of its verbal attributes. *Acustica*, 30:146–159, 1974b.

Gordon P. Walker. *Towards a physical model of the guitar.* PhD thesis, University of Wales, Cardiff, Wales, 1991.

L. Wedin and G. Goude. Dimension analysis of instrumental timbre. *Scandinavian Journal of Psychology*, 13:228–240, 1972.

David L. Wessel. Timbre space as a musical control structure. Technical report, IRCAM, Ircam - Centre Georges-Pompidou, December 1978.

Jim Williams. *A guitar maker's handbook.* Guitarcraft, Dudley, NSW, Australia, April 1986a.

Jim Williams. Letter to the editor. *Guild of American Luthiers*, 5:7, 1986b.

Jim Williams. private communication. June 2003.

Erling Wold, Thom Blum, Douglas Keislar, and James Wheaton. Content-based classification, search and retrieval of audio. *IEEE Multimedia*, pages 27–36, 1996.

J. Wolfe, J. Smith, G. Brielbeck, and F. Stocker. A system for real time measurement of acoustic transfer functions. *Acoustics Australia*, 23(1):19–20, 1995.

A. Wood. *The Student's Physics, vol.II: Acoustics.* Blackie and Son Ltd, 1940.

Worland guitars. Worland guitars. 2004. URL http://www.worlandguitars.com/options/Tops/tops.html. (Accessed June 26, 2005).

Howard A. K. Wright. *The Acoustics and Psychoacoustics of the Guitar.* PhD thesis, University of Wales, 1996.

Howard A. K. Wright and Bernard E. Richardson. Psychoacoustical evaluation of synthesised guitar tones: Linking tone quality to construction. pages 602–608, 1995.

Howard A. K. Wright and Bernard E. Richardson. On the relationships between the response of the guitar body and the instrument's tone quality. *Proceedings of the Institute of Acoustics*, 19(5):149–154, 1997.

Paul Wyszkowski. Letter to the editor. *Guild of American Luthiers*, 3:2, 1985.

Paul Wyszkowski. Comment on the Kasha question. *Guild of American Luthiers*, 6:45, 1986.